UNIVERSITAT DE BARCELONA
FACULTAT DE QUÍMICA
DEPARTAMENT D' ENGINYERIA QUÍMICA I METAL·LÚRGIA

Combination of photo-oxidation processes with biological treatment

Doctoral Thesis

Fares Al-Momani
Directed by Dr. Santiago Esplugas

Barcelona, June, 2003

PROGRAMA BIENAL DE INGENIERIA QUIMICA AMBIENTAL

Bienio 1999-2001

Memoria presentada por Fares Al-Momani, Ingeniero Químico, para optar por el grado de Doctor en Ingeniería Química.

Fares Al-Momani

La presente tesis ha sido realizada en el Departamento de Ingenieria Química y Metalurgia de la Universidad de Barcelona, bajo la dirección del Dr. Santiago Esplugas Vidal, quien autoriza su presentación:

Dr. Santiago Esplugas Vidal

Barcelona Abril del 2003

En el primer lugar quiero expresar mi mas profunda gratitud al Dr. Santiago Esplugas por la dirección, soporte y colaboración prestada, sin los que hubiera sido imposible la pronta y satisfactoria realización de este trabajo.

También deseo hacer constar mi agradecimiento al Dra. Carmen Sans por su apoyo durante todas las fases de esta investigación, especialmente en los temas biológicos y por la ayuda que me ha ofrecido cuando la he necesitado, muchísima gracias de verdad Carmen.

A Claudita, le doy las gracias de todo corazón por haberme animado y apoyado en todos los momentos. Un agradecimiento especial a mi familia por todo su cariño y aliento. Aunque están a gran distancia los tengo siempre en mi corazón.

A Nadia, Sandra, Oscar y Anastasius por todos los momentos que hemos pasado juntos en el laboratorio durante estos años, donde hemos compartido muchísimas cosas, muchas gracias por todo.

Así mismo quiero agradecer todos mis amigos dentro y fuera de la Universidad. los me han acompañado durante estos cuatro años. Durante este tiempo han sido como mi segunda familia, gracias Miguel, Monia , Zaid, Mohammed, Verónica, Cristina, Neus, Eva, y a todos los otros

Mi sincero agradecimiento a la Agencia Española de Cooperación Internacional (AECI) y la Universidad de Barcelona por la beca concedida en mi favor durante el tiempo de mis estudios de doctorado.

Mi agradecimiento para Dra. Evelyne Touraud y Dr. Jean Roussy, asi como a todos los que mi hicieron posible mi estancia en Ales-France, gracias Fouad, Tiaa y todos los nuevos amigos.

A al secretaria del Departamento de Ingeniería Química y Metalurgia por toda su colaboración en los aspectos administrativos.

Also I would Like to express my deep and special grateful to friends who help me a lot during the last 8 years and their were always beside me supporting and helping to let me do my best effort, thank you Thaker, Reema my sisters Alaa y Sara you are always in my mind and my heart.

The ability to think straight, some knowledge of the past, some vision of the future, some skill to do useful service, some urge to fit that service into the well-being of the community- these are the most vital things education must try to produce.

Virginia Gildersleeve

INDEX

1. Introduction

Comprising over 70% of the Earth's surface, water is undoubtedly the most precious natural resource that exists on our planet. Without the seemingly invaluable compound comprised of hydrogen and oxygen, life on Earth would be non-existent: it is essential for everything on our planet to grow and prosper. Although we as humans recognize this fact, we disregard it by polluting our rivers, lakes, and oceans. Subsequently, we are slowly but surely harming our planet to the point where organisms are dying at a very alarming rate. In addition to innocent organisms dying off, our drinking water has become greatly affected as is our ability to use water for recreational purposes. In order to combat water pollution, we must understand the problems and become part of the solution.

1.1 Point and non-point sources:

According to the American College Dictionary, pollution is defined as: "to make foul or unclean; dirty." Water pollution occurs when a body of water is adversely affected due to the addition of large amounts of materials to the water. When it is unfit for its intended use, water is considered polluted. Two types of water pollutants exist: point source and non-point source. Point sources of pollution occur when harmful substances are emitted directly into a body of water. A non-point source delivers pollutants indirectly through environmental changes. An example of this type of water pollution is when fertilizer from a field is carried into a stream by rain, in the form of run-off which in turn effects aquatic life. The technology exists for point sources of pollution to be monitored and regulated, although political factors may complicate matters (Wilcock, 1988). Nonpoint sources are much more difficult to control. Pollution arising from nonpoint sources accounts for a majority of the contaminants in streams and lakes.

1.2 Causes of pollution:

Many causes of pollution including sewage and fertilizers contain nutrients such as nitrates and phosphates. In excess levels, nutrients over stimulate the growth of aquatic plants and algae. Excessive growth of these types of organisms consequently clogs our waterways, use up dissolved oxygen as they decompose, and block light to deeper waters. This, in turn, proves very harmful to aquatic organisms as it affects the respiration ability or fish and other invertebrates that reside in water. Pollution is also caused when silt and other suspended solids, such as soil, wash-off plowed fields, construction and logging sites, urban areas, and

eroded river banks when it rains (Street et al., 1925). Under natural conditions, lakes, rivers, and other water bodies undergo Eutrophication, an aging process that slowly fills in the water body with sediment and organic matter. When these sediments enter various bodies of water, fish respiration becomes impaired, plant productivity and water depth become reduced, and aquatic organisms and their environments become suffocated. Pollution in the form of organic material enters waterways in many different forms as sewage, as leaves and grass clippings, or as runoff from livestock feedlots and pastures. When natural bacteria and protozoan in the water break down this organic material, they begin to use up the oxygen dissolved in the water. Many types of fish and bottom-dwelling animals cannot survive when levels of dissolved oxygen drop below two to five parts per million. When this occurs, it kills aquatic organisms in large numbers which leads to disruptions in the food chain.

1.3 Additional forms of water pollution:

Three last forms of water pollution exist in the forms of petroleum, radioactive substances, and heat. Petroleum often pollutes water bodies in the form of oil, resulting from oil spills. The exxon Valdez is an example of this type of water pollution. These large-scale accidental discharges of petroleum are an important cause of pollution along shore lines. Besides the super tankers, off-shore drilling operations contribute a large share of pollution. One estimate is that one ton of oil is spilled for every million tons of oil transported. On the other hand, the number of organic compounds have been synthesised since the turn of the century now exceeds, half a million, and some 10,000 new compound are added each year, as results, many of these compounds are now found in the wastewater from most industrial (Brown and Barnwell, 1985).

Radioactive substances are produced in the form of waste from nuclear power plants, and from the industrial, medical, and scientific use of radioactive materials. Specific forms of waste are uranium and thorium mining and refining. The last form of water pollution is heat. Heat is a pollutant because increased temperatures result in the deaths of many aquatic organisms. These decreases in temperatures are caused when a discharge of cooling water by factories and power plants occurs.

1.4 Classifying water pollution:

The major sources of water pollution can be classified as municipal, industrial, and agricultural. Municipal water pollution consists of wastewater from homes and commercial

establishments. For many years, the main goal of treating municipal wastewater was simply to reduce its content of suspended solids, oxygen-demanding materials, dissolved inorganic compounds, and harmful bacteria. In recent years, however, more stress has been placed on improving means of disposal of the solid residues from the municipal treatment processes. The basic methods of treating municipal wastewater fall into three stages: primary treatment, including grit removal, screening, grinding, and sedimentation; secondary treatment, which entails oxidation of dissolved organic matter by means of using biologically active sludge, which is then filtered off; and tertiary treatment, in which advanced biological methods of nitrogen removal and chemical and physical methods such as granular filtration and activated carbon absorption are employed. The handling and disposal of solid residues can account for 25 to 50 percent of the capital and operational costs of a treatment plant. The characteristics of industrial wastewaters can differ considerably both within and among industries. The impact of industrial discharges depends not only on their collective characteristics, such as biochemical oxygen demand and the amount of suspended solids, but also on their content of specific inorganic and organic substances. Three options are available in controlling industrial wastewater (Thomas 1982). Control can take place at the point of generation in the plant; wastewater can be pretreated for discharge to municipal treatment sources; or wastewater can be treated completely at the plant and either reused or discharged directly into receiving waters.

1.5 Legislation

Several forms of legislation have been passed in recent decades to try to control water pollution. In 1970, the Clean Water Act provided 50 billion dollars to cities and states to build wastewater facilities in USA. This has helped control surface water pollution from industrial and municipal sources throughout the United States. When congress passed the Clean Water Act in 1972, states were given primary authority to set their own standards for their water. In addition to these standards, the act required that all state beneficial uses and their criteria must comply with the “fishable and swimmable” goals of the act. This essentially means that state beneficial uses must be able to support aquatic life and recreational use. Because it is impossible to test water for every type of disease-causing organism, states usually look to identify indicator bacteria. One for a example is a bacteria known as fecal coliforms. These indicator bacteria suggest that a certain selection of water may be contaminated with untreated sewage and that other, more dangerous, organisms are

present. These legislations are an important part in the fight against water pollution. They are useful in preventing Environmental catastrophes.

Here in Spain, water Act 29/1985 points out that "*water is not a commercial product like any other but, rather, a heritage which must be protected, defended and treated as such*". In Article 16, it is pointed out that specific measures against water pollution by individual pollutants or groups of pollutants presenting a significant risk to or via the aquatic environment have to be adopted. Those measures are aimed at the progressive reduction of that pollutants and, for priority hazardous substances, the cessation or phasing out of discharges, emissions and losses within 20 years after their adoption at community level.

2. Constituents found in wastewater

Wastewater characterized in term of its physical, chemical and biological composition, the principle physical, chemical and biological constituents of wastewater and their sources are reported in table 2.1. It should be noted that many of the parameters listed in table 2.1 are interrelated. For example, temperature, physical property, affects both chemical and biological activity in the wastewater and the amount of gases dissolve in the wastewater

Table 2.1: Physical, chemical, and biological characteristics of wastewater and their sources (Metcalf and Eddy, 1985)

Characteristic	Source
Physical properties	
Color	Domestic and industrial waste, natural decay of organic
Odor	Decomposing wastewater, industrial wastes
Solids	Domestic water supply, domestic and industrial wastes Soil erosion inflow/infiltration
Temperature	Domestics and industrial wastes
Chemical constituents	
Organic	Domestic, commercial, and industrial wastes
Carbohydrate	Domestic, commercial, and industrial wastes
Fats, oil and grease	Agricultural wastes
Pesticides	Industrial wastes
Phenols	Domestic, commercial, and industrial wastes
Proteins	Domestic, commercial, and industrial wastes
Priority pollutants	Domestic, commercial, and industrial wastes
Surfactant	Domestic, commercial, and industrial wastes
Volatile-organic compounds	Domestic, commercial, and industrial wastes
Other	Natural decay organic matter
Inorganic	
Alkalinity	Domestic wastes, domestic water supply, groundwater infiltration
Chlorides	Domestic wastes, domestic water supply, groundwater infiltration
Heavy metals	Industrial wastes
Nitrogen	Domestic and agricultural; wastes
pH	Domestic, commercial and industrial wastes
Phosphorus	Domestic, commercial and industrial wastes; natural runoff
Priority pollutants	Domestic, commercial and industrial wastes
Sulfer	Domestic water supply; domestic, commercial, and industrial wastes
Gases	
Hydrogen sulfide	Decomposition of domestic wastes
Methane	Decomposition of domestic wastes
Oxygen	Domestic water supply, sarface-water infiltration
Biological constituents	
Animals	Open watercourses and treatment plant
Plants	Open watercourses and treatment plant
Protists	
Eubacteria	Domestic wastes. Surface-water infiltration, treatment plants
Archaebacteria	Domestic wastes. Surface-water infiltration, treatment plants
Viruses	Domestic wastes

2.1 Contaminant of concern in wastewater treatment

The important contaminants of concern in wastewater treatment are listed in table 2.2. Secondary treatment standards for wastewater are concerned with the removal of biodegradable organic, suspended solids, and pathogens. Many of the more stringent standards that have been developed recently deal with the removal of nutrients and priority pollutants (Levine et al., 1985). Recently, The European Union made out a list of dangerous compounds (see Table 2.3), considered as contaminants, to which constantly new substances are added ("black list" of the E.U.,)

Table 2.2: Important contaminants of concern in wastewater treatment:

Contaminants	Reasons for importance
Suspended solids	Suspended solids can lead to the development of sludge deposits and anaerobic conditions when untreated wastewater is discharge in the aquatic environment
Biodegradable organic	Composed principally of proteins, carbohydrates, and fats, biodegradable organic are measured most commonly in terms of BOD (Biological oxygen demand) and COD (chemical oxygen demand) if discharged untreated to the environment, their biological stabilisation can lead to the depletion of natural oxygen resources and to the development of septic conditions
Pathogens	Communicable diseases can be transmitted by the pathogenic organisms in wastewater
Nutrients	Both nitrogen and phosphorous, along with carbon, are essential nutrients for growth. When discharge to the aquatic environment, these nutrients can lead to the growth of undesirable aquatic life. When discharge in excessive amounts on land, they can also lead to the pollution of groundwater
Priority pollutants	Organic and inorganic compounds selected on the basis of their known or suspected carcinogenicity, mutagenicity, teratogenicity, or high acute toxicity. Many of these are found in wastewater
Refractory organics	These organics tend to resist congenital methods of wastewater treatment. Typical examples include surfactant, phenols, and agricultural pesticides
Heavy metals	Heavy metals are usually added to wastewater from commercial and industrial activities and may have to be removed if the wastewater is to be used
Dissolved inorganics	Inorganic constituents such as calcium. Sodium, and sulphate are added to the original domestic water supply as a result of water use and may be have to be removed if the wastewater is to be reused

2.2 Physical characteristics

The most important physical characteristics of wastewater is total solids content which is composed of floating matter settable matter, colloidal matter and matter in solution. Other important characteristic are shown in table 2.4

Table 2.4 physical characteristic (Metcalf and Eddy, 1981)

Characteristic	Definition
Total solids	All the matter that remains as residue upon evaporation at 103 to 105 $^{\circ}$C
Settleable solids	Solids that will settle to the bottom of a con-shaped container in 60 min period
Total volatile solids	The organic fraction that oxidize and drive off as gas at 550± 50 $^{\circ}$C
Turbidity	Measure of the light-transmitting property of water is another test used to indicate the quantity of waste discharge and natural waters with respect to colloidal and residual suspended

Table 2.3: Black list of chemicals substances selected by the E.U. (Harrison, 1992)

Group	Included substances
Chloride hydrocarbons	Aldrin, dieldrin, chlorobenzene, dichlorobenzene, chloronaphthalene, chloroprene, chloropropene, chlorotoluene, endosulfane, endrin, hexachlorobenzene, hexachlorobutadiene, hexachlorocyclo-hexane, hexachloroethane, PCBs, tetrachlorobenzene, trichlorobenzene.
Chlorophenol	Monochlorophenol, 2,4-dichlorophenol, 2-amino-4-chlorophenol, pentachlorophenol, 4-chloro-3-methylphenol, trichlorophenol.
Chloroanilines and nitrobenzenes	Monochloroanilines, 1-chloro-2,4-dinitrobenzene, dichloroaniline, 4-chloro-2-nitrobenzene, chloronitrobenzene, chloronitrotoluene, dichloronitrobenzene.
Policyclic Aromatic Hydrocarbons	Antracene, biphenyl, naphthalene, PAHs
Inorganic substances	Arsenic and its compounds, cadmium and its compounds, mercury and its compounds
Solvents	Benzene, carbon tetrachloride, chloroform, dichloroethane, dichloroethylene, dichloromethane, dichloropropane, dichloropropanol, dichloropropene, ethylbenzene, toluene, tetrachloroethylene, trichloroethane, trichloroethylene.
Other	Benzidine, chloroacetic acid, chloroethanol, dibromomethane, dichlorobenzidine, dichloro-diisopropyl-ether, diethylamine, dimethylamine, epichlorhydrine, isopropylbenzene, tributylphosphate, trichlorotrifluoroethane, vinyl chloride, xilene.
Pesticides	Cyanide chloride, 2,4-dichlorophenoxyacetic acid and derivatives, 2,4,5-trichlorophenoxyacetic acid and derivatives, DDT, demeton, dichloroprope, dichlorvos, dimethoate, disulfoton, phenitrothion, phenthyon, linuron, malathion, MCPA, mecoprope, monolinuron, omethoate, parathion, phoxime, propanyl, pirazone, simacine, triazofos, trichlorofon, trifularin and derivatives.

2.3 Chemical characteristics:

Chemical characteristics of wastewater are included in four parts:

2.3.1. Organic matter:

In wastewater of medium strength, about 75% of the suspended solids and 40% of the filterable solids are organic matters. These solids are derived from animals, plant kingdome and the activities of man in the synthesis of organic. The principle groups of organic substances found in wastewater are proteins (40 to 60 percent) carbohydrate (25 to 50 percent) fats and oils (10 percent), urea and wastewater contains small quantity of large number of different synthetic organic molecules ranging from simple to extremely complex in structure (Metcalf and Eddy, 1979)

Measurement of organic matter:

A number of different tests have been developed to determine the organic contents of wastewater. In general, the test may be divided into those used to measure gross concentration in the range of 10^{-2} to 10^{-3} $mg.L^{-1}$. Laboratory methods commonly used today to measure gross amounts of organic matter (greater than 1 $mg.L^{-1}$) in wastewater include, (1) biological oxygen demand BOD (2) chemical oxygen demand COD (3) total organic compound TOC, complementing these laboratory tests is the theoretical oxygen demand (ThOD), which is determined from the chemical formula of the organic matters.

Trace organic in the range of 10^{-12} to 10^{-3} mg.L-1 is determined using instrumental methods including gas chromatography and mass spectroscopy. Within the years the sensitivity of the methods has improved significantly.

1) Biological Oxygen Demand(BOD):

The most widely used parameters of organic pollution applied to both wastewater and surface water is the 5-day BOD (BOD_5). This determination involves the measurement of the dissolved oxygen used by microorganisms in the biochemical oxidation of organic matter. This test has some limitations discussed later. Why, then if the test suffers from serious limitations, is further space devoted to it in this field? The reason is that BOD test results are now used: 1) to determine the approximate quantity of oxygen that will be required to biologically stablize the organic matters present. 2) To determine the size of wastewater treatment facilities 3). To measure the efficiency of some treatment processes and, 4) to determine compliance with wastewater discharge permits.

To insure that meaningful results are obtained, the sample must be suitably diluted with specially prepared dilution water, so that adequate nutrients and oxygen will be available during the incubation period. Full discussion of BOD measurements will be given in experimental part (Moore et al., 1950).

Biochemical oxidation is slow process and theoretically takes at infinite time to go to completion. Within a 20-day period, the oxidation of the carbonous organic matter is about 95-99 percent complete, and in the 5-day period used for the BOD test. Oxidation is from 60 to 70 percent complete. The 20°C used are an average value for slow-moving streams in temperate climate and is easily duplicated in an incubator. Different results would be obtained at different temperature because biochemical reaction rates are temperature dependent.

The kinetics of the BOD reaction are, for practical purposes, formulated in accordance with first order reaction kinetics and may be expressed as

$$\frac{dL_t}{dt} = -k_1 t \qquad (2\text{-}1)$$

Where L_t is the amount of the first stage BOD remaining in the water at time t and k is the first reaction rate constant. This equation can be integrated as

$$\text{Ln } L_t \Big|_0^t = -kt \mid \qquad (2\text{-}2)$$

$$\frac{L_t}{L} = \exp(-kt) = 10^{-kt} \qquad (2\text{-}3)$$

Where L or the BOD_L is the BOD remaining at time =0 (i.e. the total or ultimate first-stage BOD initially present):

A typical value of k (base exp, at 20°C) is 0.23 day. The value of reaction-rate constant varies significantly however, with the type of waste.

Other type of BOD is nitrogenous biochemical oxygen demand (NBOD) and carbonaceous biochemical oxygen demands (CBOD) are well known.

Limitations of the BOD test:

A highly concentration of active, acclimated seed bacteria is required.

Pre-treatment is needed when dealing with toxic waste, and effects of nitrifying organisms must be reduced.

Only the biodegradable organic are measured .

The test does not have stoichiometric validity after the soluble organic matter present in solution has been used.

An arbitrary, long period of time is required to obtain result.

Over the above the most serious limitations is that the 5-day period may or may not correspond to the point where soluble organic matter that present has been used. The lacks of stoichiometric validity at all time reduce the usefulness of the test results.

2) Chemical Oxygen Demand (COD):

The COD test is used to measure the content of organic matter of both wastewater and natural waters. The oxygen equivalent of the organic matter, that can be oxidized is measured by using a strong chemical oxidizing agent in an acidic medium. Potassium dichromate has been found to be excellent for these purposes. The test must be performed at an elevated temperature. A catalyst (silver sulphite) is required to aid the oxidation of certain classes of organic compounds. Since some inorganic compounds interface with the test, care must be taken to eliminate them. The principle reaction using dichromate as the oxidizing agent may be represented in general way by unbalanced equation

$$\text{organic matter } (C_a H_b O_c) + Cr_2O_7^{-2} + H^+ \xrightarrow{CATALYST} Cr^{+3} + CO_2 + H_2O \qquad (2.4)$$

The COD test used to measure the organic matter in the wastes that contain compound which are toxic to biological life. The COD of a waste is, in general, higher than the BOD because the more compounds can be chemically oxidized than can be biologically oxidized. For many types of wastes, it is possible to correlate COD with BOD. This can be very useful because the COD can be determine in three hours, compared with five day for BOD.

3) Total Organic Carbon TOC:

Another means for measuring the organic matters present in the water is the TOC test, which is especially applicable to small concentrations of organic matter. This test is performed by injecting a known quantity of sample into a high-temperature furnace or chemically-oxidizing environment. The organic carbon is oxidized to carbon dioxide in the presence of a catalyst. The carbon dioxide that is produced is quantitatively measured by means of an infrared analyzer. Acidification and aeration of the sample prior to analysis eliminate errors due to the presence of inorganic carbon. The test can be performed rapidly and is becoming more popular. Certain resistant organic compound may not be oxidized, and the measured TOC value will be slightly less than the actual amount present in the sample.

2.4.2.Inorganic matter:

Several inorganic components of wastewater and natural waters are important in establishing and controlling water quality. The concentrations of inorganic substances in water are increased both by the geologic formation with which the water comes in contacts and by the wastewater, treated or untreated, that are discharge to it. An example of such inorganic compound that may present in the water and the wastewater are chlorides, nitrogen's, phosphorus, sulfur, heavy metals (nickel (Ni), manganese (Mn), lead(Pb), chromium(Cr), cadmium(Cd), zinc(Zn), copper(Cu)), iron(Fe) and mercury(Hg)).

2.4.3.Gases:

Gases commonly found in untreated wastewater include nitrogen (N_2), oxygen (O_2), carbon dioxide (CO_2), hydrogen sulfide (H_2S), ammonia (NH_3), and methane (CH_4)

2.4 Biological characteristics

The environmental engineer must have considerable knowledge of the biological characteristics of wastewater as the principal group of micro-organisms, the pathogenic

organisms found in wastewater, the organisms used as indicators of pollution and the methods used to enumerate the indicator organisms (Mara, 1974).

Wastewater contains many biological groups as:

Micro-organisms they were found in both surface water and wastewater it includes eucaryotes, eubacteria, and archaebacteria

Bacteria are single cell procaryotic. Most bacteria can be grouped by form into four categories: spheroid, rod or spiral, and filamentous.

Fungi are aerobic, multicellular, nonphotosynthtic, chemohetrophic, and eucaryotic protists. Most fungi obtained their food from dead organic matter

Algae can be a great nuisance in surface waters because, when condition are right, they will rapidly reproduce and cover streams, lakes, and reservoirs.

Protozoa are single-cell eucaryotic microorganisms without cell wall. Many majorities of protozoa are aerobic although some anaerobic types are known.

Plants and animals: it is an important range in size from microscopic rotifers and worms to macroscopic crustaceans

Viruses: are obligate parasitic consisting of a strand of genetic material-deoxyribonucleic acid (DNA) or ribonucleic acid (RNA) with protein coat. Viruses do not have ability to synthesize new compounds.

3. Wastewater treatment processing:

3.1 Physical unit operations:

Those operations for treatment of wastewater in which is brought about of or through the application of physical force are known as physical unit operation, and they were the first methods to be used (Fair et al., 1966) .

This unit operations most commonly used in wastewater treatment include; flow metering, screening, mixing, sedimentation, accelerated gravity settling, floatation, filtration, gas transfer and volatilisation.

3.2 Chemical unit processes:

Those processes for treatment of wastewater in which is brought about of or through the chemical reactions are known as chemical unit processes. The most common chemical processes used are summarized in table 3.1

Table 3.1 Applications of chemical unit processes in wastewater treatment:

Process	Application
Chemical precipitation	Removal of phosphorus and enhancement of suspended solids removal in primary sedimentation facilities used for physical-chemical treatment
Adsorption	Removal of organic not removed by convential chemical and biological treatment methods. Also used for Dechlorination of wastewater before final discharge for treated effluent
Disinfection	Selective destruction of disease-causing organisms (can be accomplished in various ways)
Dechlorination	Removal of total combined chlorine residual that exists after chlorination (Can be accomplished in various ways)
Disinfection by chlorine dioxide	Selective destruction of disease- causing organisms
Disinfection with bromine chloride	Selective destruction of disease- causing organisms
Disinfection with ozone	Selective destruction of disease- causing organisms
Disinfection with ultraviolet light	Selective destruction of disease- causing organisms
Other chemical applications	Different objective of treatments

3.3. Advanced treatment processes

3.3.1. Supercritical water oxidation (SWO)

It is an innovatory technique for rapid destruction of the organic contaminates without formation harmful products. Pure water consider to be in supercritical condition if its temperature and pressure exceeds 374.2°C and 221 bar respectively. At this point, the volume

of water is three times that at room temperature, with density of 0.322 $g.mL^{-1}$. As a result of that, this water has the ability to destroy many organic matters, water act as highly oxidative environment that oxidized this organic compound to carbon dioxide and water. The process is very efficient and no longer has high-energy costs due to using high power semiconductors.
DCP degradation by SWO have been performed by many investigators (Li et al., 1994; Lin et al., 1998). The oxidation capacity of SWO process could be improve by adding oxidants as hydrogen peroxide. DCP, conversions of 99.99% were obtained with hydrogen peroxide at 450ºC, while 87.6% conversion by oxygen addition at 500ºC was achieved (Lee et al., 1990). With respect to phenol, many studies were perform in this field, lastly Lee et al 2002 have been study the effect of addition of NaOH in SCWO efficiency, results show that the effects of NaOH on the decomposition of chlorophenols, and phenol SCWO are not negligible, and the effects of NaOH on the decomposition of other organic compounds under SCWO conditions should be considered for determining optimum operating conditions and reactor designs.

3.3.2. Electrochemical oxidation:

One of the big advantages of the electrochemical processes is that the electrons are given or consumed in the electrodes, providing a clean reagent and no harmful chemical molecules implied in the process.
This approach basically involves using the principles of Fenton's chemistry plus electricity to degrade organic compounds in contaminated water and wastewater. In process, hydroxyl radicals are created by applying an oscillating low-amperage (<10 amps) electric current to an aqueous solution of PH<5 that contains hydrogen peroxide. (No iron is added because the electrode supplies the iron catalyst for the Fenton reaction). This produce free radicals that attack the organic compound in the solution, including organometallic complexes and PCB's (Scrudato, 1996).
Several important factors that affect the reaction rate are heat, current, electrode configuration, composition, and surface area.
Nevertheless, this process contain certain inconveniences:

1. The electrochemical treatment is an expensive process in comparison with other processes also the mechanism in water is quite complex.
2. The necessity to conductive effluent, therefore in case that the treated solution doesn't present a good conductivity a salt should be added.

The electrochemical oxidation of all the organic compounds is thermodynamically favoured in front of the competitive reaction of oxygen production for water oxidation. However, the kinetics of oxidation of the water is much quicker than the kinetics of oxidation of the organic compounds, due to its biggest concentration (Sakuria et al., 1999 and Palau, 1999).

The mechanism of the electrochemical processes generally implies three stages: the electrocoagulation, the electroflotation and the electroxidation (Sienliewicz et al., 1999):

$$\begin{aligned} RH &\xrightarrow{-e^-} RH^+ \\ RH^+ &\xrightarrow{-H^+} R^\bullet \\ R^\bullet + R^\bullet &\rightarrow R-R \end{aligned} \qquad (3\text{-}1)$$

The anodic oxidation is generally considered as a direct technique, it implies the direct transfer of an electron from the organic molecule to the electrode. The pH and the nature of the electrodes influence in a decisive way the formed products.

Few studies have been found in the literature regarding the electrochemical oxidation of phenols and DCP. Phenolic compounds were showed to be electrochemical Oxidizable (Huang et al., 1992), electrochemical oxidation of chlorinated phenols was found to be hampered to anodes due to fouling problems (Rodgers et al., 1999). Recently, Electro-Fenton and photoelectro-Fenton processes have been performed efficiently for mineralization different organic matters such as aniline (Brillas et al., 1998a), 4-chlorophenol (Brillas et al., 1998b) and 2,4-D (Brillas et al., 2000).

3.3.3. Wet oxidation:

Wet oxidation processes, is the oxidation of organic and/or inorganic compounds in aqueous phase by oxygen or air, and higher pressure and temperature conditions. The temperature depends on the nature of the compounds to degrade (normally oscillates between 150 and 350ºC). At the same time, pressure goes from 20 to 200 bar. During wet oxidation processes organic matter removal of 75 to 90% COD could be obtained (Li et al., 1991). The mechanism of wet oxidation has been deeply studied and seems to take place by means of a free radical process. Among the compounds that have been catalogued as readily oxidizable by means of wet oxidation are aliphatic, aliphatic chlorides and aromatic which do not contain halogenated functional groups, such as phenols or anilines. Compounds contain halogen and nitro functional groups have been found to be difficult to degraded by this method (Scott, 1997).

3.3.4. Adsorption of organic compounds onto activated carbon:

Adsorption on activated carbon is a potential wastewater treatment method, this method could be used efficiently for organic and inorganic removals. Adsorption treatment process can be classified as mass transfer operation in which the contaminant is transferred from water phase, to the surface of active carbon (solid phase), where is accumulated for its subsequent extraction or destruction. The adsorption onto activated carbon is widely used for wastewater treatment. It is a common suggested treatment for color and odors removals, also it can be used efficiently for organic compounds and toxic compounds removals.

The adsorption of 2,4-dichlorphenol (DCP) onto activated carbon has been widely studied, it showed to be well absorbable compounds onto activated carbon (Sacher et al. (2001). DCP removal has been performed successfully by means of biological activated carbon (Ha et al., 2000; 2001), with the advantage of the bioregeneration of the activated carbon. Recently, GAC (granular activated carbon) has been also combined with photocatalysis (Malato et al., 2001). ErolAyranci et al., (2001) studied the adsorption and electrosorption behavior of phenol, 1-, 2- and 3-chlorophenol and 2,6-dichlorophenolat at high-area carbon-felt (C-felt) electrodes by in situ UV spectroscopy . It was demonstrated that the initial concentrations (about 1 mM) of these compounds can be reduced by 77% or more from wastewaters by adsorption at the C-felt.

3.3.5. Chemical oxidation:

This type of treatment just used, when the biological treatments have low effect. It can be used as pre-treatment step to the biological treatment. The more popular use of such treatment process When wastewater contain nonbiodegradable and/or toxic contaminates and normal chemical processes can not treat or transform them to biodegradable and/or none toxic compound. Also it used when the wastewater contain high contaminants concentrations. For all of that the chemical oxidation is an effective treatment.

At this point it should be distinguish between:

a) Classical oxidation treatment

b) Advanced oxidation processes (Rodriguez et al., 2000)

The classical oxidation treatment, consist of adding to the water that contain contaminants and an oxidizing agent. After which simple chemical oxidation occur to remove contaminants. The most oxidizing agent used are:

- Chloride: represent strong and cheap oxidizing agent that can be used efficiently for waste treatment. However, the only disadvantage is the low selectivity, the case that imply high dosage and chlororganics by-products formation
- Oxygen: consider as a moderate oxidizing agent, its low cost operating conditions make it an attractive choice
- Hydrogen peroxide: is one of the most proposed oxidizing agent recommended for large variety of systems, it can be applied alone or with catalyst, however sometimes the peroxide alone do not work with some organic matters
- Ozone: it is strong oxidizing agent, which has the same advantage as oxygen and peroxide. The most problem in application such treatment is the difficulty and the instability of gas controlling (Beltran et al., 1998).

It was observed that, contaminate can not be treated biological or mineralised if they are at highly chemical stability. In these cases a more effective processes should be used for convincing purification.

Advanced Oxidation Processes (AOP's): -

(AOPs) were defined by Glaze et al., (1987) as near ambient temperature and pressure water treatment processes which involve the generation of highly reactive radicals (specially hydroxyl radicals) in sufficient quantity to effect water purification. These processes are characterized that no more toxic compound can be produced during the reaction. Also via AOP's complete organic matter minerlization could be achieved. Hydroxyl radical is specially oxidation agents that attack the majority of organic matters. The kinetic of these reactions is first order for ($OH^{\bullet}$) radical concentration, and to the species to be oxidize. Rate constant in general are in order 10^{8}-10^{10} $M^{-1}.s^{-1}$, where the hydroxyl radical concentration between 10^{-12}-10^{-10} M. Table 3.2 shows the oxidation potential for oxidizing agent used in water treatments, it can be seen that the hydroxyl radical is among the most potential agents.
The hydroxyl radical characterized by it is low selectivity, but it is attractive oxidants that can be used in the wastewater treatment. Several organic compounds can be eliminated or degrade immediately by use of hydroxyl radical. However, some organic are not attacked by this action like the acetic acid, oxalic acid, chlorides derivatives as chloroforms and tetrachloroethan. Table 3.3 presents different groups of compound Oxidizable by $OH^{\bullet}$.

The variety on AOP´s comes from the fact that there are many ways for hydroxyl radical production, this permit fulfilment for the requirements of any treatment. Above all of that, it should be taken in account that these AOP's are made by use of some expensive reactants; H_2O_2, UV and/or O_3. Thus, they should not used if there are other more economical process.

Table 3.2 oxidation potential for some agents used in wastewater treatment (Beltran et al., 1997a and Oussi et al., 1997)

Oxidizing agent	Oxidation potential (V)
Florine	3.03
Hydroxyl radical	2.80
Atomic oxygen	2.42
Ozone	2.07
Hydrogen peroxide	1.77
Permenganate	1.67
Chloro dioxide	1.50
Chlorine	1.36
Bromine	1.09
Iodine	0.54

Table 3.3. Oxidizable compounds by hydroxyl radicals (Bigda, 1995)

Compounds	
Acids	Formic, gluconic, lactic, malic, propionic, tartaric
Alcohols	Benzyl, *tert*-butyl, ethanol, ethylene glycol, glycerol, isopropanol, methanol, propenediol
Aldehydes	Acetaldehyde, benzaldehyde, formaldehyde, glyoxal, isobutyraldehyde, trichloroacetaldehyde
Aromatics	Benzene, chlorobenzene, chlorophenol, creosote, dichlorophenol, hydroquinone, p-nitrophenol, phenol, toluene, trichlorophenol, xylene, trinitrotoluene
Amines	Aniline, cyclic amines, diethylamine, dimethylformamide, EDTA, propanediamine, n-propylamine
Dyes	Anthraquinone, diazo, monoazo
Ethers	Tetrahydrofuran
Ketones	Dihydroxyacetone, methyl ethyl ketone

Another aspect should not be forgotten in the application of the AOP's is water organic charge, in general expressed as COD (chemical oxygen demand). Normally the wastewater that has COD value below (≤10 g/L) can be treated with these processes, but if the quantity of COD is more, the necessity of the reactant are increase, with negative effect on treatment cost. In these cases, it is more convenient use other processes like wet oxidation (see figure 3.1).

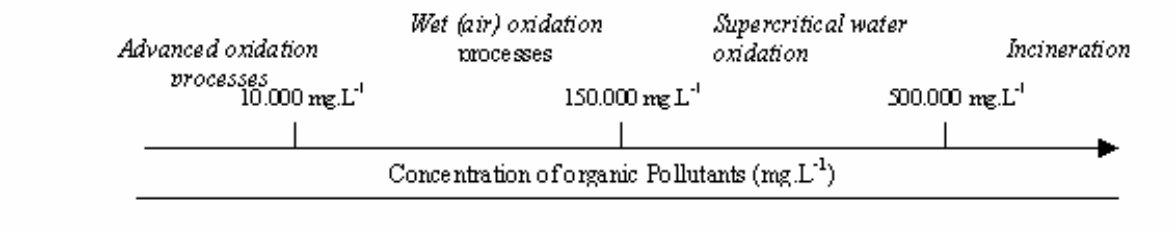

Figure 3-1: Suitability of water treatment technologies according to COD contents (Andreozzi et al., 1999)

3.3.5.1 Processes based in the ultraviolet light radiation

3.3.5.1.1 Photochemical process

The principle of the photochemical reaction, is the addition of energy for the chemical compound in form of radiation, which absorbed by the group of molecules to reach an excited state. The solar energy can be use as the source of such radiation energy for degradation of some compounds. But in some case this energy is not sufficient; for example, in case of phenol, solar energy is insufficient for breaking the aromatic ring. Hence, normally ultraviolet light radiation is used.

Different investigation indicate that, several organic contaminants can be decomposed partial or totally into other substances less toxic and more biodegradable by oxidation based on UV-light (Oussi et al., 1997). It should be recorded that, the use of low-pressure mercury lamp, that emits light with wavelength 253.7 nm, are not efficient to eliminate all contained organic matters in water. They can be used powerfully for the degradation of the aromatics, but they are incompetent in elimination the colours aliphatic. In other hand, medium pressure mercury lamps emit spectra between 254 and 400 nm, are not only efficient in generation of hydroxyl radicals, when it is combined with H_2O_2, but also they caused electron transition in many organic matters.

In the photochemical reactions, the mean step is the generation of the hydroxyl radical by photolyses of the water (Cervera et la., 1983) according to the reaction (3.2).

$$H_2O \xrightarrow{h\nu} H + OH^{\bullet} \qquad (3.2)$$

This reaction is an excessive source of radicals, also in the reaction media it may generate large quantity of reaction intermediates that absorb part of the radiation, leads to considerable effect in the photooxidation kinetics of the contaminants, this make the process valid for effluents with low contaminate concentration**.**

The photochemical treatment has good effect in solving the problem of refractors compound, However, it has disadvantages that it can not be applied in high scale due to ultraviolet light high production cost. Also, not all the radiation emitted by the source is used, just the absorbed radiation, and this is just small fraction of light produced attack the organic matter for chemical change, which indicate slow photodegradation kinetic. For increased the rate of this process, some additives are added like; addition of oxidant H_2O_2 and/or O_3, addition catalyst (Photo-Fenton) or photocatalysis(TiO_2)

3.3.5.1.2 UV/H_2O_2 process

Light absorbed by a molecule can result in electronic excitation, which increase the molecule's ability to lose or gain electrons. This makes the excited state more suitable as an oxidizing or reducing agent, that in turn makes it more likely and a highly reactive species such as the hydroxide radical ($OH^{\bullet}$) can be produced from an electron transfer process between the excited state and contacting medium.

The ultraviolet/H_2O_2 (UV/ H_2O_2) process involves the photolysis of hydrogen peroxide. The most accepted mechanism for this H_2O_2 photolysis is the rupture of the O-O bond by the action of ultraviolet light forming two hydroxyl radical (3.4) (Beltrán et al., 1997b):

$$H_2O_2 \xrightarrow{h\nu} 2\,OH^{\bullet} \qquad (3.4)$$

Some of the practical difficulties with the UV photolysis of H_2O_2 are:

- Low wavelength (below 200-400 nm) are required to make the process efficient (Tachiev et al., 1998 and Helz et al., 1997).
- Turbid waters containing strong UV absorbers such as aromatics organic compounds require higher light concentration, which increases the cost of the process
- It is not applicable to in situ treatment.

The process required an acidic pH, which can be achieved sometimes by the addition of acid or ferric oxalate. The method of irradiation is not limited to the UV light and can include natural sunlight. This may require a longer processing time, but that may be outweighed by the convenience of using natural light. Chemicals that can be treated with this technique include aromatic hydrocarbons and substituted aromatic hydrocarbon, phenols, alkanes, alkynes, ethers, and ketones, both in their substituted and non substituted forms.

The rate of the aqueous H_2O_2 photolysis was found to be pH dependent and increases when alkaline conditions are used, Probably because at 253.7 nm, the anions peroxide HO_2^- has higher molar absorption coefficient (240 vs 18.6$M^{-1}.cm^{-1}$) (Glaze et al., 1987). After that the $OH^\bullet$ radical can attack to the hydrogen peroxide leading to the following sequence of equations:

$$H_2O_2 + OH^\bullet \rightarrow HO_2^\bullet + H_2O \qquad (3.4)$$

$$H_2O_2 + HO_2^\bullet \rightarrow OH^\bullet + O_2 + H_2O \qquad (3.5)$$

$$2\,HO_2^\bullet \rightarrow H_2O_2 + O_2 \qquad (3.6)$$

when these reactions occur in medium that contain organic contaminate the reaction begin forming different type of radicals that degrade these contaminants.

This system has advantage that if it works with ozone, it provides cheaper hydroxyl radical, which make the ozone more easier to handle.

The hydroxyl radical generated in presence of an organic substrate can react in three different ways(Legrini et al., 1983):

1. With hydrogen abstraction: $OH^\bullet + RH \rightarrow R^\bullet + H_2O$ (3.7)

2. With electrophilic addition: $OH^\bullet + PhX \rightarrow HOPhX^\bullet$ (3.8)

3. With electron transfer: $OH^\bullet + RX \rightarrow RX^{\bullet+} + OH^-$ (3.9)

The recombination radical-radical should also be taken into account (3.10):

$$2\,OH^\bullet \rightarrow H_2O_2 \qquad (3.10)$$

literature review show that UV/H_2 O_2 has been used for degradation of different types of organic ; 2,4-dichlorophenol (DCP) and other chlorophenols removal were studied by Benítez et al. (2000a). Hirvonen et al. (2000) made a comparison between DCP degradation rate by UV/H_2O_2 process in alkaline conditions and direct UV (20-W 254 nm lamp) irradiation, in the study they reported that the addition of hydrogen peroxide at acidic pH increased the reaction rate by one order of magnitude. Alnaizy et al. (2000) studied phenol degradation with a UV/ H_2O_2 process in a completely mixed, batch photolytic reactor, the UV irradiation source was a low-pressure mercury lamp. The study indicate that there is an optimum H_2O_2 / phenol molar ratio for efficient degradation in the range of 100-250.

3.3.5.1.3 Photocatalysis

The basic principle of photocatalysis process is a semiconductor photo excitation as result of radiation absorption, normally near ultraviolet spectrum. Under near UV irradiation, a suitable semiconductor material may be excited by photons possessing energies of sufficient magnitude to produce conduction band electrons and valence band holes. These charge carriers are able to induce reduction or oxidation, respectively, and react with both water and organic compounds. The holes are extremely oxidants and should thus be able to oxidize almost all chemicals, as well as water, resulting in the formation of hydroxyl radicals (Munter et al., 2001). Many catalysts have been tested, although TiO_2 in the anatase form seems to possess the most interesting features, such as high stability, good performance and low cost (Andreozzi et al., 1999).

DCP complete mineralization was achieved during photocatalysis process with TiO_2 and 6-W 254 nm Hg lamp (Ku et al., 1992). Giménez et al. (1999) also tested the photocatalytic treatment of DCP by using TiO_2 and solar light, proving that reaction was first order with respect to DCP concentration and comparing the efficiencies of two different photocatalytic reactors.

3.3.5.1.4. UV/Fe(III):

UV/Fe(III) consider one of the more common treatment process based in UV-light. Fe(III) solutions in the presnce of UV irradiation acts as photo-catalyst. Throughout photo-catalytic process not only the absorbed UV photons lead to organic matter degradation but also ferric ion undergoes a photo-redox reaction producing more hydroxyl radicals.

$$Fe(III) + H_2O \xrightarrow{h\nu} Fe(II) + OH^{\bullet} + H^{+} \qquad (3.11)$$

Rodríguez et al., 2000 have been studieded the degradation of nitobenzen by UV/Fe(III) process, 80% of nitrobenzen degradation was found to achieve during 60 min irradiation time. Phenol degradation via UV/Fe(III) proceese was found to follow first order kinetic (Rodríguez et al., 2002).

3.3.5.1.5. Vacuum ultraviolet process (VUV)

The VUV consists on the UV spectral domain where air (oxygen) strongly absorbs radiation; its border with the UV-C is at 190 nm, and spectroscopic work at shorter wavelengths can

only be performed in vacuum or in non-absorbing gases. VUV photochemical processes are becoming possible with the development of excimer light sources emitting in this domain (Legrini et al., 1993).

It is an interesting method for the degradation of organic pollutants in liquid or gaseous phase. Besides the photolysis of the target compound, VUV photolysis of water is a highly efficient way of hydroxyl radical generation Eq.3.12, which can then attack the substrate:

$$H_2O \xrightarrow{hv} \frac{1}{2}H_2 + OH^{\bullet} \qquad (3.12)$$

The complete photomineralization of DCP by VUV oxidation has been reported by Baum et al., (1995). Oppenl et al., (2000) have been studied phenol photodegradation via VUV lihght, the study point out the advantage of phenol total mineralization by the production of effecitnt hydroxyl radicals.

3.3.5.1.6.Fenton and Photo-Fenton

a) Fenton and Fenton like reaction

More than one century ago, H.J.H. Fenton discovered that using hydrogen peroxide and iron salt like catalyst could oxidize many organic molecules. Recently it has been discovered the mechanism of Fenton oxidation that bases on the generation of hydroxyl radical by the catalytic decomposition of the H_2O_2 in acidic media (Bigda,1995). In presence of Fe(II), the peroxide breaks down to $OH^{\bullet}$ and OH^{-}, according to the following equations (3.14 to 3.16) (Nesheiwat and Swanson, 2000):

$$Fe(II) + H_2O_2 \rightarrow Fe(III) + OH^{-} + OH^{\bullet} \qquad (3.13)$$

$$Fe(III) + H_2O_2 \rightarrow Fe(II) + H^{+} + HOO^{\bullet} \qquad (3.14)$$

$$2\,H_2O_2 \rightarrow H_2O + OH^{\bullet} + HOO^{\bullet} \qquad (3.15)$$

The iron catalyst can be either Fe (II) or Fe(III) salts, although ferrous iron may be preferred. Nowadays both sulfate and chloride iron salt can be used. It is interesting to note that, the possibility of iron recycling make the process more feasible, for iron recycling the procedure is the following: raising the PH, separating the iron floc, and re-acidifying the iron sludge.

In this process radical generation begins once the hydrogen peroxide and iron ions come in contact. The hydroxyl ($OH^{\bullet}$)radicals formed are very powerful oxidizer and are short-lived species. ($OH^{\bullet}$) is one of the most powerful oxidizer known, next to fluorine in its reactivity.

The reaction rate is limited by the rate of (OH^-) generation, which is directly related to the concentration of the iron catalyst, and although less so, by the specific wastewater being treated.

Several mechanisms for the reaction of hydroxyl radical are possible. However, two mechanisms are most common effective in organic matter destruction. Oxygen addition mechanisms, where hydroxyl radical adds to unsaturated compound to form a free-radical product:

$$OH^{\bullet} + C_6H_6 \rightarrow C_6H_6(OH)^{\bullet} \qquad (3.16)$$

and hydrogen abstraction, where water and an organic free radical are formed

$$OH^{\bullet} + CH_3OH^{\bullet} \rightarrow CH_2OH^{\bullet} + H_2O \qquad (3.17)$$

The oxidation of an aromatic ring compound such as phenol is a classic example of the use of Fenton's reagents to reduce the toxicity of industrial effluents. In the process, carboxylic and dicarboxylic acids are produced, and if the oxidation is carried to completion, CO_2 and water are formed. Substituted aromatic ring structure can be also oxidized with Fenton's reagent to carboxylic acids and dicarboxylic acids and theoretically all the way to CO_2 and water.

In this way, toxic or non-biodegradable ring structure can be made less toxic and more amenable to biological oxidation. The reaction is highly exothermic and is associated with foaming and gas emissions.

Effect of temperature

The rate of Fenton reaction increase with increasing the temperature, with more effect pronounced at temperatures between 5°C and 20°C. As the temperature increases above 40-50°C the efficiency of H_2O_2 utilization decreases due to the accelerated decomposition of H_2O_2 into oxygen and water. Successive addition of H_2O_2 may be required when treating wastewater with high levels of contaminants in order to moderate the rise in temperature as the reaction proceeds.

PH effect

A low pH is important to keep ferric ion in solution. At a pH less that 3, Fe(III) is in the solution; at a pH greater than 3 and less than 5, Fe(III) is out of solution in colloidal form; and above pH 5, Fe(III) precipitates as $Fe_2O_3 \bullet H_2O$.

Chemical oxidation selectivity

Ultimately, the reagent's ability to destroy contaminate through an oxidation reaction depends on the radical's ability to attack the chemical structure sought for destruction. $OH^{\bullet}$ attack on aromatic compounds in an electrophlic substitution. Therefore, electron-withdrawing substitutuents slow down the reaction and electron -donating groups accelerate it.

Among the groups oxidized by the Fenton reagent are acids, alcohols, aldehydes, aromatics, amines, and dey. More-extension lists of chemicals that can and cannot be oxidized by the Fenton reagent are provided in table 3.3 (Bigda 1995). Most of the chemicals encountered in a typical contamination situation are oxidizable by this technique. In general, small and inexpensive bench-scale experiments are recommended to evaluate the efficiency of the reaction and to determine what kind of compounds, desired or undesired, are forming.

The most common application of Fenton reaction has been in an on-site reactor vessel either to treat an effluent stream from an industrial or chemical process or to treat contaminated medium. In general the procedure for the Fenton reaction involves

- Adjusting the pH of wastewater pH to 3-5
- Adding iron catalyst in an aqueous solution
- Adding the peroxide slowly

As the reaction proceeds, the pH declines, first at the point where the iron sulfate is added, and then a more-pronounced decline at the point where hydrogen peroxide is added. This occurs partly due to the fragmenting of organic material into organic acids. This pH change indicates that the reaction is proceeding as desired, and it is monitored as a sign of such progress

There are several advantage associated with carrying out the reaction in a vessel

- Better control over the chemical added with respect to mixing and minimizing wasted chemicals
- The ability to recycle the iron catalyst by redissolving and filtering the iron hydroxide sludge after neutralization, without the need for expensive regeneration.

The ability to use the effluent of the reaction vessel to preheat the feed (because the process is exothermic).

- The ability to pretreat the feed to possibly reduce its chemical oxygen demand (COD) and bacterial toxicity and thus enhancing the biodegradability of the effluents.

There are also several disadvantage associated with using a vessel. The fixed cost and the operating cost associated with such an assembly are higher than those of an in situ design. And, because different industrial locations have different contaminants, the ability to use identical units at several sites is limited.

A sharp and sudden increase in the rate of the reaction can occur due to the temperature increase and possible pressure build-up in a closed environment. Several factors might lead to this

1. A low initial temperature resulting in high activation energy. There is an initial slow reaction phase that is followed by strong reaction and as harp increased in temperature.
2. Any excess of hydrogen peroxide available, because of an inappropriate addition rate or high pH. This causes the iron salt to precipitate and may cause a runway condition to occur.

b) Photo-Fenton

The degradation rate of an organic pollutant by means of Fenton or Fenton-like is strongly enhanced by UV light irradiation with wavelength superior to 200 nm (photo-Fenton and photo-Fenton like process). Under these conditions, the photolysis allows the regeneration of the Fe^{+2} by means of Fe^{+3} complexes of (3.18) (Chen et al., 1997):

$$Fe(OH)^{2+} \xrightarrow{h\nu} Fe(II) + OH^{\bullet} \qquad (3.18)$$

Chamarro et al. (2001) used Fenton process for the degradation of phenol, 4-chlorophenol, 2,4-dichlorophenol and nitrobenzene. The stoichiometric coefficient for Fenton reaction was approximately 0.5 mol of organic compound/mol H_2O_2. The process was found to eliminate the toxic substances and increased the biodegradability of the treated water. Ormad et al., (2001) compared the degradation of a DCP solution by Fenton and photo-Fenton process: During Fenton reaction only a small abatement of DCP was observed, a 78% mineralization

was achieved by the photo-Fenton process (10 mM H_2O_2, Fe(II) 10 mg.L^{-1}, 36-W black light lamp). Recently Esplugas et al. (2002) have been studied the degradation of phenol by different oxidation processes including photo-Fenton. Fenton and photo-Fenton processes was found to be the more efficient for phenol degradation.

3.3.5.2 Ozonation (O_3)

The ozone is a powerful oxidizing agent; it is able to participate in a great number of reactions with organic and inorganic compound. Among the most common oxidizers, only hydroxyl and fluorine have oxidation potential more than the ozone. The principles disinfectant action of the ozone is known from century. However, it is in the last twenty years when this chemical agent has acquired a great importance in wastewater treatments. Thus, the ozonation can constitute a AOP's for itself, as hydroxyl radical coming from the decomposition of ozone which is catalyzed by hydroxyl ion or the initiated by the presence of traces of other substances, like transition metal cations (Beltrán et al., 1997a).

Indeed, in an ozonation process, it should be considered two possible pathway of oxidation. The direct pathway through the reaction between ozone and the dissolved compounds, and radical pathway through the reaction of radicals generated from ozone decomposition (hydroxyl radical) and dissolved compounds (Baraza, 2000). The combination of both pathways for elimination of compounds depends on the nature of the compounds, the pH of the medium and of the ozone dose. On one hand, the molecular ozone can react in a direct way with the dissolved pollutants by electrophilc attack of the major electronic positions of the molecule. This mechanisms predominate when the pollutant is very electophilic reagent, for example, phenols, and phenol derivatives. The reactions of the ozone with organic compound usually occurred by means of the ozonation of the double bond or in the nucliphy centre. (Non shard pair of electrons) obtaining aldehydes, acetone or carbonyls. The other mechanism, of indirect type, consists on the decomposition of the ozone to other secondary oxidants, mainly hydroxyl radical that react quickly with the pollutants. These mechanisms predominate, with low reactive molecules, such as hydrocarbons, benzene or chlorobenzene (Hoigne and Bader, 1979).

Together with the process of oxidation, the ozonization diminishes the colour and the turbidity, besides disinfecting the treated waters. Another important note is that the ozone is not very selective, for what can degrade and/or eliminate the pollutants.

The mechanism of the ozone decomposition in water is the following:

$$O_3 + H_2O \rightarrow HO_3^+ + OH^- \quad (3.19)$$

$$HO_3^+ + OH^- \leftrightarrow 2\,HO_2 \quad (3.20)$$

$$O_3 + HO_2 \rightarrow HO + 2\,O_2 \quad (3.21)$$

$$HO + HO_2 \rightarrow H_2O + O_2 \quad (3.22)$$

Numerous studies have been carried out on the reactivity of the ozone with diverse polluting substances and kinetic models of the ozonization reaction have settled down of diverse organic and inorganic compound (Hoigné and Bader, 1983 a and b).

The ozone treatment process can be supplemented with the use of ultraviolet radiation and/or hydrogen peroxide.

3.3.5.2.1. UV/ O_3 process

The ozonation constitutes of the AOP's that presents several advantages in front of conventional chemical oxidizing agents, as the chlorine or the chlorine dioxide. However, refractory compound as some saturated alcohol's, coloured compound, low molecular weight compound and carboxylic acids are difficult to degrade by means of ozonation, since both ozone reactions pathway are very weak. This is due to the low value of first order kinetic constant for the direct reaction ozone-pollutant and the insufficient hydroxyl radical concentration generated by decomposition of the ozone. Unless the pH of the means rises, what would imply the use of external basic agents. Therefore a bigger concentration of radical $OH^{\bullet}$ is needed (Beltrán et al., 1997a).

The treatment with ozone can also be enhanced by use of ultraviolet radiation (254 nm) to generate more hydroxyl radicals. The extinction coefficient of the O_3 at 254 nm is of 3300 $M^{-1}.cm^{-1}$, which is very superior that of the H_2O_2 (Andreozzi, 1999). If an effluent, which has dissolved ozone, is exposed to the UV radiation, photolysis takes place, by dissociation of O_2 molecule to oxygen atom in the state ^1D. This the last one can react with a molecule of water to produce hydrogen peroxide that in turn can be decomposed by photolysis or to react with the ozone. The global reaction that takes place is the following:

$$H_2O + O_3 \xrightarrow{hv} 2\,OH^{\bullet} + O_2 \quad (3.23)$$

Thus, this system contains three ways to produce OH radicals and/or to oxidize the pollutant for subsequent reactions: UV radiation, ozone and hydrogen peroxide. Considering that hydrogen peroxide photolysis is very slow compared with the rate at which ozone is decomposed by HO_2^- , it seems that a neutral pH reaction of ozone with HO_2^- is the main pathway. The mechanisms of radical production through over this process is presented in figure 3.2

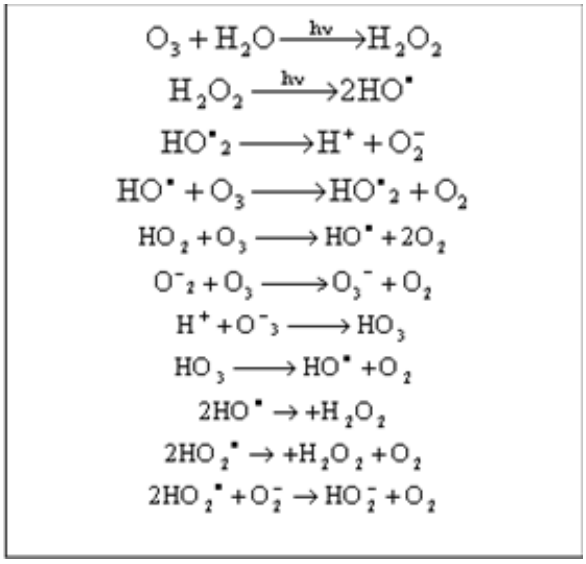

Figure 3.2: Mechanism of ozone radical reactions (Glaze et al., 1987)

3.3.5.2.2 H_2O_2 / O_3 process

Another way to increase the production of hydroxyl radical is combination of ozone with hydrogen peroxide. This combined system produces bigger conversion yields than the ozonation. It can be used in those cases that the direct reaction ozone-pollutant follows a slow kinetic regime. Hydrogen peroxide in water break-up and partially dissociated in the species of ionic (HO_2^-), which reacts with ozone causing the decomposition of the last giving a series of reactions. By that both radicals hydrogen peroxide and ozone participate in the reaction and degrade more effectively the existence organic (Adam et al., 1994). The global reaction that takes place is (3-26):

$$H_2O_2 + 2\,O_3 \rightarrow 2\,OH^{\bullet} + 3\,O_2 \qquad (3.26)$$

That has as initiation stage (3.27) (Staehelin and Hoigne, 1982):

$$HO_2^- + O_3 \rightarrow HO_2^\bullet + O_3^\bullet \qquad (3.27)$$

Because this system doesn't depend on the radiation transmission to activate the molecules of O_3 or H_2O_2, its biggest advantage is being able to work without problems in cloudy waters. The process H_2O_2/O_3 has been studied with several compounds, it gives bigger degradation rate. With several compounds it has been a gaussiana relationship, increased the degradation speed with the quantity of peroxide, until a point for which the reaction is inhibited, because the excess H_2O_2 consume radical hydroxyl in the reaction (3.28) (Chamarro et al, 1996):

$$H_2O_2 + OH^\bullet \rightarrow HO_2^\bullet + H_2O \qquad (3.28)$$

Paillard et al., (1988) studied the degradation of herbicides (s-triazina) found that the good relationship (mg of hydrogen peroxide/mg ozone) was around 0,5. Studies regarding DCP removal by the O_3/UV process (e.g. Trapido et al., 1997; Hautanemi et al., 1998; Kuo, 1999) have been studied the degradation of DCP by different ozone combination.

3.3.5.2.3.UV/H_2O_2 / O_3 process

Another possible alternative for the obtaining more hydroxyl radical is to combine the binary systems UV/ H_2O_2, O_3/UV and O_3/ H_2O_2, obtaining the tertiary system O_3/UV/ H_2O_2. This process is very potent and it allows a considerable reduction of the total carbon and/or quick mineralization of pollutants. It is the most effective treatment for highly polluted effluents. In accordance with the stiochiometry. Two ozone molecules eliminated by molecule of peroxide produce two hydroxyl radical according to:

$$2\,O_3 + H_2O_2 \xrightarrow{h\nu} 2\,OH^\bullet + 3\,O_2 \qquad (3.29)$$

Zeff and Barich (1990) studied the oxidation of different organic compound in water, as Methlyne chloride, chlorobenzene, benzene, toluene, ethilbenzen, trichloroethilen, etc by means of this system, and they proved that this method is more efficient than the treatment of

each treatment alone or in binary combinations. Mokrini et al., (1997) studied the effect of this combination in the phenol oxidation at different pHs. A 40% of TOC reduction was achieved by this method. With regard to DCP, no articles have been found in the literature about the oxidation of these compounds by means of this process.

3.3.5.2.4. O_3/UV/Fe process

The combination of ozone with light and iron as catalyst improves the oxidative capability of the catalytic ozonation O_3/Fe. Three process may account for this improvement of the efficiency of the process. On one hand, Fe(III) species undergo a photoredox process with UV and near-UV light, giving rise to Fe(II) and $OH^{\cdot}$ radicals according to equation 3-34 (Safarzadeh-Amiri et al., 1996; Mazellier et al., 1997):

$$Fe^{3+} \xrightarrow[H_2O]{h\nu} Fe^{2+} + OH^{\bullet} + H^{+} \qquad (3.30)$$

On the other hand, Fe(III) is considered to increase the number of hydroxyl radicals through the reduction of O_3 with the Fe^{2+} generated by the photoreduction of Fe^{3+} (Abe and Tanaka, 1999), similar to the mechanism proposed for the photo-Fenton reaction. The mechanism is quite unclear (Ruppert et al., 1994)

$$Fe^{2+} + O_3 \rightarrow FeO^{2+} + O_2 \qquad (3.31)$$

$$FeO^{2+} + H_2O \rightarrow Fe^{3+} + OH^{\bullet} + OH^{-} \qquad (3.32)$$

If hydrogen peroxide is present in the medium, directly or by ozone photolysis, it can react with Fe(II) by Fenton reaction (3335), regenerating Fe(III) and closing a loop mechanism Fe(III)/Fe(II) while hydroxyl radicals are generated.

$$Fe^{2+} + H_2O_2 \rightarrow Fe^{3+} + OH^{-} + OH^{\bullet} \qquad (3.33)$$

Besides this, the initial oxidation of organic pollutants generates oxygenated intermediates, e.g. intermediates with carboxylic functional groups, which can react with Fe(III) and form complexes. These complexes are also photoactive and produce CO_2, organic radicals and ferrous ions on irradiation, contributing to the mineralization of these pollutants without the participation of hydroxyl radicals (Safarzadeh-Amiri et al., 1996a; Abe and Tanaka, 1999).

$$RCO_2Fe(III) \xrightarrow{h\nu} R^{\bullet} + CO_2 + Fe(II) \qquad (3.34)$$

The addition of iron ion (Fe^{3+} or Fe^{2+}) has been reported to accelerate the UV-enhanced ozonation of several pollutants (Abe and Tanaka, 1997, 1999). Ruppert et al . (1994) studied the degradation of 4-chlorophenol solutions by means of different AOPs. The O_3/UV/Fe(II) was found to be the most effective method, achieving complete mineralization in few minutes. Complete mineralization of DCP among other chlorophenols was achieved also by O_3/UV/Fe(III) as reported by Abe and Tanaka (1997), where the effect of Fe(III) was found to depend on its concentration. Abe and Tanaka as well (1999) studied the effect of this combination with nitrophenols, attributing the main effect to the photodegradation of aliphatic intermediates by Fe(III) complex. The degradation of aniline and 4-chlorophenol has been studied by Sauleda and Brillas (2001) by means of O_3/UVA/Fe(II), reporting that both quickly mineralized by the O_3/UVA and O_3/UVA/Fe(II).

3.4. Biological treatment

With proper analysis and environmental control, almost all the wastewater can be treated biologically. Therefore, it is essential to understand the characteristics of each biological process to ensure that the proper environment is produced and controlled effectively

3.4.1. Objective of biological treatment

The general objectives of the biological treatment of wastewater are to coagulate, remove the nonsettleable colloidal solids and to stabilize the contained organic mater (Metcalf and Eddy, 1985). For domestic wastewater, the objective is simply reduce the organic content, and in many cases, the nutrients such as nitrogen and phosphorous. However, sometimes the removal of trace organic compounds that may be toxic is also an important treatment objective. In agricultural wastewater treatment, the objective is to remove the nutrients, specifically the nitrogen and phosphorous, that are capable to stimulating the growth of aquatic plants. Beside all of that, in industrial wastewater, the objective is to remove and reduce the concentration of organic and inorganic compound.

3.4.2. Role of microorganisms

The removal of carbonaceous BOD, the coagulation of nonsettleable colloidal solids, and the stabilization of organic matter are accomplished biologically using of microorganisms, principally bacteria. The microorganisms are used to convert the colloidal and dissolved

carbonaceous organic mater into various gases and into cell tissue. Because cell tissue has specific gravity slightly greater than that of water the resulting cells can be removed easily from treated liquid by gravity settling (Grady etal., 1980),

3.4.3. Introduction to microbial metabolism

Understanding of the biochemical activities of the important microorganisms is the basic information to design a biological treatment process. The two major topics considered here are (1) the general nutritional requirements of the microorganisms (2) the nature of microbial metabolism based on the need for molecular oxygen.

In order the microorganisms to reproduce and function properly an organisms must have (Benfield et al, 1980)

1) a sours of energy
2) carbon for synthesis of new cellular material
3) inorganic elements or nutrients

Organic nutrients (growth factor) may also be required for cell synthesis. Carbon and energy source usually referred to as substrate.

Two of the most common sources of cell carbon for microorganisms are organic matter and carbon dioxide. Organisms that use organic carbon for the formation of cell tissue are called heterotrophs. Organisms that derive cell carbon from carbon dioxide are called autotrophs.

The conversion of carbon dioxide to cell tissue is a reductive process that need net input of energy. The energy needed for cell synthesis may be supplied by light or by chemical oxidation reaction (phototrophs) (Eckenfekder et al., 1987).

The principal inorganic nutrients needed by microorganisms are nitrogen (N), sulphur(S), potassium (P), magnesium (Mg), calcium (Ca)… etc. In addition to these inorganic nutrients needed, organic nutrients may also be needed by some organisms.

3.4.4. Bacterial growth (Atkinson etal.,1974)

Effective environmental control in biological waste treatment is based on understand of the basic principle governing the growth of microorganisms. Bacteria can reproduce by binary fission, by a sexual mode or by budding. Generally, they reproduce by binary fission (i.e. by dividing, the original cell becomes two new organisms). The time required for each fission, which is termed the generation time, can vary from days to less than 20 min. For example, if

the generation time is 30 min, one bacteria would yield 16 777 216 bacteria after period of 12 h. This computed value is a hypothetical figure, for bacteria would not continue divide indefinitely because of various environmental limitations such as substrate concentration, nutrient concentration, or even system size.

Different growth rate can be used for bacterial growth like, growth in term of bacterial numbers, growth in term of bacterial mass and growth in mixed cultures.

To ensure that the microorganisms will grow, they must be allowed to remain in the system long enough to reproduce. This period depends on their growth rate, which is related directly to the rate at which the meatbolize or utilize the waste. Assuming that the environmental conditions are controlled properly. Controlling the growth rate of the microorganisms can ensure effective waste stabilization.

In both batch and continuous culture systems the rate of growth of bacterial cells can be define by the following relationship

$$r_g = \mu X \qquad (3.35)$$

Where r_g = rate of bacterial growth, gTVSS.L^{-1}.s^{-1}

μ = Specific growth rate, s^{-1}

X = concentration of microorganisms gTVSS

Because dX/dt= r_g for both culture the following relationship is also valid for batch reactor

$$dX/dt = \mu X \qquad (3.36)$$

In batch culture, if one of the essential requirements (substrate and nutrients) for growth were present in only limited amounts, it would be depleted first and growth would cease, in continuous culture, growth is limited. Experimentally it has been found that the effect of a limiting substrate or nutrient can often be defined adequately using the following expression proposed by Monod (1949)

$$\mu = \mu_m \frac{s}{k_s + s} \qquad (3.37)$$

Where μ= specific growth rate, s^{-1}

μ_m= maximum specific growth rate, s^{-1}

s=concentration of growth-limiting substrate in solution, g.L^{-1}

k_s=half velocity constant, substrate concentration at one-half the maximum growth rate, g.L^{-1}

If the value of μ is substituted in Eq (3-35), the resulting expression for the rate growth rate is

$$r_g = \frac{\mu_m Xs}{k_s + s} \qquad (3.38)$$

In both batch and continuous-growth culture systems, a portion of substrate is converted to new cell and a portion is oxidized to inorganic and organic en products. Because the quantity of the new cell produced has been observed to be reproducible for given substrate, the following relationship has been developed the rate of substrate utilization and the rate of growth.

$$r_g = -Yr_{su} \qquad (3.39)$$

Y= maximum yield coefficient, g/g (defined as the ratio of the mass of cell formed to the mass of substrate consumed).

r_{su} = Substrate utilization rate, $g.L^{-1}.S^{-1}$

On the bases of laboratory study, it has been concluded that yield depends on (1) the oxidation state of the carbon source and nutrient elements,(2) the degree of polymerization of the substrate,(3) pathways of the metabolisms,(4) the growth rate, and(5) various physical parameters of cultivation.

If the value of r_g from Eq. (3.37) substituted in Eq. (3.38), the rate of substrate utilization can be defined as follow:

$$r_{su} = -\frac{\mu_m XS}{Y(k_s + S)} \qquad (3.40)$$

In Eq. (3.40) the term μ_m / Y is often replaced by the term k, defined as the maximum rate of substrate utilization per unit mass of microorganisms :

$$k = \frac{\mu_m}{Y} \qquad (3.41)$$

If the term k is substituted for the term μ_m / Y in Eq (3.41), the resulting expression is

$$r_{su} = -\frac{kXS}{(k_s + S)} \qquad (3.42)$$

In bacteria systems used for wastewater treatment, the distribution of cell age is such that not all the cells in the system are in the log-growth phase. Consequently, the expression for the rate of growth must be corrected to account for the energy required for cell maintenance. Other factors, such as death and perdition, must also be considered. Usually, these factors are lumped together, and it is assumed that the decrease in cell mass caused by them is

proportional to the concentration of organisms present. This decrease is often identified in the literature as the endogenous decay. The endogenous decay term can be formulated as follows:

$$r_d \text{ (Endogenous decay)} = -k_d X \qquad (3.41)$$

Where k_d =endogenous decay coefficient, s^{-1}

When Eq (3.41) is combined with Eq (3.37) and (3.34), the following expression are obtained for the net rate of growth

$$r'_g = \frac{\mu_m XS}{K_S + S} - k_d X \qquad (3.43)$$
$$r'_g = -Yr_{su} - k_d X$$

Where r'_g = net rate of bacterial growth, $gTVSS.L^{-1}.s^{-1}$

The corresponding expression for the net specific growth rate is given by Eq (3.44), which is the same as the expression proposed by Van U (1967)

$$\mu' = \mu_m \frac{S}{K_s + S} - k_d \qquad (3.44)$$

Where μ' = net specific growth rate, s^{-1}

The effect of endogenous respiration on the net bacterial yield are accounted for by defining an observed yield as follow

$$Y_{OB} = \frac{r_g'}{r_{su}} \qquad (3.44)$$

so another way to write eq(3.46) is:

$$\mu' = Y_{OB}\mu_m \frac{S}{K_s + S} - k_d \qquad (3.47)$$

The temperature effect of the biological reaction-rate constant is very important in assessing the overall efficiency of a biological treatment process. Temperature not only influences the metabolism activities of the microbial population but also has and thoughtful effect on such factors as gas-transfer rates and settling characteristics of the biological solids. The effect of temperature on the reaction rate of a biological process is usually expressed in the form expressed by Eq(3.46). Some typical values of the θ for some commonly used biological processes are presented in table (3.4).

Table 3.4 Temperature activity coefficient for various biological treatment processes

	θ value	
Process	Range	Typical
Activated sludge	1.00-1.08	1.04
Aerated lagoons	1.04-1.10	1.08
Trickling filters	1.02-1.08	1.035

$$r_T = r_{20}\theta^{(T-20)} \qquad (3.48)$$

Where

r_T = reaction rate at T°

r_{20} = reaction rate at 20 °

θ = temperature activity coefficient

T = temperature in °C

3.4.5. Basic types of Bioreactors

There are two basic types of biological and chemical reactors:

- ✓ Continuous Stirred Tank Reactor (CSTR)
- ✓ Plug flow reactors.

CSTR are easily visualized as vessels or tanks that are stirred to achieve uniformity throughout the tank. A very important characteristic of the CSTR is that the concentration of the reactants in the outlet is equal to the concentration of the reactants in the vessel regardless of the concentration of the reactants in the inlet (Crosby et al., 1980).

Plug flow reactors can be modeled as a pipe where the reactants move as a plug along the pipe. The concentrations of the reactants will vary along the pipe and there is no mixing between the beginning and the end of the system. In bio- application different reactors configuration systems are available such as fluidized bed bioreactor system, packed bed bioreactor, air sparged fixed bed bioreactor and rotating media bioreactor.

Bioreactors can be operated in three ways:

Batch reactors: are simplest type of mode of reactor operation. In this mode, the reactor is filled with medium and the reaction is allowed to proceed. When the reaction has finished the contents are emptied for downstream processing. The reactor is then cleaned, re-filled, re-inoculated and the process starts again.

Continuous reactors: fresh media is continuously added and bioreactor fluid is continuously removed. As a result, cells continuously receive fresh medium and products and waste products and cells are continuously removed for processing. The reactor can thus be operated for long periods of time without having to be shut down. Continuous reactors can be many times more productive than batch reactors. This is partly due to the fact that the reactor does not have to be shut down as regularly and also the growth rate of the bacteria in the reactor that can be more easily controlled and optimized. In addition, cells can also be immobilized in continuous reactors, to prevent their removal and thus further increase the productivity of these reactors (Adams et al., 1974).

The fed batch reactor is the most common type of reactor used in industry. In this reactor, fresh media is continuous or sometimes periodically added to the bioreactor but unlike a continuous reactor, there is no continuous removal. The reactant is emptied or partially emptied when reactor is full or fermentation is finished. As with the continuous reactor, it is possible to achieve high productivities due to the fact that the growth rate of the cells can be optimized by controlling the flow rate of the feed entering the reactor.

Sequencing batch reactors:

The SBR process has widespread application where mechanical treatment of small wastewater flows is desired. Because it provides batch treatment, it is ideally suited for wide variations in flow rates. Furthermore, operation in the "fill and draw" mode prevents the "washout" of biological solids that often occurs with extended aeration systems.Another advantage of SBR systems is that they require less operator attention and produce a very high quality effluent (Arora et al., 1987).

The SBR process operates on a fill and draw batch system (Buitron et al., 2001) wherein the reactor acts as a biological reactor and settling tank at various stages of the treatment cycle (see figure 3.3). Wastewater may be accumulated in a batch and then delivered to a reaction tank (s) which contains activated sludge. The batch is subject to biological treatment for a prescribed period of time with both anoxic and aerobic cycles possible. At the end of the reaction period, the batch is allowed to settle, after which the clarified treated effluent is decanted from the top of the tank. The sludge remains in the tank to provide the biological population for the subsequent cycle. Excess biomass is pumped on a regular basis to a sludge holding tank for digestion and disposal.

The various stages in the SBR sequence are:

Stage 1: Filling

During this stage the SBR Tank is filled with the influent wastewater. In order to maintain suitable F/M (food to microorganism) ratios, the wastewater should be admitted into the tank in a rapid, controlled manner. This method functions similarly to a selector, which encourages the growth of certain microorganisms with better settling characteristics

Stage 2: Reaction

This stage involves the utilization of biochemical oxygen demand (BOD) and ammonia nitrogen, where applicable, by microorganisms. The length of the aeration period and the sludge mass determines the degree of treatment. The length of the aeration period depends on the strength of the wastewater and the degree of nitrification (conversion of the ammonia to a less toxic form of nitrate or nitrite) provided for in the treatment.

Stage 3: Settling

During this stage, aeration is stopped and the sludge settles leaving clear, treated effluent above the sludge blanket. Duration for settling varies from 45 to 60 minutes depending on the number of cycles per day.

Stage 4: Decanting

At this stage of the process effluent is removed from the tank through the decanter, without disturbing the settled sludge.

Stage 5: Idle

The SBR tank waits idle until a batch accumulates and it is time to start a new cycle with the filling stage.

Stage 6: Sludge Wasting

Excess activated sludge is wasted periodically during the SBR operation. As with any activated sludge treatment process, sludge wasting is the main control of the effluent quality and microorganism population size. This is how the operator exerts control over the effluent quality by adjusting the mixed liquor suspended solids (MLSS) concentration and the Mean Cell Residence Time (MCRT).

In this process, the SBR tank acts as the equivalent of several components in the conventional activated sludge treatment process, as follows:

1. *Aeration Tank:* the SBR tank acts as an aeration tank during the reaction stage where the activated sludge is mixed with the influent under aerated conditions.
2. *Secondary Clarifier:* the SBR tank acts as a secondary clarifier during the settling and

decanting stages where the mixed liquor is allowed to settle under quiescent conditions, and the overflow is discharged to the next stage of treatment.
3. *Sludge Return System:* the activated sludge, following settling in the SBR tank, is mixed with the influent similar to the sludge return system, except that the feed is transferred to the sludge rather than the sludge being transferred to the front end of the plant.

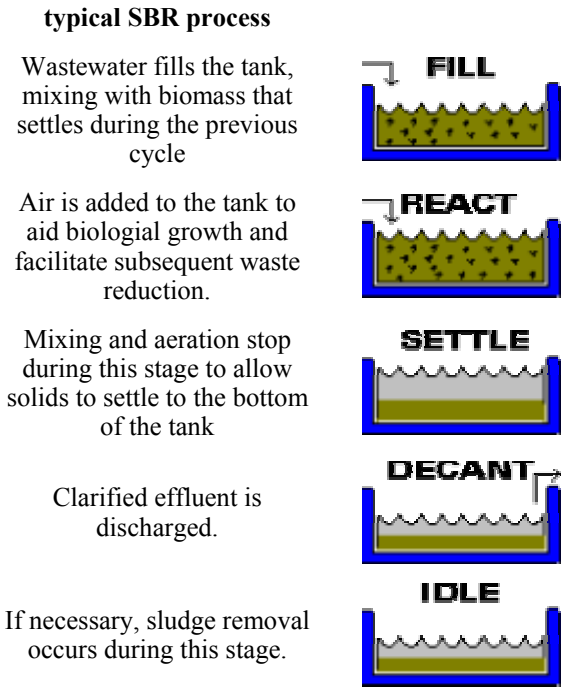

Figure 3.3: SBR process operation steps:

3.5. Combined AOP's with Biological treatment

As commented before, biological treatment of wastewater, groundwater, and aqueous hazardous wastes is often the most economical alternative when compared with other treatment options. The ability of a compound to undergo biological degradation is dependent on a variety of factors, such as concentration, chemical structure and substituents of the target compound. The pH or the presence of inhibitory compounds can also affect the biological degradation. Although many organic molecules are readily degraded, many other synthetic and naturally occurring organic molecules are biorecalcitrant (Adams et al., 1994).

Treatment process of any type of wastewater depends on the characteristics of water itself. Figure 3.4 presents a strategy that can be followed in treatment of different types of water. Accordingly, water can be classified into three categories; biodegradable, hardly biodegradable and non-biodegradable wastewater.

Biodegradable wastewater is one of the most easily waste (green line figure 3.4), it can be treated directly in biological process. This aspect is interesting from an economic point of view, since the costs of having immobilised and operation of a biological process is much smaller (Scott and Ollis, 1994; Marco et al., 1997). Investments costs for biological processes range from 5 to 20 times less than chemical ones such as ozone or hydrogen peroxide, while treatment costs range from 3 to 10 times less (Scott and Ollis, 1996; Marco et al., 1997 and Mathews et al 1991).

For hardy biodegradable wastewater (yellow line) there are two alternatives, the selection of any of these alternatives depends on wastewater characteristics. Wastewater that contain high level of organic matter can be diverted first to biological treatment to eliminate all the biodegradable compound and then to chemical process. In second stage chemical process bio-recalcitrant waste can be totally minerlized or it can be oxidized into smaller by-product which are more biodegradable and then recycled to biological process to finalize the treatment.

With respect to non-biodegradable wastewater (red line), a potentially viable solution is the integration of chemical and biological treatment processes (Gilbert, 1987; Heinzle et al., 1995; Marco et al., 1997; Ledakowicz, 1998; Beltrán et al., 2000b). In the first process the toxic and/or non-biodegradable compounds would be eliminated until the point where no longer inhibition due to their toxicity and/or the non-biodegradability, This can be achieved by organic compound oxidation all over the chemical process. In order to be able to combine chemical process outlet with biological process, it is necessary to determine the variation of biodegradability as a function of the chemical reaction. Once the solution biodegradability improved it can be feed to biological treatment, else more oxidation may needed. In the last years the study has been increased in this area. It is necessary to mention as examples the effect of the AOP's in the biodegradability of organic compound (Takahashi et al.,1994) different AOP's were combined with a biological process for the treatment of textile effluents (Ledakowicz and Gonera, 1999).

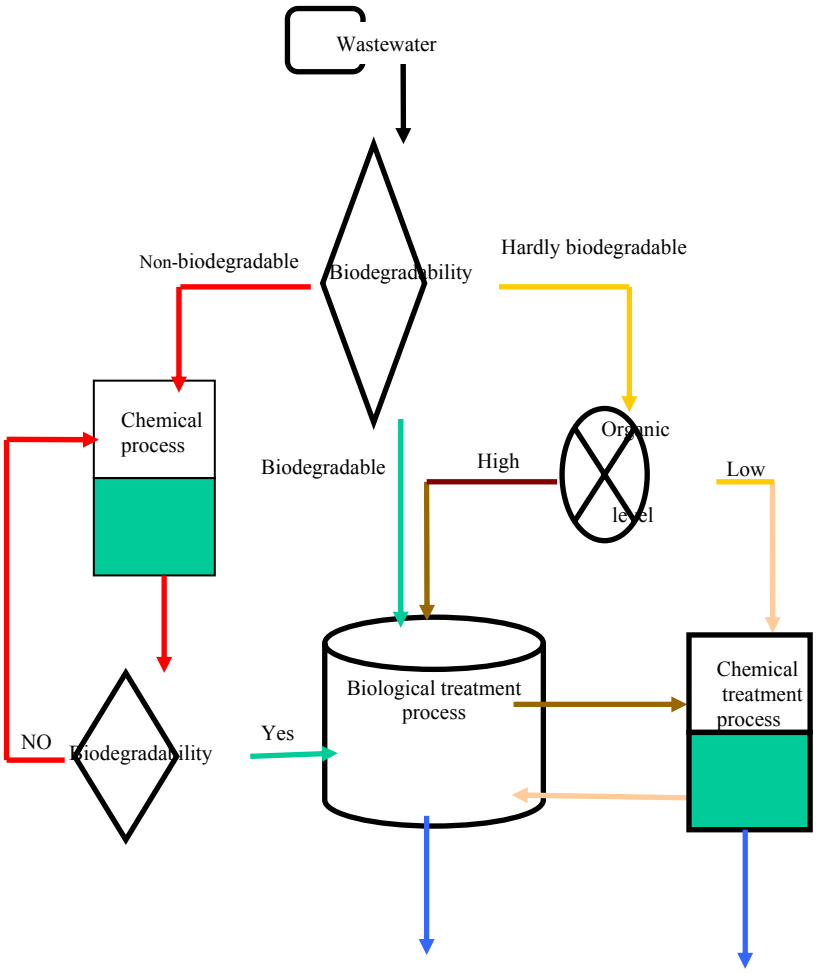

Figure 3.4: strategy for Wastewater treatment processing.

4. Studied compounds

4.1. phenol (POH):

Among the organic chemical contaminants, phenolic compounds are the objects of big interest in the preservation of the environmental medium. Phenol (POH) has been chosen in this study as a model compound; as results of its hard biodegradation ability via conventional treatment processes. Also it has simple molecular structure that permits a follow-up easy to aqueous solution, making it one of most common contaminants found in many industrial wastewater La Grega et al. (1994) .

4.1.1. Source and utilization

Phenol is produced through both natural and anthropogenic processes. It is naturally occurring in some foods, in human and animal wastes, and in decomposing organic material, and it is produced endogenously in the gut from the metabolism of aromatic amino acids.

The phenol exists either free or in a composed form. It is obtained from coal tar and is widely used as a disinfectant for industrial and medical applications (US, EPA (2002). As reason of its wide utilization, phenol exist in sewage of several industrial plants, (plant of coke, plant of wood and low temperature carbonization). It also serves as a chemical intermediate for manufacture of nylon 6-resins, antioxidant, medicines, ink, paints, herbicides, as well as other man-made fibers epoxy, phenolic resins and petroleum solvents (Alnaizy et al. (2000),. Approximately half of the U.S. consumption is directly related to the housing and construction industries, in applications such as germicidal paints and slimicides.

Phenol is present in the atmosphere as an emission from motor vehicles and as a photooxidation product of benzene. Moreover, phenol can be extract from the hydrolysis of lignine. It is also a product of human organism metabolism, it exists in urine with a concentration of 40 $mg.L^{-1}$.

By its germicide action, the phenol has been used during several times like disinfectant (in spray form), but the corrosive or harm effects on skin and mucous, limit its utilization as pharmaceutical product. Above the earlier industries, the major

consumption of phenol is through the production of phenol-formaldehyde resins and manufacturing of e-caprolactame.

4.1.2. Properties and features

Phenol (C_6H_5OH) is a strong transparent of unpleasant odour compound. It has crystal shape, very soluble in water at ambient temperature and in several organic solvents (aromatic hydrocarbons, alcohols, ethers, acidic hydrocarbons halogeneses). It has low solubility in hydrocarbon aliphatics. It can form salts with the strong bases, called phenoxides. The major part of these salts is especially soluble in water those of the sodium or potassium. The OH group transmits a big reactivity to grouping phenyle what encourages substitution reactions mainly in positions «ortho» and «para».

The main physical and chemical properties of the phenol, are represented in table.4.1

Table 4.1:Physical and chemical properties of phenol

Properties	Value
Description	Colorless to light pink solid
Molecular weight ($g.mol^{-1}$)	94.11
Boiling point (ºC)	181.91
Fusion point (melting) (ºC)	40.6
Density ($g.cm^{-3}$)	1.092 at 0 ºC 1.071at 20 ºC 1.050 at 50 ºC
PH	4.5 – 6
PKa (in water)	$1.28.10^{-10}$
Molecular formula	C 6 H 5 OH
Vapor pressure	0.3513 torr at 25° C
Odor	*threshold* 40 ppb (150 $mg.m^{-3}$) (Amoore and Hautala, 1983)
Solubility	86,000 ppm in water, very soluble in alcohol, carbon tetrachloride, acetic acid and liquid sulfur dioxide; soluble in chloroform, ethyl ether, carbon disulfide; slightly soluble in benzene
Henry's Law Constant	3.97 x 10 -7 atm. $m^3.mol^{-1}$ (25 °C)

4.1.3. Effects of phenol

Phenol is a very corrosive poison that absorbs by contact with skin, by inhalation or by ingestion. Ochronosis, or discoloration of the skin, and other dermatological disorders may result from dermal phenol exposure (Ohtsuji and Ikeda (1972)). Phenol poisoning is associated with headache, fainting, vertigo, and mental disturbances.

Phenol is toxic to bacteria and fungi, and it is used as a slimicide and disinfectant. Because of its anesthetic effects, phenol is used in medicines such as ointments, ear and nose drops, cold sore otions, throat lozenges and sprays (such as those sold under the Cepastat and Chloraseptic labels) and antiseptic lotions. The greatest potential source of exposure to phenol is in the occupational setting, where phenol is used in manufacturing processes (Ogata et al.,1986) . People are also exposed via consumer products, such as medicines and lotions, and some foods and tobacco smoke.

Phenol is readily absorbed by the inhalation, oral and dermal routes. The portal-of-entry metabolism for the inhalation and oral routes appears to be extensive and involves sulfate and glucuronide conjugation and, to a lesser extent, oxidation. Once absorbed, phenol is widely distributed in the body, although the levels in the lung, liver, and kidney are often reported as being higher than in other tissues (on a per-gram-tissue basis).

4.2. Chlorophenols

4.2.1. Source and utilization

Some chlorophenols are used as pesticides. Others are used in antiseptics. Small amounts are produced when water is disinfected with chlorine. They are also produced while bleaching wood pulp with chlorine to make paper. They have obtained notoriety as hazardous substances, because most of them are toxic and present long persistence in the environment. Laboratory studies carried out with animals showed that they developed liver and immune system effects.

High levels of chlorophenols given to pregnant female rats in their drinking water reduced the number of babies they had, and caused low birth weights (ATSDR, 1999).The presence of these substances has been detected in surface and ground waters (Howard, 1989). In Table 4.2, data related to the presence of these substances in different industrial and municipal effluents is presented.

Table 4.2. Concentration of chlorophenolic compounds in different effluents (Howard, 1989)

Industry	Concentration of 2-chlorophenol ($\mu g.L^{-1}$)	Concentration of 2,4,6-trichlorophenol ($\mu g.L^{-1}$)
Secondary sewage effluent	1.7	-
Herbicide production waste	2.88	-
Leather tanning and finishing	-	2200 – 5900
Foundries	-	240 – 1400
Aluminium forming	-	260 – 1800

Table 4.3 presents the solubility of some of these compounds, which will determine its presence in different types of water. As it can be observed, they are in general readily soluble in water.

Table 4.2 Solubility of some chlorophenols in water (Ullmann's, 1991)

Compound	Solubility at 20ºC ($g.L^{-1}$)
2-Chlorophenol	28.5
3-Chlorophenol	26.0
4-Chlorophenol	27.1
2,4-Chlorophenol	4.5
2,4,6-Trichlorophenol	0.8
Pentachlorophenol	0.014

4.2.2. Toxicity

In chlorophenol production, irritation symptoms of nose, eyes, respiratory tract, and skin resulting in chloroacne have been observed. The results of epidemiology studies on the long-term effects of chlorophenols are quite contradictory and have not allowed the experts to reach any firm conclusions (Mark et al, 1992).

The substance can be absorbed into the body by inhalation of its aerosol, through the skin and by ingestion (see International Chemical Safety Cards). TLV (Threshold Limit Value) has not been established. Lethal dose (LD_{50}) for rats has been found to be 580 $mg.kg^{-1}$ (oral) and 1730 $mg.kg^{-1}$ (percutaneous). Insuffiicent data are available on the effect of this substance on human health. Increasing attention is devoted at the present time to the risks of 2,4-dichlorophenol in relation to skin adsorption under the EPA's testing program for high-production-volume chemicals. EPA recommends that drinking water contain no more than 0.03 $mg.L^{-1}$.

4.2.3. Environmental considerations of chlorophenols (Ullmann's, 1991)

Chlorophenols constitute a group of organic substances that are introduced into the environment as a result of quite a lot of actions, such as waste incineration, uncontrolled use of wood preservatives, pesticides, fungicides and herbicides, etc, as well as by-products formed during bleaching of pulp with chlorine and in the disinfection by chlorination to get drinking water (Ahlborg and Thunberg, 1980).

All chlorophenol possess bactericidal activities that increase with the degree of chlorination. Chlorophenols are highly toxic to algae. Most of plants are very sensitive to the phytotoxicity of chlorophenols. As for aquatic organisms, fish and other aquatic organisms absorb chlorophenols through their gills, gastrointestinal tract or skin. The EPA recommends that a maximum average 2,4-dichlorophenol concentration in surface waters not exceed 2.02 $mg.L^{-1}$.

Chlorophenols may be present in the aquatic environment in many forms. They may be dissolved in free or complexed form, adsorbed on suspended inert solid or benthic sediments, or carried in biological tissues. Volatilization transfers the chlorophenol from the water to the air but does not otherwise affect it. Biodegradation is the principal means by which chlorophenols are removed. It must be induced because the antimicrobial activities of these products require that the bacteria adapt.

4.2.4. Chemical properties (Ullmann's, 1991)

Chlorophenols are versatile intermediates in chemical syntheses because both the hydroxyl group and the aromatic ring can react by both electrophilic and nucleophilic substitution.

Electrophilic substitution is favored by the presence of chlorine atoms on the aromatic nucleus. Nucleophilic substitution for one or more of the chlorine atoms, although disfavored by the presence of the other chlorine atoms, nevertheless it is widely used, for example to prepare various substituted diphenyl ethers, which serve as efficient herbicides.

4.3. 2,4-Dichlorophenol (DCP)

4.3.1. Source and utilization

2,4-Dichlorophenol (DCP) is used in manufacturing of 2,4-dichlorophenoxyacetic acid (2,4-D) and 2-(2,4-dichlorophenoxy) propionic acid (2,4-DP). Industrially, DCP can be obtained by chlorinating phenol, *p*-chlorophenol, *o*-chlorophenol, or a mixture of these compounds in cast-iron reactors.

4.3.2. Physical properties.

DCP is solid at ambient temperature (colourless crystals) and has a strong characteristic odor. It is slightly soluble in water, but highly soluble in alcohols. Some physical properties of DCP are presented in Table 1.8.

4.3.3.Uses

As it has been commented above, the main use of 2,4-dichlorophenol is as a key intermediate in the synthesis of chloride-based herbicides, such as 2,4-dichlorophenoxyacetic acid (2,4-D) and 2-(2,4-dichlorophenoxy)propionic acid (2,4-DP). It is also found in the selective postemergence herbicide (applied between the emergence of a seedling and the maturity of a crop plant), diclofop-methyl and as a selective preemergence herbicide (used before emergence of seedling above ground).

Table 1.8. Physical properties of 2,4-dichlorophenol (Ullmann's, 1991)

Physical property	Value
Melting point	45ºC
Boiling point	
at 101 kPa	210.9ºC
at 13 kPa	146ºC
at 0,13 kPa	53ºC
Density (50ºC)	1.388 $g.mL^{-1}$
Vapor Pressure (53ºC)	133 kPa
Specific heat (20ºC)	190 $J.mol^{-1}.K^{-1}$
Viscosity (50ºC)	2.65 mPa.s
Solubility in water (20ºC)	4.5 $g.L^{-1}$
Flash point (closed cup)	113ºC

4.4. Dyes:

4.4.1. Utilization :

Dyes constitute a group of organic substances that use in different coloring processing; azoic dyes are the largest chemical class of dyes used regularly for textile and paper printing dyeing (Philippe et al. 1998). Since they are persistent and highly soluble in water, reactive dyes are the most important groups in cellulose dyeing (cotton, polyesters). Other dyes with different characteristic are used for other type of applications; Acid dyes are commonly used in dying polyamide fibers (Nylanthrene dyes are ideally suited to polyamide 6 or 6.6. dyeing).

4.4.2.Environmental considerations of dye pollution

Dyes are introduced into the environment as a result of several man-made activities. Nowadays, there are more than 5000 commercial dye products, most of these dyes used in textile industry. Thus, this industry is considered as one of the major resource of highly polluted wastewater (Brown et al. (19939)). Fixation rate of a specific dye may vary according to functional groups used to fabricate such a kind of dye. In general more than 40% of initial dye mass remain in the dye bath, and hence its wastewater highly contaminated (Galindo et al., 2001).

Modern commercial dyes are very stabile in water solution and they contain high composition ratio of aromatic rings. Thus, it was believed that theses dyes molecule are non-biodegradable and some of them are toxic to bacteria, Some studies using activated sludge suggest that bio-transformation is slow for water-soluble dyes (yoo et al., 2002). Reactive dyes have been reported to go through the biological treatment systems with out being removed (Hu et al., 1999)

5. Objectives

As it was mentioned in the introduction, the high cost derived from the use of AOP can make attractive the possibility of coupling AOP with a biological treatment. In case of low biodegradable compounds, the oxidation of organic compounds by AOPs usually produces oxygenated organic products and low molecular weight acids that are more biodegradable. With toxic compounds, the AOP would be extended until the point that no inhibition due to toxicity was observed.

As presented in the previous section (section 4), phenol, DCP and dyes wastewater constitute a risk to human health and produce a public concern. Phenol and DCP were chosen in this study as a model compound; because of their high toxicity for bacterial population in biological treatment processes and due to their wide presence in different types of industrial wastewater. Moreover. environmental pollution by textile dyes also set a severe ecological problem which is increased by the fact that most of them and their by products are difficult to discolor using standard biological methods (Yoo et al., 2002, Lopez et al., 2002).

Based on all that, three general objectives motivate this work;

- To study the possibility of using the advanced oxidation process (AOP's), based on photo-oxidation, for the treatment of low biodegradable and/or toxic compounds, which cannot be treated by a conventional biological treatment.
- To examine the biodegradation of these target compound after being photo-treated.
- To explore the effect of VUV and UV light in colour removal of textile dyes and textile wastewater, in addition to biodegradability development of the pre-treated solutions

To achieve these objectives, it has been considered convenient

- ✓ To study the effect of degradation and mineralization rate of phenol and DCP by means of photo-oxidation process. In fact, this goal was performed in two parts:

1. Photo-oxidation based on UV light. During this part the following processes were studied, direct UV photolysis, UV combined with hydrogen peroxide (UV/H_2O_2), UV combined with ferric ion (UV/Fe(III)), Fenton reaction , Fenton like and photo-Fenton

2. Photo-oxidation based on UVA light. This part was carried out via two reactors; single lamp photo-reactor and multi lamps photo-reactor. Again during this part the following processes were studied in each reactor: UVA photolysis, UVA combined with hydrogen peroxide (UVA/H_2O_2), UVA combined with ferric ion (UVA/Fe(III)) and photo- Fenton.

- ✓ To explore the effect of these AOPs on the biodegradability enhancement of phenol and DCP aqueous solutions. All over this part, BOD_n, BOD_n/COD and BOD_n/TOC ratios were used as biodegradability indicators.

- ✓ To try to identify the main intermediates produced in the oxidation of these solutions, trying to relate the present intermediates with changes in the biodegradability of the solutions.

- ✓ To follow the change in oxidation state all over the previous processes and relates the change in oxidation state to biodegradability enhancement.

In the second part of this work ***biological process*** were studied. For this biodegradation part, it was decided to select photo-Fenton pre-treated solution to feed the bioreactor, because these solution give the highest biodegradability under small initial reactant concentration and short irradiation time.

Phenol is consider as a weak biodegradable contaminates. Thus, its biodegradation were performed in two batch bio- reactors:

I. Single biological treatment of direct phenol bio-oxidation.
II. Coupled biological treatment process including, phenol pre-treated by photo-Fenton followed by biodegradation.

The specific objectives of this part were:

- ✓ To study the aerobic biological degradation for phenol and phenol pre-treated solutions.
- ✓ To compare between single and coupled biological treatment processes in bio-oxidation efficiency.
- ✓ To check biodegradation kinetics and investigate the effect of pre-treatment step in kinetic parameters improvements

With respect to DCP, the direct biodegradation was not possible, so the study was performed only at pre-treated solution. Two different reactors were used;

I. Non acclimated activated sludge bioreactor .
II. Acclimated sludge bio-reactor with the sludge previously acclimated to phenol solution

Moreover, a full coupled chemical- biological process was performed for DCP biodegradation. T***he coupled process consist of photo-Fenton carried out multi lamps photo -reactor and sequencing batch bio.reactors (SBR)***. in this part, two type of biodegradation were checked up: aerobic and anaerobic treatment.

The specific objectives were:

- ✓ To examine the difference between biodegradation of DCP pre-treated solution in acclimated and non-acclimated biological process.
- ✓ To study DCP pre-treated solution biodegradation in aerobic and anaerobic SBR, and to compare between the two processes.
- ✓ To study the effect of pre-treated solution biodegradability change in biological reactor performance.

6. Equipments and reactants

6.1 Equipments

Photo-reactors

The Photo-oxidation processes were carried out in four different photo-reactors;

- **Reactor 1: Tubular photo-reactor:**

The first experimental series of photo-oxidation processes were performed in tubular photo reactor whose scheme is shown in figure (5.1).

The reactor equipped with:

1. 5 L liquid reservoir
2. Four germicides low-pressure mercury lamps, placed parallel to the reactor axis (see figure 5.2). The lamps nominal power is 15 W each (60 W in total), and emit radiation basically at 253.7 nm.
3. Reflectors: Low-pressure mercury lamps are a rounded with one quarter cylinder cross section reflectors (see figure 5.2)
4. The reaction zone: Consists of a cylindrical quarts tube 100 cm in longitude with an exterior diameter of 2.2 cm and an interior parameter of 1.85 cm. It is mounted within quartz tube with a diameter of 5.0 cm. Air circulating in the tubular space between the two tubes for cooling.
5. recirculating pump primate fluid circulation at different flow rate.

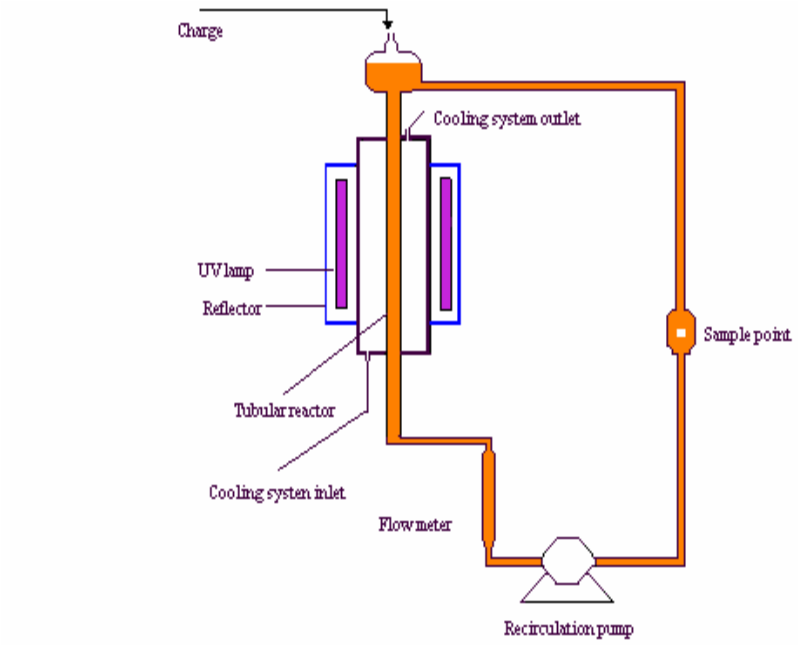

Figure (5.1 a) Tubular Photo- reactor

Figure (5.1b) Tubular photo- reactor

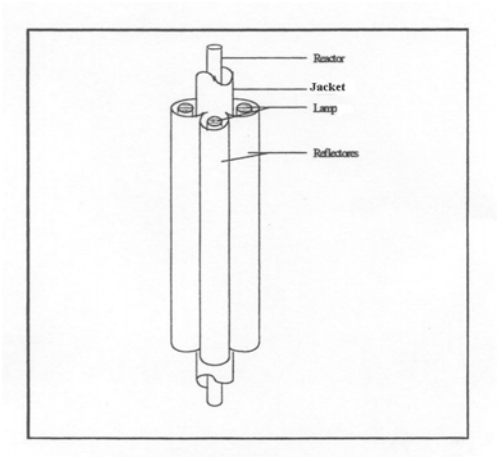

Figure (5.2) low-pressure mercury lamps and reflector configuration in photo-reactor

- **Reactor 2 : Single lamp stirred tank photo-reactor:**

This reactor consist of:

1. A jacketed thermostatic 1.5L stirred tank (figure 5.3).
2. Blackblue lamp with nominal power of 4 W emits radiation at 350 nm. The lamp placed in tank center
3. Magnetic stirrer that provides good mixing inside the reactor.

4. Thermostatic bath (Haake C-40) for temperature control inside the reactor.
5. Feeding and purging pumps
6. Neutralizing tank.

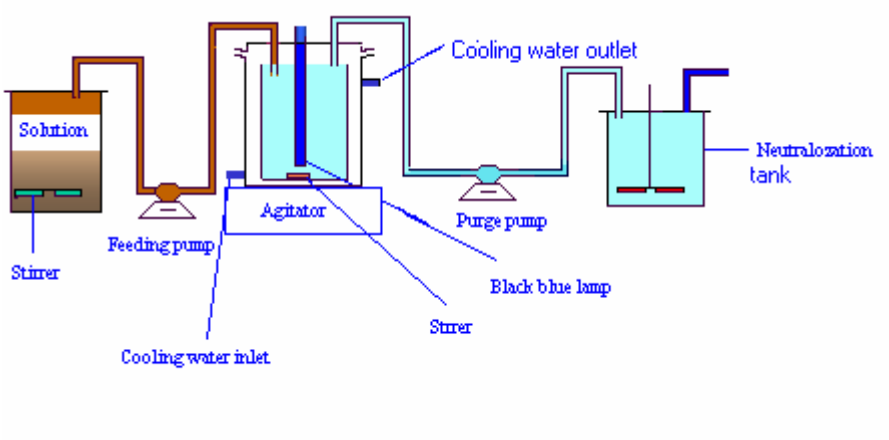

Figure 5.3; Single lamp stirred tank photo-reactors .

- **Reactor 3: Multi lamps stirred tank photo-reactor:**

This reactor equipped with :

1. A jacketed thermostatic 2L stirred tank (figure 5.4)
2. Three blackblue lamp with nominal power is 8W each (24W in total) placed in triangular configuration inside the reactor, these lamps emit radiation at wavelength of 360 nm.
3. Magnetic stirrer that provides good mixing inside the reactor
4. The same thermostatic bath (Haake C-40) was used to control the temperature inside the reactor
5. Feeding and purging pumps
6. Neutralizing tank.

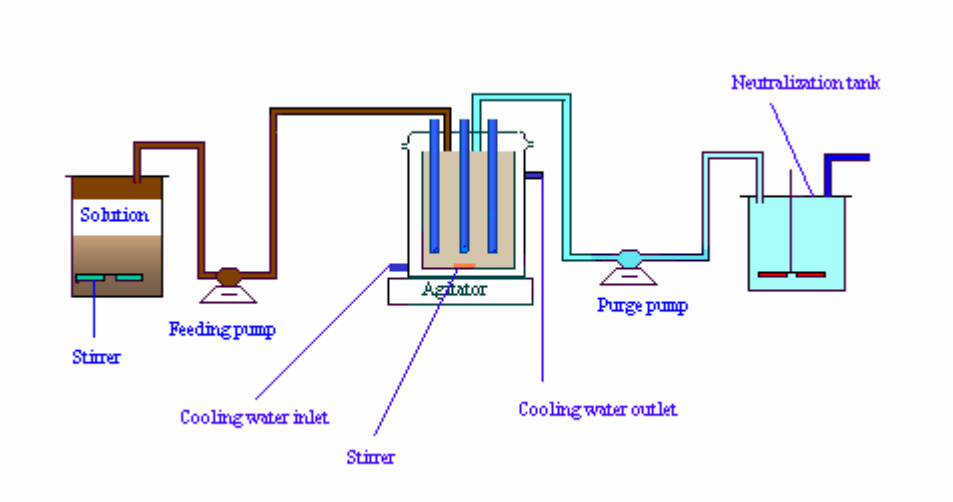

Figure 5.4: multi lamp stirred tank photo-reactors .

Experimental procedure:

In all the three previous reactors the same procedure was followed to perform the experiments

The procedure was as follow:

- Preparation of phenol or DCP solutions by dissolving the weighted quantity of solid phenol or DCP in water.
- When necessary, the required quantity of the catalyst Fe(II) or Fe(III) was added to the solution and mixed perfectly to assure the dissolution of all particle and got a homogenous solution.
- Prepare the needed quantity of hydrogen peroxide (H_2O_2).
- Calibrate the pH meter.
- When needed, adjust the pH of the solution
- Charge the reactor with the treated solution.
- Switch on mixing or liquid circulation (a recirculation flow rate at reactor 1 was 100L/h).
- After several time of mixing or liquid circulation, take the initial sample (sample at time zero).
- Switch on the cooling.
- Add the quantity of hydrogen peroxide (H_2O_2) to the reactor, and switch on the UV light source at the same time.

- Take samples at different time intervals, tests it for H_2O_2 consumption and quenched with sodium hydrogen sulphite to avoid further reactions. The samples were used later for analysis.
- clean the reactor

Reactor 4: Tubular photo-reactor :

Dyes photolysis were carried out in annular 2 L photo-reactor (figure 5.5). The reactor consist of:

1. Irradiated volume of 420 mL.
2. Reaction zone consists of a cylindrical quartz tube, 85cm in length, 1.5 cm external diameter and 5.5 mm irradiation thickness.
3. Low pressure mercury lamp (Pen Ray UV-P) surrounded with a quartz tube. The lamp with nominal power of 120W emit irradiation principally at 253.7 and 184.9nm (VUV).
4. recirculation pump that re-circulates liquid through the radiation zone.
5. online temperature and pH measurement

In this reactor two type of quartz can be used; Suprasil qurtz and Infrasil quartz. In fact, the change in quartz type is useful to move from VUV to UV irradiation. Infrasil quartz are know to prevents VUV irradiation (184.9 nm) to reach the reaction zone. Thus using this quartz leads to only UV photolysis.

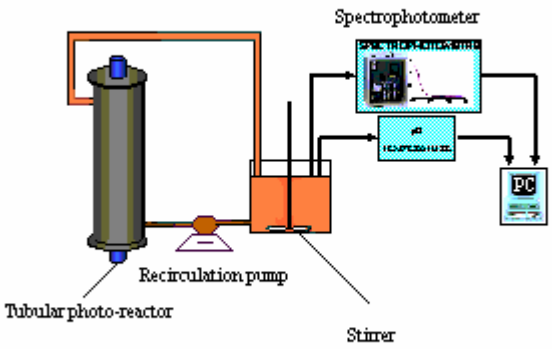

Figure 5.5: Tubular photo-reactor.

The experimental procedure was as follows:

- Dye solutions were prepared at the required concentration (100 $mg.L^{-1}$) by dissolving the weighted quantity of solid dye in water.
- Calibrate the PH meter.
- Measure initial pH, conductivity and absorbance for all dyes at time zero.
- Charge the reactor with the water solution (1L), circulate water through the reactor and switch on the UV lamp for 15 min (15 min is the time needed for Pen Ray UV-lamp to reach steady energy output).
- After 15 min water was removed and the reactor was charged with dye solution and start timing.
- Dye was circulated via centrifugal pump at a recirculation rate 180$L.h^{-1}$.
- Samples were with drown at different time intervals
- When almost all the color was eliminated the reaction stopped.
- Clean the reactor
- Samples were used later for absorbance, COD, BOD and inhibition test analysis.

Biological reactors:

Stirred tank bioreactor

Aerobic biological oxidation experiments were completed in 1.5L stirred tank reactors (figure 5.6). The reactor equipped with air diffuser at which an airflow rate of 100 Lh^{-1} was continuously supplied and distributed uniformly all over the reactor, also it supply with agitator that make the solution inside the reactor homogenous. Biomass used is activated sludge from municipal wastewater treatment plant at Gava (Barcelona, Spain).

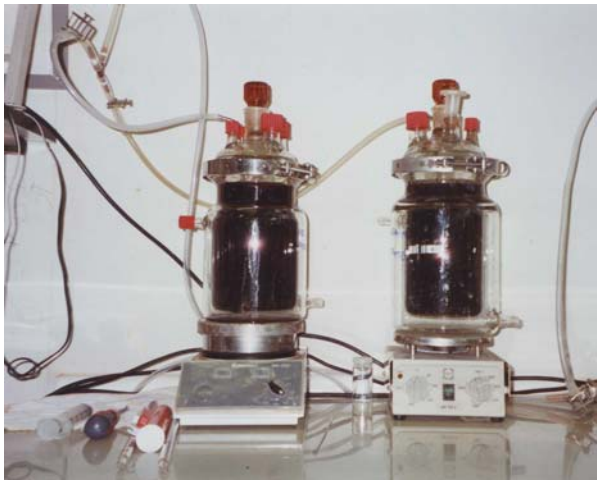

Figure 5.6 biological stirred tank reactors

Experimental procedure.

For both phenol and DCP bio-oxidation almost the same procedure was used, so in this section only DCP bioreactor will be presented,

1. Acclimated- reactor

   In this reactor it was used biomass acclimated previously to phenol solution. When choosing phenol it was thought that its chemical structure more or less similar to the possible DCP intermediates produced from photo-Fenton reaction. To start-up this reactor the following steps was followed:

   The reactor was operated at semi-continues mode

   ⊕ The reactor was initially charged with the following mixture:
   - 400 mL of biomass from a municipal waste water treatment plant (Gavà, Barcelona)
   - 250 mL of a 100 $g.L^{-1}$ phenol solution
   - 850 mL of municipal waste water
   - macronutrients (3 mL of NH_4Cl solution, 3 mL of $CaCl_2$ solution, 3 mL of $FeCl_3$ solution, 3 mL of $MgSO_4$ solution and 9 mL of phosphate buffer solution).

   For the first time, HRT was fixed at10 days. Based on that, determined volume has to be taken out from the reactor and fed with fresh solution daily:

   $$q = \frac{V}{HRT} = \frac{1500\,mL}{10\,days} = 150\,mL.day^{-1}$$

   pH, TSS (total suspended solids) and TOC (Total organic carbon) were measured everyday

   ⊕ After this cycle (10 days), and when it was clear that the reactor work efficiently by mixing phenol with municipal wastewater, different phase was started by feeding the reactor with pure 100 $mg.L^{-1}$phenol solution (instead of mixture

municipal waste water / phenol solution). That is, 1100 mL of the solution was taken out from the reactor and the corresponding volume of phenol solution (with the needed macronutrients) was fed to the reactor. Initial seeding was 1.5 $g.L^{-1}$ and HRT of 1.5 days, so the daily volume to be fed was 1 L. the same previous analyses were carried out.

⊕ After 7 cycles (11 days), the reactor was considered to be acclimated to the phenol solution. Then the pre-treated solution was fed, by mixing it with the 100 $mg.L^{-1}$ phenol solution in different percentages (from 20% photo-treated solution / 80% phenol solution up to 100% photo-treated solution) and at different HRTs (from 10 days up to 12 hours).

⊕ Daily procedure with the reactor was as follows:

- Stop the magnetic stirring and the feeding of air to allow the biomass to settle down.
- Take out the determine volume of solution (q = 1500 mL/HRT).
- Feed the reactor with fresh solution of the corresponding phenol/photo-treated solution/macronutrients mixture, previously neutralized at pH 7.
- Perform pH, TSS, TVSS (total volatile suspended solids) and TOC analyses.

- When HRT = 12 hours, this procedure was done twice a day.

2. Non-acclimated reactor.

This reactor was fed with 1.5 $g.L^{-1}$ of activated sludge from a wastewater treatment plant (Gave, Spain). The start-up and daily procedure of this reactor consisted of the following steps:

⊕ The reactor was initially charged with the following mixture:

- 400 mL of biomass from a municipal wastewater treatment plant (Gavà, Barcelona)
- 1100 mL of municipal waste water
- macronutrients (3 mL of NH_4Cl solution, 3 mL of $CaCl_2$ solution, 3 mL of $FeCl_3$ solution, 3 mL of $MgSO_4$ solution and 9 mL of phosphate buffer solution)

A hydraulic retention time (HRT) of 10 days was fixed. The corresponding volume to be taken out from the reactor and fed daily with fresh solution. Analyses carried out every day were: pH, TSS and TOC.

⊕ After few days, the pre-treated solution was started to be fed. 1100 mL of the solution was taken out from the reactor and the corresponding volume of a mixture with 20% photo-treated solution / 80% municipal waste water was fed to the reactor. A HRT of 10 days was fixed, so the daily volume of new solution to be fed was 150 mL. Daily analyses carried out were pH, TSS, TVSS and TOC.

⊕ The percentage of pre-treated solution was gradually increased, from 20% photo-treated solution / 80% municipal waste water up to 100% photo-treated solution, and HRTs was progressively reduced as well from 10 days to 12 hours.

⊕ Daily procedure with the reactor was as follows:

- Stop the magnetic stirring and the feeding of air to allow the biomass to settle down.
- Take out the corresponding volume of solution (q = 1500 mL/HRT).
- Feed the reactor with fresh solution of the corresponding municipal wastewater / photo-treated solution, previously neutralized at pH 7.
- Perform pH, TSS, TVSS (total volatile suspended solids) and DOC analyses.
- When HRT = 12 hours, this procedure was done twice a day.

Sequencing batch reactors (SBR):

Biodegradation via SBR´s were performed in a coupled photochemical-biological reactor. The coupled processes is presented in figure 5.6. Photochemical reactor (left hand side figure 5.7) is the multi lamp stirred tank photo-reactor presented previously. In the right hand side of figure 5.6 appear the SBR reactor.

SBR reactor consist of:

1. A 1.5 L biological reactor
2. Air diffuser and agitation.
3. Programming unit
4. Alimentation and purge pumps

5. Pneumatic valve
6. Temperature controller

Experimental procedure.

In this part only simple description will be pointed about the procedure used in SBR operations. A detailed explanation on different aspects of SBR and coupled process will be presented in couple process discussion:

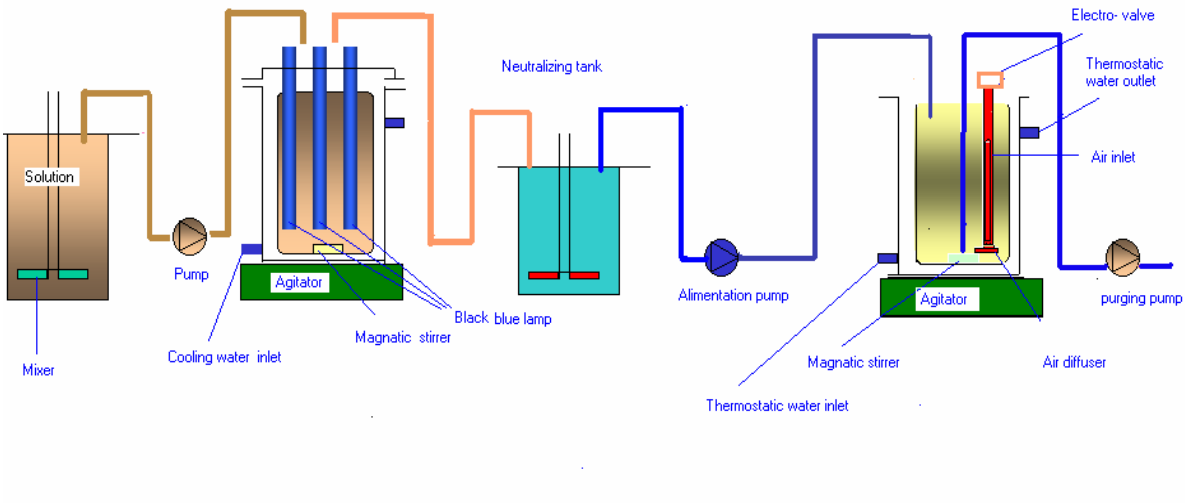

Figure 5.6: Photochemical-biological reactor installation

The aerobic oxidation was carried out with photo-Fenton pre-treated solution. The outlet solutions of photo-Fenton process were discharge to a tank, neutralized to pH around 7.0, and mixed with nutrients solutions (NH_4Cl, $CaCl_2$, $FeCl_3$, $MgSO_4$ and buffer solution NaH_2PO_4 adjusted to pH 7.2 with KOH) according to the procedures explained in Standard Methods (1985). SBR bioreactor was operated under five well defined phases: fill, react, settle, down and idle. Detailed explanation of each step is explained in introduction (section 3.4.8.)

The daily procedure was as follow :

- At the beginning of each cycle, the solution fed automatically to the SBR via alimentation pump, samples at zero time was with drawn.
- Agitation and airflow were switched on automatically.
- The solution left to react according to cycle time (8 days or 3 hr). During each cycle pH, TOC, TSS. TVSS analysis were carried out.
- At the end of each cycle, agitation and airflow were switched off
- Bioreactor allow to settle for 1 hr and purging pump connected to remove the treated solution from the reactor.
- New solution was charged by alimentation pump for another bio-oxidation cycle.

6.2. Reactants:

- Phenol (> 99%, Merck)
- 2,4-Dichlorophenol, $C_6H_4Cl_2O$ (>98%, MERCK)
- Textile dyes
- Iron Sulfate $FeSO_4,7H_2O$ (98%, Panreac)
- Hydrogen Peroxide (30%, Merck)
- Sodium Hydrogen Sulphite solution (40% W/V, Panreac)
- Sulfuric Acid (95-98%, Fluka)
- Oxalic Acid Dihydrate (99.5%, Panreac)
- Uranyl Nitrate (> 98%, Panreac).
- Potassium Dihydrogen Phosphate (purissimum–CODEX, Panreac)
- Sodium Nitrate(99%, Probus)
- Potassium Dichromate(99%, Probus)
- Mercury Sulfate, $HgSO_4$(98%, Probus)
- Silver Sulfate, Ag_2SO_4(98%, Probus)
- Sodium Hydroxide (97.5%, Probus)
- Phosphoric Acid (85%, Probu)

6.3. Analytical Methods

6.3.1. Actinometry

The most utilized method for determination the radiation potential of any radiation source is the actinometry. It is based on the photochemical decomposition of oxalic acid in the presence of uranyl ion (Heidt et al., 1979, Esplugas et al., 1983). The decomposition of oxalic acid, in pH range between 3-7, and conversion is less than 20%, the reaction that takes place is (6.1)

$$UO_2^{2+} + H_2C_2O_4 \rightarrow UO_2^{2+} + CO_2 + CO + H_2O \qquad (6.1)$$

By the knowledge of the actinometer and the lamp characteristics, the radiation intensity can be calculated. Full analysis for reactors actinometry is given in appendix A1.

6.3.2. pH.

The pH measurements were carried out with a Crison GLP-22 pH-meter, calibrated with two buffer solutions of pH 4 and 7. The analysis was not performed on line, but after each sample withdrawal.

6.3.3. High Performance Liquid Chromatography (HPLC)

Phenol and DCP concentrations through out the experiments were determined by high performance liquid chromatography (HPLC)in reverse phase.

The HPLC used consists of sex parts: Waters degasser, Waters Controller(Waters 600), Autosampler (Waters 717), columns oven, temperature controller and photodiode array detector (Waters 996). Operated with Millennium software.

The column used has the following characteristics: Packing: SPHERISORB ODS2, particle size: 5 μm, length: 25 cm and 0.46 cm inner diameter. The mobile phase used was a mixture water/acetonitrile and phosphoric acid (60:40:0.5%), isocratically delivered at a flow rate of 1 $mL.min^{-1}$. The wavelength of the UV detector was selected from the absorption spectra of phenol and DCP (see figure 6.1). Maximum absorption of phenol and DCP were found to be 280 nm. For each sample, 10 μL sample was injected at 25ºC (set point). Under these conditions, phenol and DCP was found to

appear at 6 and 15 min retention time, respectively. Calibration was done by means of component standards (phenol and DCP) at different concentrations.

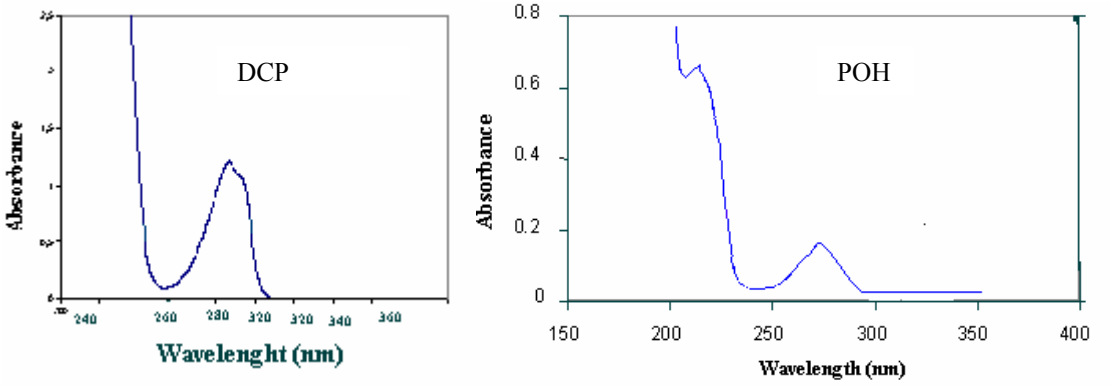

Figure 6.1Absorption spectrum for DCP and POH

6.3.4 Determination the chemical oxygen demand (COD)

Chemical oxygen demand (COD) depends on the amount of oxygen present to oxidize the contained organic matter in the solution.

The chemical oxygen demand was determined by the procedure stipulated in Standard Methods 5220 D: closed reflux, colorimetric method (Standard Methods, 1985). The test procedure be made of heating to an elevated temperature (150°C) a known sample volume with excess of potassium dichromate in presence of acid (H_2SO_4) for a period of two hours in a sealed glass tube. During this time the organic matter oxidize this can be noticed by the change in the colour of the dichromate of yellow colour to green colour (chromic ion) equation (6.2). Catalyst as silver sulphate (Ag_2SO_4) is added for the oxidation of certain classes of organic matter.

$$Cr_2O_7 + 14H^+ + 6e^- \leftrightarrow 2Cr^{3+} + 7H_2O \qquad (6.2)$$

The method is completed by colorimetric determination of the amount of chrome produced. This can be done rapidly and easily by using the spectrophotometer. It is an exact method used in many laboratories nowadays.

Since we use strong oxidizing agent, so if there are a presence for any chlorides in the solution it can oxidize by the dichromate

$$6Cl^- + Cr_2O_7^{2-} + 14H^+ \rightarrow 3Cl_2 + 2Cr^{3=} + 7H_2O \qquad (6.3)$$

To eliminate this interdiction a solution of mercury sulphate should be used ($HgSO_4$) in the mixture, so the mercury will react with the chlorine ion to form ($HgCl_2$) and no effect of the chlorine to the test will be noticed

The COD test solutions needed to be prepared are:

- Digester solution (0.2 N $K_2Cr_2O_7$), prepared by adding to 500 mL distilled water 10.216 g of $K_2Cr_2O_7$ primary standard grade, previously dried at 103°C for 2 h, 167 mL of concentrated H_2SO_4 and 33.3 g of $HgSO_4$. dissolve, cool to room temperture it in 500 mL water and dilute it to 1000 mL.
- catalyst solution prepared by addition Ag_2SO_4 to acidic solution of concentrated sulphuric acid in the ration 5.5 g Ag_2SO/kg H_2SO_4 and dissolve it perfectly

The test done by adding in standard tubes 10 mL; 2.5 mL of the sample 1.5 mL of the digester and 3.5 mL of the catalyst. Tight cap tubes and invert each several times to mix perfectly . Place the sample tubes in heater (150°C) for 2 hours. Afterward, let the sample cool to room temperature and then measure the absorbency by spectrophotometer with wavelength 585 nm. To got the relation between the absorbency and the COD, calibration were done for the spectrophotometer by using sample with know COD value in the range 20-900 $mgO_2.L^{-1}$ so a calibration curve for the relation COD and the absorbency where done to give directly COD value.

6.3.5 Determination the total organic carbon (TOC):

The TOC measurements was determined by combustion method and analysis the resultant CO_2 in the combustion gases. The equipment used is Dohrmann TOC analyzer DC-190. The system contains combustion tube felled with platinum catalyst, through which pass an oxygen (99.999% purity) flow of 200 $cm^3.min^{-1}$. The temperature of the reaction zone maintains at 680°C. The samples are introduced into combustion chamber by automatic sampler after which combustion occur (total oxidation to CO_2 and H_2O). The gases flux go out of the reactor pass condenser and gas /liquid separator to eliminate almost all the water. The remaining droplet of water can by remove from the gas stream by the dehumidfactor, which operates at almost temperature (0-10)°C. The dry gas that contain CO_2 pass a scrubber that separate halogens and finally reach an infrared detector for determine the exact amount of total

carbon which is in this case is the same as the total organic carbon. The standard solution used to calibrate the TOC device is a solution of byphthalate that contain 100 mg $C.L^{-1}$.

6.3.6 Determination of the biological oxygen demand

Biochemical Oxygen Demand (BOD) is related to the amount of biodegradable organic matter in a water sample. During oxidative degradation of organic matter, aerobic microorganisms which perform it consume oxygen present in water as dissolved gas. BOD is expressed as weight of oxygen consumed per unit volume of water during a defined period of time at a defined temperature, e.g. mg $O_2.L^{-1}$ (or ppm) during 5 days at 20ºC.

Biological oxygen demand BOD was performed in a 500 mL volume bottle supplied with oxytop system. It is a manometric respirometer that relates oxygen uptake to the change in bottle total pressure as result of oxygen consumption.

The general procedure for the BOD test can be summerized as follow:

1. Preparation the buffer solution and the supplementary nutrients

The buffer and nutrients solutions used in the test prepared as follow

- *Phosphate buffer solution* , 1.5 N: Dissolve 207 g sodium dihydrogen phosphate, $NaH_2PO_4 \cdot H_2O$ in water. Neutralize to pH 7.2 with 6N KOH and dilute to 1 L.
- *Magnesium sulfate solution*, 0.41N*:* Dissolve 101 g $MgSO_4.7H_2O$ in water and dilute to 1 L.
- *Ferric chloride solution*, 0.018N*:* Dissolve 4.84 g $FeCl_3.6H_2O$ in 1 L water.
- *Calcium chloride solution*, 0.25N*:* Dissolve 27.7 g $CaCl_2$ in 1 L water. Glucose-glutamic acid solution: dry reagent –grade glucose and reagent-grade glutamic acid at 103°C for 1 h. Add 150 mg glucose and 150 mg glutamic to distilled water and dilute it to 1 L
- Glucose-glutamic acid solution: Dry reagent-grade glucose and reagent-grade glutamic acid at 103°C for 1 h. Add 15.0 g glucose and 15.0 g

glutamic acid to distilled water and dilute to 1 L. Neutralize to pH 7 using 6N potassium hydroxide.

2. Preparation the seeding microorganisms:

Microorganisms that are used in the BOD test are non-acclimated organisms The preparation of these consist of taken volume activated sludge bacteria solution, (in our case taken from the activated sludge system operating at the sewage works of Gava Barcelona, Spain). Decant it, then remove the supernatant, and take the bottom layer, which contain the bacteria. (if the bacteria were stored in the refrigerator it should be pulled out and let to got temperature of 20±5°C. Water sample for which BOD_5 to be tested, should be aerated in period of 30 min to assure that there is sufficient oxygen during microorganisms incubation

Preparation of testing bottle

There are many range of BOD that could a sample contains. Depending on this BOD range the total volume of solution used in the test changes. The range of BOD and the correlated volume needed were shown in table 6.1

Table (6.1) The range of BOD and the correlated volume

Range of BOD_5 ppm	Sample volume	Multiplication factor
0-40	432 ml	1
0-80	365 ml	2
0-200	250 ml	5
0-400	164ml	10
0-800	97 ml	20
0-2000	43.5 ml	50
0-4000	22.7 ml	100

For each BOD, test three bottle should be arranged. The first which called blank bottle it just contains the bacteria buffer solution and distill water, the second contain the sample, buffer solution and glucose/glutamic acid solution, this use to measure the inhibiting effect of the sample, and finally the third that contain the buffer and the sample.

In the present case, BOD values were lower than 40 mg $O_2.L^{-1}$, so the total volume of the sample was fixed at 432 mL. Each volume was filled with the following amounts of each solution: 425 mL of sample, 2.595 mL of buffer solution, 0.865 mL of NH_4Cl, $MgSO_4$ and $CaCl_2$ solutions, and 0.650 mL of biomass (this amount was fixed by the guidelines given by the Standard Methods, 5210 D). For each BOD test, a "blank bottle" has to be arranged, containing the bacteria, buffer and nutrient solutions and Millipore water. Samples, previously aerated, are allowed to reach 20ºC in the refrigerator, then 2 NaOH tablets are added in a quiver and the bottles are sealed with the Oxitop membrane, reset the zero and kept in the incubator thermostatically controlled at a 20 ± 1 °C with agitation for up to 5 or 21 days.

Calculation

The value of n-day BOD calculated by using the formula

$$BOD_n = (D_{ns} - D_b) * N \qquad (6.4)$$

Where:

D_n = BOD measured after n-days in the sample bottle

D_b = BOD measured after n days in the blanc bottle

N= Multiplication factor

6.3.7. Determination of total suspended solids at 103-105 ℃

Suspended solids or non-filterable solids refer to matter suspended in water and wastewater. Solids may affect water or effluent quality adversely in a number of ways. Solids analyses are important in the control of biological and physical wastewater treatment processes and for assessing compliance with regulatory agency wastewater effluent limitations

A well mixed sample is filtered through a weighed standard glass fiber filter, porosity 45µm. And the residue retained on the filter is dried to a constant weight at 103 to 105 °C. The increase in weight of the filter represent the total suspended solids.

Procedure:

Preparation of glass-fiber filter:

- Clean the filter three time with 200-mL distilled water at each time

- Dry the filter in an oven at 103 to 105 °C for 1 h, if the filter will be use to measure volatile solids, an ignition at 550 °C for 15 min should be done for each filter
- Cool the filter in desecrator to balance temperature and weight
- Take the weight of the filter

Sample analysis:

- Assemble filtering apparatus and filter and begin suction
- Add 10 mL to the apparatus and continue in filtration for 5 min
- Remove the filter from the apparatus with precaution not to loss any solid it contain
- Place it in oven at temperature of 103 to 105 °C for one hour
- After one hour remove the filter, let it cooled for 20 min
- Take the weight of filter

Calculation:

$$\text{mg total suspended solids/L} = \frac{(A-B)\times 1000}{\textit{sample}\ \text{volume, mL}} \qquad (6\text{-}5)$$

Where:

A= weight of filter+ dried residue, mg

B= weight of filter, mg

6.3.8. Determination of total volatile suspended solids at 550℃

The residue from the pervious test is ignited at 550±50°C. And then keep to cool for 15 min in a dry atmosphere, the lost weight represent the volatile suspended solids

Calculations

$$\text{mg volatile solids/L} = \frac{(B-C)\times 1000}{\text{sample volume, mL}} \qquad (6\text{-}6)$$

Where:

B= weight of filter + volatile residue, mg

C= weight of filter at the final period, mg

6.3.9 Inhibition test of activated sludge

Inhibition test on activated sludge provides a good indication of biodegradable organic matter in a water sample. The test gives rapid indication of water medium toxicity for non-acclimated biomass population. Moreover, as a result of easy application procedure and the test short time (3 h) it may be advantageously take place of BOD_5 measurement. During bio-oxidation of organic matter, aerobic microorganisms consume oxygen present in water as dissolved gas, and oxygen concentration in water decrease. Thus, if the dissolved oxygen measured with time at presence of microorganisms, this can be relates to the amount of organic matter.

The test was carried out in a 300 mL volume bottle supplied with dissolved oxygen elected.

The general procedure for the inhibition test can be summarized as follow:

Preparation of synthetic medium

A simple biodegradable solution , called synthetic media, was prepared. Synthetic medium solution contain the following components (see table 6.2). After preparation, the pH of the solution was 7.5±0.5.

Table 6.2 components used in preparation of synthetic medium.

Component	*Quantity*
Peptone	*16 g*
East extract	*11g*
Urea	*3g*
Sodium chloride	*0.7g*
Calcium chloride di-hydrate	*0.4g*
Magnesium sulfate hepta-hydrate	*0.2 g*
Distilled Water	*1000 ml*

Preparation the seeding microorganisms:

Microorganisms that are used in the test are non-acclimated organisms The preparation of these consist of taken volume activated sludge bacteria solution, (in our case taken from the activated sludge system operating at Ales, France). Decant it, then remove the supernatant, and take the bottom layer, which contain the bacteria.. Water sample should

be aerated in period of 30 min to assure that there is sufficient oxygen during microorganisms incubation

Preparation of testing bottle

For each water sample, five bottles was prepared. Table 6.3 present the quantity needed for preparation each bottle:

- The first three bottles (F_{T1}, F_{T2} and $F_{T3)}$ water sample at concentrations 0.1, 1.0 and 10 % V/V is mixed with synthetic medium, activated sludge and water.
- The fourth bottle(F_b), called blanc, contain only activated sludge and synthetic medium this bottle use to check that the activity of sludge in an easily biodegradable water solution.
- In the fifth bottle, the oxygen consumption as result of any physico-chemical reaction in water medium, this easy perform to be sure that during the test the only oxygen consumption due to bio-oxidation take place. This bottle contains no sludge.

Table 6.3: Preparation of testing bottle

Activated sludge	3 $gTVSS.L^{-1}$				
Reactant concentrations	F_{T1}	F_{T2}	F_{T3}	F_b	F_{pc}
Water sample (ml)	0.3	3	30	0	30
Synthtic medium (ml)	10	10	10	10	10
Activated sludge (ml)	10	10	10	10	0
Water (ml)	279.7	277	250	280	260
Total volume	300	300	300	300	300

Thus, for each water sample, the bottles were filled with the needed solution at a temperature of 20ºC, dissolved oxygen was measured in each bottle at time zero. Then, the activated sludge was added and measurement started immediately each 10 min for 3 hour.

7. treatment of DCP and POH by AOP´s based on UV-light

In the present series of experiments, AOP´s based on UV-light with wavelength 254.7 nm were carried out. Experiments were carried out in tubular photo-reactor (Reactor 1, section 6.1), actinometrical results show that the photon flux of this reactor is 13.3 μ Einstein.S^{-1}. The effect of different AOP´s on the degradation and biodegradability of DCP and POH solutions were studied. The influence of different AOP´s operational conditions, initial reactant concentrations, irradiation time and pH was examined, as well as the effect of all these conditions in pre-treated solutions biodegradability. Furthermore, first order kinetic constant and half-life time ($t_{1/2}$), during AOP´s reactions was determined.

Before starting with any treatment, stripping and volatilization effect on DCP and POH aqueous solutions was checked. Results are shown in Appendix A2, Table DCP-S and DCP-V. Experimental results show that, for both processes, and after two hours of treatment less than 10% losses of DCP were found. moreover, during the first 40 minutes (approximate time necessary to remove DCP in some AOP´s) less than 4% removal was observed. Consequently, this amount may suppose negligible.

7.1 Treatment of DCP and POH by direct UV- light

7.1.1. Photo-degradation

100 mg.L^{-1} of DCP and POH solutions were treated by direct UV-light photolysis (table DCP-UV and POH-UV Appendix A2). Figure 7.1 presents the normalized concentration of DCP and POH as function of irradiation time as well as the normalized TOC evolution. It can be seen in the figure that, both DCP and POH follow the same degradation tendency, with delay time of about 3 min in DCP response. Aqueous DCP and POH solutions was not able to absorb all UV light (see spectra in installation section 6.3), hence their direct photolysis by UV light is quite slow. During 2 hours reaction time no more than 53% POH and 56% DCP could be eliminated. Esplugas et al., (2002) have been studied POH degradation by UV light, in the study 24% POH degradation was obtained during 30 min, in our study at the same time POH degradation of 20% was obtained which is in consistence with the published results. This degradation was combined with 13 and 16 % total organic carbon (TOC) removal for

DCP and POH respectively. This point out that UV-light alone is inefficient method for DCP and POH degradation.

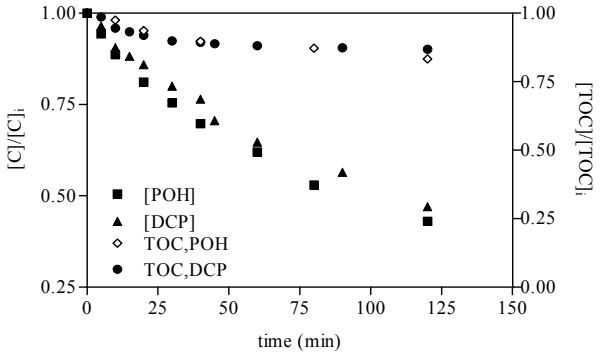

Figure 7.1: Normalized concentrations of DCP, POH and change in TOC Vs. irradiation time in direct UV-light photolysis.

For both compounds, first order kinetic constant based in DCP and POH degradation by UV was calculated Eq.(7.1).

$$\ln \frac{[C]}{[C_0]} = -K_0 t \qquad (7.1)$$

where C is the concentration at any time, C_0 is the initial concentration and K_0 is the first order kinetic constant. Results are presented in Figure 7.2. The degradation of DCP and POH by direct UV-photolysis follows first order kinetics (R^2 =0.98). As expected, DCP and POH degradation rate constant is so low due to the weak effect of UV in eliminating these compounds. First order reaction rate constant of 0.00664 min^{-1} and half-life time ($t_{1/2}$) of 118 min were obtained for DCP. Trapido et. al., (1997) have been studied the degradation of chloro-phenols by UV light, the reported apparent rate constant for DCP degradation with UV-light is 0.0071 min^{-1} which is in the same order of magnitude found in this study. On the other hand, POH shows better reactivity for UV photolysis: first order reaction rate constant of 0.0075 min^{-1} and half-life time ($t_{1/2}$) of 95 min was reported. Results obtained in POH case are in good agreement with the ones tabulated by Esplugas et al. (2002), (K_o =0.0088 min^{-1} and $t_{1/2}$ 79 min).

An important parameter that gives an idea how efficient direct photolysis process is the quantum yield. According to reactor geometry and the actinometrical results, the quantum yield at initial time has been determined; ϕ_{POH} = 7.2±0.1 mmol.$Einstein^{-1}$ and ϕ_{DCP} = 3.2±0.2 mmol.$Einstein^{-1}$. Rodriguez et al., (2002) have been studied the

degradation of POH by UV light, the reported quantum yield (ϕ_{POH} = 11.2±0.1 mmol.Einstien^{-1}) is in the same order of magnitude found in this study.

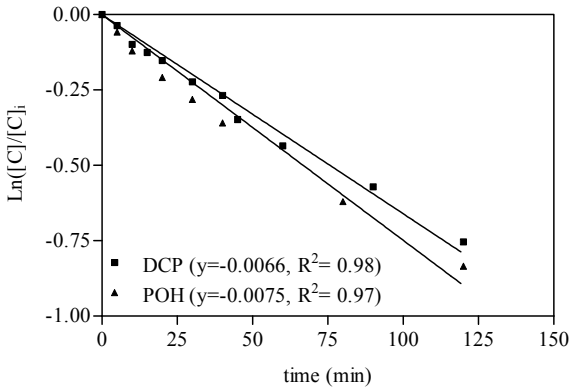

Figure 7.2: first order kinetic constant for DCP and POH degradation by direct UV photolysis

7.1.2. Influence of UV-light in biodegradability

Biodegradability of water systems is normally measured by applying different types of biodegradation tests. BOD_n (BOD_5 or BOD_{21}), BOD_n/COD and BOD_n/TOC have been proposed by a number of authors as biodegradability indicator (Gilbert, 1987; Marco et al., 1997, Yu and Yu, 2000; Chamarro et al., 2001). Other biodegradability measurements including substrate destruction, oxygen uptake, EC_{50} toxicity measurements, cell growth counts and intracellular ATP levels have been also reported (Scott and Ollis, 1995). In the proceeding part of this study BOD_n (BOD_5 or/and BOD_{21}), BOD_n/COD and BOD_n/TOC will be used as biodegradability indicators.

First of all, the ability of 100 mg.L^{-1} DCP and POH solution to go through biodegradation process was measured; BOD_5, BOD_{10}, BOD_{21} and the inhibition test for activated sludge were used as biodegradation parameters. Experiments show that DCP at concentration of 100 mg.L^{-1} is not readily biodegradable as indicated by its BOD_n (BOD_5=0.0 and BOD_{21}=0.0). However, POH did not show the same affinity. BOD_5 measurement shows that POH is hardly biodegradable compound (BOD_5 =27 mg O_2.L^{-1}, BOD_5/COD ratio is 0.12). But, it was found that POH biodegradability decrease by increasing its concentration in solution (at 1000 mg.L^{-1} POH solution BOD_5/COD ratio is 0.017). Chamarro et al. (2001) have been studied the biodegradability of different phenolic compounds. In their study, BOD_5/COD ratio for POH and DCP were 0.18 and 0.0 for POH and DCP respectively which is in a good agreement with present results. Figure 1.3 presents the oxygen consumption by activated sludge when DCP and POH were added to easily

biodegradable carbon source at different dilutions. As it can be seen, the presence of DCP at small volume percentage (0.1% V/V) leads to decrease in oxygen consumption by aerobic bacteria. It can be also noticed that, the oxygen consumption decreases by increasing the DCP concentration in the synthetic medium, and total inhibition occurred when the concentration is 10 % V/V. In case of POH, concentration of (10 % V/V) leads to negligible decrease in oxygen consumption so POH under these conditions is not inhibited. Nonetheless, as the concentration increases negative effect in bacterial culture was noticed and almost total inhibition was observed when pure POH was used as sole carbon source.

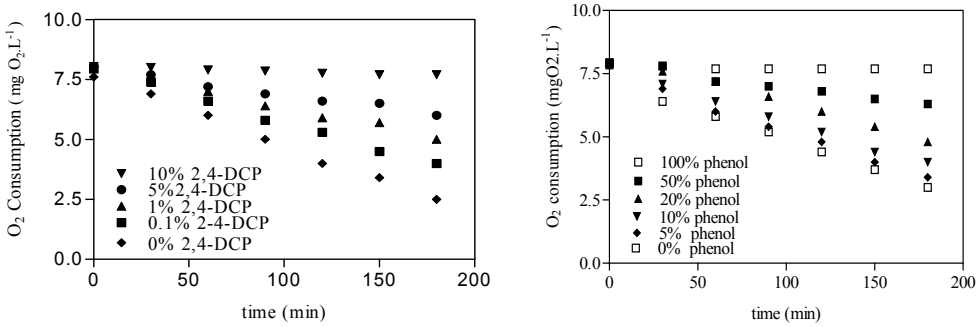

Figure 7.3: Inhibition test of oxygen consumption by activated sludge for 100 $mg.L^{-1}$ DCP and 100 $mg.L^{-1}$ POH solution.

The photolyzed DCP and POH solutions with UV were tested for their biodegradability. Due to inefficient UV process in DCP degradation, there was no change in biodegradability of the photolyzed solution (BOD_5, BOD_{10} and BOD_{21} were zero). An explanation of that could be accredited to the inherent toxicity of high remaining DCP in the solution.

Unlike to DCP, direct POH photolysis guide to somewhat biodegradability enhancement; after 2 hour treatment the biodegradability measured as BOD_5/COD and BOD_5/TOC ratios increased from 0.12 and 0.35 up to 0.19 and 0.46 respectively.

7.1.3 Change on oxidation state:

Although during UV photolysis not all intermediates have been identified, the degradation of DCP and POH into other by-products was followed by the change in degree of oxidation. Two parameters were studied on purpose; COD/TOC and the average oxidation state (AOS). Both parameters (AOS and COD/TOC ratio) give a

remarkable information on how chemical substances in the effluent become more oxidized. lower COD/ TOC ratios imply higher degree of oxidation while higher ratios means low oxidation, this parameter ranging theoretically between 4 and 5.3 for alkanes and 0.6 for very oxidized substances like oxalic acids (Marco et al., 1997). In the same time, AOS calculated from the formula 7.2 (Stumm and Morgan, 1991): takes value of +4 for CO_2, the most oxidize state of C, and –4 for CH_4, the most reduced state of carbon. Mean oxidation stages of organic carbons of several organic compounds were listed in Stumm and Morgan (1991).

$$\text{AOS} = \text{Average Oxidation State} = \frac{4(\text{TOC} - \text{COD})}{\text{TOC}} \qquad (7.2)$$

where TOC is in mol $C.L^{-1}$ and COD in mol $O_2.L^{-1}$.

Both parameters were followed during DCP and POH degradation. Due to inefficient degradation capacity of this process for both compounds, There were slight variations in oxidation state of organic matter produced from the degradation. With respect to DCP, all over the reactions small change in both parameters was noticed; COD/TOC decrease from 2.71 down to 2.32 while AOS increase from -0.061 up to 0.51. Also tiny effect was noticed through out POH oxidation; COD/TOC was decrease from 2.82 to 2.46 and AOS was changed from –0.23 up –0.31. This may suggest the resistivity of POH and DCP against direct UV photolysis. Another point to mentioned here, is the relation between biodegradability and the change in oxidation state of the organic matters, it was noticed that a good relation exist; high oxidation of organic matter leads to better improvement in biodegradability, as result of photo-oxidation the organic matter into small by-product which are more able to biodegradation.

7.2. Treatment of DCP and POH by UV/ H_2O_2

7.2.1 Photo- degradation

Since direct UV-photolysis of both components was low, it was decided to study the effect of UV/H_2O_2 process in DCP and POH degradation in addition to biodegradability improvement. Homogeneous photochemical methods ,if they wok, are advantageous over photo-catalytical methods, since they do not demand a separation procedure of solid catalyst after treatment. For an effective treatment, photolysis requires strong energy UV light and chemical oxidants such as hydrogen peroxide and ozone. In this

process the degradation enhanced by the presence of hydrogen peroxide, which leads to hydroxyl radicals formation according to Eq. (3.3)

$$H_2O_2 + h\nu \rightarrow 2OH^{\bullet} \qquad (3.3)$$

Although neither hydrogen peroxide nor UV when it used alone oxidize all DCP or POH. The combination of UV and H_2O_2 enhances strongly the degradation efficiency (see figure 7.4 and 7.5), (results are in table DCP-UV/H_2O_2-1 to DCP-UV/H_2O_2-6 and table POH-UV/H_2O_2-1 to POH-UV/H_2O_2-3 Appendix A2). DCP and POH degradation rates increase by addition of hydrogen peroxide (H_2O_2). During UV/H_2O_2 process, DCP attacked either by UV photons or hydroxyl radicals generated from H_2O_2 photolysis. So, as H_2O_2 initial concentration is increased, more hydroxyl radical are available to attack the aromatic ring and so more elimination of DCP and POH achieved. Based on the experimental results, a concentration of 200 mg.L^{-1} H_2O_2 during 90 min irradiation are needed for 100% DCP removal, and 400 mg.L^{-1} H_2O_2 was sufficient to degraded all POH with the same irradiation time. However, during the reaction not all the added amount of H_2O_2 was consumed. Quantofix test shows at the end of the reaction least 50 mg.L^{-1} H_2O_2 in case of DCP and 100 mg.L^{-1} POH remained in the reactor vessel. Moreover, using 100 mg.L^{-1} of H_2O_2 for DCP and 300 mg.L^{-1} POH during the same irradiation time gave 96% removal of the both (DCP and POH) and the remaining H_2O_2 was less than 15 and 60 mg.L^{-1} respectively. This may be assume as a good degradation point where the treatment can be stopped for DCP and POH, since the presence of high concentration of H_2O_2 in wastewater has a lot of side effect in the bio-activity of bacterial population if the water is post-treated in biological systems, so elimination of this residues should be done. Accordingly, UV/ H_2O_2 is able to eliminate major part of DCP and POH without environmental effect under the following conditions: 100 mg.L^{-1} of H_2O_2 and 90 min irradiation time for DCP and 200 mg.$L^{-1}$of H_2O_2 and 90 min irradiation time for POH. Trapido et al., (1997) in the study of DCP degradation by UV/H_2O_2 have been recommended a high molar ratio between hydrogen peroxide to DCP, due to low hydrogen peroxide extinction coefficient.

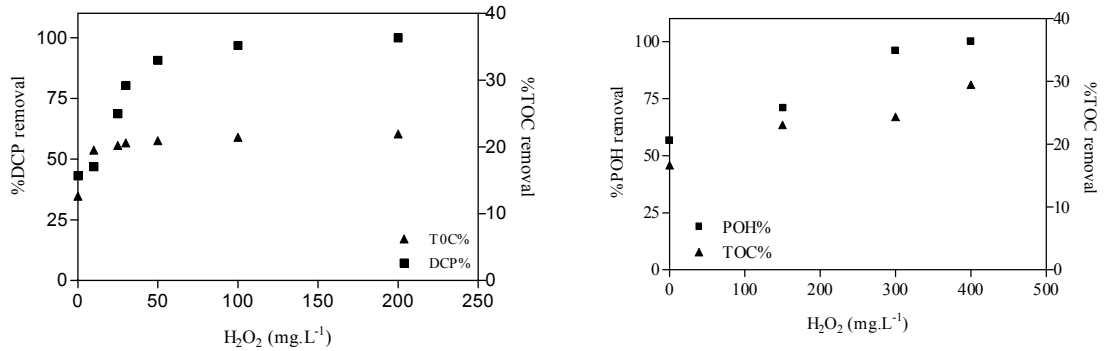

Figure 7.4: DCP, POH and TOC removal as function of initial H_2O_2 concentration during UV/ H_2O_2 process. Reaction time 90 min .

Both DCP and POH degradation rates at different initial H_2O_2 concentrations were also compared by calculating to first order reaction rate constants and half life time ($t_{1/2}$) with respect to DCP and POH concentrations. The regression analysis of the concentration curves versus reaction time indicated that the decomposition rate of these compounds could be described by first order kinetics (see figure 7.5 for DCP, results of phenol not shown). The first order kinetic constants and the half-life time at different H_2O_2 initial concentrations are presented in table (7.1). As it was noticed before, that the reaction rate is accelerated by increasing the initial concentration of H_2O_2. Results for DCP photo-degradation are in agreement with Trapido et al., (1997) (0.00708 min^{-1}).

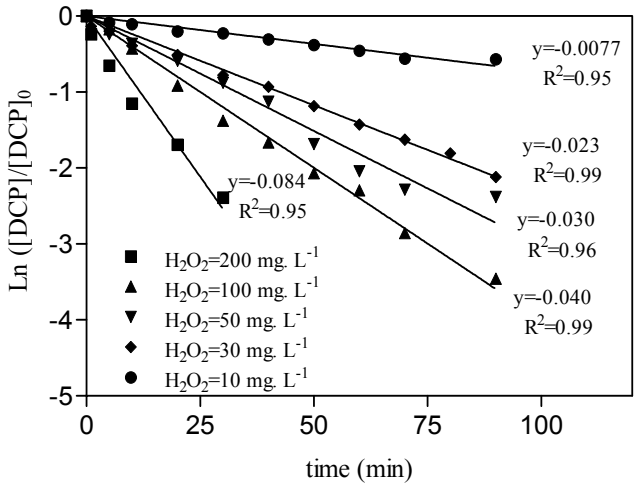

Figure 7.5: First order kinetic constant for DCP degradation by UV/H_2O_2 photolysis

Table 7.1: First order kinetic constants and the half life time at different H_2O_2 initial concentrations for UV/H_2O_2 process

DCP			*POH*		
$[H_2O_2]$ ($mg.L^{-1}$)	*$t_{1/2}$ (min)*	*K_0 (min^{-1})*	*$[H_2O_2]$ ($mg.L^{-1}$)*	*$t_{1/2}$ (min)*	*K_0 (min^{-1})*
10	> 90	0.0077		---	---
30	48	0.023		---	---
50	22	0.03	150	53	0.011
100	15	0.04	300	18	0.0284
200	5	0.084	400	114	0.0478

7.2.2. Influence of UV/H_2O_2 process in biodegradability

Biodegradability test were also applied for the solutions treated by UV/H_2O_2. Experimental results demonstrate that UV/H_2O_2 process has the capacity to remove all DCP from the solution at higher initial H_2O_2 concentration. However, it was not able to make any improvement in the biodegradability of the DCP treated solutions (Table 7.2), in spite that 44% chemical oxygen demand (COD) was removed. This can refer to toxicity of DCP by-products formed during this process, which are not readily biodegradable. Also, at small initial concentrations of H_2O_2 the toxicity exerted by remaining DCP could be reason for low biodegradability values. Adams et al., (1997) studied DCP biodegradability, and found that DCP at low concentrations (below 25 $mg.L^{-1}$) is biodegradable, different that, in this study it was obtained that 10%V/V of DCP in aqueous solution leads to total inhibition of oxygen consumption, that can be justify BOD behaviour.

Table 7.2: Evolution of biodegradability (BOD_5 and BOD_5/COD) and COD for DCP solution treated with UV/H_2O_2 process

$[H_2O_2]_i$ ($mg.L^{-1}$)	DCP%	COD_i (mg $O_2.L^{-1}$)	COD_f (mg $O_2.L^{-1}$)	BOD_5 (mg $O_2.L^{-1}$)	COD %	BOD_5/COD
200	100	118	66	2	44	0.03
100	97	122	72	1	41	0.014
50	91	135	82	1	39	0.012
30	80	116	82	0	31	0.00
25	69	120	84	0	32	0.00
10	44	122	95	0	30	0.00

With regard to POH biodegradability, as mentioned before POH can be classified as hardly biodegradable compound. During UV/H_2O_2 treatment it was noticed an improvement in the biodegradability of the treated solution as result of degradation the original POH solution into other by-products which found to be more biodegradable (see figure 7.6). The change in biodegradability and hence the proportion of organic matter able to bio-oxidation. At 400 mg.L^{-1} H_2O_2, BOD_5, BOD_5/COD and BOD_5/TOC increased for the pre-treated solution respectively up to 33 mgO_2.L^{-1}, 0.26 and 0.60 mgO_2.mg^{-1}C.

7.2.3 Change on oxidation state

The oxidation state of the formed intermediates throughout UV/H_2O_2 reaction was examined. Figure 7.7 presents the evolution of COD/TOC and AOS as a function of initial H_2O_2 concentration for both components.

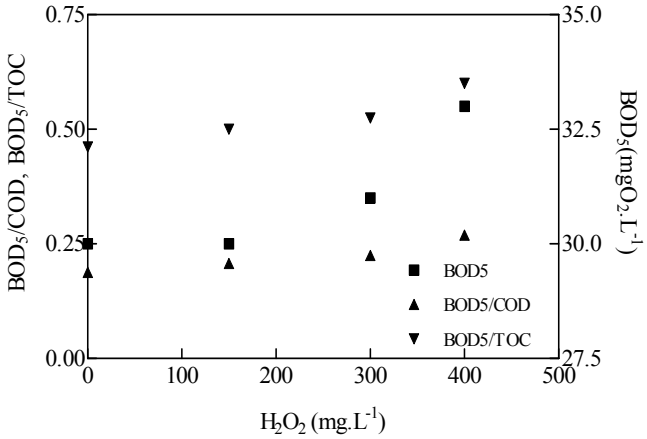

Figure 7.6: BOD_5, BOD_5/TOC and BOD_5/COD Evolution of POH treated solution with UV/H_2O_2 process

The degree of oxidation of the contained organic matter increases as the initial hydrogen peroxide used increases. On the other hand, it can be seen that for both DCP and POH, the change in oxidation state for the produced intermediates all over reaction is small, for example at the highest H_2O_2 initial concentration used (200 mg.L^{-1}), COD/TOC ratio was found to decay 26% and 18 % for DCP and POH respectively, meaning that organic substances present in the solution faced a weak oxidation, The same tendency could be noticed for the change in the AOS state. The weak oxidation of the organic matter could be explain the tiny change in the biodegradability values.

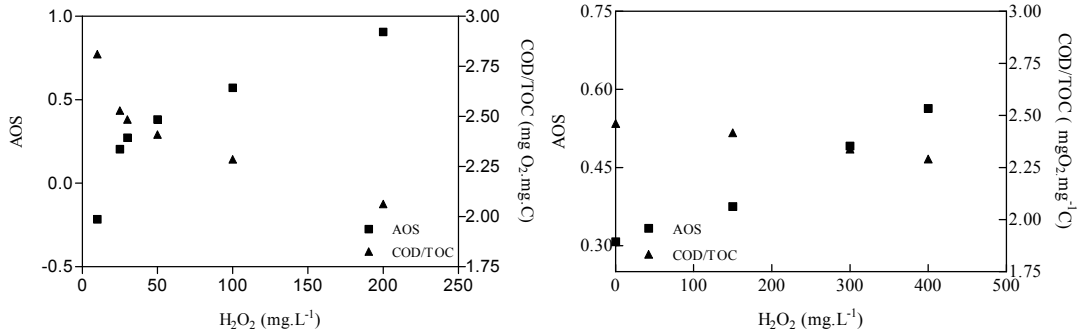

Figure 7.7: Evolution of COD/TOC and AOS as a function of initial H_2O_2 concentration for DCP and POH in UV/ H_2O_2 process. Reaction time 90 min.

7.3. Treatment of DCP and POH by UV/Fe(III)

7.3.1. Photo-degradation

As presented in the introduction (section 3.5), iron in its ferrous and ferric form acts as photo-catalyst and requires a working pH below 4. In the photo-catalytic process not only the absorbed UV photons lead to organic matter degradation but also ferric ion undergoes a photo-redox reaction producing more hydroxyl radicals. In this part, experiments were carried out to determine the influence of UV/Fe(III) combination in DCP and POH photo-degradation as well as biodegradability improvement (tables DCP-UV/Fe(III) –1 to DCP-UV/Fe(III) –4 and POH-UV/Fe(III) –1 to POH-UV/Fe(III) –4 Appendix A2). Experiments were carried out at different initial Fe(III) concentration. The effect of UV/Fe(III) process in degradation rate of both components (DCP and POH) is illustrated in figure (7.8), where total DCP, POH and TOC removal percentages are plotted versus Fe(III) initial concentration. Figure 7.8 shows that, Fe(III)/UV combination efficiency is greater than UV radiation alone, addition of Fe (III) enhanced the UV efficiency in DCP and POH degradation. The degradation rate of both DCP and POH distinctly increased with increasing amounts of iron salt. It was also noticed that, the major degradation percentage is obtained during the first 60 min of the reaction (total irradiation time is 90 min). Furthermore, it was observed that for DCP the degradation reached its maximum value when 35 mg.L^{-1} Fe(III) was used, adding more amount of Fe (III) has small effect on the degradation outcome and the degradation take a plateau form, while POH degradation tendency increase by increasing the initial Fe(III) concentration. An explanation of DCP behaviour could be deduced to higher addition of iron salt that produced with the librated chlorine ions

brown turbidity that slowed down the absorption of UV light required for photolysis and cause the recombination of hydroxyl radicals (Ghaly et al., 2001). The mean use of ferric chloride to obtain the desired Fe (III) initial concentration, has been reported to be hydroxyl radical scavengers (Maletzky and Bauer, 1998). Nonetheless in our research group this effect was studied in many installations and tiny effect in chloride ion was observed.

Under the experimental conditions, 60% of DCP was removed from the solution, this according to the following operational conditions: 70 $mg.L^{-1}$ initial Fe(III) concentration and 90 min irradiation time, during this time 21% of TOC was found to be mineralized. With respect to POH, 70 $mg.L^{-1}$ Fe(III) and 90 min lead to 73.6 % POH elimination and 19.21 % TOC mineralization.

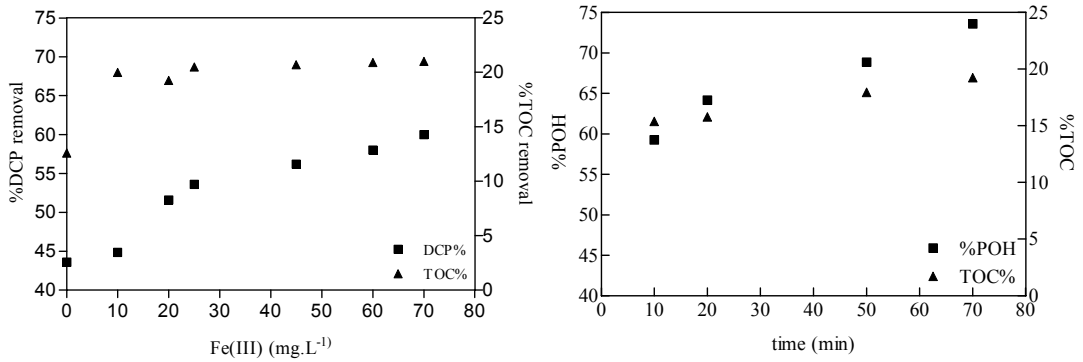

Figure 7.8: Evolution of DCP, POH and TOC as function of initial Fe (III) concentration during UV/ Fe (III) process. Reaction time 90 min

Throughout the reactions, especially in DCP case, the solution pH was measured and it was found to decrease to 2.8 (3.0 in case of POH) in the first min of the reaction, so there were no any precipitates of iron hydroxide. Under our experimental conditions ($[Fe(III)]_0 > 5$ $mg.L^{-1}$ and pH around 2.8), $Fe(OH)^{2+}$ is the predominant monomeric Fe(III) aqua-complex (Mazellier et al., 1999), consequently the following equilibria is established.

$$Fe^{+3} + H_2O \Leftrightarrow Fe(OH)^{2+} + H^+ \qquad (3.11)$$

Thus Fe (III) species undergo a photo-redox reaction giving more hydroxyl radicals

$$Fe^{+3} + H_2O \xrightarrow{h\nu} Fe^{2+} + OH^{\bullet} + H^+ \qquad (7.3)$$

The redox potential of Fe (III)/Fe (II) couples is 0.77 V. The simultaneous re-oxidation of Fe (II) into Fe (III) by oxygen as well as by appropriate products in the solution present an interesting catalytic aspect to the process.

The reaction rates based in first order kinetics and half-life time were calculated (see figure 7.9 for DCP, results for phenol are nor presented). Table 7.3 presents kinetic results for both components. It was noticed, POH is more affected by UV/Fe(III) process than DCP, in all experimental conditions the rate of degradation and half-life time for POH is higher than that of DCP.

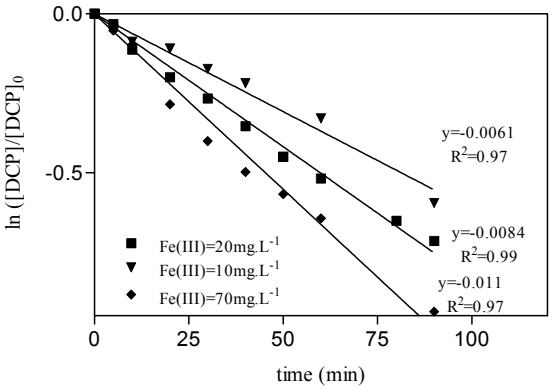

Figure 7.9: First order kinetic constant for DCP degradation by UV/Fe (III) process.

Table 7.3: First order kinetic constants and the half life time at different Fe (III) initial concentrations for UV/ Fe (III) process

	DCP		*POH*	
[Fe (III)], (mg. L^{-1})	*$t_{1/2}$ (min)*	*K_0 (min^{-1})*	*$t_{1/2}$ (min)*	*K_0 (min^{-1})*
10	> 90	0.0061	80	0.0086
20	89	0.0084	61	0.010
70	55	0.011	46	0.0153

7.3.2.Influence of UV/ Fe (III) process in biodegradability

Unlike UV/H_2O_2 process, UV/ Fe (III) is not capable at all to remove all DCP from the solution, even at high Fe (III) initial concentrations. The presence of DCP in a solution affects the bacterial culture and may lead to inhibition and recalcitrant conditions. For that reason, the solutions treated by this process show no change in biodegradability (see table 7.4).

POH shows difference tendency (see figure 7.10), when using 10 mg .L^{-1} Fe(III) the BOD_5/COD and BOD_5/TOC ratios increased up to 0.194 and 0.50 respectively. This suggests a good enhancement in the biodegradability compared with original POH

solution (BOD_5/COD) 0.12 was occurred. Moreover, adding more Fe(III) enhance more the biodegradability; at 70 mg .L^{-1} Fe(III) both ratios increased to 0.23 and 0.57.

Table 7.4: COD and BOD values for DCP treated by UV/Fe (III) process.

$[Fe(III)]_i$ ($mg.L^{-1}$)	DCP%	COD_i ($mg\ O_2.L^{-1}$)	COD_f ($mg\ O_2.L^{-1}$)	BOD_{5f} ($mg\ O_2.L^{-1}$)	COD%	BOD_5/COD
10	45	133	98	0	26	0
20	51	121	96	0	21	0
25	54	122	98	0	20	0
45	56	121	92	0	24	0
60	58	122	90	0	26	0
70	61	122	88	0	28	0

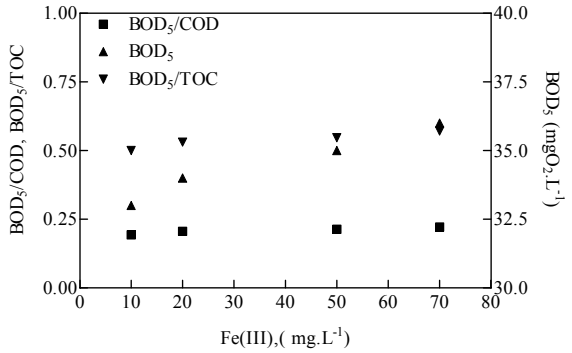

Figure 7.10: BOD_5, BOD_5/COD, BOD_5/TOC evolution of POH treated solution as function of initial Fe(III) used in UV/Fe(III) process. Reaction time 90 min.

7.3.3 Change on oxidation state

The change in oxidation state during UV/Fe(III) reaction was also examined in figure 7.11. A small change in the oxidation state in the reaction solution was observed for both DCP and POH. Addition more concentration of iron salts doesn't lead to helpful change in the organic matter oxidation state.

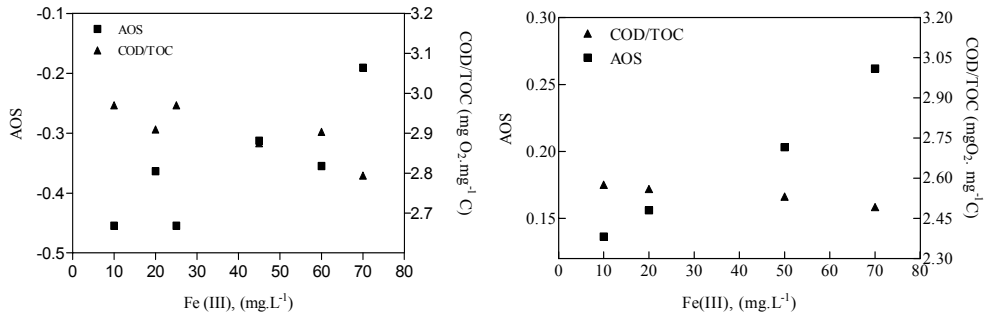

Figure 7.11: Evolution of COD/TOC and AOS as a function of initial Fe (III) concentration for DCP and POH in UV/Fe (III) process. Reaction time 90 min.

7.4. Treatment of DCP and POH by Fenton's and Fenton like reagents:

7.4.1. Degradation

Fenton's reagents reported by Fenton (1894) is mainly a mixture of ferrous Fe (II) ion and hydrogen peroxide which produces $OH^{\bullet}$ radicals according to the reaction

$$Fe(II) + H_2O_2 \rightarrow Fe(III) + OH^{\bullet} + OH^{-} \qquad (3.13)$$

Although the reagent has been used in mechanistic investigation in organic chemistry, its potentiality in wastewater treatment has only begun in recent years (Eisenhuar 1964, Barbini et al., 1987). It has been demonstrated that, Fenton reagents is able to destroy POH, chlorinated POH and herbicides in water media, as well as reducing chemical oxygen demand (COD) in municipal wastewater. It is being employed for the treatment of wastewater contaminated with phenolic pollutants. The usefulness of the Fe(II)/H_2O_2 process as potential oxidants of soil contamination has also been investigated (Watts et al., 1993).

The use of Fe (II)/H_2O_2 for wastewater treatment is attractive due to the fact that iron is highly abundant and non-toxic element, and 30% aqueous hydrogen peroxide solution (normal concentration used in Fenton applications) is easy to handle and environmentally kind. However, requirement of stoichiometric amount of Fe(II) (high amount of iron ions) may be assume as process limitation.

It is also known that hydrogen peroxide decomposed catalytically by Fe(III) and generates hydroxyl radicals in the process (Walling,1975). Thus, ferrous ion in Fenton reagents can be replaced with ferric ion. The mechanism proposed for free ferric ion evolves the hydroxyl ($OH^{\bullet}$) and hydroperoxyl radicals ($HO_2^{\bullet}$) according to

$$Fe(III) + H_2O_2 \Leftrightarrow H^{+} + Fe(OOH)^{2+} \qquad k_1=2\cdot10^{-3} \qquad (7.4)$$

$$Fe(OOH)^{2+} \rightarrow HO_2^{\bullet} + Fe^{2+} \qquad (7.5)$$

$$Fe(II) + H_2O_2 \Leftrightarrow OH^{\bullet} + Fe(III) + OH^{-} \qquad (7.6)$$

$$HO_2^{\bullet} + Fe(II) \rightarrow Fe^{3+}HO_2 \qquad k_2=3\cdot10^{6}\ M^{-1}s^{-1} \qquad (7.7)$$

$$H_2O_2 + OH^{\bullet} \rightarrow H_2O + HO_2^{-} \qquad k_3=2.7\cdot10^{7}M^{-1}s^{-1} \qquad (7.8)$$

Throughout Fenton reaction rate constant for reaction of ferrous ion with hydrogen peroxide is high and Fe (II) oxidize to Fe (III) in a few seconds to minutes in the presence of excess amounts of hydrogen peroxide. For this reason, it is believed that a

majority of the waste destruction catalyzed by Fenton reagent is simply Fe (III)-H_2O_2 catalyzed destruction process, and Fenton reagent with an excess of hydrogen peroxide is essentially a Fe (III)/ H_2O_2 process (known as a Fenton like reagent or modified Fenton).

Effect of initial H_2O_2 concentration:

The results of DCP and POH degradation by Fenton and modified Fenton at different initial hydrogen peroxide and fixed Fe(II) or Fe(III) concentrations (10 $mg.L^{-1}$) is shown in figure 7.12 (table DCP-H_2O_2/Fe(II)-1 to DCP-H_2O_2/Fe(II)-3 and POH-H_2O_2/Fe(II)-1 to POH- H_2O_2/Fe(II)-3 Appendix A2). Both DCP and POH could be degraded under Fenton and modified Fenton conditions. Rising the concentration of H_2O_2 direct to increase DCP degradation, in 60 min reaction time,100% DCP degradation was achieved when 100 and 115 $mg.L^{-1}$ of H_2O_2 was used for Fenton and modified Fenton respectively. At the same time, total POH removal was obtained during 30 min and 350 and 355 $mg.L^{-1}$ of H_2O_2 respectively, Result are in somewhat in agreement with Esplugas et al, 2002 where total POH degradation was achieved with 334 $mg.L^{-1}$ H_2O_2, 3 $mg.L^{-1}$ Fe(II) and 20 min reaction time.

As comparison between DCP and POH degradation, it can be seen that with respect to DCP the major degradation occur when initial concentration of 75 $mg.L^{-1}$ H_2O_2 was used (almost 90%), increasing the concentration lead to small improvement in the degradation. But in POH case, it is clear that increasing the initial hydrogen peroxide concentration produce more degradation, as result to the presence of more organic matter able to degradation and continuous hydroxyl radical formation. It is remarkable to indicate that no difference was obtained if the reaction starts with Fe (II) or Fe (III) since the degradation percentage are in the same order of magnitude.

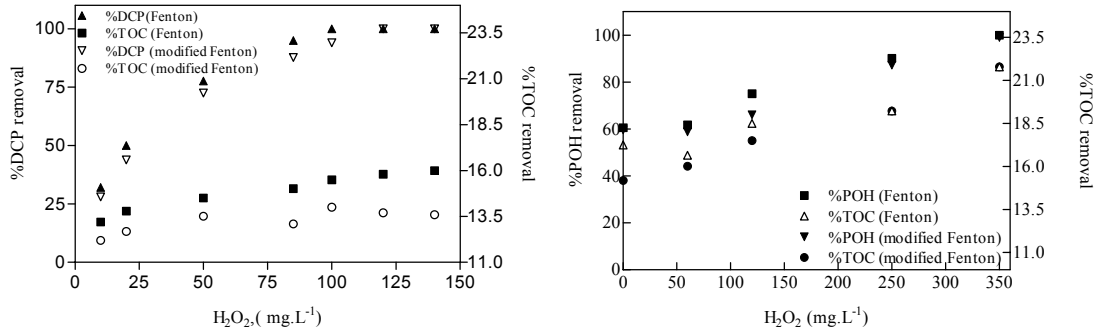

Figure 7.12: Evolution of DCP, POH and TOC removal in Fenton and modified Fenton as function of initial H_2O_2.$[Fe(II)]_i$ or $[Fe(III)]_i$ =10 $mg.L^{-1}$ and 60 min reaction time (30 min in POH case)

With regard to TOC reduction, during DCP degradation, both processes (Fenton and modified Fenton), at the same initial H_2O_2 concentrations, gave almost the same mineralization rate (15% as an average). By the other hand, different mineralization was obtained during POH photo-degradation: varying initial hydrogen peroxide concentration leads to some change on TOC reduction; increasing the initial H_2O_2 from 60 to 150 $mg.L^{-1}$ increase the mineralization rate by 13 %. Furthermore, it was also noticed that no difference in mineralization rate between Fenton and modified Fenton.
First order kinetics constant and half-life time as a function of initial H_2O_2 concentration for Fenton and Modified Fenton are summarized in Table 7.5. As comparison between DCP and POH, it can be seen that POH degradation rate is faster that DCP degradation rate. In all the studied conditions; both first order kinetic constant and half-life time of POH is superior of that of DCP. Yet, it should not forgot the high initial H_2O_2 concentrations needed on POH case.

Table 7.5: First order rate constant and half-life time $t_{1/2}$ as function of initial H_2O_2 for Fenton and modified Fenton reaction. $[Fe\ (II)]_i$ or $[Fe\ (III)]_i$= 10 $mg.L^{-1}$ 60 min reaction time (30 min for POH) and free pH evolution

	DCP			*POH*		
Process	H_2O_2 ($mg.L^{-1}$)	K_0 (min^{-1})	$t_{1/2}$ (min)	H_2O_2 ($mg.L^{-1}$)	K_0 (min^{-1})	$t_{1/2}$ (min)
Fenton	20	0.0134	> 60	60	0.039	16
	50	0.0241	34	250	0.091	7
	85	0.0399	29	350	0.22	2
Modified Fenton	20	0.009	> 60	60	0.035	17
	50	0.020	39	250	0.083	7.5
	85	0.0266	35	350	0.16	2.5

Effect of initial iron ion concentrations:

Another set of Fenton experiments were carried out changing the initial amount of Fe (II) with fixed H_2O_2 initial concentration 20 and 30 $mg.L^{-1}$ for DCP and POH respectively (see figure 7.13). Increasing the concentration of Fe(II) lead to small development in elimination rate of DCP or POH. In the contrary, at higher initial Fe (II) a decrease in the degradation efficiency was noticed. It was also observed that, TOC

removal evolution in both reactions is in the same order of magnitude as before (15% for DCP and 18% for POH).

Explanation of that could be attribute to the catalytic effect of Fe(III)- formed during the reaction- in the decomposition of H_2O_2 to H_2O and O_2 (Murphy et al., 1989). There is also some evidence that Fe (III) and H_2O_2 react to produce several Fe(III)-hydroperoxy complexes like Fe $(HO_2)^{2+}$ and Fe $(OH)(HO_2)^{2+}$ which decompose to produce the hydroperoxy radical $HO_2^{\bullet}$ and Fe (II). If $HO_2^{\bullet}$ is formed, it is relatively non-reactive with organic matter (De Laat and Gallard,1999), and this may distress DCP or POH reactivity.

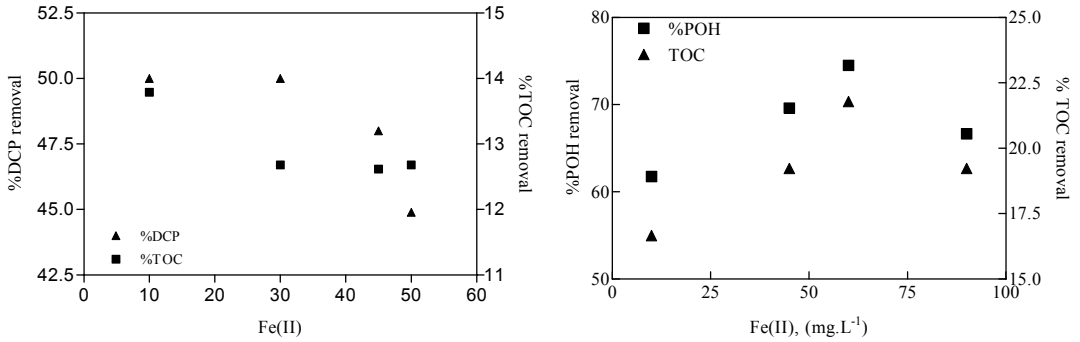

(A) (B)

Figure 7.13: Evolution of DCP, POH and TOC removals as function of initial Fe (II) in Fenton process. (A) $[H_2O_2]_i$ = 20 mg.L^{-1}, 60 min reaction time and free pH evolution, (B) (A) $[H_2O_2]_i$ = 30 mg.L^{-1}, 30 min reaction time and free pH evolution.

7.4.2. Dechlorination

The formation of inorganic chlorine during DCP degradation through Fenton reaction was followed. Figure 7.14 presents the chloride ion evolution and DCP elimination as function of reaction time. Chlorine ion concentration increased slowly during Fenton reaction. 26% dechlorination was achieved for 77% of DCP elimination, and at 95.0% of DCP elimination, the dechlorination was 44%. The non-stoichiometric conversion of chlorine during DCP degradation may explain by the formation of other chlorinated compounds.

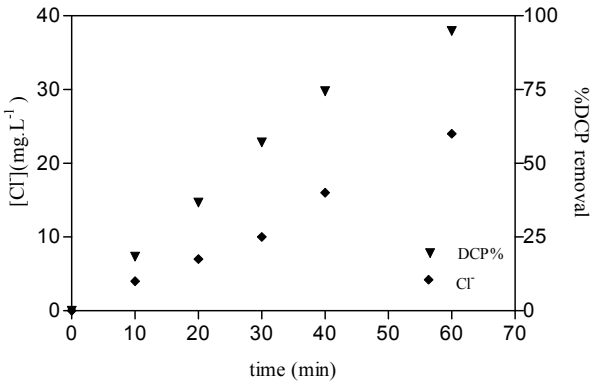

Figure 7.14: Evolution of chlorine ion and DCP removal as function of reaction time $[H_2O_2]_i$=85 $mg.L^{-1}$, $[Fe(II)]_i$ =10 $mg.L^{-1}$ and free pH evolution.

7.4.3. Influence of Fenton and Fenton like reagents in the biodegradability

Effect of initial H_2O_2 concentrations

The biodegradability measured as BOD_n/COD and BOD_n/TOC ratio was studied for solution treated by Fenton and modified Fenton. In case of DCP solution it was noticed that, BOD_5 value was so small. So, it was decided to measure both BOD_{10} and BOD_{21}. The change in BOD_n as function of initial H_2O_2 concentration used in Fenton and Fenton like reactions was followed. Figures 7.15 and 7.16 present BOD_5, BOD_{10}, BOD_{21}, and contaminants removal percentage as function of initial H_2O_2 used in Fenton and modified Fenton reactions respectively. During POH degradation, treated solution was tested for BOD_5 and BOD_{21} values, and it was observed no difference between BOD_5 and BOD_{21}, so it was decided in the proceeding experiments to measure only BOD_5.

BOD_5 values started to increase as DCP or POH deplete from the solution. For DCP degradation, considerable BOD_n change was detected when DCP concentration was less than 15 % of the initial concentration (BOD_5= 1 $mgO_2.L^{-1}$). Moreover, significant BOD_n values were obtained when all DCP has been disappeared from the solution (H_2O_2 used 100 $mg.L^{-1}$ and BOD_5=8 $mgO_2.L^{-1}$). Further oxidation (by adding more H_2O_2) after elimination all DCP also leads to some improvement in the BOD values (at 140 $mg.L^{-1}$ H_2O_2 BOD_5 =10 $mgO_2.L^{-1}$). However, cost associated with addition more hydrogen peroxide and the low biodegradability enhancement value suggests stopping the reaction at this limit. Through Fenton reactions, BOD_n behavior could be ascribed as follow: at the beginning there were high concentration of DCP. As it was observed in the inhibition test figure 7.3 mixing DCP with other readily biodegradable organic

matters directs to bio-oxidation inhibition. That is the reason why BOD remains constant until almost all DCP vanish from the solution and then the biodegradation start to increase. Moreover, the result suggests that elementary DCP intermediates are not readily biodegradable, and they need supplementary oxidation to degrade it to higher biodegradable material.

With regard of POH, its elimination in the solution acquire small improvement in biodegradability for 40 % increment in POH removal in Fenton reaction only 4 and 6 $mgO_2.L^{-1}$ of BOD_5 and BOD_{21} respectively was obtained.

The same tendency was observed for both DCP and POH treated with modified Fenton reaction, the BOD_5 increases as the degradation of the original contaminates increaser. And maximum BOD_5 was obtained when all the recalcitrant compound were removed.

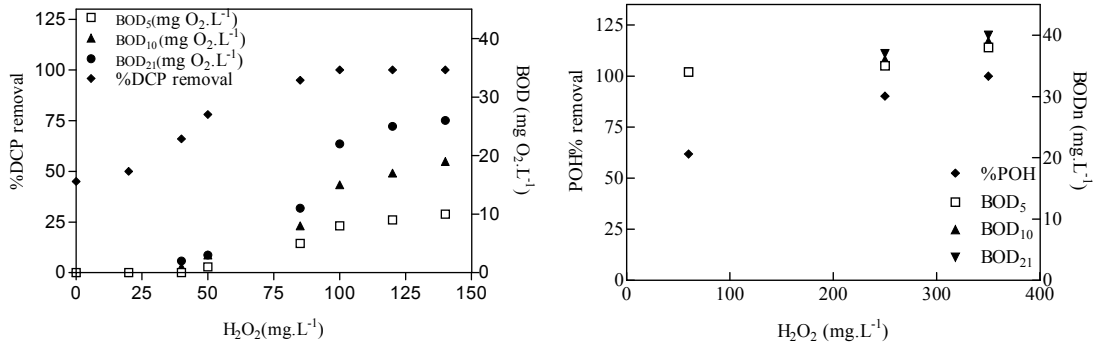

Figure 7.15: Evolution of BOD_n, DCP removal and POH removal as function of initial H_2O_2 in Fenton reaction. $[Fe(II)]_i$ = 10, 60 min reaction time (30 min for POH) and free pH evolution.

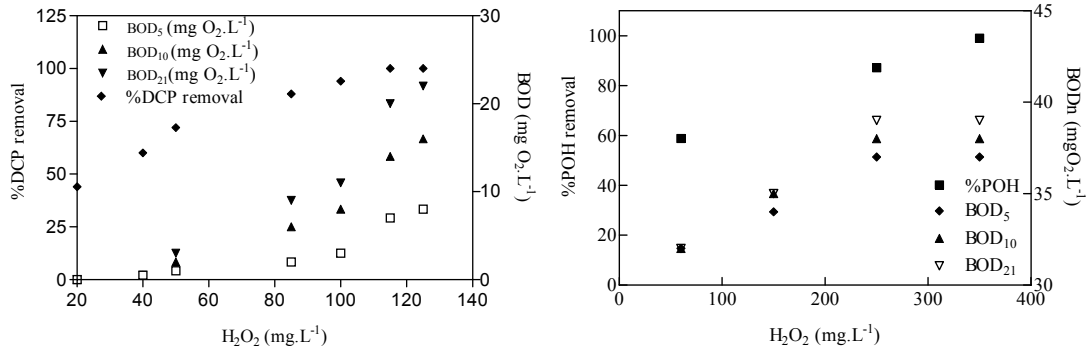

Figure 7.16: BOD_n, DCP removal and POH removal removals percentage evolution as function of initial H_2O_2 in modified Fenton reaction. $[Fe\ (III)]_i$ = 10 $mg.L^{-1}$, 60 min reaction time (30 min for POH) and free pH evolution

BOD_n/COD ratios for Fenton and Fenton like reactions are shown on figures 7.17 and 7.18. Both ratios increase substantially as the initial H_2O_2 concentration increases. Maximum enhancement in the biodegradability was obtained when all the DCP and

POH disappeared from the solution. At this point, BOD_5/COD ratio of DCP treated solution increase from 0 up to 0.12 and 0.13 (0.33 and 0.36 BOD_{21}/COD) after Fenton modified Fenton pre-treatment respectively. For POH this ratio increased up to 0.28 for Fenton and 0.24 for modified Fenton. Generally BOD_n/COD ratio of 0.4 is considered the cut-off point between biodegradable and difficult to biodegrade waste (Metcalf and Eddy, 1985). This biodegradation limit could be achieved by additional Fenton oxidation; 20 $mg.L^{-1}$ increment in H_2O_2 initial concentration increased BOD_{21}/COD ratio of DCP treated solution to 0.40. Nevertheless, Fenton like reaction was not able to reach this limit by adding the same amount of hydrogen peroxide.

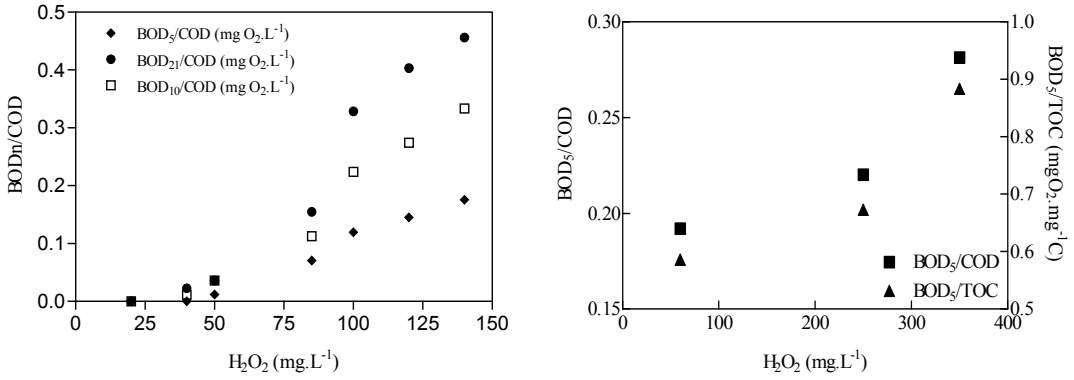

(A) (B)

Figure 7.17: Change in Bon_n/COD ratios as function of initial H_2O_2 concentration in Fenton reaction. (A) DCP with $[Fe(II)]_i$ = 10 $mg.L^{-1}$, 60 min reaction time ((30 min for POH) and free pH evolution, (B)POH with $Fe(II)]_i$ = 10 $mg.L^{-1}$, 30 min reaction time and free pH evolution.

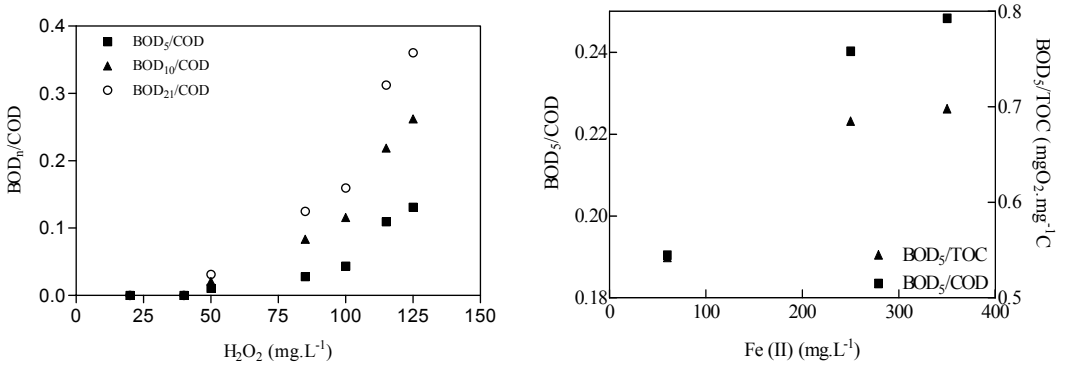

(A) (B)

Figure 7.18: Change in BOD_n/COD ratios as function of initial H_2O_2 concentration for modified Fenton reaction. (A) DCP with $[Fe(II)]_i$ = 10 $mg.L^{-1}$, 60 min reaction time ((30 min for POH) and free pH evolution, (B)POH with $Fe(II)]_i$ = 10 $mg.L^{-1}$, 30 min reaction time and free pH evolution.

The ratio BOD_n/TOC is another biodegradability indicator. Experimental values of BOD_n/TOC ratio for Fenton and Fenton like reactions were studied for both DCP and POH

under the same previous conditions. Results are presented figures 7.18 7.19 for POH and DCP respectively. At 100 % DCP removal the ratio increased from 0.0 to 0.21 (BOD_{21}/TOC 0.60) for Fenton and 0.20 (BOD_{21}/TOC 0.60 and 0.57) for Fenton like reaction. In the same way BOD_5/TOC ratio for POH treated solution increased up to 0.88 and 0.7 for Fenton and Fenton like respectively.

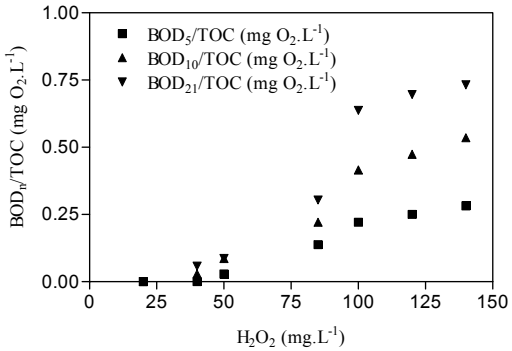

Figure 7.19: Change in BOD_n/TOC ratios as function of initial H_2O_2 concentration for DCP in Fenton and modified Fenton reactions. $[Fe (II)]_i$ or $[Fe (III)]_i$ = 10 $mg.L^{-1}$, 60 min reaction time and free pH evolution.

Effect of initial iron ion concentrations

Experiments carried out with different initial iron concentration were tested for biodegradability improvement. With DCP solution Fenton reactions were carried out using initial H_2O_2 concentrations of (10 and 20 $mg.L^{-1}$), and varying the initial Fe (II) or Fe (III) concentration. throughout these experiments, a maximum DCP removal achieved was (50%). So, no enhancement in biodegradability of treated solution attained.

POH treated solution by Fenton process under different initial Fe(II) concentrations and 20 $mg.L^{-1}$ H_2O_2 shows some improvement in biodegradability. Figure 7.20 presents the change in BOD_5/TOC and BOD_5/COD ratios as function of initial Fe (II) concentration for POH treated solution in Fenton and modified Fenton processes. It can be seen that with Fe(II) initial concentration of 10 $mg.L^{-1}$ BOD_5/COD and BOD_5/TOC ratios developed up to 0.19 and 0.59 respectively. Moreover, for higher amount of Fe(II) the biodegradability enhancement was small; increasing the concentration to 90 $mg.L^{-1}$ leads to increment in the same previous ratios (up to 0.22 and 0.66 respectively).

7.4.4. Change on oxidation state

Effect of initial H_2O_2 concentrations

With respect to the degree of oxidation, figures 7.21 and 7.22 present the change in AOS and COD/TOC ratio as function of initial H_2O_2 during Fenton and modified Fenton reactions. During DCP degradation, H_2O_2 has a remarkable influence in organic mater oxidizing in reaction medium, even at small initial concentration. Increasing the initial H_2O_2 concentration by 20 $mg.L^{-1}$ changes the AOS from -0.233 to 0.057 and COD/TOC ratio from 2.82 to 2.62. The same tendency was observed for modified Fenton reaction; the degree of oxidation increase by increasing the initial H_2O_2 used. This indicates that adding more hydrogen peroxide leads to supplementary hydroxyl radicals production which attack non selectively the organic matter leading to degraded it to more oxidized material.

Dissimilar to that was observer in POH photo-oxidation, 150 $mg.L^{-1}$ H_2O_2 direct only to change in AOS from -0.085 to 0.68 and COD/TOC ratio from 2.72 to 2.13. This indicates that under experimental condition POH and its intermediates faced weak oxidation, for further oxidizing agent needed to be added to change contained organic mater oxidation sate. Similar tendency was noticed in modified Fenton reactions.

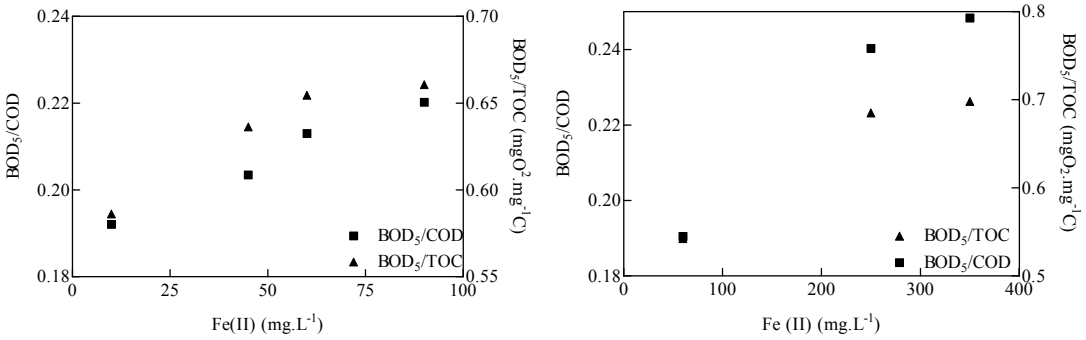

(A) (B)

Figure 7.20: Change in BOD_5/TOC and BOD_5/COD ratios as function of initial Fe (II) concentration for POH treated in A)Fenton and B) modified Fenton reactions. $[H_2O_2]_i$ = 20 $mg.L^{-1}$, 30 min reaction time and free pH evolution

The tiny change in oxidation state of POH and its intermediates may explain the insignificant enhancement on biodegradability during Fenton reaction, in spite the fact that POH is considered as weak biodegradable component.

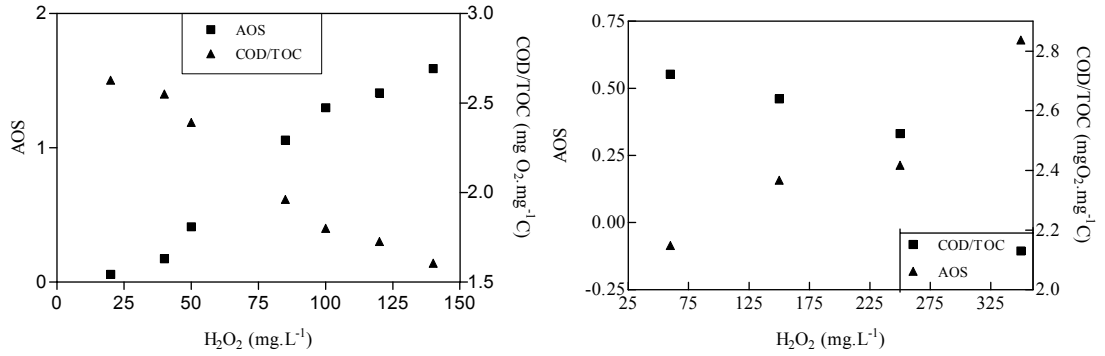

(A) (B)

Figure 7.21: AOS and COD/TOC evolution of as a function of initial H_2O_2 concentration for Fenton process. process (A) DCP $[Fe\ (II)]_i$ = 10 $mg.L^{-1}$, 60 min reaction time and free pH evolution, (B) POH $[Fe\ (II)]_i$ = 10, 30 min reaction time and free pH evolution

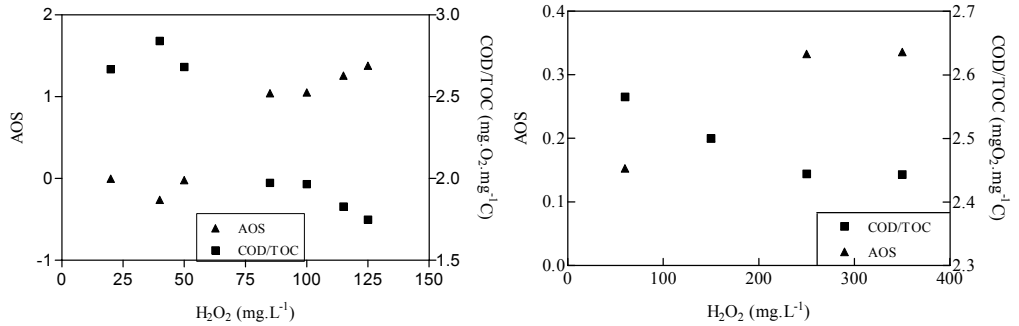

(A) (B)

Figure 7.22: AOS and COD/TOC evolution of as a function of initial H_2O_2 concentration for modified Fenton process (A) DCP $[Fe\ (II)]_i$ = 10 $mg.L^{-1}$, 60 min reaction time and free pH evolution, (B) POH $[Fe\ (II)]_i$ = 10, 30 min reaction time and free pH evolution

Effect of initial iron ion concentrations

The degree of oxidation of DCP, POH and their intermediates during Fenton eactions at different Fe (II) is presented in figure 7.23. Unlike the H_2O_2 tendency, the increment in the initial Fe(II) concentration lead to very small change in the degree of organic matter oxidation. Change the initial iron concentration from 10 to 60 $mg.L^{-1}$ with 20 $mg.L^{-1}$ H_2O_2 in Fenton reaction guide to increase AOS from –0.13 to 0.1 and decrease COD/TOC ratio from 2.7 to 2.6 for DCP. Again at higher Fe(III) concentration it was found that small decline occurred in the oxidation state. The same tendency was observed for POH solution; increasing Fe(II) concentration from 10 to 90 $mg.L^{-1}$ with 30 $mg.L^{-1}$ H_2O_2 in Fenton reaction guide to increase AOS from –0.08 to 0.03 and decrease COD/TOC ratio from 2.72 to 2.64.

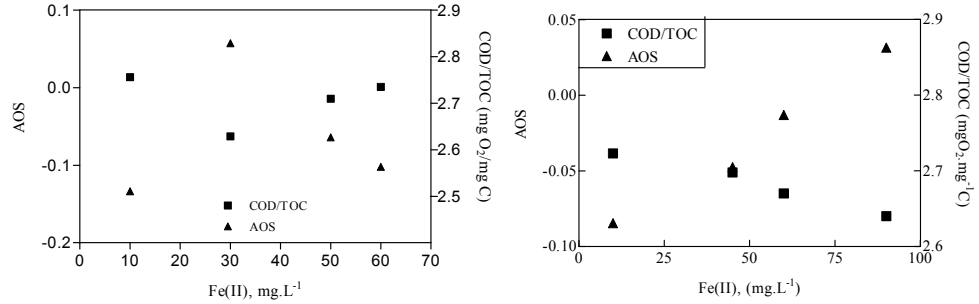

(A) (B)

Figure 7.23: AOS and COD/TOC evolution of as a function of initial Fe (II) concentration for Fenton process. process (A) DCP $[H_2O_2]_i$ = 20 mg.L^{-1}, 60 min reaction time and free pH evolution, (B) POH $[H_2O_2]_i$ = 30 mg.L^{-1}, 30 min reaction time and free pH evolution,

7.5. Treatment of DCP and POH by photo-Fenton

7.5.1. photo-degradation

The rate of degradation of organic pollutant with Fenton/ Fenton like reagents can strongly accelerated by irradiation with UV-light. The combination of UV light with Fenton or Fenton like reaction (photo-Fenton or photo-Fenton like reactions) is advantageous, not only it leads to the formation of additional hydroxyl radicals via photon absorption but also to ferrous catalyst recycling by reduction of Fe (III). By this, the concentration of Fe(II) increases and therefore the reaction is accelerated (Lipczynska-Kochany, 1991).

The increase in Fenton and modified Fenton efficiency with UV-visible irradiation, from now on photo-Fenton, is accredited to:

- Photo reduction of ferric ion: irradiation of ferric ion (and/or ferric hydroxide) produces ferrous ion according to Eq. (7.12). The ferrous ion produced reacts with hydrogen peroxide generating a second hydroxyl radical and ferric ion, and the cycle continue.

$$Fe(III)(OH)^{2+} + h\nu \rightarrow Fe(II) + OH^{\bullet} \qquad (7.9)$$

- Efficient use of light: the absorption spectrum of hydrogen peroxide does not extend beyond 360 nm and has a low molar absorption coefficient beyond 250 nm. On the other hand, the absorption spectrum of ferric ion (and/or hydroxo ferric ion) extends to near UV-visible region and has relatively large molar absorption coefficient, thus making more efficient use of the lamp output when polychromatic light is employed. Consequently, photo-oxidation and

mineralization can be proceed by irradiation with visible light (Pignatello, 1992).

- Photolysis of Fe (III)-organic intermediate chelates: the initial oxidation of organic pollutants generates oxygenated intermediates (i.e. intermediates with hydroxyl and/or carboxyl functional group) which can react with Fe (III) and form complex. These complex are also photoactive and produce CO_2 organic radicals and ferrous iones on irradiation Eq.(1.13) (Balzani, et al., (1970))

$$Fe(III)(RCO_2) + h\nu \rightarrow Fe(II) + CO_2 + R^{\bullet} \qquad (7.10)$$

All this results in an increased rate of destruction of organic pollutant as the reaction progresses.

Effect of Initial H_2O_2 concentrations

It was seen in the previous section that, using Fenton and modified Fenton gave the same result. So, in this section only reaction with Fe(II) will be treated. The degradation of DCP and POH was strongly sensitized by combination of hydrogen peroxide, Fe (II) with UV-light (table DCP-PHF-1 to DCP-PHF-6 and table POH-PHF-1 to POH-PHF-3 Appendix A2), due to the favourable absorption spectrum of the reactants. (Pignatello et al.,1992), this process generates $OH^{\bullet}$ radicals according to:

$$H_2O_2 \xrightarrow{h\nu} 2OH^{\bullet} \qquad (3.3)$$

Hydroxyl radicals are known to react with saturated organic chemicals by H-abstraction from alkyl or hydroxy groups (Walling, 1975) or by an electron transfer process Eqs. (7.16 and 7.15) (Bossmann et al., 1998):

$$RH + OH^{\bullet} \rightarrow R^{\bullet} + H_2O \qquad (7.11)$$

$$RH + OH^{\bullet} \rightarrow (RH)^{+\bullet} + OH^{-} \qquad (7.12)$$

Photo-Fenton reactions at different molar concentration of H_2O_2 were carried out to find out the influence of hydrogen peroxide in DCP and POH degradation. Figures 7.24 and 7.25 present the degradation of both DCP, POH and total organic carbon evolution (TOC) as function of reaction time during photo-Fenton reaction according to the following conditions: 100 $mg.L^{-1}$ DCP or POH, fixed initial Fe(II) concentration 10 $mg.L^{-1}$, 40 min irradiation time for DCP, 15 min for POH and different H_2O_2 initial concentrations.

H_2O_2 has an important rule in $OH^{\bullet}$ production in photo-Fenton reaction, the degradation rate was found to be dependent on the initial H_2O_2 concentration, at free pH and small

initial Fe(II) concentration 10 mg.L^{-1}. It was also observed that H_2O_2 consumed rapidly over the reaction periods, and this leads to significant degradation of DCP and POH. what's more, it was noticed that reaction rate decline when the initial H_2O_2 concentration decrease in the reaction medium. In case of DCP, 100% disappearance of the apparent DCP during 40 min reaction time was obtained when H_2O_2 concentration of 50 mg.L^{-1} was used. However, 220 mg.L^{-1} H_2O_2 was needed to remove 83% of POH solution, it was observed that, the major degradation was observed during the first 20 min of the reaction, this may suggest that the reaction time can be reduced with no affect in POH degradation efficiency. Thus, it was decided to stop POH treatment at this limit and try to modify the reaction condition to get 100% POH elimination. The elimination of all DCP and 83% POH was combined with 21 and 33% TOC removal respectively. which indicates that small conversion of the contained organic material was mineralized to CO_2 and water.

Another set of experiments were carried out for POH solution at high fixed Fe(II) concentration 60 mg.L^{-1} (Table POH- H_2O_2/PHF-4 to POH-H_2O_2/PHF-8 Appendix A2). This concentration was found during Fenton reaction to give high degradation. Summary of experimental results are shown in figure 7.26. Under these experimental condition high oxidation was noticed to take over for 100 mg.L^{-1} POH solution. Only 15 min irradiation time and 300 mg.L^{-1} H_2O_2 was sufficient to degraded all POH in to other intermediates

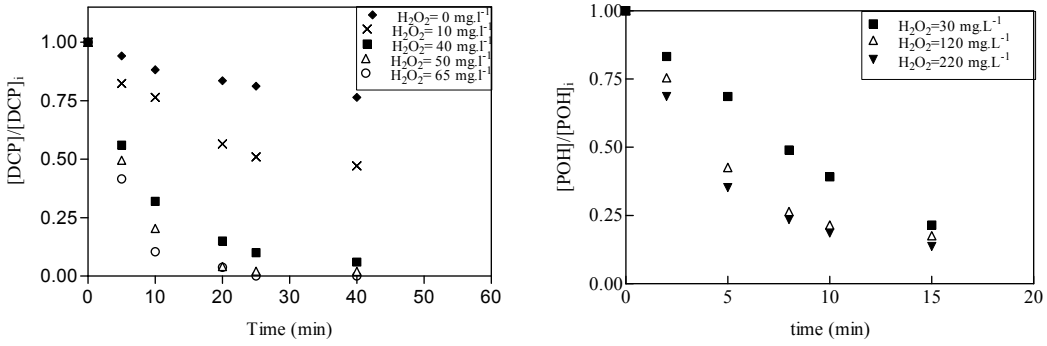

Figure 7.24: DCP and POH degradation in photo-Fenton reaction at different initial H_2O_2 concentrations. $[Fe\ (II)]_i$ =10 mg. L^{-1},free pH evolution.

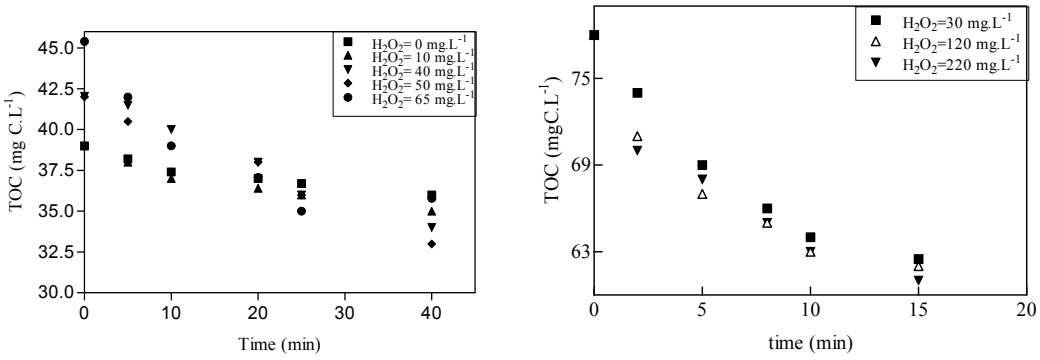

(A) (B)

Figure 7.25: Total organic carbon evolution (TOC) in photo-Fenton reaction and different initial H_2O_2concentrations, A) DCP and B) POH. $[Fe\ (II)]_i$ =10 mg. L^{-1}, free pH evolution.

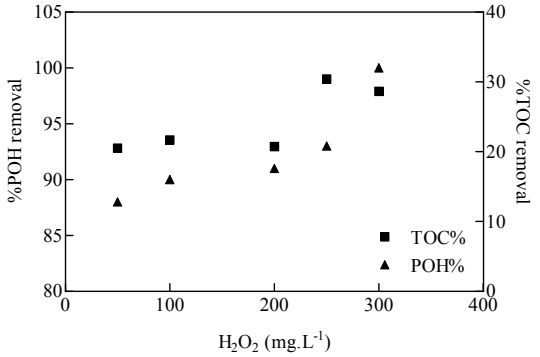

Figure 7.26: POH degradation in photo-Fenton reaction and different initial H_2O_2 concentrations. $[Fe\ (II)]_i$ =60 mg. L^{-1},free pH evolution, 15 min reaction time.

It was expected that increasing the concentration of H_2O_2 reduced the rate of degradation of DCP or POH, due to " self-scavenging" Effect of $OH^{\bullet}$ by H_2O_2 Eq. 7.12 (Stefanet al.,1996 and Kang et al.,1999); and this may be used to get an optimum value for hydrogen peroxide needed for total degradation. Even though the hydroperoxy radical ($HO_2^{\bullet}$) formed in this process, its reactivity with organic compounds is low (Herrera et al., 1998).

$$OH^{\bullet} + H_2O_2 \longrightarrow HO_2^{\bullet} + H_2O \qquad (7.12)$$

However, in our experiments this effect has not been detected. Although all DCP and POH were disappeared from the reaction solution, increasing initial H_2O_2 guide to oxidize the formed intermediates. Figure 7.27 presents the evolution of COD and TOC removal as function of H_2O_2 initial concentration for DCP solution. It can be seen that, rising the initial H_2O_2 concentration direct to more oxidation of the contained organic matter. 50 % of COD conversion was obtained when 50 $mg.L^{-1}$ H_2O_2 was used, while it reached to 61% when H_2O_2 was increased to 70 $mg.L^{-1}$. This implies that the photo-

Fenton reaction could be used for total mineralization of organic compound to CO_2 and H_2O, as it will see later. The same tendency was noticed in case of POH solutions.

The degradation rate of DCP and POH by photo-Fenton process was also studied based in first order kinetic model [Eq. (7.1)]. Logarithmic of normalized reactant concentrations vs. irradiation time is plotted in figure 7.28 (results for POH not presented). The kinetic constant value and half-life time at different initial hydrogen peroxide concentrations are presented in table 7.6.

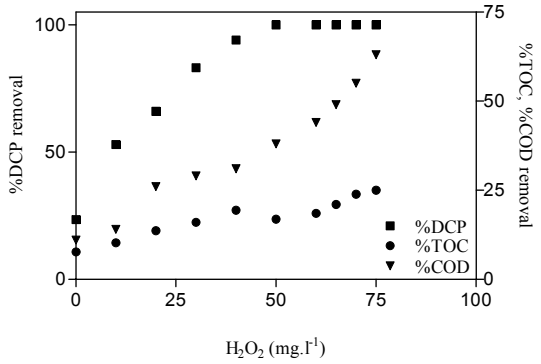

Figure 5.27: DCP, TOC and COD removal percentage as function of H_2O_2 in photo-Fenton process. [Fe (II)]$_i$ =10 mg. L^{-1} experimental time 40 min.

Table 7.6: Values of reaction rate constants, half-life time for DCP and POH degraded by photo-Fenton at different initial H_2O_2 concentrations. [Fe(II)]$_i$ =10 mg.L^{-1} experimental time 40 min (15 min in POH case) and free pH evolutions

DCP			*POH*		
$[H_2O_2]$ ($mg.L^{-1}$)	*$t_{1/2}$ (min)*	*K_0 (min^{-1})*	*$[H_2O_2]$, ($mg.L^{-1}$)*	*$t_{1/2}$ (min)*	*K_0 (min^{-1})*
0	> 40	0.0163	30	8	0.0965
10	28	0.0266	120	4.1	0.136
40	8	0.1007	220	3.5	0.153
50	4.5	0.1062			

DCP and POH degradation rate is highly dependent in H_2O_2 initial concentration. It is remarkable to mention here the high affect of H_2O_2 in the first order kinetic constant of POH, significant improvement of the degradation rate was noticed by increasing the initial hydrogen peroxide concentration. Moreover, a considerable difference between the kinetic constants was noticed with respect to POH solution, as it can be seen in the table POH under experimental condition is more faster than DCP. However, it should

not forgot the high amount of H_2O_2 used in phenol and the difference in irradiation time which make the comparison between both compound just qualitative.

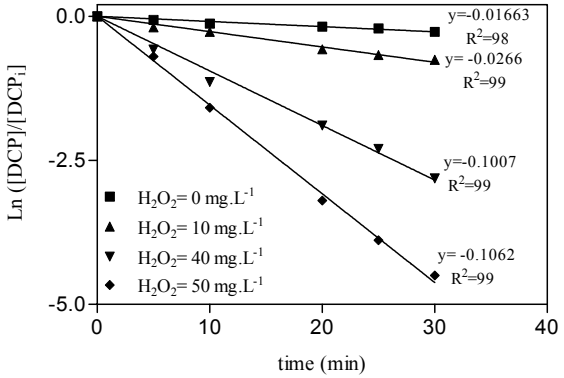

Figure 7.28: First-order plot for degradation of DCP as function of initial H_2O_2. $[Fe(II)]_i$=10 mg:L^{-1} and free pH evolution.

Effect of initial iron ion concentration

Iron has important rule in photo-Fenton reactions. Iron species in solution are considered to act as catalysts and have beneficial effect in forming oxidizing species in continuous cycle Fe (II)/ Fe (III)/ Fe (II) (see Eq. 7.13 and 7.15). So, it was decided to study the effect of iron in the degradation of DCP and POH to obtain the optimal Fe (II) amount.

$$Fe^{+2} + H_2O_2 \rightarrow Fe^{3+} + OH^{\bullet} + OH^{-} \quad (7.13)$$

$$Fe^{3+} + H_2O \xrightarrow{h\gamma} Fe^{2+} + OH^{\bullet} + H^{+} \quad (7.14)$$

$$H_2O_2 \xrightarrow{h\gamma} 2OH^{\bullet} \quad (7.15)$$

Photo-Fenton reactions were carried out with various amounts of the iron salt and fixed H_2O_2 initial concentration (table DCP-PHF-7 to DCP-PHF-15 and POH-PHF-9 to POH-PHF-11 appendix A2). Figure 7.29 presents the degradation of DCP and POH as function of time for different initial Fe (II) concentration and fixed initial H_2O_2 (10 mg.L^{-1} for DCP and 50 mg.L^{-1} for POH. Removal percentage and TOC reduction as function of initial Fe (II) for both compound (DCP and POH) are presented in figure 7.30

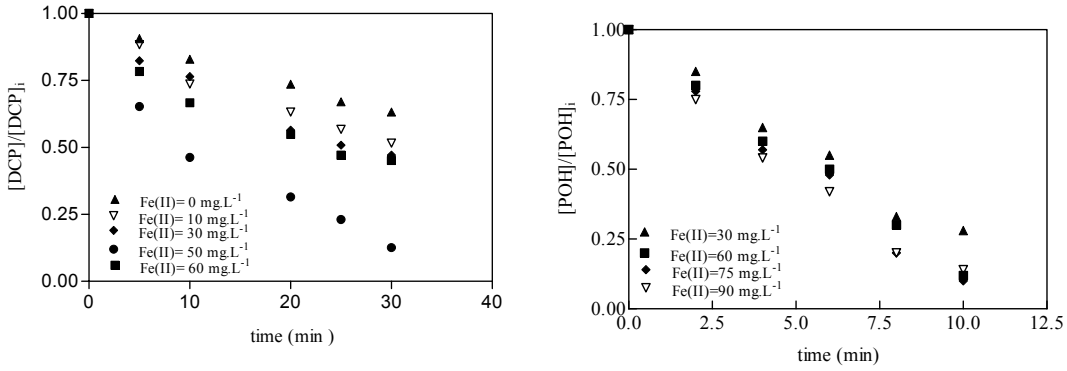

(A) (B)

Figure 7.29: DCP and POH degradation as function of time for different Fe (II) initial concentration. (A) $[H_2O_2]_i$= 10 mg.L^{-1} and experimental time 40 min. (B) $[H_2O_2]_i$= 50 mg.L^{-1} and experimental time 15min and free pH evolution.

The figures illustrate that addition of Fe (II) enhance the efficiency of photo-Fenton reaction in DCP degradation. The degradation rate distinctly increased with increasing amounts of iron salt. However, it was noticed that, specially in DCP case, the reaction reach a concentration at which catalytic reaction effect is weak, and addition of the iron salt above this point (50 mg.L^{-1} for DCP) did not improved the degradation, but rather perceptible decrease in the degradation rate occurred.

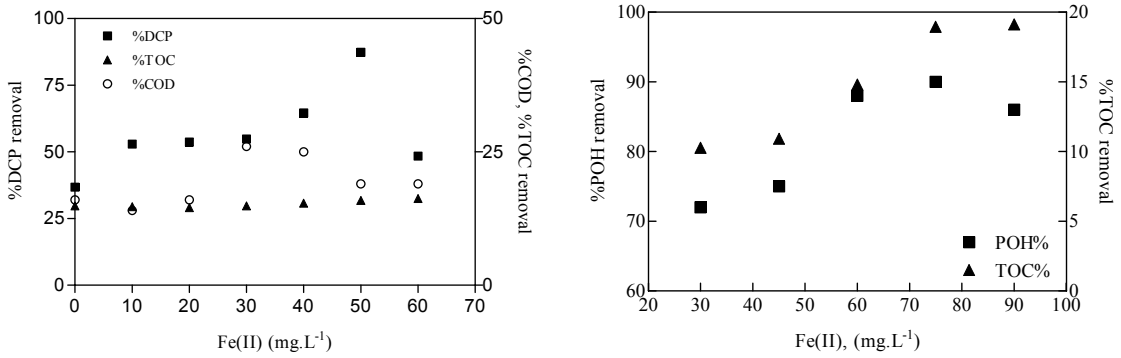

(A) (B)

Figure 7.30: DCP, POH and TOC removal percentages as function of initial Fe(II). (A) $[H_2O_2]_i$= 10 mg.L^{-1} and reaction time 40 min. (B) $[H_2O_2]_i$= 50 mg.L^{-1} and reaction time 15min and free pH evolution.

This may be explained due to the fact that during several elementary steps of reaction mechanism, iron can consume radicals with potentially negative effect in the reaction rate. Unlike that, this effect was insignificant on POH degradation. Ghaly et al., (2001) studied the degradation of p-chlorophenols by photo-Fenton reaction, and they reported that higher addition of iron salt resulted in brown turbidity that slowed down the

absorption of UV light required for photolysis and cause the recombination of hydroxyl radicals. In this case Fe (II) act as scavenger for $OH^{\bullet}$ radicals. On the other hand, the use of large quantities of Fe in solution has negative effect from the applied point of view, since it implies the need of an additional treatment step for Fe(II) removal. So, it is desirable that the ratio of H_2O_2 to Fe (II) should be as small as possible, and both radicals recombination and sludge production from iron complex can be evaded. Under the studied conditions, increasing the initial Fe(II) from 30 to 50 $mg.L^{-1}$ direct to increase DCP degradation from 54 up to 87% and POH degradation from 65 to 82%.

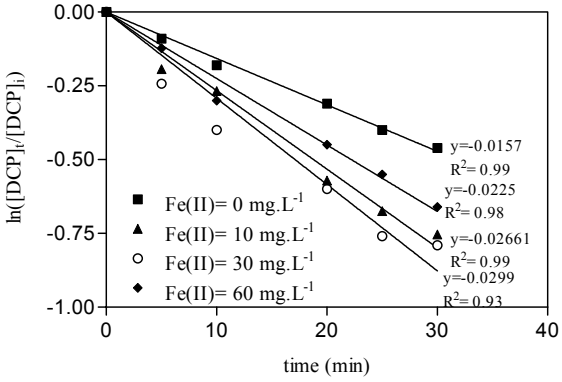

Figure 7.31: First-order plot for degradation of DCP as function of initial Fe (II) in photo-Fenton reaction:$[H_2O_2]_I$= 10 $mg.L^{-1}$ and free pH evolutions.

First order kinetic model also applied to photo-Fenton reaction at different Fe(II) initial concentration. Figure 7.31 (only DCP presented). Unlike the H_2O_2, it can be seen that at higher amount of iron no significant increase the degradation rate. Kinetic constant values and half-life time are presented in table 7.8. The results suggest that the maximum degradation of DCP can be obtained at Fe (II) initial concentration a round 50 $mg.L^{-1}$. Moreover a slight decrease in the reaction constants when initial iron concentration augmented to 60 $mg.L^{-1}$, as result of iron scavenging effect. The same affinity was noticed for POH kinetics, but the catalytical effect deactivation was trivial and take place at higher initial Fe(II) concentration (75 $mg.L^{-1}$).

Table 7.7: Values of reaction rate constants of the degradation of DCP and POH at different initial Fe (II) concentrations. DCP initial condition :$[H_2O_2]_I$= 10 , 40 min reaction time and free pH evolution, POH:$[H_2O_2]_I$= 50 $mg.L^{-1}$,15min reaction time and free pH evolution.

DCP			*POH*		
Fe (II) *($mg.L^{-1}$)*	K_o *(min^{-1})*	$t_{1/2}$ (min)	*Fe (II)* *($mg.L^{-1}$)*	K_o *(min^{-1})*	$t_{1/2}$ (min)
0	0.0157	>30	30	0.101	4.8
10	0.0266	28	60	0.1474	4.2
30	0.0229	28	75	0.1545	4.2
50	0.0642	10	90	0.1413	4.66
60	0.0225	20	-	-	-

Effect of initial pH:

pH value affects the oxidation of organic substances both directly and indirectly. During the photo-Fenton process the major dominated reactions are Fenton, photolysis of hydrogen peroxide and photo-reduction of ferric ion, (Eqs. 7.16 to -7.18) respectively (Fenton, 1894, Baxendale and Wilson, 1956, Faust and Hoigne 1990).

$$H_2O_2 + Fe^{+2} \rightarrow OH^{\bullet} + Fe^{+3} + OH^{-} \quad (7.16)$$

$$H_2O_2 + UV \rightarrow 2OH^{\bullet} \quad (7.17)$$

$$Fe^{+3} + UV + H_2O \rightarrow OH^{\bullet} + Fe^{+2} + H^{+} \quad (7.18)$$

As indicated in Eq. (7.16) the amount of $OH^{\bullet}$ formed through Fenton process is affected by solution pH. The $OH^{\bullet}$ can be efficiently formed under acidic conditions. On the contrary, H_2O_2/UV process is independent of pH conditions, according to Eq. (7.17). It has been reported that photo-Fenton process can effectively remove toxic and refractory organics such as landfill leachate (Kim et al.,1997) nitrogen containing organics (Maletzky and Bauer, 1998), colour in dye manufacturing wastewater (Kang J-W et al 1999) at pH 3, 3.5 and 5. In other words, the photo-Fenton process can remove pollutant under acidic and neutral conditions.

The effect of initial pH at photo-Fenton process is presented in Figure 7.32 (table DCP-PHF-16 to DCP-PHF-21 appendix A2). For both POH and DCP a maximum degradation was obtained at acidic pH (pH=3.0), then the degradation decrease for pH

above 4.5 because at higher pH value iron ions may precipitate as hydroxide and that reduced the transmission of the radiation.

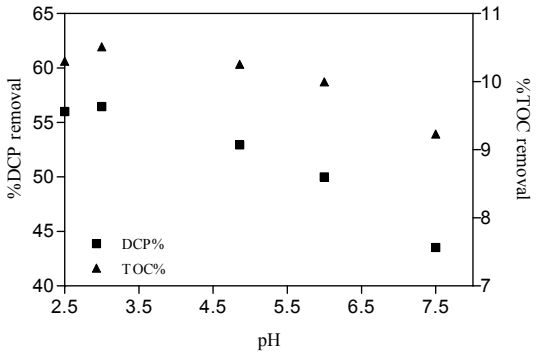

Figure 7.32: Evolution of DCP degradation as function of pH, $[H_2O_2]_i$= 10 mg.L^{-1}, $[Fe\ (II)]_i$ =10 mg.L^{-1} and reaction time 40 min.

During photo-Fenton reaction there were pH drop from any initial pH to 2.8. The overall pH drop is corresponds to an increase in the $[H^+]$ concentration in solution by a factor of almost 7 (Ormad et al., 2001). This suggests that at this pH value 2.8 Eq. (7.19) is controlling during the degradation process and not the $OH^\bullet$ radical generation.

$$Fe(III) + H_2O_2 \rightarrow Fe(II) + HO_2^\bullet + H^+ \qquad (7.19)$$

However, Fenton reaction leading the pH of the system in the opposite direction

$$Fe(II) + H_2O_2 \rightarrow Fe(III) + OH^\bullet + OH^- \qquad (7.20)$$

It is known that superoxide radical $HO_2^\bullet$ has a considerably lower one-electron standard potential $HO_2^\bullet / O_2^-$ Eº =0.75 V compared to the $OH^\bullet$ radical with $(OH^\bullet / OH^-)$ Eº =1.90 V. This may give an explanation of the Photo-Fenton rate slowing down as the reaction proceeds.

Another important point, in case of DCP, considers the evolution of HCl during the mineralization of DCP proceeding according to Eq (7.26).

$$HO - C_6H_3 - Cl_2 + H_2O_2 + \frac{11}{2}O_2 \rightarrow 6CO_2 + H_2O + 2HCl \qquad (7.21)$$

Effect of initial DCP and POH concentration

The change of initial DCP concentrations was also studied (table DCP-PHF-22 and POH-PHF-11 appendix A2). Fixed concentrations of hydrogen peroxide and iron (II) was chosen to study the degradation rate, and all experiments were held at room

temperature and free pH evolution. Experimental results are stipulated in figure 7.33 and 7.34.

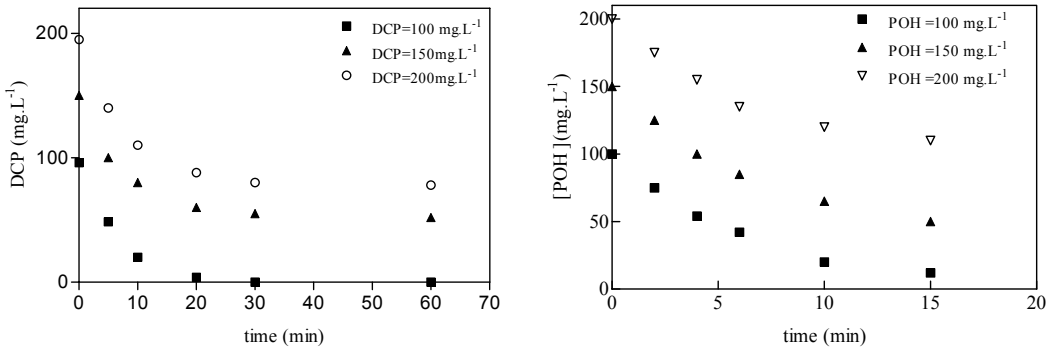

Figure 7.33: DCP and POH evolution as function of time for different initial concentrations, initial condition; for DCP are $[H_2O_2]_i$= 50 mg.L^{-1} $[Fe(II)]_i$ = 10 mg.L^{-1} and free pH evolution, for POH $[H_2O_2]_i$= 50 mg.L^{-1} $[Fe(II)]_i$ = 60 mg.L^{-1}.

Although it was started with the same reactant concentrations (50 mg.L^{-1} H_2O_2 and 10 mg.L^{-1} Fe(II) for DCP , 50 mg.L^{-1} H_2O_2 and 60 mg.L^{-1} Fe(II) for POH), it was noticed that, the rate of degradation is related to initial contaminant concentration. 100% of DCP was removed when 50 mg.L^{-1} initial H_2O_2 concentrations was used, while it is only 60 % for 200 mg.L^{-1} H_2O_2. It is interesting to note that, for all DCP initial concentrations, TOC% is in the same order of magnitude. The same affinity could be seen through POH degradation (87 %POH degradation at 100 mg.L^{-1} and 35% at 200 mg.L^{-1} initial POH concentration).

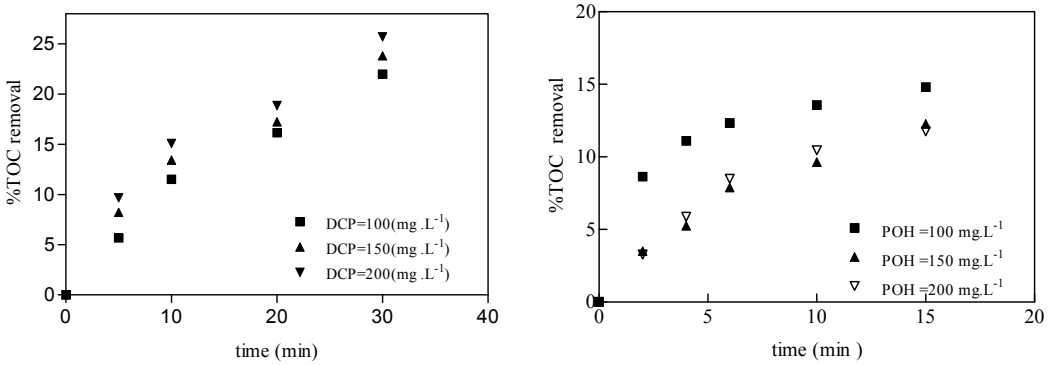

Figure 7.34: Evolution of TOC vs. reaction time for different DCP and POH initial concentrations, initial condition; for DCP are $[H_2O_2]_i$= 50 mg.L^{-1} $[Fe(II)]_i$ = 10 mg.L^{-1} and free pH evolution, for POH $[H_2O_2]_i$= 50 mg.L^{-1} $[Fe(II)]_i$ = 60 mg.L^{-1} .

From figure 7.33 it can be noticed that, DCP and POH degradation concentration follow zero order kinetic, for DCP average zero order kinetic constant of 0.0045 $mol.min^{-1}$ was obtained. The same of that is POH, results are presented in table 7.8 for zero order kinetic constant K_z ($mol.min^{-1}$) and half- life time $t_{1/2}$ (min).

Table 7.8: Values of reaction rate constants of POH degradation at different initial concentrations. $[H_2O_2]_I$= 50 $mg.L^{-1}$, $[Fe(II)]_I$= 50 $mg.L^{-1}$, 15 min reaction time and free pH evolution.

$[POH]_i$ ($mg.L^{-1}$)	K_z ($mol.min^{-1}$)	$t_{1/2}$ (min)
100	0.0521474	4
150	0.0046	8
200	0.043	20

Effect of UV light irradiation time:

To elucidate the effect of UV-light in the degradation rate. Experiments were done using UV/H_2O_2 and photo-Fenton process (table DCP-PHF-23 and DCP-PHF-24 appendix A2). The first 8 min of both reactions were carried out in the dark (with out UV-light), after that, UV light was switched on until the end of the experiments (see figure 7.35) (results concerning DCP). During the first 8 min, DCP degradation was 12 % for UV/H_2O_2 and 21 % for photo-Fenton, while the degradation augment to 45% and 43% when UV applied during the remaining 22 min of the experiment. The total DCP removal was 76% and 83% in the two respective cases. In spit that dark reactions were applied at appropriate condition for formation hydroxyl radicals as result of existence high initial concentration of H_2O_2, at the moment UV light switched on there were noticeable increase in the degradation rate. Also it can be seen the fast response of photo-Fenton reaction to the presence of UV-light comparing with H_2O_2/UV system. Moreover, it can observe from the figure that the reaction rate is so fast during the first 10 min after UV switched on and after that it almost constant.

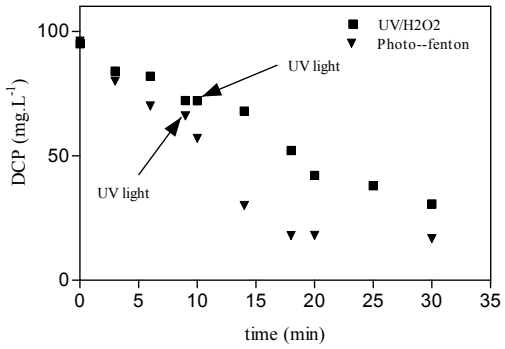

Figure 7.35:Variation of DCP as function of UV irradiation time for: UV/H_2O_2 and photo-Fenton processes, $[H_2O_2]_i$ =30 $mg.L^{-1}$, $[Fe(II)]_i$ =10 $mg.L^{-1}$

7.5.2. Dechlorination

During photo-Fenton reaction chlorine ions were formed continuously, providing that dechlorination takes place in the oxidation processes. Chlorine ion concentration increased during the first 40 minutes of the reaction (as indicated in table DCP-PHF-4). For 94% of DCP elimination, 55% of dechlorination was achieved, and at 100% of DCP elimination, the dechlorination was 73% (figure 7.36). From DCP decrease and Cl^- ion formation, it is readily seen that the rates of these two processes are not similar. This may suggest the formation of aromatic and aliphatic chlorinated compounds (Abe and Tanaka, 1997). Trapido et al. (1997) reported that a 62% dechlorination can be obtained for 97% of DCP elimination, which is in agreement with the achieved experimental results.

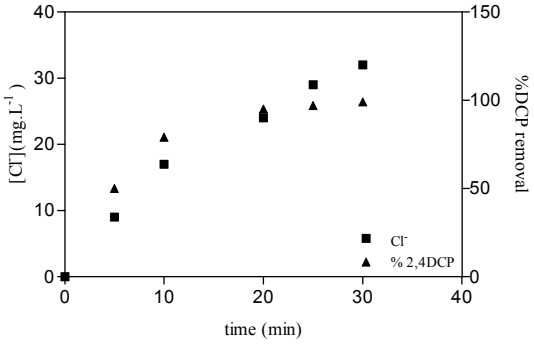

Figure 7.36: Evolution of chloride ion and DCP % elimination as function of reaction time. $[H_2O_2]$=50 $mg.L^{-1}$, [Fe(II)]=10 $mg.L^{-1}$.

7.5.3 Influence of photo-Fenton in Biodegradability

To study the effect of photo-Fenton process in the biodegradability of DCP and phenol pre-treated solutions, it was necessary to examine all the conditions that affect contaminant (DCP or POH) degradation.

Effect of initial H_2O_2 concentrations

To study the effect of hydrogen peroxide in biodegradability of DCP and POH treated by photo-Fenton, the solutions studied before were neutralized and tested for their biodegradability.

BOD_n of phenol and DCP solution as function of initial H_2O_2 concentration and fixed Fe(II) initial concentration 10 $mg.L^{-1}$ is presented in figure 7.37. In general, an increase in the BOD_n of the pre-treated solution points out improvement in solution bio-compatibility. It was observed that, BOD_n of DCP treated solution increases as the initial hydrogen peroxide increase, being BOD_5 =13, BOD_{10} =14 and BOD_{21} =17

$mgO_2.L^{-1}$ when all DCP disappeared form the solution. The same tendency could be observed for POH, as much H_2O_2 added as more is the BOD_5 enhancement. The use of 150 $mg.L^{-1}$ H_2O_2 (at this concentration almost 70% POH was removed)leads to BOD_5 increment from 27for original POH solution up to 44 $mgO_2.L^{-1}$. It is remarkable to note that, the variation of biodegradability between BOD_5 and BOD_{21} for POH pre-treated solution is insignificant so it was decided just to present BOD_5 evolution.

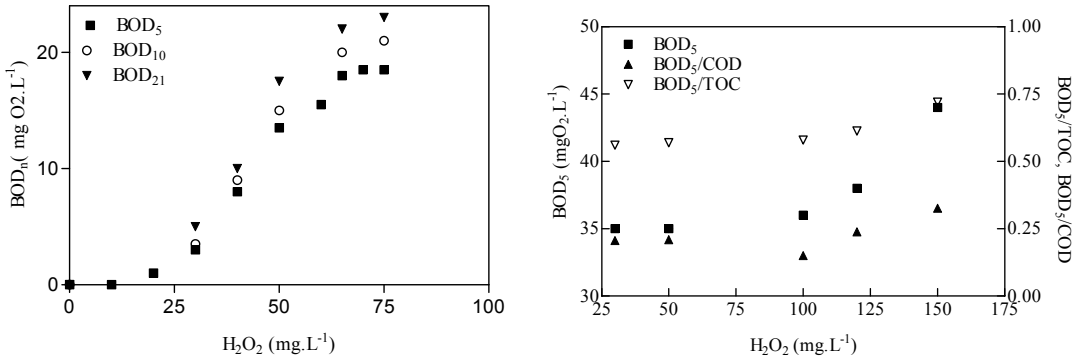

(A) (B)

Figure 7.37: BOD_n as function of initial H_2O_2 concentration for A) DCP Initial conditions, DCP are $[Fe(II)]_i$= 10 mg-L^{-1}, 40 min reaction time and POH solution treated by photo-Fenton. and B)POH Initial conditions, $[Fe(II)]_i$= 10 mg-L^{-1}, 15 min.

BOD_5/COD and BOD_5/TOC ratios for both components (DCP and POH) are shown on Figures 7.37 and 7.38. As expected increasing the amount of hydrogen peroxide used in the reaction increases the biodegradability (measured as BOD_5/COD and BOD_5/TOC). The increment in BOD_5/COD and BOD_5/TOC ratios after pretreatment is an indicative of biodegradability improvement due to increase in contained organic matter proportion (COD or TOC) willing to bio-oxidation. Both ratios increase substantially by elimination and /or degradation more DCP or POH, a values of 0.19 BOD_5/COD and 0.4 BOD_5/TOC (0.24 and 0.57 for BOD_{21}/COD and BOD_{21}/TOC respectively) was achieved at the moment where 100% DCP removed. For POH (under the same previous conditions 83%POH removal) these ratios (BOD_5/COD and BOD_5/TOC) increased up to 0.32 and 0.85 respectively. As it was mentioned before, biodegradable domestic wastewater has a BOD_5/COD ratio between 0.4 to 0.8 and BOD_5/TOC ratio between 0.6 to 1.6 and it is considered substantially biodegradable (Metcalf and Eddy, 1985). These limits could be attained by additional oxidation. For DCP solutions, adding extra 15

mg.L^{-1} H_2O_2 increased BOD_5/COD and BOD_5/TOC ratios up to 0.40 and 0.53 respectively. With respect to POH another conditions were tested to reach these limits.

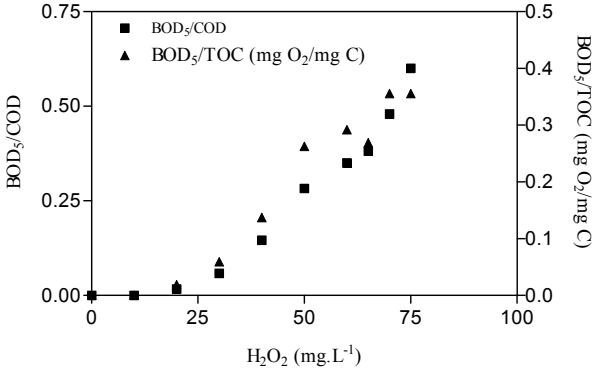

Figure 7.38: BOD_5/COD and BOD_5/TOC as function of initial H_2O_2 concentration for DCP solution. [Fe (II)]$_i$= 10 mg-L^{-1}, 40 min reaction time.

Figure 7.39 presents BOD_5/COD and BOD_5/TOC ratio for POH solution treated with following conditions: different initial H_2O_2, initial Fe (II) 60 mg-L^{-1} and 15 min reaction time. All photo-Fenton conditions used in this set lead to a significant improvement in biodegradability of treated solution up to domestic wastewater limit (BOD_5/COD > 0.40). However, during these experiments, different tendency in what presented before was observed. At higher hydrogen peroxide concentration (from 200 up to 300 mg.L^{-1}) the biodegradability of the solution follows the same evolution as was expected, that is an increase of the biodegradability by increasing the initial hydrogen peroxide used in the reaction. But, for lower hydrogen peroxide concentration (from 50 to 200 mg.L^{-1}) the results are the opposite what was expected. It was observed higher biodegradability at lower initial hydrogen peroxide, and proceeding more in oxidation other by-product formed which is less biodegradable. The explanations for that, could be attribute to degradation of POH during the earlier oxidation into other by-products like catecols, quinones and hydroquinone which are less biodegradable than POH itself (Lunok et al., 1992 and Liao et al., 1995). Hence, addition more hydrogen peroxide degrades such components to other by-product, which are readily biodegradable. So, the biodegradability starts to increase again. Moreover, significant improvement in biodegradability for POH treated solution was acquired under this conditions. With only 15 min irradiation time, 50 mg-L^{-1} H_2O_2 and 60 mg.L^{-1} Fe(II) biodegradability value of BOD_5/COD =0.71 was achieved. This represents significant improvement

compared with original POH solution (BOD_5/COD =0.12). The same increment also obtained at conditions: 15 min irradiation time, 300 mg-L^{-1} H_2O_2 and 60 mg.L^{-1} Fe(II).

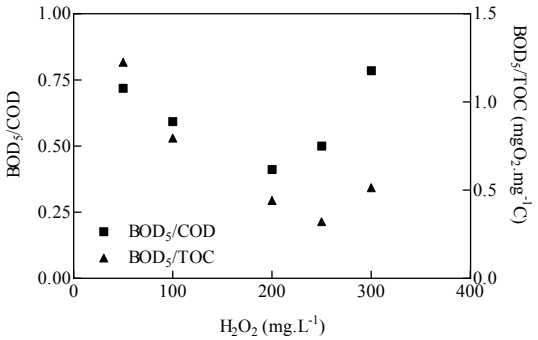

Figure: 7.39: BOD_5/COD and BOD_5/TOC as function of initial H_2O_2 concentration for POH solution. [Fe (II)]$_i$= 60 mg-L^{-1}, 15 min reaction time.

As presented before, the presence of DCP in small concentrations may lead to oxygen consumption inhibition. Figure 5.40 presents the change in the biodegradability (BOD_5/COD and BOD_5/TOC) as a function DCP removal percentage, for photo-Fenton experimental conditions $[H_2O_2]_i$= 50 mg.L^{-1}, $[Fe(II)]_i$ =10 mg.L^{-1} 40 min and free pH evolution. The BOD_5/COD and BOD_5/TOC ratios were found to start to increase when the amount of DCP removed was more than 20% of the original concentration. Moreover, noticeable increment in the biodegradability was observed when all DCP eliminated (0.0 to 0.18 and to 0.32) for BOD_5/COD and BOD_5/TOC respectively.

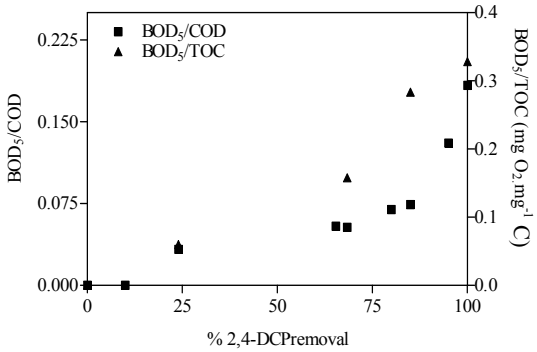

Figure 7.40: BOD_5/COD and BOD_5/TOC as a function DCP removal percentage. $[H_2O_2]_i$= 50 mg.L^{-1}, [Fe(II)]i =10 mg.L^{-1} 40 min and free pH evolution.

Effect of iron salts concentrations

The biodegradability improvement of solutions carried out in photo-Fenton at different initial Fe (II) concentration were tested. The following photon-Fenton conditions were used for each component; a) DCP: two initial H_2O_2 concentration 10 and 30 mg.L^{-1}, 40

min reaction time and free pH evolution, b) POH: two fixed H_2O_2 concentration 50 and 300 mg.L^{-1} and 15 min reaction time. The BOD_n for the treated solution was followed during the reactions.

For DCP solutions with initial H_2O_2 concentration 10 mg. L^{-1}, There where small increment in the BOD_n values as result of remaining DCP. Figure 5.41 presents the BOD_n values of DCP pre-treated solution carried out with photo-Fenton at initial H_2O_2 concentration of 30 mg.L^{-1} and different Fe(II) concentrations. The figure point out the enhancement in the BOD_n as function of initial Fe (II). At the beginning, BOD_n increases as initial Fe (II) and DCP removal percentage increased, and it reach the maximum value at the point when all the DCP disappears from the solution (11 mg $O_2.L^{-1}$ BOD_5 and 14 mg $O_2.L^{-1}$ BOD_{21}). Further addition of Fe (II) does not lead to BOD_n improvement. An explanation for that, as it was noticed during DCP degradation, higher iron ion concentration slow down the UV absorption and act as scavenger for $OH^{\bullet}$. Consequently, the DCP removal from the solution decreases, the presence of DCP in solution has affect bacterial culture activity. Hence, the BOD_n value decrease.

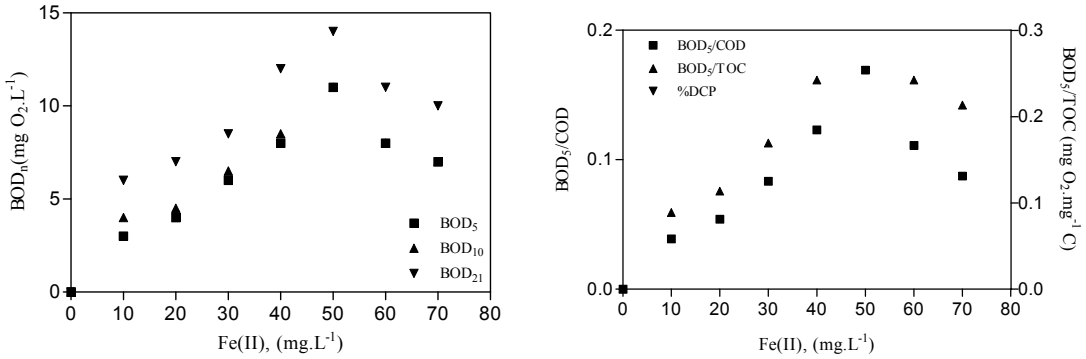

Figure 7.41: BOD_n, BOD_5/COD and BOD_5/TOC as function of initial Fe (II) concentration for DCP in photo-Fenton, $[H_2O_2]_i$= 30 mg-L^{-1}, 40 min reaction time.

The same tendency was detected for POH treated solutions at photo-Fenton experiment conditions of 50 mg.$L^{-1}H_2O_2$, 15 min reaction time and free pH evolution (see figure 7.42). With initial Fe(II) concentration of 30 mg.L^{-1} BOD_5 was found to be 80 mg$O_2.L^{-1}$, increasing initial iron concentration up to 90 mg.L^{-1} leads only to enhancement in BOD_5 up to 105 mg$O_2.L^{-1}$ which indicate slight improvement in the treated solution biodegradability.

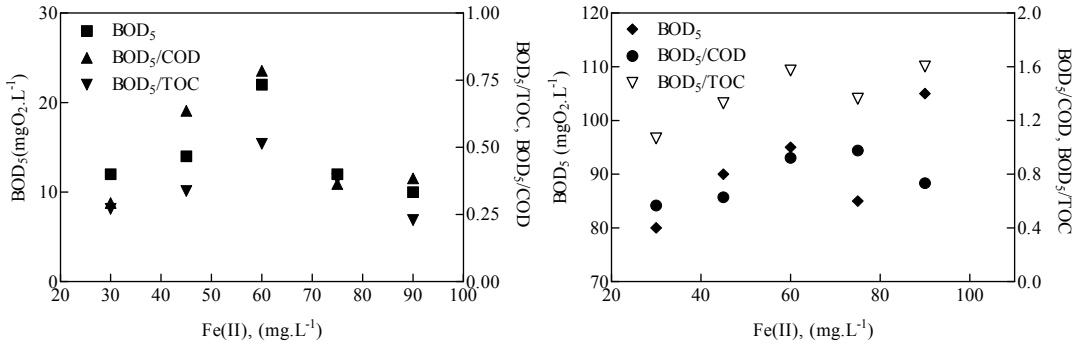

(A) (B)

Figure 7.42: BOD_5, BOD_5/COD and BOD_5/TOC as function of initial Fe (II) concentration for POH treated solution, A) $[H_2O_2]_i$= 50 mg-L^{-1}, 15 min reaction time and free pH evolution, B) $[H_2O_2]_i$= 10 mg-L^{-1}, 15 min reaction time and free pH evolution .

BOD_5/COD and BOD_5/TOC ratios for treated solutions were checked to see the increase in the contained organic matter fraction (COD or TOC) able to biodegradation. Figures 7.41 and 7.42 present biodegradability parameters (BOD_5/COD and BOD_5/TOC) as function of initial Fe(II) used for DCP and POH solutions. The biodegradability improves by adding more Fe(II) due to oxidize and/or degradation more DCP and POH. For 100% DCP removal BOD_5/COD of 0.17 and BOD_5/TOC of 0.33 were acquired. But, adding more Fe(II) for supplementary oxidation was not successful for more biodegradability enhancement.

With respect to POH treated solution, under the same previous conditions ($[H_2O_2]_i$= 10 mg-L^{-1}, 15 min reaction time and different initial Fe(II)concentrations). Different tendency was observed. Increasing the initial Fe(II) guide to increase the biodegradability all over the reaction. once more a considerable biodegradability value was achieved; with only 15 min irradiation time, 50 mg.$L^{-1}H_2O_2$ a biodegradability value of BOD_5/COD =0.73 was achieved.

Also POH biodegradability under high initial H_2O_2 concentrations and different initial Fe(II) was tested. Figure 7.43 illustrates BOD_5/COD and BOD_5/TOC as function of initial Fe (II) concentration for the treated solution. Under these conditions, the catalytic reaction deactivation and scavenging effect of Fe(II) was found to occur at Fe(II) of 50 mg.L^{-1}. Consequently, the biodegradability was found to take maximum vale at this concentration, after words the tendency diminish. Also with these condition, important biodegradability value of 0.78 was obtained.

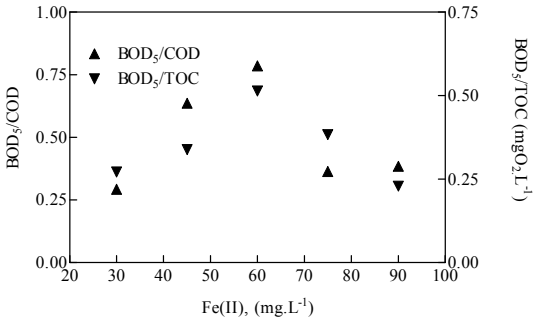

Figure 7.43: BOD_5/COD and BOD_5/TOC as function of initial Fe (II) concentration for photo-Fenton, $[H_2O_2]_i$= 300 mg-L^{-1}, 40 min reaction time.

Figure 7.44 presents the change in the biodegradability (BOD_5/COD and BOD_5/TOC) as a function DCP removal percentage, for photo-Fenton reaction done at initial Fe (II) concentration 30 mg. L^{-1} and $[H_2O_2]_i$= 30 mg. $L^{-1}$for 40 min and free pH evolution. Experimental results confirm the previous observations.

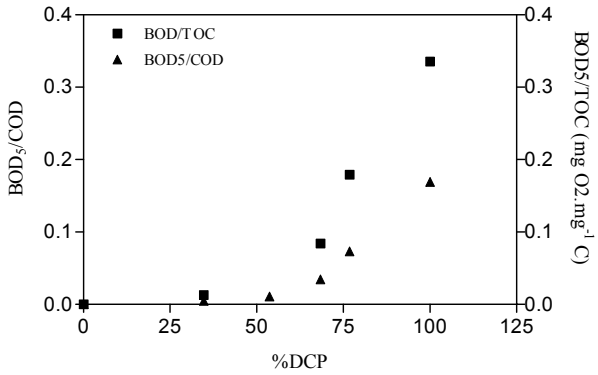

Figure 7.44: BOD_5/COD and BOD_5/TOC change as a function DCP removal, $[Fe(II)]_i$ = 30 mg. L^{-1} and $[H_2O_2]_i$= 30 mg. $L^{-1}$for 40 min and free pH evolution.

Effect of pH

The pH effect on biodegradability variation was also studied, for DCP solution treated with photo-Fenton at initial concentration 10 mg. L^{-1}Fe (II) , 10 mg. L^{-1} H_2O_2 and 40 min experimental time. There was no change in the biodegradability due to the presence more than 45 mg. L^{-1} DCP. Subsequently, experiments were repeated increasing the initial H_2O_2 concentration to 30 mg.L^{-1}. Figure 7.45 demonstrates the change of BOD_5/COD and BOD_5/TOC for solutions treated under these conditions. Results indicate that under the same initial reactant concentrations (10 mg.L^{-1} Fe (II), 30 mg.L^{-1} H_2O_2 and 40min irradiation time). The better biodegradability obtained when photo-

Fenton carried out at acidic pH as a result of more organic matter oxidation (at pH 3 BOD_5 was 98 $mgO_2.L^{-1}$ and at pH 7 BOD_5 was 88 $mgO_2.L^{-1}$)

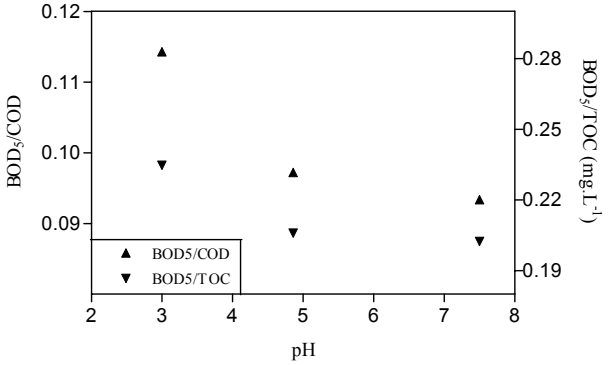

Figure 7.45: Change of BOD_5/COD and BOD_5/TOC as function of initial pH. $[Fe\ (II)]_i$=10 $mg.L^{-1}$ and $[H_2O_2]_i$= 30 $mg.L^{-1}$ and 40min experimental time

POH solution treated with photo-Fenton at different initial pH was also studied. Results confirm the previous results; an increment of 15% in BOD_5/COD was obtained by decreasing the initial solution pH from 5.5 down to 3.0.

Effect of initial contaminate concentration

Biodegradability improvement of solution treated by photo-Fenton at different initial DCP and POH solution concentrations (100, 150 and 200 $mg.L^{-1}$) were studied. As a result of their effect on biomass; biodegradability was found to be dependent in initial contaminants concentrations (DCP and POH). Solution with 100 $mg.L^{-1}$ initial DCP treated with 50 $mg.L^{-1}$ H_2O_2, 10 $mg.L^{-1}$ Fe(II) and 40 min shows biodegradability development from 0.0 up to 0.18, while there were no improvement in biodegradability for the other two concentrations (150 and 200) treated under the same conditions, due to present significant DCP concentrations. The same influence in biodegradability was noticed in POH solutions, a considerable development was noticed for 100 mgL^{-1}phenol solution and no improvement at concentrations 150 and 200$mg.L^{-1}$.

7.5.4.Change on oxidation sate

Effect of initial H_2O_2 concentrations

Figure 7.46 presents the AOS and COD/TOC evolution as function of initial hydrogen peroxide in photo-Fenton reactions for both DCP and POH. Oxidation state increase as the

initial amount of hydrogen peroxide H_2O_2 increase. At photo-Fenton initial conditions 10 $mg.L^{-1}$ Fe (II), 40 min reaction time and free pH evolution, increase the initial H_2O_2 from 0 to 60 $mg.L^{-1}$; AOS for final treated solution was found to increase from 0.13 up to 2 and COD/TOC decrease from 2.58 down to 1.33 for DCP. In POH case the change in oxidation sate was more smaller; under the same previous conditions change the initial H_2O_2 from 30 to 150 $mg.L^{-1}$ direct to change the AOS of the final solution from –0.39 up to 0.1 and COD/TOC ratio from 2.93 to 2.59. It is interesting to remark that, throughout oxidation, DCP is more affected by H_2O_2 variation than phenol. Furthermore, As noticed before that under these conditions DCP biodegradability (BOD_5/COD) solution increased to 0.18 while a biodegradability of 0.32 was obtained for POH. This may suggests that small POH oxidation may guide to good biodegradability improvement.

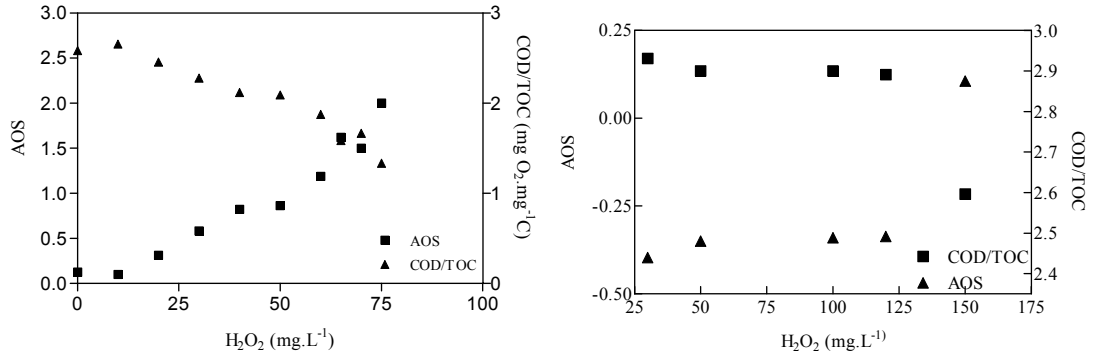

Figure 7.46: AOS and COD/TOC evolution as function of initial hydrogen peroxide (A) DCP. $[Fe\ (II)]_i$= 10 $mg.L^{-1}$, 40 min reaction time and free pH evolution .B) (A) POH , $[Fe\ (II)]_i$= 10 $mg.L^{-1}$, 15 min reaction time and free pH evolution .

The change in oxidation state as function of DCP removed is presented in figure 7.47. again the tendency imply high oxidation sate obtained by more DCP photo-oxidation.

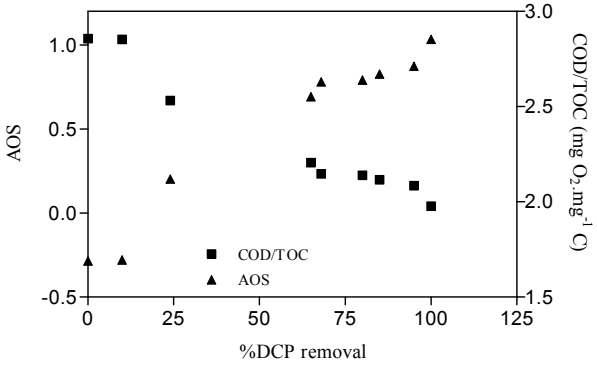

Figure 7.47: AOS and COD/TOC evolution as function of DCP removed. $[Fe\ (II)]_i$= 10 $mg.L^{-1}$, $[H_2O_2]_i$= 50, 40 min reaction time and free pH evolution .

Effect of initial iron ion concentration

With respect to the effect of iron dose in the oxidation state, Figure 7.48 demonstrates the AOS and COD/TOC change as function of initial Fe(II) concentration for both components (DCP and POH) at fixed initial H_2O_2 concentration (10 and 50 mg.L^{-1} for DCP and phenol respectively). Iron dose have very small effect in oxidation state change throughout photo-Fenton reaction. At the beginning of the reaction the tendency seems to be proportional to Fe(II) added, increasing the oxidation as iron dose increases until maximum value reached; after that the degree of oxidation appear almost constant. increase the initial Fe(II) from 0 to 50 mg.L^{-1}, AOS for final treated solution was found to increase from -0.22 up to 0.47 and COD/TOC decrease from 2.81 down to 2.66 for DCP, while increase the iron dosage from Fe(II) 30 to 75 mg.L^{-1} for POH, the same values increased from 1.17 up to 1.9 and from 1.88 down to 1.4.

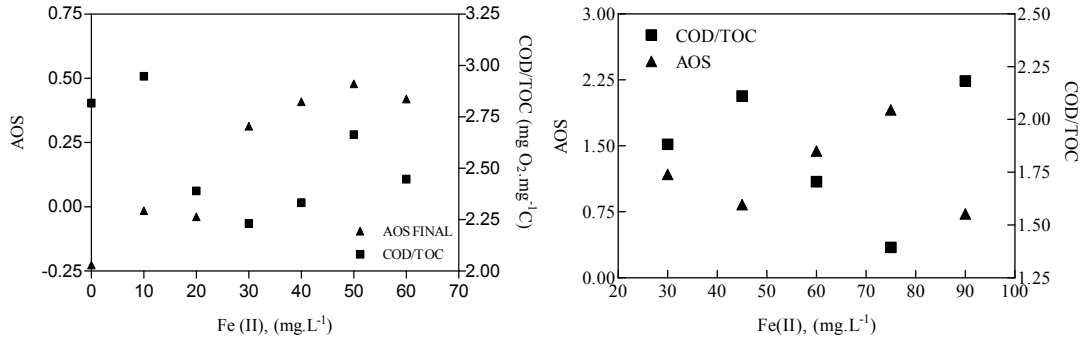

(A) (B)

Figure 7.48: AOS and COD/TOC as function of initial Fe(II). Initial conditions, A) DCP $[H_2O_2]_i$= 10 mg-L^{-1}, 40 min reaction time and B) POH $[H_2O_2]_i$= 50 mg-L^{-1}, 15 min reaction time.

Effect of UV irradiation time

As it introduced before, UV light has a noticeable rule in the production of hydroxyl radicals, so it was decided to study the effect of irradiation time in oxidation state change. Figures 7.49 and 7.50 present the change in oxidation state as function of

reaction time for DCP at different H_2O_2 and Fe (II) initial concentrations.

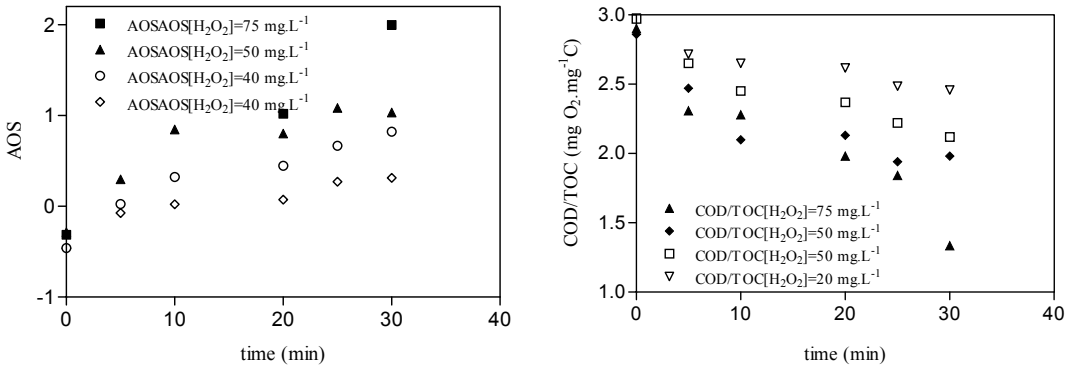

Figure 7.49: AOS and COD/TOC Evolution as reaction time for different initial H_2O_2 Concentrations. [Fe (II)]$_i$= 10 mg.L^{-1} and free pH evolutions

The oxidation state of DCP changes all over photo-Fenton reaction, which indicates that the original DCP oxidizes and then its degraded into other intermediates with higher oxidation state. H_2O_2 has a remarkable effect on oxidation state, while a small effect could be noticed for the initial amount of iron. It can also be realize the scavenger effect of Fe (II) at higher concentrations which leads to small oxidation of the contained organic matter (DCP and its intermediates at this case).

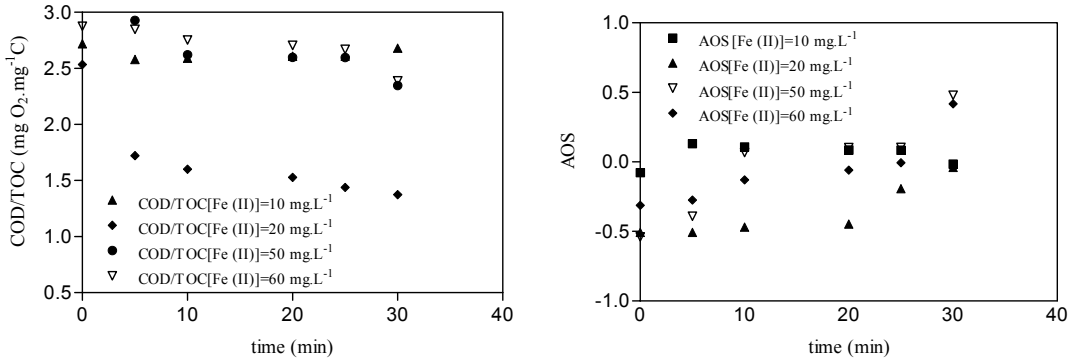

Figure 7.50: AOS and COD/TOC Evolution as reaction time for different initial Fe (II) Concentrations. [H_2O_2]$_i$= 10 mg.L^{-1} and free pH evolutions

7.5.5. Optimum conditions

Based on all the previous results, optimum reactant concentrations and operational conditions were selected based in DCP and POH elimination and significant biodegradability enhancement. Accordingly, optimum conditions for DCP are: H_2O_2 50

$mg.L^{-1}$, 10 $mg.L^{-1}$ Fe(II) during 40 min reaction time, free pH evolution and 25 ^{o}C. No more Fe (II) was used since in this case photo-Fenton will be used as pre-treatment, so higher Fe(II) concentrations will produce sludge problems when the pre-treated solution were neutralized.

With respect to POH optimum conditions taken in account are those lead to better biodegradability and low economical pre-treatment cost: H_2O_2 50 $mg.L^{-1}$, 75 $mg.L^{-1}$ Fe(II) and 15 min reaction time and free pH evolution.

7.6 High concentrated POH solutions

POH under low concentration is hardly biodegradable material, its biodegradability decrease by increasing its concentration in aqueous solution (for 100 and 1000 $mg.L^{-1}$ POH solution BOD_5/COD is 0.12 and 0.017 respectively). Since POH may be found in different industrial wastewater at different concentration limits, and hence consider not readily biodegradable. In this section, it was decided to study the effect of photo-Fenton process in biodegradability improvement of high concentration POH solution (1000 $mg.L^{-1}$). As the procedure used for biodegradability improvement is the same that followed in the earlier section, in this part only photo-Fenton operation conditions and the BOD_5/COD values will be presented. Several experiment at different initial reactant concentration were carried out (see table POH-PHF-13 in appendix A2).

Effect of initial H_2O_2 concentrations

Different experiments were carried out changing the concentration of hydrogen peroxide. Figure 7.51 presents the evolution of POH and TOC removal percentage as function of reaction time for photo-Fenton effluent solution. During the experiments there was a partial degradation of the original POH, as it can be seen in the figure, the concentration of phenol decreases as function of irradiations time, and finally only 10% of the original concentration remain in the reaction vessel. This was combined with 25% total organic carbon removal.

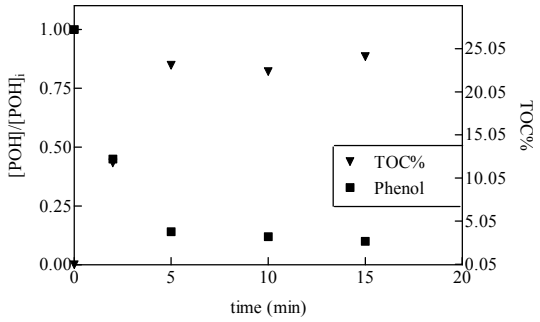

Figure 7.51: Variation of POH concentration and TOC removal percentage COD/TOC and ratio for photo-Fenton effluent solution (1000 mg.L^{-1} POH, 3000 mg.L^{-1} H_2O_2 and 1500 mg.L^{-1} Fe(II))

Biodegradability evolution as function of initial H_2O_2 and two different Fe(II) concentration are shown in figure 5.52. All photo-Fenton studied conditions lead to a significant improvement in biodegradability of the treated solution, compared with the original POH solution. As it was expected, the increase in hydrogen peroxide concentration leads to more oxidation of POH into smaller by-products, and thus increases biodegradability. The effect of this oxidation step can be seen clearly in figure 7.52 where the biodegradability of the photo-Fenton effluent solution increased from 0.017 to 0.72 for solution with initial POH concentration 1000 mg.L^{-1}, as the dosage of hydrogen peroxide increased.

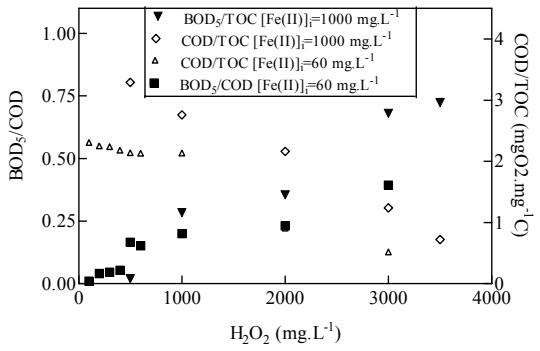

Figure 7.52: Evolution of the biodegradability and oxidation state Vs. H_2O_2 concentration at Fe(II)=60 mg.L^{-1} for photo-Fenton effluent solution, $[POH]_i$=1000 mg.L^{-1}, pH_0=3

The POH degradation and byproduct formation that happens during photo-Fenton reaction, can be followed by studying the change in oxidation state (COD/TOC) of the component. Adding a small quantity of hydrogen peroxide, a slight oxidation occurred in the effluent solution (COD/TOC =2.31) compared with that of the initial POH solution (COD/TOC =2.63). But as proceed in addition more hydrogen peroxide, which leads to more hydroxyl

radicals production, and hence organic matter degradation to other smaller byproduct with low state of oxidation increase. Accordingly, the biodegradability change depends on the change in the by-products.

Effect of iron initial concentrations

The effect of changing the iron concentration for the photo-Fenton reaction with 1000 $mg.L^{-1}$ POH at three fixed H_2O_2 concentrations (1000, 2000 and 3000 $mg.L^{-1}$) is shown in figure 7.51. For the first two concentrations, experimental results show that an increase in iron concentration increases the biodegradability until it reaches a maximum value, after which there is no effect for the catalyst Fe(II) in biodegradability. However, for 3000 $mg.L^{-1}$ H_2O_2 concentration, the iron effect on the biodegradability is different. The biodegradability tendency as a function of Fe(II) shows a direct relation, for which an increase in the Fe(II) concentration leads to an increase in the biodegradability. This may attribute to the presence of highly oxidative environment (high H_2O_2 amount) that leads to continuous organic matter oxidation, and hence generation of more biodegradable intermediates.

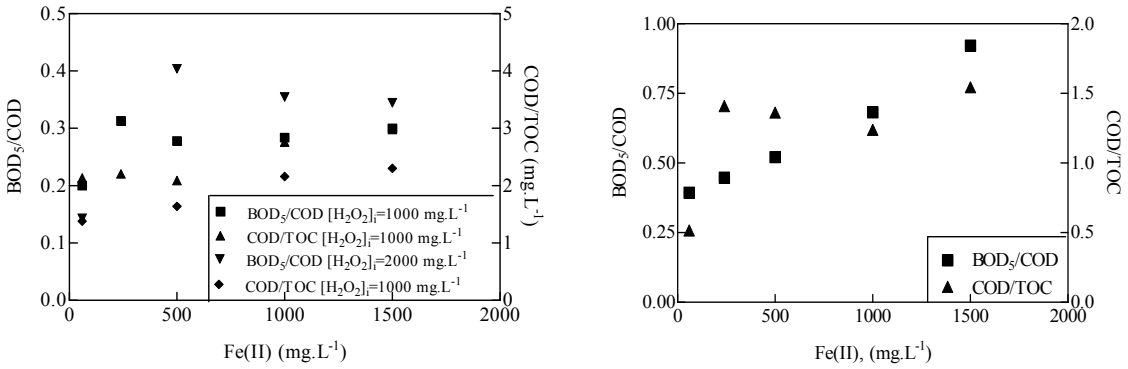

Figure 7.53: Evolution of the biodegradability and state of oxidation Vs. Fe(II) concentration at A) $[H_2O_2]$=1000 and 2000 $mg.L^{-1}$, B) $[H_2O_2]$=1000 $mg.L^{-1}$ for photo-Fenton effluent solution, $[POH]_i$=1000 $mg.L^{-1}$, 15 min irradiation time and free pH evolutions.

The maximum biodegradability reached for the concentration 1000 $mg.L^{-1}$ of POH is 0.92, which corresponds to a concentration of 1500 $mg.L^{-1}$ of iron and a 3000 $mg.L^{-1}$ of H_2O_2. This value is significantly high compared with the biodegradability of the original POH (1000 $mg.L^{-1}$) that is of 0.017.

7.6. Aerobic biological oxidation:

After increasing the biodegradability of DCP and POH solutions, the aerobic biological oxidation of the pre-treated solutions were tested at laboratory scale. For this experimentation part, DCP and POH will be discussed separately.

7.6.1. Aerobic biological oxidation of DCP:

Photo-Fenton pre-treated solution with $BOD_5/COD = 0.18$ was used, since it was the first point where all the DCP disappear from the solution and there was almost no biomass inhibition effect. This pre-treated solution is obtained from the following photo-Fenton operational conditions: 40 min experimental time, and initial concentrations 50 and 10 $mg.L^{-1}$ of H_2O_2 and Fe (II) respectively. The pre-treated solution was fed to two different aerobic biological reactors. The first one was contained biomass acclimate to POH during 4 weeks, while the second reactor operated with activated sludge coming from wastewater treatment plant.

7.6.1.1. Acclimated reactor:

This reactor was started up, by taking 1.5 $g.L^{-1}$ TSS of biomass and feeding it with 100 $mg.L^{-1}$ POH solution during 4 weeks, this time was sufficient to reach maximum TOC% removal. After that feeding of the reactor was change to be mixture of DCP pre-treated solution and POH with different percentage (DCP photo-treated to residual wastewater) and hydraulic retention times (HRTs). The percentage (DCP photo-treated to POH) was change gradually and finally the reactor was operated with 100% photo-Fenton pre-treated solution. Table 7.9 shows a summery of the experimental results at steady state for each HRT. Initial total organic carbon(TOC_i) after feeding the reactor, final total organic carbon (TOC_f) before the next feeding, total organic carbon removal percentage (TOC_r) Eq. (7.22) are tabulated. From the table it can figure out that, all working conditions reach TOC_r superior to 50 %. TOC_r increases by increasing the organic load rate (OLR). The maximum TOC_r achieved is 89 %, this results was obtained when the reactor was fed with 70% photo-Fenton pre-treated solution and 2 days HRT. This may suggest the possibility to treat photo-Fenton pre-treated solution by biological co-digestion with domestic wastewater.

$$TOC_r = \frac{(TOC_i - TOC_f)}{TOC_i} \qquad (7.22)$$

When feeding with pure photo-Fenton pre-treated solution and short hydraulic retention time (12 to 24 h) organic carbon removal (TOC_r) decreases in spite that the OLR increased. This may due to changing the feed characteristic (100% pre-treated solution) However, it can be seen that after the ORL increased for 1 day HRT, the TOC_r start to increase. Figure 7.54 presents TOCi, TOC_f and TOCr percentage for 100% of photo-Fenton pre-treated solution and 12 h HRT.

Table 7.9 Summary of the experimental results for acclimatized reactor

Feed(1)	HRT (days)	OLR ($mg.C.L^{-1}.day^{-1}$)	TOC_i ($mg.C.L^{-1}$)	TOC_f ($mg\ C.L^{-1}$)	TOC_r %
20/80	10	10.9	18.1	6.9	61.7
20/80	10	9.8	23.3	11.0	52.7
20/80	5	13.0	14.4	5.0	65.1
20/80	2	29.7	33.3	4.9	85.4
30/70	2	19.9	24.7	6.0	75.7
50/50	2	25.3	24.6	5.4	77.9
70/30	2	34.1	37.1	4.1	89.0
100/0	1	46.1	35.1	16.6	52.7
100/0	0.5	69.2	33.1	14.0	57.7

(1) %Photo-Fenton pre-treated solution to POH

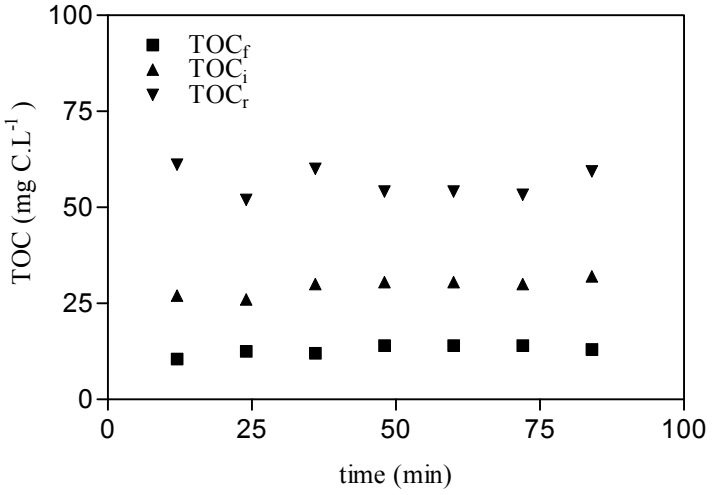

Figure 7.54: Initial, final and TOC removed for the acclimated reactor operating at 100% of photo-Fenton pre-treated solution and HRT = 12 hours.

7.6.1.2. Activated sludge reactor:

This reactor was started up by mixing the photo-Fenton pre-treated solution with activated sludge ($1.5\ g.L^{-1}$) and municipal wastewater. As in the acclimated reactor, different

percentages of the pre-treated solution and different HRTs were used. Table 7.10 gives a summery of the same parameters examined in the acclimated reactor during operating at steady state. The same as found before, the TOC_r increases proportionally by increasing the (OLR). Once more, maximum TOC_r of 81.5 % was achieved when the reactor was fed with 70% photo-Fenton pre-treated solution and 30% municipal wastewater. However, when the feed solution was changed to be 100% photo-Fenton pre-treated solution there was a decrease in TOC_r. Also, it is interesting to note that activated sludge reach it is maximum TOC_r % when the feed ratio has 70% of the pre-treated solution. Even though, the removal efficiency for acclimated reactor is slightly higher, it could be indicated that, DCP treated solution could be efficiently treated by co-digestion with domestic wastewater, with no need of biomass acclimation. Moreover, it is interesting to note also that, in this part the bioreactor was fed with pre-treated solution that has biodegradability of 0.18. While during photo-Fenton reaction it was noticed that better biodegradability could be achieved 0.33, which mean that bioreactor efficiency can be improve more.

Table 7.10 Summary of the experimental results for acclimatized reactor

Feed(2)	HRT (days)	OLR ($mg.C.L^{-1}.day^{-1}$)	TOC_i ($mg.C.L^{-1}$)	TOC_f ($mg.C.L^{-1}$)	TOCr %
20/80	10	21.7	23.8	12.4	47.9
20/80	5	43.0	39.3	12.7	67.6
20/80	2	93.4	63.8	11.8	81.4
30/70	2	41.4	45.8	9.6	79.0
50/50	2	61.9	67.5	14.6	78.4
70/30	2	137.0	76.6	14.9	80.5
100/0	2	16.0	21.8	10.2	53.2
100/0	1	32.0	28.2	10.8	61.5
100/0	0.5	64.0	29.4	13.0	55.8

(2) %Photo-Fenton pre-treated solution to wastewater

7.6.1.3. Kinetic study:

According to Monod model (see chapter 3.4), biological degradation of compounds in wastewater can be describe as:

$$-\frac{1}{X}\frac{dS}{dt} = \frac{\mu_m S}{Y(K_s + S)} \qquad (3.37)$$

If one of the essential requirements (substrate and nutrients) for growth were present in only limited amounts, it would be depleted first and growth would cease.

Experimentally it has been found that under low substrate concentration (K_s>>>S) Monod model can be defined adequately using the following first order kinetic expression [Beltran et al., 2000].

$$-\frac{1}{X}\frac{dS}{dt}=\frac{kS}{(K_s+S)}=K_{ob}S \qquad (7.23)$$

where K_{ob} is biological first order kinetic constant ($L.g^{-1}$ VSS. h^{-1}). Eq. (7.24) is integrated with initial condition $S=S_o$ for t=0:

$$\ln(\frac{S_0}{S})=K_{ob}t \qquad (7.24)$$

According to Eq. (7.23), plot of ln (S_0/S) versus time must lead to straight lines. Figure 7.55 to 5.58 show results of kinetic study for acclimated and non-acclimated bioreactor operated with 100% DCP pre-treated solution at different HRT, calculations where performed with 95% confidence level, (table DCP-Bio-1 to table DCP-Bio-4 Appendix A3).

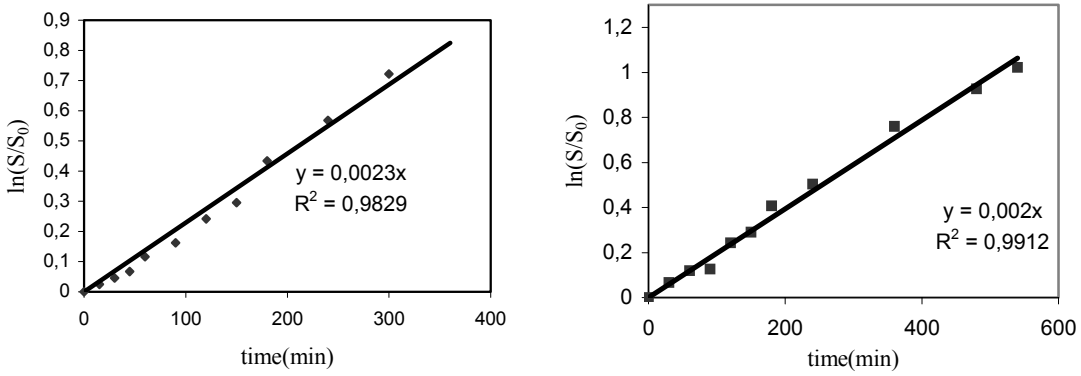

(A) (B)

Figure 7.55. Kinetic study of the biodegradation of 100% pre-treated solution carried out in the non-acclimated reactor. Conditions: T = 22ºC, pH ≈ 7.2, TVSS = 0.35 $g.L^{-1}$, (A)HRT = 2 days and (B) T = 22ºC, pH ≈ 7.2, TVSS = 0.35 g.L⁻ HRT = 1 days.

A good correlation of the experimental points to straight line during each period ($r^2 > 0.93$) confirms the validity of the proposed model. Table 7.11 provides the K_{ob} values for both reactors fed with 100% photo-Fenton pre-treated solution and 12 and 24hr HRTs. As it can be noticed, kinetic constants for acclimated reactor are to some extent higher than activated sludge reactor, both at 24 hours (1.3 vs. 0.78 $L.gTVSS^{-1}.h^{-1}$) and 12 hours HRT (1.62 vs.

1.02 $L.gTVSS^{-1}.h^{-1}$). In is interesting to note that, in acclimated reactor working at 1 day HRT to different kinetics were noticed. The presence of such kind of kinetics may be attributed to the presence of two types of substrate with two different biodegradability value. Thus, at the beginning the biomass oxidize the more biodegradable compound and after that start the second kinetic to degraded the remaining organic matter

Table 7.11: Kinetic constant values (K_{ob}) for both reactors (acclimated and non acclimated reactors) at different photo-Fenton pre-treated percentage and HRTs.

Reactor	HRT	X (g TVSS.L^{-1})	K_{ob} ($L.gTVSS^{-1}.h^{-1}$)
Acclimated reactor (pre-treated solution 100%)	1 day	0.08	1.28
Non-acclimated reactor (pre-treated solution 100%)	1 day	0.13	0.78
Acclimated reactor (pre-treated solution 100%)	12 h	0.1	1.62
Non-acclimated reactor (pre-treated solution 100%)	12 hr	0.13	1.02

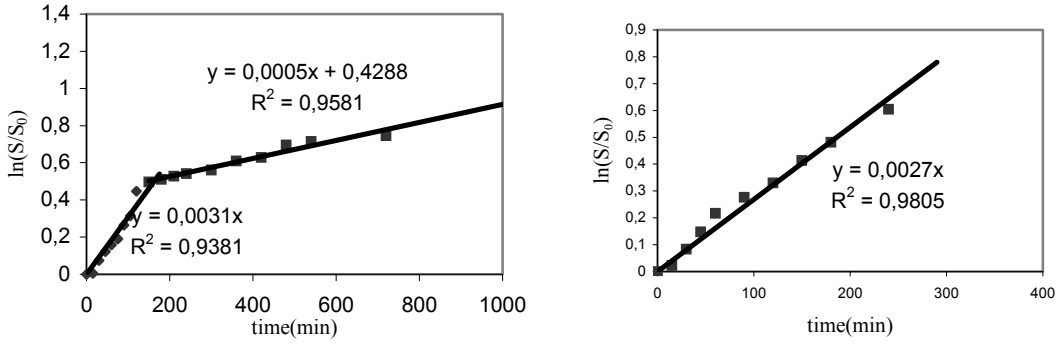

(A) (B)

Figure 7.57: Kinetic study of the biodegradation of 100% pre-treated solution carried out in the acclimated reactor. Conditions: (A) T = 22ºC, pH ≈ 7.2, TVSS = 0.13 $g.L^{-1}$, HRT = 1 days, (B) (A) T = 22ºC, pH ≈ 7.2, TVSS = 0.13 $g.L^{-1}$, HRT = 12 h

7.6.2. Aerobic biological oxidation of POH:

In this part, aerobic biological oxidation was combined with photo-Fenton process, to study the effect of pre-treatment step in efficiency and biodegradation rate of POH treated solutions. Pure POH solution has a biodegradability value of (BOD_5/COD=0.12 and 0.017 for 100 and 1000 $mg.L^{-1}$). For each initial POH concentration (100 and 1000 $mg.L^{-1}$), two reactors were operated in batch conditions. In the first one, pure POH was used as sole carbon source and in the second one photo-Fenton pre-treated solution with significant biodegradability was used. Dissimilar to DCP reactor, in this part cycle duration was

change in the way that at the end only non-biodegradable organic matter remains in the reactor. A comparative study between aerobic biological degradation for pure POH and combined processes (photo-Fenton and aerobic biodegradation) was realized. Initial chemical oxygen demand (COD_i), initial total organic carbon (TOC_i), final chemical oxygen demand before next feeding (COD_f), final total organic carbon (TOC_f), removal percentage in both parameters (COD_r% and TOC_r%) as well as cycle duration for single and combined processes for two concentrations of POH (100 and 1000 ppm) is shown in table 7.12 and table 7.13.

As it can be seen, for 100 $mg.L^{-1}$ POH solution, with initial TOC and COD of 76.6 and 191.3 $mg.L^{-1}$ respectively, the average COD percentage removal observed during single process reaction was 89% (final COD and TOC are 4 $mgO_2.L^{-1}$ and 3.3 $mgC.L^{-1}$ respectively) and this was reached with cycle duration of 132 hours, while COD removal of 98% could be obtained in combined process with only 25 hours cycle duration. This result shows that a single biological treatment needs high cycle duration to reach a significant TOC and COD removal, but using combined processes, high COD and TOC conversion can be reached easily within low and practical cycle duration limits.

Table 7.12: Removals of COD, and TOC in the aerobic biological process for single process and combined Process, initial POH concentration 100 $mg.L^{-1}$.

Single process 100 $mg.L^{-1}$ POH

Run	TOC_i ($mg.L^{-1}$)	COD_i ($mg.L^{-1}$)	TOC_f ($mg.L^{-1}$)	COD_f ($mg.L^{-1}$)	COD_r% Removal	TOC_r% Removal	Cycle duration (hr)	€/kg TOC removed
1	70	138	20.36	17.1	81	71	110	12.9
2	91	189	17.5	14.3	78	82	140	14.2
3	102	213	10	16.8	76	87	110	10.5
4	73	176	14.3	18.0	80	80	120	12.5
5	90	178	13.0	17.1	83	85	150	14.7
6	68	118	15	16.2	77	77	135	14.6
7	90	189	16	16.2	80	82	138	14.0

Coupled processes with Photo-Fenton (100 $mg.L^{-1}$ POH, 300 $mg.L^{-1}$ H_2O_2, 60 $mg.L^{-1}$ Fe(II))

Run	TOC_i ($mg.L^{-1}$)	COD_i ($mg.L^{-1}$)	TOC_f ($mg.L^{-1}$)	COD_f ($mg.L^{-1}$)	COD %	TOC% Removal	Cycle duration (hr)	€/kg TOC removed
1	80	150	5.5	4.6	97	93	55	8.8
2	87	160	3.6	2.9	96	96	46	10.9
3	88	164	5.0	2.9	98	94	47	8.95
4	84	155	3.5	2.5	98	96	50	8.6

Coupled processes with Photo-Fenton (100 $mg.L^{-1}$ POH,50 $mg.L^{-1}$ H_2O_2, 75 $mg.L^{-1}$ Fe(II))

Run	TOC_i ($mg.L^{-1}$)	COD_i ($mg.L^{-1}$)	TOC_f ($mg.L^{-1}$)	COD_f ($mg.L^{-1}$)	COD% Removal	TOC% Removal	Cycle duration (hr)	€/kg TOC removed
1	85	189	5	4.0	97	94	23	4.5
2	88	195	3	3.0	98.5	97	24	4.4
3	87	192	5	3.0	98.5	94	26	4.7
4	85	189	3	3.0	98.5	96	27	4.5

Furthermore, table 7.12 presents simple cost estimation for single and combined processes, estimation was completed based in operational such as (electricity used in agitation, UV-light and air production) and cost of chemical reagent added in both chemical and biological reactor. It can be seen that coupled processes (using photo-Fenton as pre-treatment followed by biodegradation) decrease the organic matter removal cost by a factor of 3 (from 13.2 €/kg TOC removed in single biological process down to 4.3 €/kg TOC removed in coupled processes). This suggests that combined AOP´s is a good strategy for high treatment efficiency and low costs. Beside that, it should not overlook the high fixed capital cost as result of high biological reactor volume (big cycle duration) in single process that confirm the economy of coupled processes.

With respect to 1000 $mg.L^{-1}$ POH solution, the removal percentage of TOC and COD for the two processes reached a highly significant value of 98%. However, the combined process shows a better tendency due to its small cycle duration compared with the single process (50 to 180). With respect to operational and reagents costs, it is clear that single biological process has better cost for kg TOC eliminated than coupled process (15.5 to 72 in single and couple process respectively). So far, the high operational cost obtained in coupled processes refer to the high initial H_2O_2 and iron used in photo-Fenton reaction to

improve the biodegradability. Nonetheless, at these concentrations (3000 mg.L^{-1} H_2O_2, 1500 mg.L^{-1} Fe(II)) the biodegradability (BOD_5/COD) was achieved 0.92. This value is two times the recommended biodegradability of municipal wastewaters (BOD_5/COD≈ 0.4). Thus, high unwanted chemical reagents were used in this case that affected negatively the processes economy. Further investigations should be carried out to study further operation conditions and reagents concentrations, to be able to decide the more reasonable process.

Table 7.13: Removals of COD, and TOC in the aerobic biological process for single process and combined Process, initial POH concentration 1000 mg.L^{-1}.

Single process with 1000 mg.L^{-1} POH

Run	TOC_i (mg.L^{-1})	COD_i (mg.L^{-1})	TOC_f (mg.L^{-1})	COD_f (mg.L^{-1})	COD_r% Removal	TOC_r% Removal	HRT (hr)	€/kg TOC removed
1	690	1470	19.5	39	97	97	180	15.46
2	846	1950	18.5	33	98	98	180	15.44
3	816	1920	18.8	33	75	98	180	15.43

Coupled processes with Photo-Fenton (1000 mg.L^{-1} POH,3000 mg.L^{-1} H_2O_2, 1500 mg.L^{-1} Fe(II))

Run	TOC_i (mg.L^{-1})	COD_i (mg.L^{-1})	TOC_f (mg.L^{-1})	COD_f (mg.L^{-1})	COD_r% Removal	TOC_r % Removal	Cycle duration (hr)	€/kg TOC removed
1		2100	18	27	95	98	48	70.6
2	936	2030	18	21	96	99	50	73
3	915	2100	18	22	97	98	48	70.6

The high removal tendency in single biological reactor can be explained as follow: microorganisms used for effluents of 1000 mg.L^{-1} biodegradation are the same used for the ones of 100 mg.L^{-1} for long time, so this type of bacteria can be assume highly acclimated to POH degradation products, and consequently high reactive, hence it has reactivity to degrade POH and its intermediates in the same efficiency. Consequently, the combined processes are expected to have economical advantages against single biological process. The same trends were noticed for TOC removal percentage, which was 79 and 95 for single and combined processes respectively.

7.6.2.1. Kinetic study:

The same model used before based on Monod model was applied for the bioreactors, a general plot following equation (7.24) is shown in figure (7.59) for 100 mg.L^{-1} POH in single process and photo-Fenton effluent solution. It can be seen that both POH and POH photo-treated solutions biodegradation follow first order kinetic. As comparison between POH and photo-treated solution it can be noticed that photo-Fenton solution degraded faster than POH solution, as presented with its higher first order kinetic constant (0.0203 and 0.96 L.g $VSS^{-1}.h^{-1}$ for POH and photo-Fenton effluent solution respectively). Table 7.14 represents value of first order kinetic constant for POH at two concentrations (100 and 1000 mg.L^{-1}) and different photo-Fenton effluent solution.

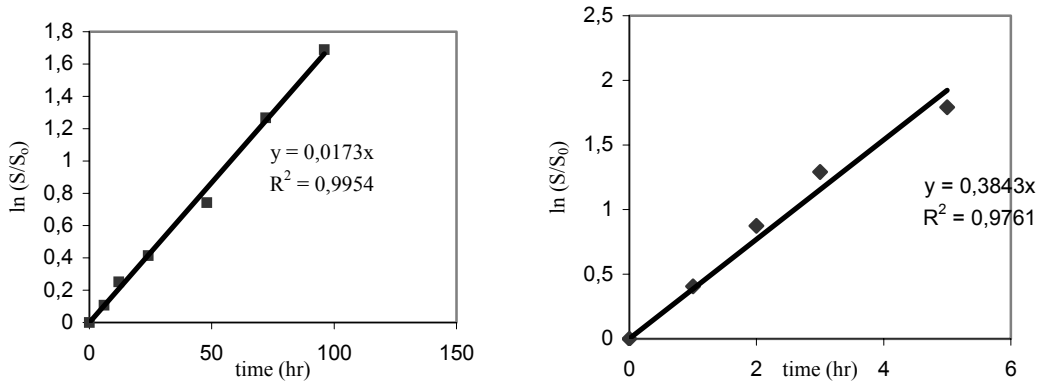

Figure 7.59: Kinetic study of aerobic biodegradation of A) POH, B) photo-Fenton effluent solution 100 mg.L^{-1} POH, 50 mg.L^{-1} H_2O_2, 75 mg.L^{-1} Fe^{+2}

In design of bioreactors it is necessary to relate the biomass evolution over the whole cycle for batch cultivation. One of the most used parameters to establish such relation is the cellular yields coefficients ($Y_{X/S}$) and the biomass death phase kinetic constant (k_d). The first one represents grams of biomass produced per gram of substrate removal, and the second one indicates the importance of the endogenous metabolism into cell culture. Considering both growth and death phases, the overall expression for the specific growth rate (μ)is see Eq. 3.36

$$\mu = Y_{X/S}\, q - k_d \qquad (7.25)$$

Where q is the specific decomposition rate of substrate. To perform calculations, specific decomposition rate q must be previously evaluated for each time of biological reaction. For simplifications equation (7.32) could be used:

$$q = -\frac{1}{\overline{X}} \quad \frac{\Delta s}{\Delta t} \qquad (7.26)$$

A plot of μ vs. q should thus give a straight line whose slope and intercept will be $Y_{X/S}$ and k_d respectively, to perform such plots the specific growth rate μ was calculated using equation (7.27)

$$\mu = \frac{1}{\overline{x}} \frac{\Delta x}{\Delta t} \qquad (7.27)$$

A general plot following equation (7.27) is shown in figure (7.60). experimental results show good distribution around the straight line which indicates the validity of the proposed model for bio-oxidation. For Photo-Fenton (100 $mg.L^{-1}$ POH, 50 $mg.L^{-1}$ H_2O_2, 75 $mg.L^{-1}$ Fe (II)), a slope of 0.0015 (g VSS g COD^{-1}) and intercept of $3.4x10^{-3}$(h^{-1}) was obtained, which corresponds to a cellular yield coefficient, and micro-organisms death phase kinetic constant respectively. Summary of all experimental results for POHs and other photo-Fenton treated solution are summarized in table 7.14.

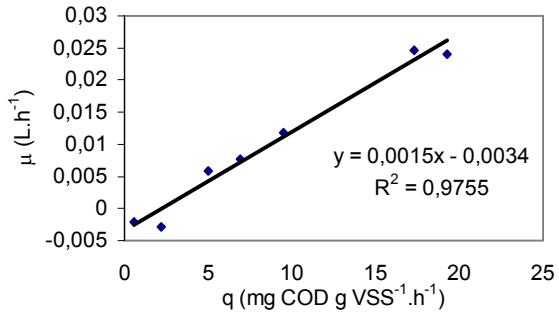

Figure 7.60: Evaluation of $Y_{X/S}$ and k_d in the aerobic biological degradation for photo-Fenton pre-Treated solution. Initial conditions 100 $mg.L^{-1}$ POH, 50 $mg.L^{-1}$ H_2O_2, 75 $mg.L^{-1}$ Fe (II).

Table (7.14) kinetic data for POH and photo-Fenton effluent solutions

Process	K_{ob} ($L.g\ VSS^{-1}.h^{-1}$)	$Y_{x/s}$ ($g\ VSS\ g\ COD^{-1}$)	K_d (h^{-1})
Single process(100 $mg.L^{-1}$ POH)	0.0203(*)	$7x10^{-3}$	$1.3x10^{-2}$
Photo-Fenton (100 $mg.L^{-1}$ POH, 60 $mg.L^{-1}$ Fe(II), 300 $mg.L^{-1}$ H_2O_2	0.3117	$4.6x10^{-3}$	$6.4x10^{-3}$
Photo-Fenton (100 $mg.L^{-1}$ POH, 75 $mg.L^{-1}$ Fe(II), 50 $mg.L^{-1}$ H_2O_2)	0.96	$1.5x10^{-3}$	$3.4x10^{-3}$
Single process(1000 $mg.L^{-1}$ POH)	0.0157	$3x10^{-4}$	$1.5x10^{-4}$
Photo-Fenton (1000 $mg.L^{-1}$ POH, 1000 $mg.L^{-1}$ Fe(II), 3000 $mg.L^{-1}$ H_2O_2	0.636	$1.7X10^{-3}$	$1.0X10^{-3}$
Photo-Fenton (1000 $mg.L^{-1}$ POH, 1500 $mg.L^{-1}$ Fe(II), 3000 $mg.L^{-1}$ H_2O_2)	0.248	$3.2X10^{-3}$	$2.7X10^{-3}$

(*) Constant values are tabulated only for first degradation kinetic

7.7. Mineralization

If organic matter degradation in photo-Fenton process were held in a highly oxidative environment, all the contained organic matter can be mineralized to CO_2 and water. Photo-Fenton reactions were carried out to mineralize 100 $mg.L^{-1}$ DCP and POH solutions. The mineralization was followed by total organic carbon reduction. As photo-Fenton reaction degradation efficiency changes by varying initial reactant concentrations, and based on the previous results, H_2O_2, Fe(II) and pH effect, it was decided to fixed Fe(II) initial concentration to 40, 60 $mg.L^{-1}$ for DCP and POH respectively (in previous section a concentration of 40 $mg.L^{-1}$ Fe (II) was found to have high DCP degradation rate), pH allowed to evolve freely. H_2O_2 initial concentration was manipulated to accomplish total mineralization. Figure 7.61 presents the TOC reduction as function of time for different initial H_2O_2 concentrations for both DCP and POH. Photo-Fenton reaction could be used for total mineralization of both components. A hydrogen peroxide concentration of 270 and 750 $mg.L^{-1}$(7.94 and 22.01 $mmol.L^{-1}$) was sufficient to remove all DCP and POH respectively. This represents a molar ratio between DCP and H_2O_2 of 4.87 This value is favorable in terms of H_2O_2 consumption for removal all the present amount of DCP. Ormad et al., 2001 reported in his studied of the DCP degradation in photo-catalytic reactor that a ratio of 3.6-4 between H_2O_2 and DCP is needed to abate all the DCP in the solution. A ratio close to 10 has been reported for many industrial pollutants and in many other studies in the field of advanced

oxidation technologies (Ruppert et al., (1993), this ratio in the same order of magnitude to that found in our study. It is interesting to note that for both DCP and POH concentration the amount of H_2O_2 used for total mineralization are less than the essential stoichiometric amount by 62% and 40% respectively, as result of hydroxyl radical production from UV light and iron photo-redox process.

Esplugas et al., (1994) and Kuo, (1999) have been studied the degradation of chlorophenols by AOP´s. They pointed out that chlorophenols mineralization follows first order kinetics. Accordingly, the mineralization of both DCP and POH were tested for first order linearity. Figure 7.62 presents the plot of logarithmic normalized TOC value as function of time for different H_2O_2 concentrations for DCP mineralization. In table 7.15 DCP and POH first order kinetic constant and half-life time for TOC mineralization are presented.

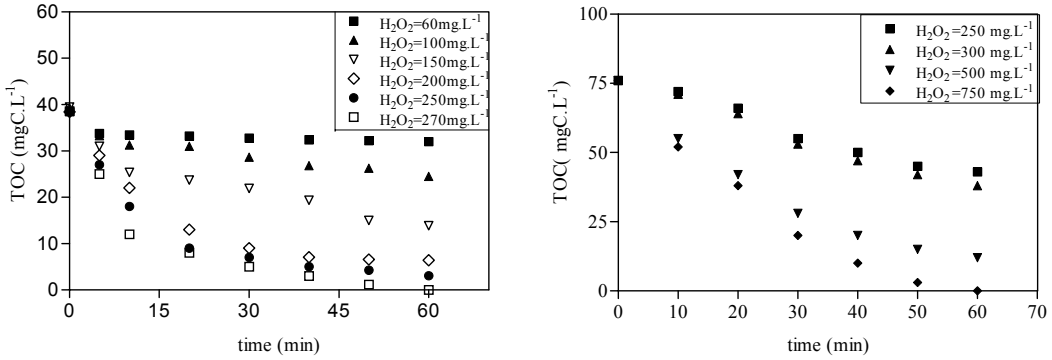

(A) (B)

Figure 7.61: Mineralization of DCP and POH at different H_2O_2 concentration, conditions A) $[Fe\ (II)]_i$=40 $mg.L^{-1}$, time=60 min and free pH evolution, B) $[Fe\ (II)]_i$=60 $mg.L^{-1}$, time=60 min and free pH evolution.

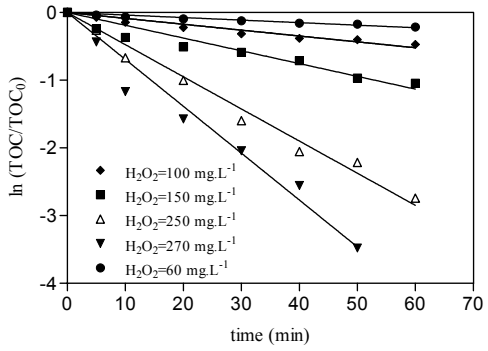

Figure 7.62: First order mineralization kinetics for DCP degradation. $[Fe(II)]_i$ = 40 $mg.L^{-1}$, and free pH evolution.

7.15: First mineralization kinetic constant and half-life time for DCP mineralization by photo-Fenton reaction

DCP			POH		
H_2O_2 ($mg.L^{-1}$)	K_{TOC} (min^{-1})	$t_{½}$ (min)	H_2O_2 ($mg.L^{-1}$)	K_{TOC} (min^{-1})	$t_{½}$ (min)
270	0.0693	8	750	0.0553	20
250	0.0475	12	400	0.0340	25
150	0.0189	40	350	0.0111	60
100	0.009	>60	250	0.0084	>60
60	0.004	>60	200	0.0061	>60

7.8. Intermediates Identification:

Both studied components were examined for intermediates identification, POH treated solution were checked in both HPLC and mass spectra. Unfortunately, results were not consistence with previous studies, only hydroquinine and resorcinol could be identified, so it was decided not to present these result in this section. Yet, DCP intermediates identification will be discussed briefly in this section :

As it was indicated before that the stoichiometric conversion for DCP mineralization and dechlorination are not equal. And this suggests the formation of aromatic and aliphatic chlorinated compounds during the oxidation reactions, which indicates the presence of chlorinated intermediates. Previous studies in detecting the DCP degradation intermediates have been resulted to number of common compounds. Abe and Tanaka, 1997 reported the presence of chlorohydroquinone between the intermediates. The formations of chlorinated intermediates have been studied by Qiu et al., (2002) and Duguet et al., (1987). Hydroquinine, muconic acid and glycolic acid have been detected by Yu and Hu (1994) in the ozonation of DCP solutions at pH 3. Ormad et al., 2001 have been identified Ketone, 2,6-Bis(1,1-dimethyl)-4-methyl-POH, Dibutyl-phthalate and n-Nitro-1, 2-benzen-dicarboxylic acid and Eculanon or isomer $C_{22}H_{14}O_7$ during DCP photo-Fenton degradation.

In our study photo-oxidation samples were analyzed by means of HPLC for DCP intermediates identifications. Different standard were used: chlorohidroquinone, 4,6-dichlororesorcinol, chlorobenzoquinone, hydroquinine, resorcinol, p-benzoquinone, formic acid and oxalic acid. Chlorobenzoquinone was identified as an earlier reaction by-product but dissimilar to a previous research (Abe and Tanaka, 1997), has not found among the final formed intermediates.

UV-light: Figures 7.63 and 7.64 present chromatograms corresponding to samples after 30 and 90 minutes of UV-irradiation respectively (experiment DCP-UV). The peak at retention time. 6.6 minutes, which was identified as chlorobenzoquinone, appeared after 15 minutes of treatment. At this time, less than 15% of the initial DCP was removed. The presence of DCP and chlorobenzoquinone may account for the no improvement of biodegradability observed at this process.

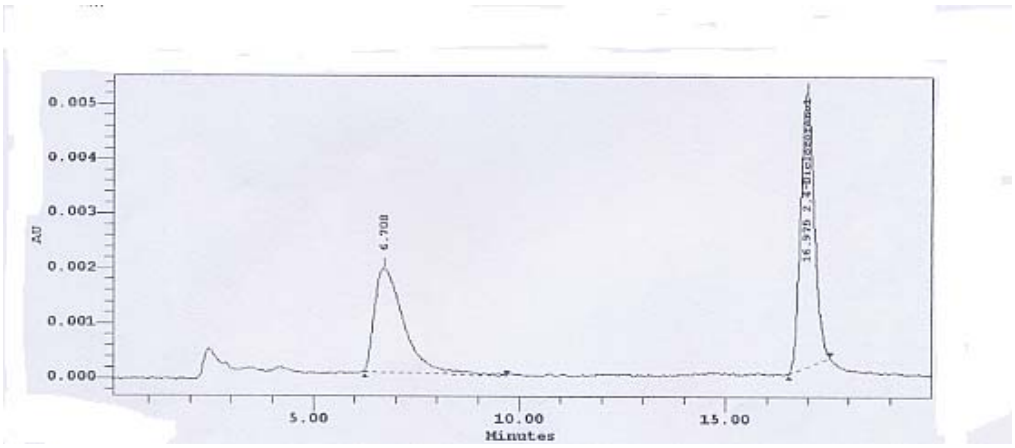

Figure 7.63: Chromatogram corresponding to sample at 30 min of direct UV-photolysis

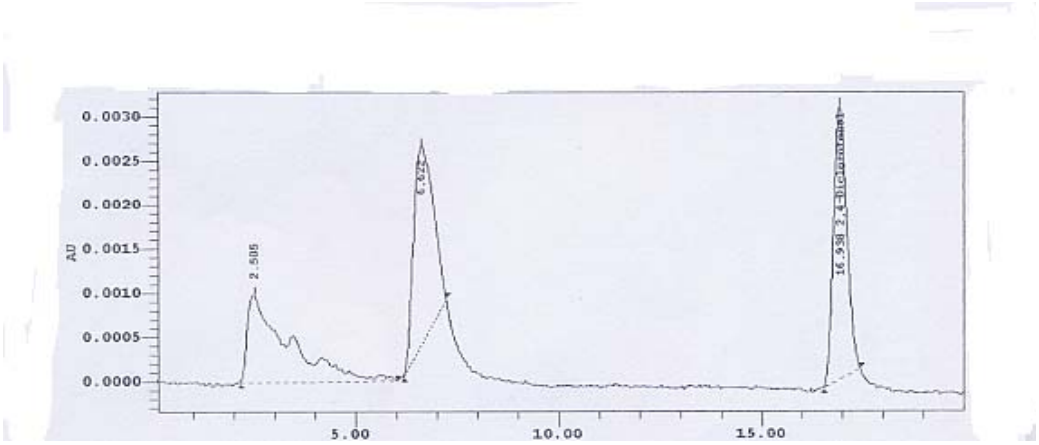

Figure 7.64: Chromatogram corresponding to sample at 90 min of direct UV-photolysis

UV/H_2O_2: Figure 7.65 and 7.66 present the chromatograms corresponding to samples after 5 and 30 min of UV irradiation respectively (experiment UV/H_2O_2-3). It can be seen that, chlorobenzoquinone is also formed during this process but more earlier than UV process (5 min). But in the contrary of UV process this intermediate disappears after 30 min of experiment by degrading it to other smaller intermediates (smaller retention time) at the end of the treatment, and hence the biodegradability of the treated solution slightly increased.

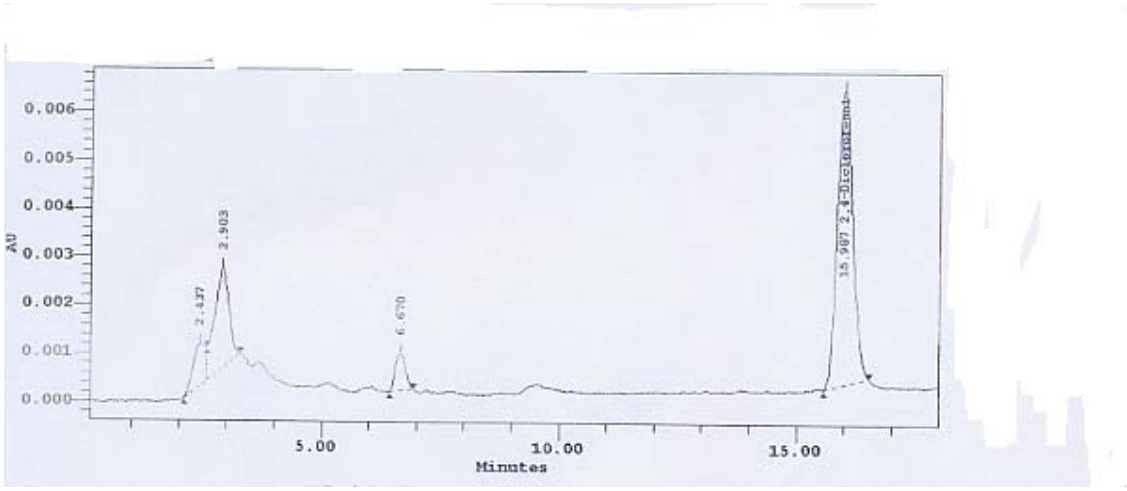

Figure 7.65: Chromatogram corresponding to sample at 5 min of direct UV/H_2O_2 photolysis

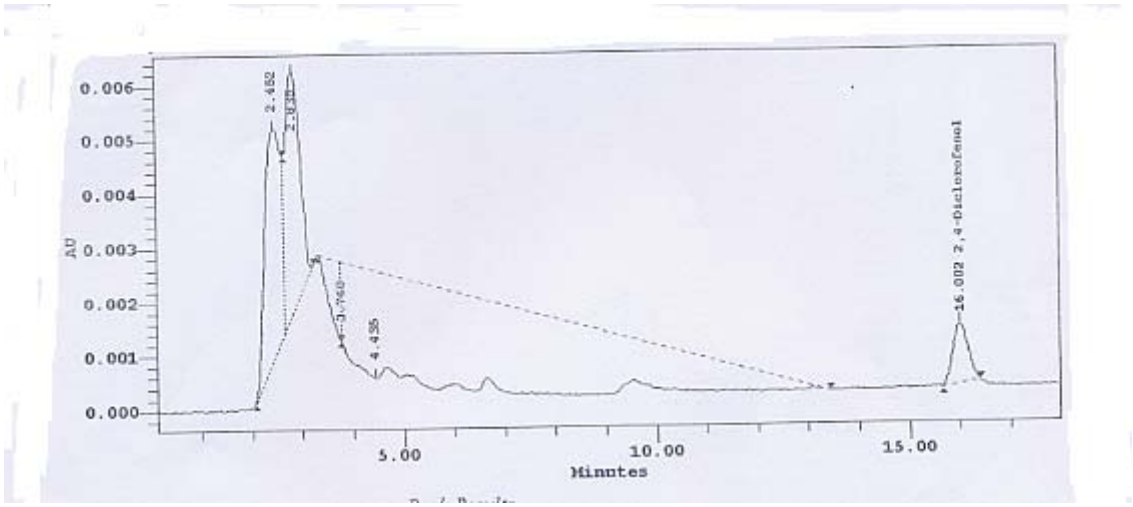

Figure 7.66 Chromatogram corresponding to sample at 30 min of direct UV/H_2O_2 photolysis

UV/Fe (III): Figure 7.67 presents sample at 30 min of experiment (experiment UV/Fe (III)-1). The same intermediates were identified in this process, which formed after 10 min of treatment and continue all over the experiment, the reason that prevents the biodegradability improvement.

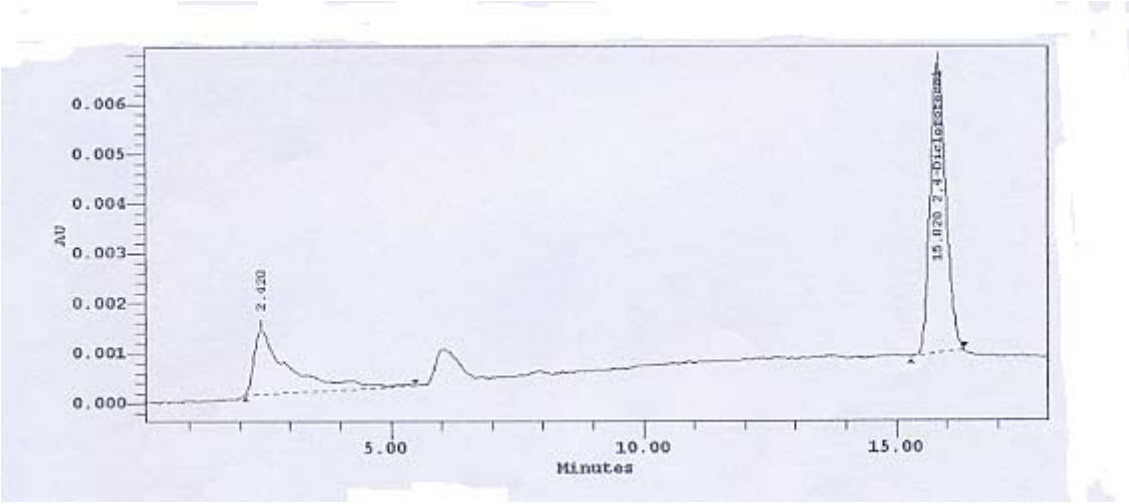

Figure 7.67: Chromatogram corresponding to sample at 30 min of direct UV/Fe(III)

Fenton reactions: Figures 7.68 and 7.69 present the chromatograms corresponding to samples after 20 for experiment DCP-H_2O_2/Fe (II)-1 and DCP-H_2O_2/Fe (II)-2 For initial H_2O_2 concentration 50 and 100 mg.L^{-1}, the formation of chlorobenzoquinone and other unknown intermediates was so fast the first 2 min of experiment and it continues through all the reaction. However when higher concentration of H_2O_2 was used 100 mg.L^{-1} the formation and disappearing of chlorobenzoquinone and the other smaller intermediets was so fast less than 20 min and just one intermediate was remaining.

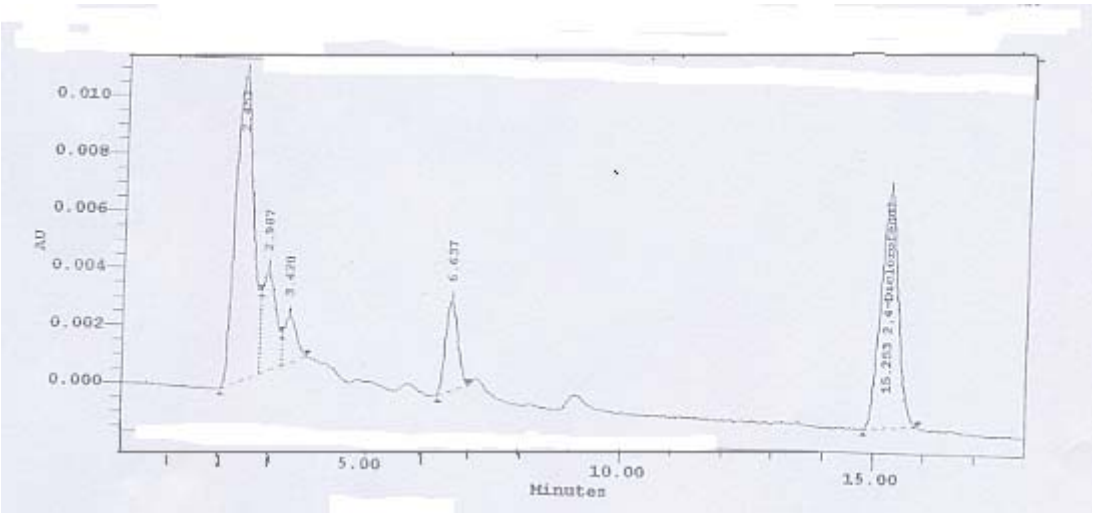

Figure 7.68: Chromatogram corresponding to sample at 20 min of Fenton reaction

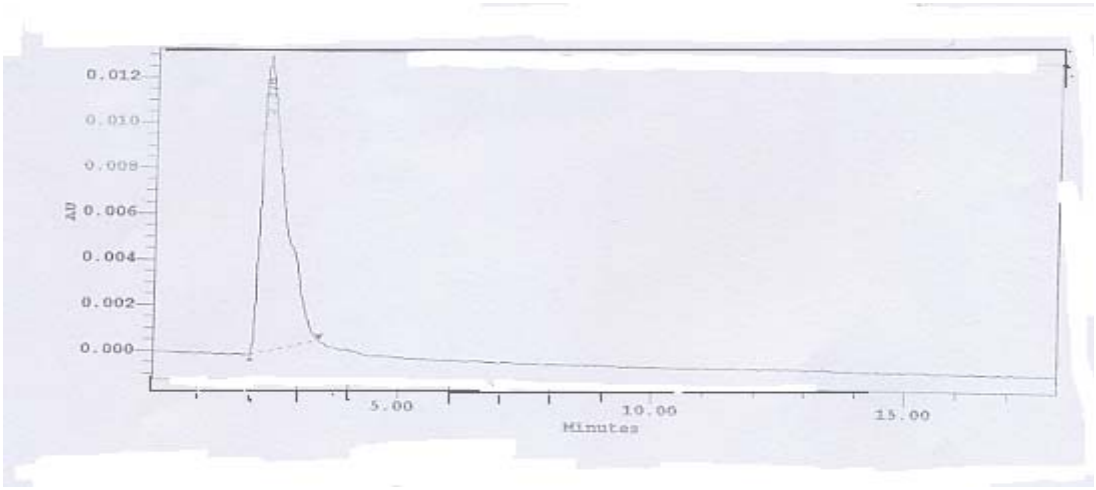

Figure 7.69: Chromatogram corresponding to sample at 20 min of Fenton reaction

Photo-Fenton: with regarded of intermediates identifications in photo-Fenton it was not easy procedure due to high reaction rate at the first min of the reaction. For that to experiments were done (experiment DCP-PHF-2 and DCP-PHF-4) respectively. Figure 7.70 and 7.71 show the chromatograms corresponding to samples after 0.5 and 1 min of experiment DCP-PHF-2. As it can be seen that, chlorobenzoquinone formed so early and unique in the reaction medium and then start the formation of other intermediates while chlorobenzoquinone disappear from the solution. For experiment DCP-PHF-4 the result are presented in figure 7.72 and 7.73 for reaction at 5 min and 30 min. it can observe that after 5 min reaction time chlorobenzoquinone has been degraded and other smaller intermediates with retention time 2.39 was formed after, this intermediates was identified to be hydroquinine. Nevertheless, this intermediates no more stay in the treated solution long time since it deplete to other smaller intermediates after 15 min reaction (see figure 7.73).

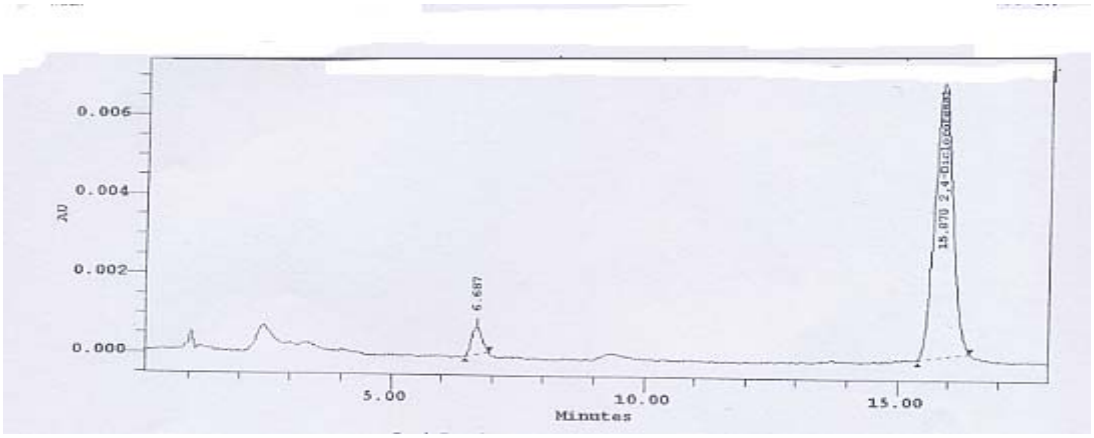

Figure 7.70: Chromatogram corresponding to sample at 0.5 min of photo-Fenton reaction

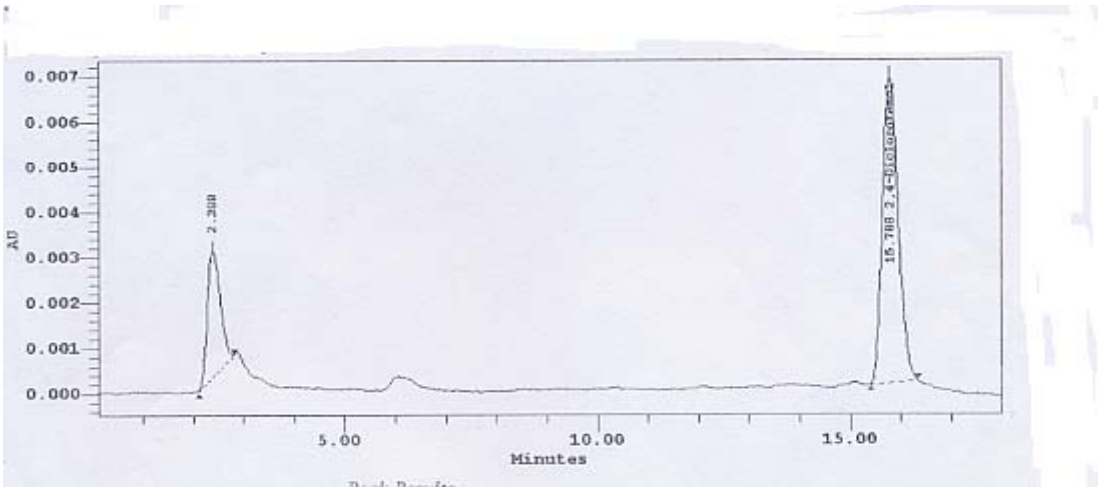

Figure 7.71: Chromatogram corresponding to sample at 1.0 min of photo-Fenton reaction

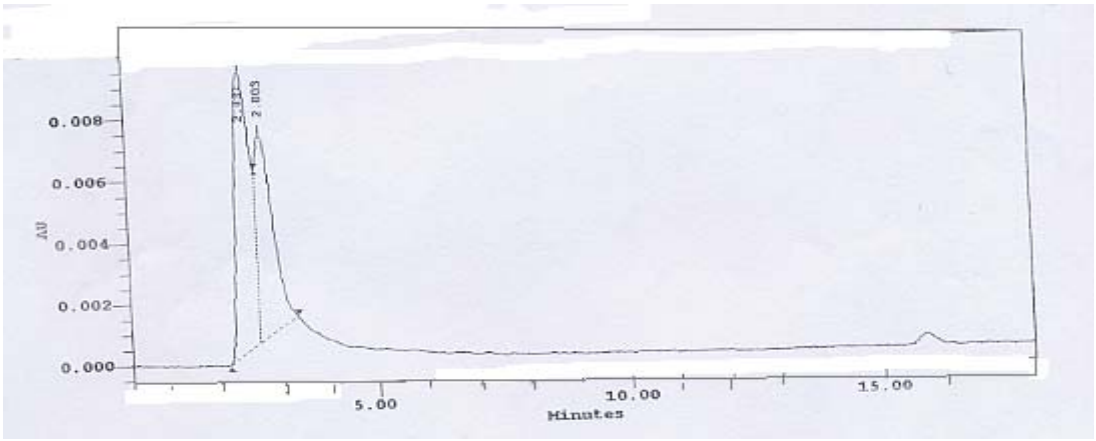

Figure 7.72: Chromatogram corresponding to sample at 5.0 min of photo-Fenton reaction

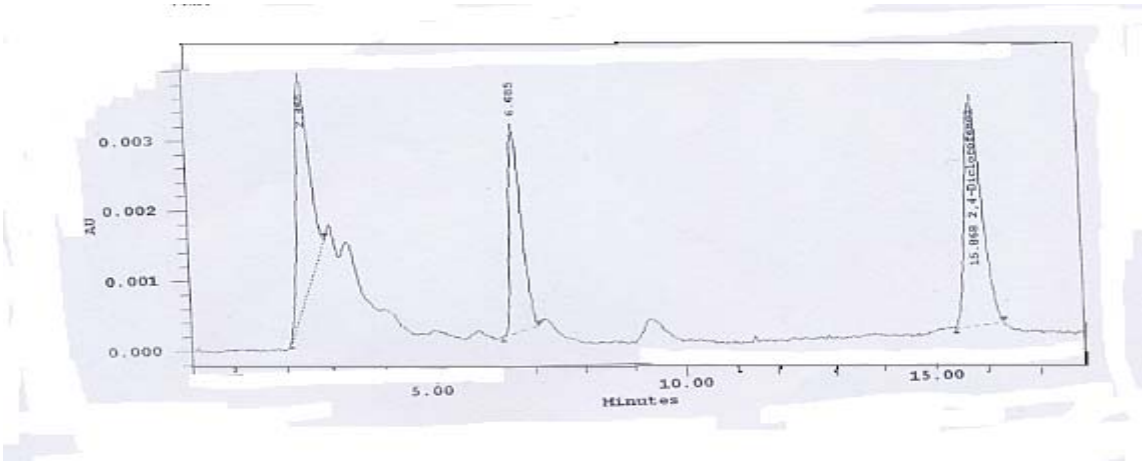

Figure 7.73: Chromatogram corresponding to sample at 30. min of photo-Fenton reaction

7.9. Comparison of the different studied processes for DCP and POH degradation

In the present section, different studied variables that have been commented before will be used for the comparison purpose between the processes: UV, UV/H_2O_2, UV/Fe (III), Fenton and Photo-Fenton, the general conditions and initial reactant concentration used in this section can be seen in legend of figure 7.74. all over the comparison theses initial condition were fixed.

In figure 7.74 the normalized DCP and POH concentrations as function of reaction time are compared for all the previous studies. Photo-Fenton process shows the best degradation results for both components (DCP and POH), while UV irradiation alone shows the slowest ones. 100%DCP was obtained with 50 mg.$L^{-1}H_2O_2$, 10 mg.L^{-1} Fe(II) and only 35 min, at the same time Fenton and UV/H_2O_2 need 80 min to gain only 80% DCP elimination with same initial Fe(II) and/or H_2O_2 concentrations. The same tendency can be seen clearly in for POH (see figure 7.74(B)).

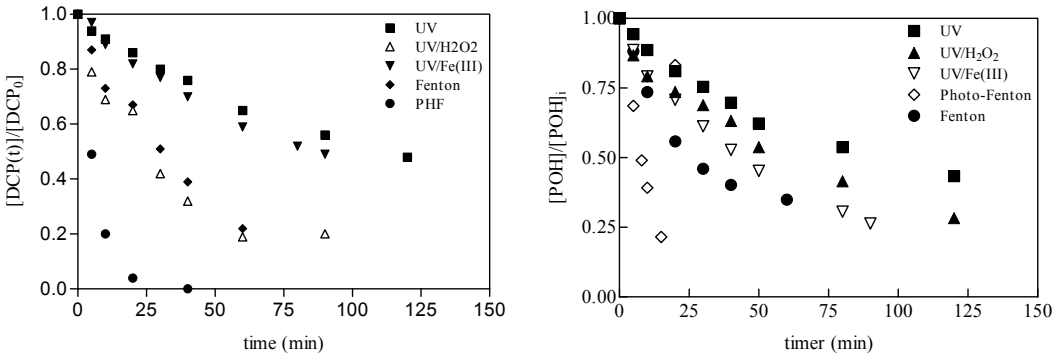

(A) (B)

Figure 7.74. Comparison of the different processes for DCP and POH removal. A) DCP, $[H_2O_2]_i$ = 50 mg.L^{-1}, $[Fe(II)]_i$= 10 mg.L^{-1}, $[Fe(III)]_i$= 70 mg.L^{-1} and free pH evolution, B) POH, $[H_2O_2]_i$ = 30 mg.L^{-1}, $[Fe(II)]_i$= 10 mg.L^{-1}, $[Fe(III)]_i$= 70 mg.L^{-1} and free pH evolution

Table 7.16 presents the pseudo-first order kinetic constant and experimental half-life time ($t_{1/2}$) for the same previous experiments. The results confirm the priority of photo-Fenton in DCP degradation over the other processes. For photo-Fenton reaction with the same previous conditions K_o is 0.11 min^{-1} and half-life time is 4.5 min, while the value the same values are 0.006 min^{-1} and 118 min respectively for UV process.

Table7.16: First rate constant and half-life time for different AOP´s. conditions for DCP, $[H_2O_2]_i$ = 50 $mg.L^{-1}$, $[Fe(II)]_i$= 10 $mg.L^{-1}$, $[Fe(III)]_i$= 70 $mg.L^{-1}$ and free pH evolution, and for POH, $[H_2O_2]_i$ = 30 $mg.L^{-1}$, $[Fe(II)]_i$= 10 $mg.L^{-1}$, $[Fe(III)]_i$= 70 $mg.L^{-1}$ and free pH evolution.

	DCP		*POH*	
Process	K_o (min^{-1})	$T_{1/2}$ (min)	K_o (min^{-1})	$t_{1/2}$ (min)
UV	0.006	118	0.008	90
UV/H_2O_2	0.03	22	0.011	53
UV/Fe (III)	0.0084	86	0.0153	46
Fenton	0.024	30	0.039	16
Photo-Fenton	0.106	4.5	0.101	4.8

TOC mineralization rate, for the different processes is presented in figure 7.75. Photo-Fenton process is found to have highest TOC reduction rate compare with other process (16% for DCP). Fenton and UV/Fe (III) provide similar results. However. it should not forgot that photo-Fenton process gives the TOC reduction during short reaction time, while other processes reaches the same value with longer time. This comparison is just qualitative one since in these reaction the purpose was to eliminate the contaminates (DCP or POH) from the solution and hence increase the biodegradability. Also, it is interesting to remained, as presented before, that photo-Fenton was able under moderate initial reactant concentration to mineralize all the TOC presented in the solution while the other process could not reach this point even at high initial reactant concentration and long reaction time.

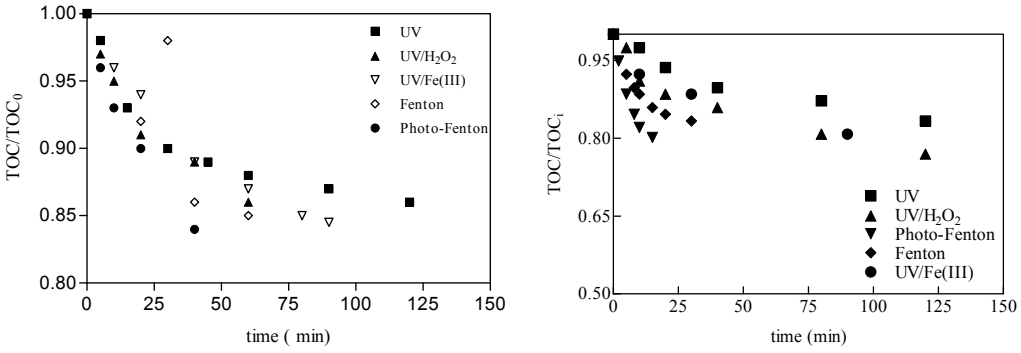

(A) (B)

Figure 7.75: TOC mineralization for different AOP´s. A) DCP, $[H_2O_2]_i$ = 50 $mg.L^{-1}$, $[Fe(II)]_i$= 10 $mg.L^{-1}$, $[Fe(III)]_i$= 70 $mg.L^{-1}$ and free pH evolution, B) POH, $[H_2O_2]_i$ = 30 $mg.L^{-1}$, $[Fe(II)]_i$= 10 $mg.L^{-1}$, $[Fe(III)]_i$= 70 $mg.L^{-1}$ and free pH evolution

Previous studies pointed out that chlorophenols mineralization follow first order kinetics (Esplugas et al., 1994 and Kuo, 1999). Therefore, the apparent first order rate

constants based in TOC mineralization for the previous process was examined. Results are presented in table in 7.17. All the processes have been found to follow first order kinetics except UV light, which shows deviation from linearity.

Table 7.17 the apparent first order rate constants based in TOC mineralization for different AOP´s

	DCP (min^{-1})	POH (min^{-1})
Process	$10^{-1}*K_{TOC}$	$10^{-2}*K_{TOC}$
UV	0.39±0.09	0.17±0.08
UV/H_2O_2	0.22±0.02	0.25±0.03
UV/Fe (III)	0.18±0.02	0.26±0.04
Fenton	0.17±0.03	0.80±0.02
Photo-Fenton	0.17±0.04	1.75±0.1

With respect to dechlorination during DCP photo-degradation, the results obtained from the first three processes (UV, UV/H_2O_2 and UV/Fe(III)) was miss leading since there were no predictability of the results, hence it was decided not to present them. Fenton and photo-Fenton results are compared in figure 7.76. Photo-Fenton process liberates more Cl^- ions than Fenton process (73 to 40% respectively). This may be explained by the main DCP degradation pathway is considered to be direct dechlorination through a nucleophilic displacement of chloride (by OH^-) hence photo-Fenton has more ability for this type of reaction due to is high hydroxyl radical production.

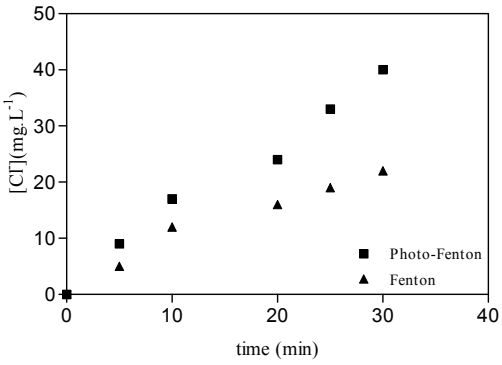

Figure 7.76: Dechlorination by Fenton and photo-Fenton process. $[H_2O_2]_i$ = 50 mg.L^{-1}, $[Fe(II)]_i$= 10 mg.L^{-1}, $[Fe(III)]_i$= 70 mg.L^{-1} and free pH evolution

As discussed earlier the degree of oxidation of organic matter can be presented by its COD/TOC ratio and AOS values. The change in oxidation state for the five processes at the same indicated conditions are plotted in figure 7.77 and 7.78. As it can be seen in the figures that photo-Fenton reaction has more oxidizing capacity compared with the other AOP processes. during 40 min reaction time COD/TOC for photo-Fenton and UV/Fe (III) reduced by 30 and 3% respectively, and AOS increase from –0.28 to 1.35 and from –0.44 to –0.21 for the same process respectively. The same tendency was noticed during POH photo-oxidation.

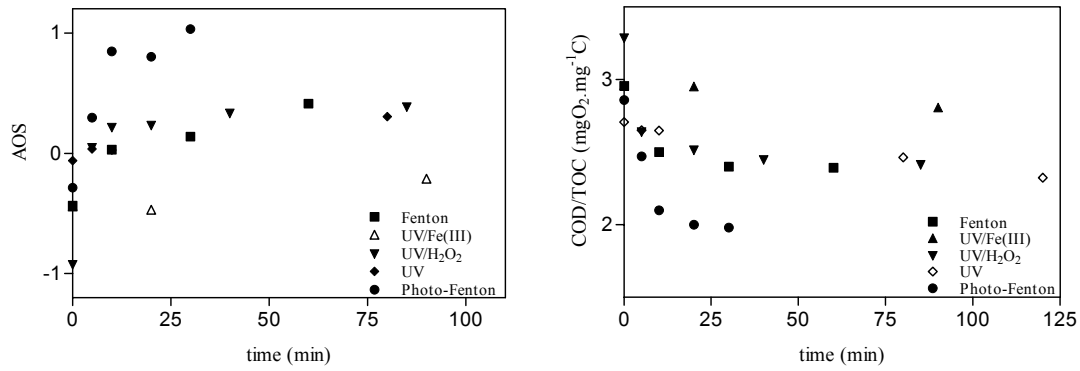

Figure 7.77: Change in oxidation state for the five processes during DCP photo-degradation. $[H_2O_2]_i$ = 50 mg.L^{-1}, $[Fe(II)]_i$= 10 mg.L^{-1}, $[Fe(III)]_i$= 70 mg.L^{-1} and free pH evolution.

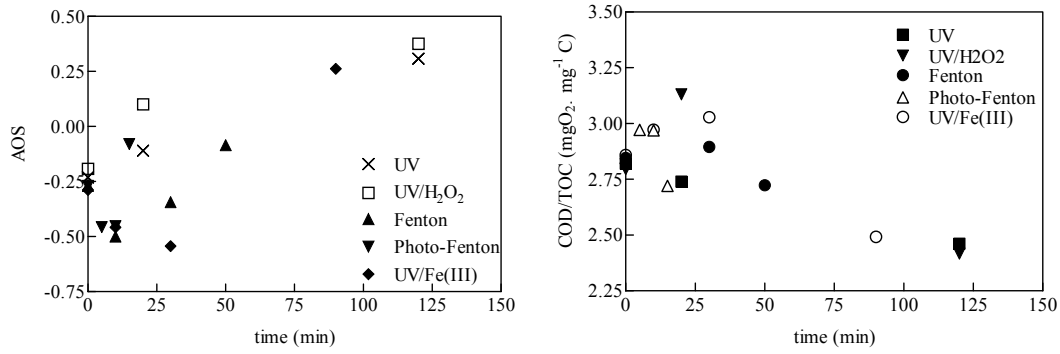

Figure 7.78: Change in oxidation state for the five processes during POH photo-degradation. $[H_2O_2]_i = 30$ mg.L^{-1}, $[Fe(II)]_i = 10$ mg.L^{-1}, $[Fe(III)]_i = 70$ mg.L^{-1} and free pH evolution.

With respect to biodegradability enhancement as discussed before the processes UV, UV/Fe (III) and UV/H_2O_2 had a negligible affect in the biodegradability improvement. For Fenton process, the increment in BOD_5 was zero while it is 3 mg O_2.L^{-1} for BOD_{21} at the same time for photo-Fenton BOD_5 and BOD_{21} was 13 and 17 respectively. Based in the present results, photo-Fenton shows better tendency in biodegradability enhancement compared with the other processes. This may aimed as mentioned before to strong ability of photo-Fenton in degraded the organic mater into other smaller intermediates which are readily more biodegradable.

Photo-Fenton process shows good efficiency in increasing the biodegradability of 100 and 1000 ppm POH solutions, by oxidation of the original solution to other more biodegradable byproducts. maximum biodegradability (measured as BOD_5/COD) of 0.92 was reached for both POH concentrations. Other photo-oxidation processes shows small improvement in biodegradability; during Fenton reaction biodegradability of 0.22 was found.

Finally, a rough costs estimation regarding operating costs and required reagents has been compared between the five studied processes. Reagents and electricity costs are shown in Table 7.18. Costs have been calculated for amount of DCP eliminated and TOC mineralized in each process. Among the studied processes, it can be seen that photo-Fenton and Fenton processes represent cheaper treatment process to degraded more phenol and/or eliminate organic matter. Other processes cost more energy to degraded in the same efficiency.

As a comparison between DCP and POH, it can be see that, POH degradation process is less than that of phenol, this may be due, as presented in the discussion to continous degradation tendency of POH at by different AOP´s.

Table 7.18: Reagents and electricity costs.

	Coste (€)
Electrecity	0.07
H_2O_2 (kg)	19
Fe(II) (kg)	7
Fe(III) (kg)	9

Table 7.19. Comparison of costs among the studied processes

Processes	DCP		POH	
	€/kg DCP eliminated	€/kg C eliminated	€/kg POH eliminated	€/kg C eliminated
UV	10.0	83.0	8.5	65
UV/H_2O_2	14.4	109.1	11	85
UV/Fe(III)	13.5	110.0	18	95
Fenton	10.0	88.0	8.5	75
Photo-Fenton	8.6	40.0	6.2	35

8. Treatment of DCP by AOP´s based on UVA-light

In this part, AOP´s were carried out based on UVA light irradiation to degraded DCP solution with initial concentration of 100 $mg.L^{-1}$. Two different reactor configurations was used, the first reactor has single blackblue lamp that emits irradiation at wavelength 350 nm (see photo-Reactor 2 section 5.1). The second reactor has multi-lamps that emit radiation basically at 360 nm (photo-Reactor 3 section 6.1). Another difference between the two reactors is the irradiation energy; single lamp reactor has power of 4W, throughout actinometry, it was found that 2.5 $\mu Einstein.s^{-1}$ photon flux entering this reactor, while multi lampss reactor has total lamp power 24W (three lamps with 8 W each), the photon flux of this reactor was 9.3 $\mu Einstein.s^{-1}$ (see appendix A1 for actinometrical calculations). For simplicity during the results discussion it will refer to the result according to single lamp and multi-lamps reactor. In both reactors the degradation and biodegradability improvement of DCP solutions were studied. As in the previous section, the influence of different operational conditions as, initial reactant concentrations, temperature, irradiation time and pH was examined, in addition to the effect of all these conditions in pre-treated solutions biodegradability. Furthermore, first order kinetic constant (K_0) and half-life time ($t_{1/2}$), during AOP´s reactions was determined. Experimental results obtained from the two reactor are tabulated in appendix A4.

8.1. Treatment of DCP by UVA /H_2O_2 and direct UVA-light

8.1.1 Photo-degradation

In these experiments both UVA-light alone and UVA-light combined with H_2O_2 were used to study the degradation of 100 $mg.L^{-1}$ DCP solutions. Figures 8.1 to 8.2 present the experimental results for single lamp reactor. In figure 8.1, DCP and TOC evolution as function of UVA-light irradiation is presented, direct UVA-light is not an efficient method to eliminate DCP solution; during 2 hour of reaction just 9% of original DCP was eliminated and only 4% total organic carbon mineralization was reached.

Addition of H_2O_2 to photo-reactor during UVA irradiation improves DCP degradation. As it was seen before, the degradation rate of DCP increases by increasing the initial hydrogen peroxide concentration. during 2 hours irradiation time, 37% of DCP removal and 13% TOC mineralization was obtained by adding 250 $mg.L^{-1}$ H_2O_2 (see figure 8.3). based on the high initial H_2O_2 concentration and the degradation value, this reactor H_2O_2/UVA is not a convenient method for DCP degradation.

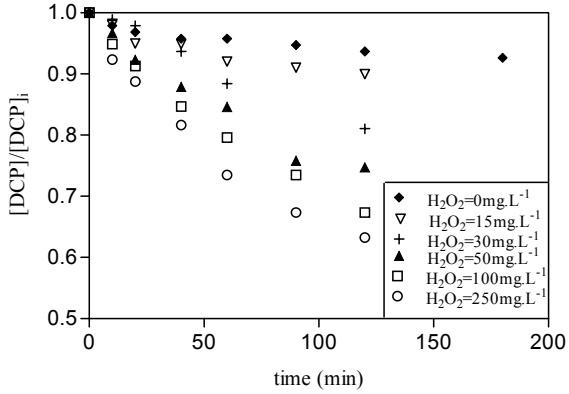

Figure 8.1 Evolution of DCP and TOC as function of UVA-light irradiation time in the single lamp reactor with different initial H_2O_2 concentrations.

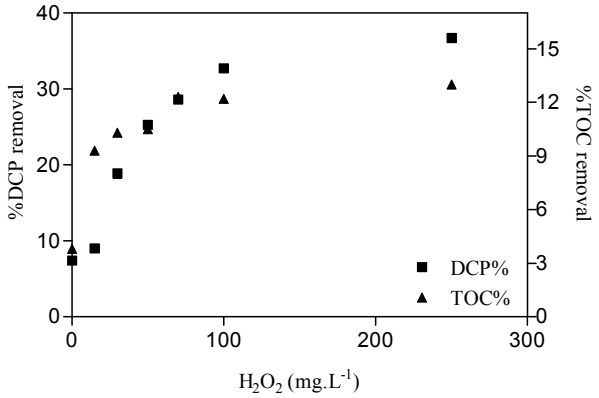

Figure 8.2: DCP and TOC removal percentage as function of H_2O_2 in UVA/H_2O_2 process for single lamp reactor, irradiation time 2 hours.

With respect to multi lamps reactor, experimental results are presented in figures 8.3 and 8.4. A significant improvement in the degradation rate could be noticed as a result of increasing the lamps irradiation energy and using new reactor configurations. Direct UVA photolysis at the same previous irradiation time (2 h) guide to 22% of DCP removal. Simultaneously, noticeable enhancement in degradation via combining UVA with H_2O_2 was achieved, up to 50% DCP degradation could be obtained using 200 mg.L^{-1} H_2O_2 and 2 h irradiation. Nonetheless, for all experimental conditions, it was noticed that no more than 12% TOC reduction can be acquired.

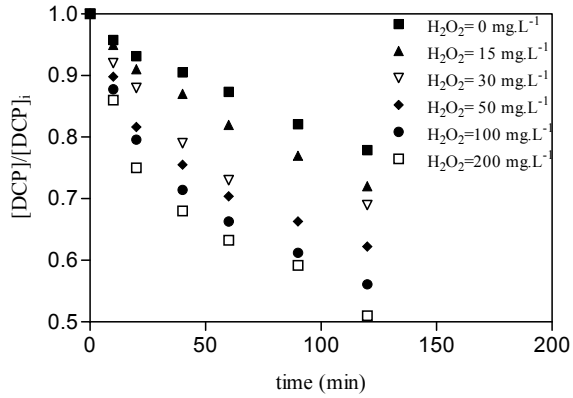

Figure 8.3: Evolution of DCP vs. reaction time for different H_2O_2 initial concentration in UVA/H_2O_2 process for multi lamps reactor.

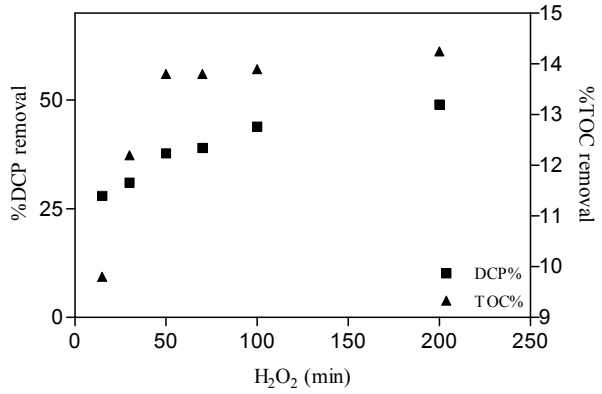

Figure 8.4: DCP and TOC removal percentage as function of H_2O_2 in UVA/H_2O_2 process for multi lamps reactor, irradiation time 2 hours.

During the reaction time, in both reactors, not all H_2O_2 amount was consumed, test shows that at least 60 mg.L^{-1} in single lamp and 30 mg.L^{-1} and multi lamps of non reacted H_2O_2 remained in the reactor vessel at the end of the reaction. The presence of high concentration of H_2O_2 in wastewater affect negatively the process feasibility. Also, it is a harmful for bacterial population if the treated wastewater diverted to second stage biological treatment. So, elimination of this residues should be done.

8.1.2 Quantum yield

An important parameter that gives an idea how efficient the direct photolysis process is the quantum yield. According to reactor geometry and the actinometrical results, the quantum yield at initial reaction time was evaluated to be equal to 1.0±0.2 mmol.Einstein^{-1} for single lamp reactor and 2.5±0.4 mmol.Einstein^{-1} for multi lamps

reactor. Significant difference can be noticed between single lamp and multi lamps reactor from quantum yield point of view.

It is interesting to mention the small difference between reactor 1 (UV-light, wavelength 254nm and nominal power 60 W) and multi lamps reactor (UVA-light, wavelength 360 nm and nominal power 24 W) with respect to quantum yield, ϕ = 3.2±0.2 mmol.Einstien^{-1} in reactor 1 and 2.5±0.4 mmol.Einstein^{-1} in multi lamps reactor. The case that indicates small difference in degradation efficiency between both reactors.

The degradation kinetic was also calculated for these reactions, experimental results were tested for first order kinetic model Eq. 7.1. The logarithmic normalized DCP as function of time for single lamp reactor is plotted in figure 8.5. First order kinetic constants values for both reactors are presented in table 8.1. A good distribution of experimental results around straight line verify the validity of the proposed model. Nonetheless, small deviation from linearity was noticed for direct UVA photolysis in single lam reactor. Half-life time could not be calculated under the present experimental conditions as all the maximum removal could be achieved is too low.

The reaction rate constant obtained using UVA-light in single lamp reactor is smaller than that achieved from multi lamps reactor by more than an order of magnitude (0.0005 to 0.0015), this confirm the precedence of multi lamps reactor configuration over single lamp reactor.

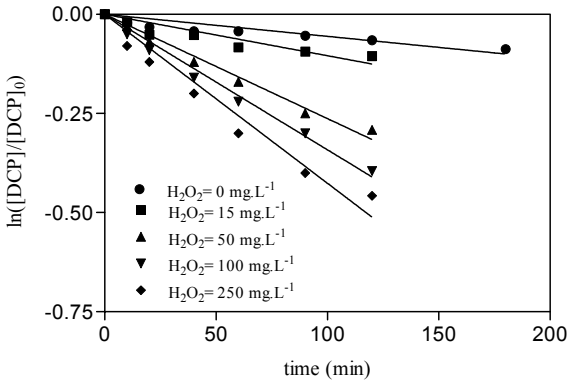

Figure 8.5: First order kinetics for DCP degradation by UVA/H_2O_2 process. At different H_2O_2 initial concentration in single lamp reactor

As a comparison between both reactors, multi lamps reactor shows more degradation efficiency than single lamp reactor. Using UVA irradiation alone DCP degradation of 9% and 22% achieved in both reactor respectively. Moreover 50% of DCP degradation could

be obtain in the multi reactor just by using 200 $mg.L^{-1}$. This limit could not be achieved in single lamp even with more initial hydrogen peroxide concentration (250 $mg.L^{-1}$ gives 39% degradation).

Table 8.1: First order kinetics for DCP degradation by UVA/H_2 O_2 process. At different H_2O_2 initial concentration for single and multi lamps reactor.

Single Lamp reactor (4W)			Multi lamps reactor (24W)		
H_2O_2 ($mg.L^{-1}$)	K_0 (min^{-1})	R^2	H_2O_2 ($mg.L^{-1}$)	K_0 (min^{-1})	R^2
0	0.0005	0.72	0	0.0015	0.94
15	0.0010	0.93	13	0.0029	0.95
50	0.0026	0.94	50	0.0038	0.91
100	0.0034	0.95	100	0.0055	0.88
250	0.0043	0.95	200	0.0063	0.90

As it was commented in quantum yield calculations, UVA multi lamps reactor is more o less similar to UV reactor. In this section, the reaction rates constant obtained by using UVA multi lamp reactor (wavelength 350 nm) is smaller than that achieved by using UV-light reactor (wavelength 254 nm), for the same initial H_2O_2 concentration (100 $mg.L^{-1}$) K_0 was 0.0034 for UVA reactor and 0.04 UV reactor. This tendency could be featured to absorption spectrum characteristics of hydrogen peroxide. It is known that hydrogen peroxide absorption spectrum extends beyond 350 nm but has favorable absorption spectrum wavelength around 250 nm, which leads to efficient H_2O_2 photolysis, generating more $OH^{\bullet}$ radicals (Pignatello et al., 1999). Thus, with UVA reactor (wavelength 350 nm) the molar absorption coefficient is low, and small fraction of H_2O_2 could be photolyzed to produce hydroxyl radicals.

8.1.3. Effect of UVA and UVA/H_2O_2 processes in biodegradability:

In this section also BOD_n/COD and BOD_n/TOC will be used as biodegradability indicators. BOD_5 and BOD_{21} of solutions treated by UVA and UVA/H_2O_2 processes were tested; the change of pre-treated solution biodegradability of both processes was negligible. For single lamp reactor and initial H_2O_2 concentration of 250 $mg.L^{-1}$ during 2 hours experimental time, the biodegradability, measured as BOD_5/COD ratio increased from zero for original DCP solution up to 0.011 for pre-treated solution. This tendency could be deduced to deficiency of these processes in elimination DCP totality.

As presented before, DCP is not readily biodegradable component, and it may cause inhibition for activated sludge. Hence, no change in BOD_n was noticed.

Different tendency was observed in multi lamps reactor, significant enhancement in biodegradability was achieved. Figure 8.6 presents the biodegradability improvement as function of initial H_2O_2 used in multi lamps reactor. It can be seen that, BOD_5, BOD_5/COD and BOD_5/TOC start to increase by increasing the hydrogen peroxide concentration as result of DCP degradation. BOD_5/COD and BOD_5/TOC ratios of 0.06 and 0.1 respectively were obtained, this is an indication in the increase of organic mater proportion able to bio-oxidation.

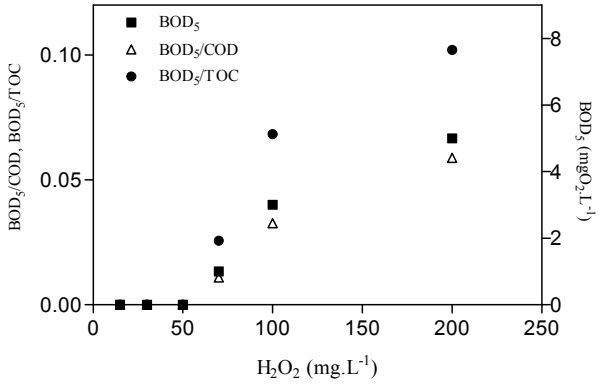

Figure 8.6: BOD_5, BOD_5/COD and BOD_5/TOC as function of initial H_2O_2 in UVA/H_2O_2 for multi lamps reactor, reaction time 90 min.

8.1.4. Change on oxidation state

The change in oxidation state all over the reactions was also followed, Figures 8.7 and 8.8 present the COD/TOC and AOS evolution as function of reaction time for single lamp reactor. The degradation of DCP solution via direct UVA process direct to small variation in the oxidation state of organic matter; during 2 hour irradiation COD/TOC decreased from 3.01 to 2.97 and AOS increased from -0.53 to -0.39.

In UVA/H_2O_2 reaction, the change in oxidation state of the organic matter was noticed to be dependent on the initial H_2O_2 used. But, the change in oxidation state all over the reaction was tiny, only 15 % decay in COD/TOC ratio was occurred at the highest H_2O_2 initial concentration (250 $mg.L^{-1}$). The same tendency was noticed for AOS variation (from –0.53 up to 0.12). The weak oxidation take place to organic matter can be an explanation to the insignificant biodegradability improvement in this reactor.

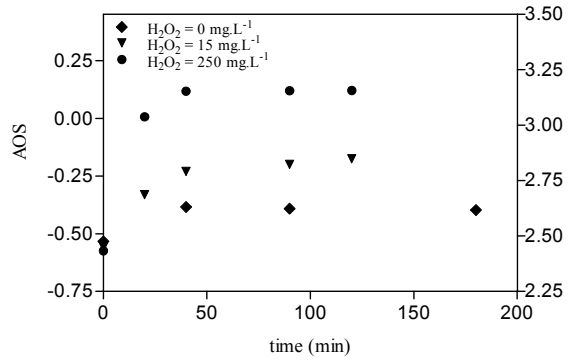

Figure 8.7 Evolution of AOS vs. reaction time for UVA/H_2O_2 process at different initial H_2O_2 concentrations in single lamp reactor.

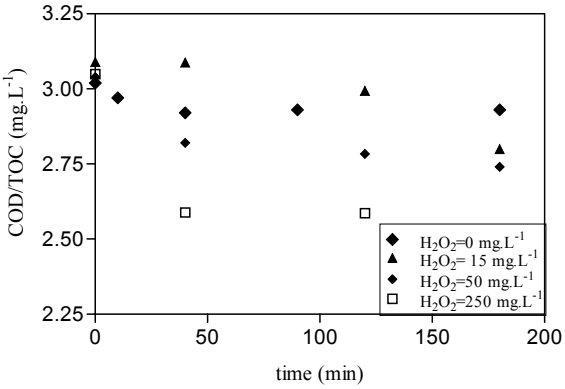

Figure 8.8: Evolution of COD/TOC vs. reaction time for UV/H_2O_2 process at different initial H_2O_2 concentrations in single lamp reactor.

In the case of multi lamps reactor (see figures 8.9 and 8.10), all through the reaction it was observer that organic matter oxidation follow the same tendency as before mainly increase the oxidation by increase the initial H_2O_2 concentration used. But, in this reactor further oxidation of organic matter was observed, this may be referred to additional irradiation energy and the new reactor arrangements. For the highest initial H_2O_2 (200 mg.L^{-1}) COD/TOC ratio decayed by 20% and AOS increase from –0.57 to 0.28.

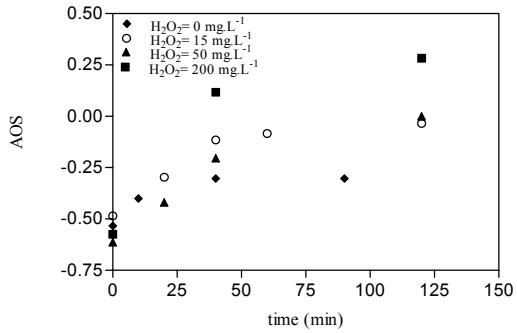

Figure 8.9: Evolution of AOS vs. reaction time for UVA/H_2O_2 process at different initial H_2O_2 concentrations in multi lamps reactor.

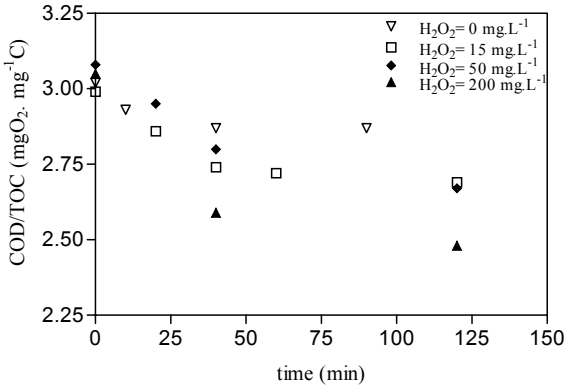

Figure 8.10: Evolution of COD/TOC vs. reaction time for UVA/H_2O_2 process at different initial H_2O_2 concentrations in multi lamps reactor.

In section 7.1 and 7.2 when UV light (λ=254 nm) was used for DCP degradation and at the same initial H_2O_2 concentration (200 $mg.L^{-1}$), the decay in COD/TOC ratio was found to be 26%, which is in the order of magnitude obtained by multi lamp reactor. Thus, from oxidation state point of view, the two reactors (UV and UVA multi lamps) are similar in oxidation the organic matter. Nonetheless, the cost associated in using multi lamps reactor with irradiation energy of 24W is more favorable over the use of UV reactor with irradiation energy of 60W.

8.2. Treatment of DCP by UVA/Fe(III) process

8.2.1 Photo-degradation

UVA/Fe(III) process was also tested. Figures 8.11 and 8.12 present the evolution of DCP as function of reaction time at different initial Fe(III) concentrations for single lamp reactor. The combination of Fe(III) with UVA-light is more efficient than UVA radiation alone. At the beginning the degradation was proportional to amount of Fe (III) added; increase the degradation by increasing initial iron salt concentration. During 90 min irradiation time and 120 $mg.L^{-1}$ Fe(II) initial concentration, 60 % of DCP was degraded. When this process was tested with UV reactor (section 7.3), it was noticed that the major degradation take place during the first 60 min of reaction time. Dissimilar to that, in the present reactions it was noticed that the degradation continue all over the reaction time (see figure 8.11). This suggests the continuous hydroxyl radicals formation. A reason for that is the absorption spectrum of ferric ion, which has a high molar absorption coefficient at wavelength around 350 nm. Consequently, permanent formation of hydroxyl radicals arise.

With respect to TOC reduction, it can be seen in figure 8.12 that, for all the studied condition TOC reduction keeps around 12%. For 60% DCP elimination (the maximum degradation obtained by this process) 12% of TOC was reduced.

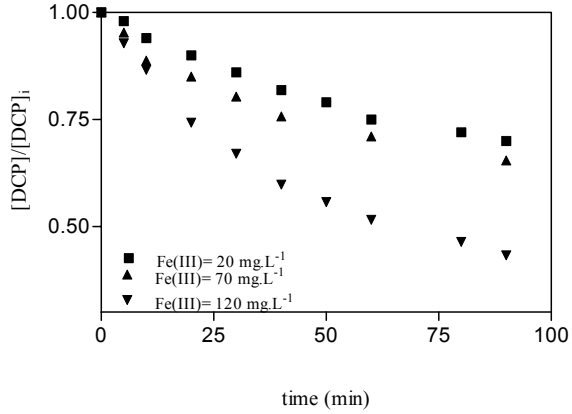

Figure 8.11 Evolution of DCP vs. reaction time at different initial Fe(III) concentrations in UVA/Fe(III) process in single lamp reactor.

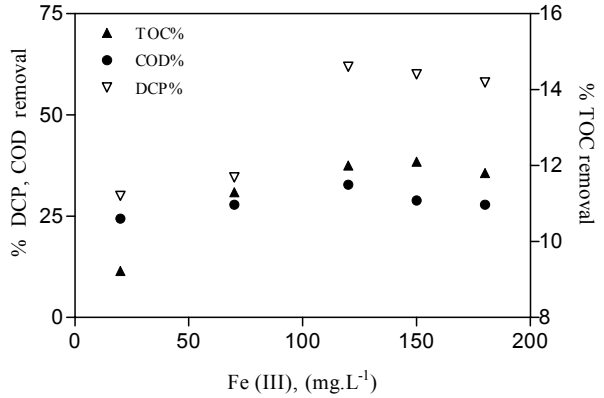

Figure 8.12 DCP, COD and TOC removal as function of initial Fe(III) in UVA/Fe(III) process in single lamp reactor reaction time 90 min.

Fe(III)/UVA process also was tested in multi lamps reactor, the evolution of DCP as function of irradiation time at different initial Fe(II) concentrations is presented in figure 8.13. the degradation tendency in both reactors (single and multi lamp) is identical; the degradation increase by increasing the Fe(III) initial concentration, and the reaction prolong all over the reaction time. Moreover, the degradation efficiency and TOC reduction seems to be superior in multi lamps reactor as a result of change in irradiation power; at 120 $mg.L^{-1}$ Fe (III) and 90 min irradiation time 70% of DCP degradation and 15% TOC reduction were accomplished.

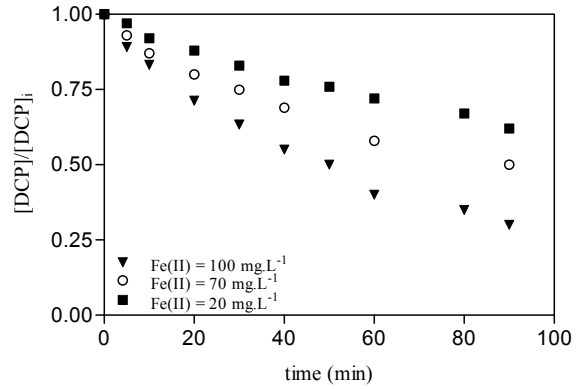

Figure 8.13 Evolution of DCP vs. reaction time at different initial Fe(III) concentrations in UVA/Fe(III) process in multi lamps reactor.

Experimental data for both reactors was tested for first order kinetic and half-life time (see table 8.2). regression analysis to straight line confirms the validity of the proposed model. It can be noticed in the table that, for both reactors DCP degradtion increase by increasing the initial Fe(II) concentration. On the other hand, remarkable change in DCP degradation efficiency was seen by increasing the irradiation energy.

Table 8.2: first order kinetics for DCP degradation by UVA/Fe(III) process. At different Fe(III) initial concentration

Single lamp reactor (4W)				*Multi lamps reactor (24W)*			
[Fe (III)], (mg. L^{-1})	*$t_{1/2}$ (min)*	*K_0 (min^{-1})*	R^2	*[Fe (III)], (mg. L^{-1})*	*$t_{1/2}$ (min)*	*K_0 (min^{-1})*	R^2
20	> 90	0.0046	0.99	20	> 90	0.0054	0.98
70	> 90	0.0062	0.95	70	90	0.0087	0.96
120	50	0.0113	0.98	100	50	0.0136	0.97

8.2.2. Effect of UVA/Fe(III) processes in biodegradability:

Solutions treated by Fe(III)/UVA light were tested for their biodegradability, BOD_5/COD and BOD_5/TOC was measured on purpose. For both reactor no significant improvement in these ratios was noticed: as it was seen in the previous section at 120 $mg.L^{-1}$ Fe(III) and 90 min irradiation time DCP elimination of 60 and 70% was obtained. At this conditions BOD_5/COD and BOD_5/TOC were increased up to 0.024 and 0.0007 in single lamp. For multi lamp reactor the same ratios augmented respectively up to 0.0385 and 0.001. Two reasons may explain this affinity:

I. The presence of DCP in solution; In the experiments, the minimum remaining concentration of DCP was 30 $mg.L^{-1}$ so it is strongly affect the BOD_5 behaviour.

II. High initial concentration of Fe(III) has negative influence in BOD_5. In spite the fact that, for BOD_5 measurements solutions treated by UVA/Fe(III) were neutralized and decanted to a proper time and only the supernatants was used in BOD tests.

8.2.3 Change on oxidation state

As before, the variation of organic oxidation states was also tested. Results are presented in Figures 8.14 to 8.17 where AOS and COD/TOC ratio were plotted against the irradiation time for different initial Fe(III) concentration. During the reaction there were an oxidation of the contained organic matter due to hydroxyl radical formation. The degree of oxidation is weakly dependent in initial Fe(III) concentration. in single lamp with initial ferric ion concentration of 120 $mg.L^{-1}$ an increment on AOS from –0.4 to 0.63 and reduction COD/TOC ratio from 2.94 down to 2.24 was obtained.

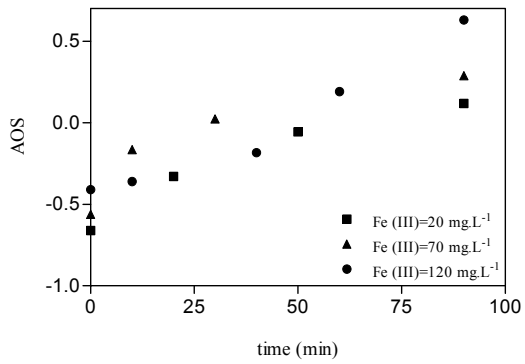

Figure 8.14: Evolution of AOS as function of reaction time in UVA/Fe(III) process, for different initial Fe(III) concentrations in single lamp reactor.

The same tendency was observed in multi lamp reactor, with better oxidation ability as result of bigger lamp energy. But still weakly dependent of initial Fe(III), increasing the initial Fe(III) concentration from 70 to 120 $mg.L^{-1}$ leads to increment in oxidation sate of the contained organic matter by 12 %.

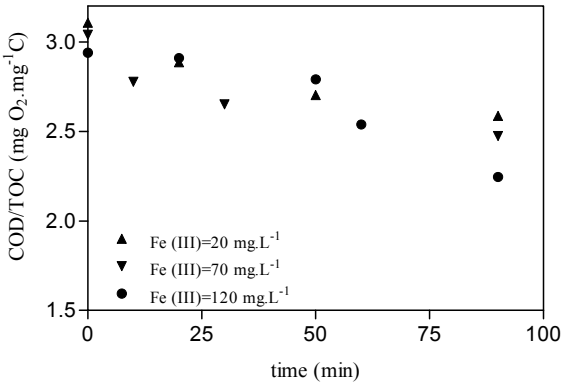

Figure 8.15: Evolution of COD/TOC as function of reaction time in UVA/Fe(III) process, for different initial Fe(III) concentrations in single lamp reactor.

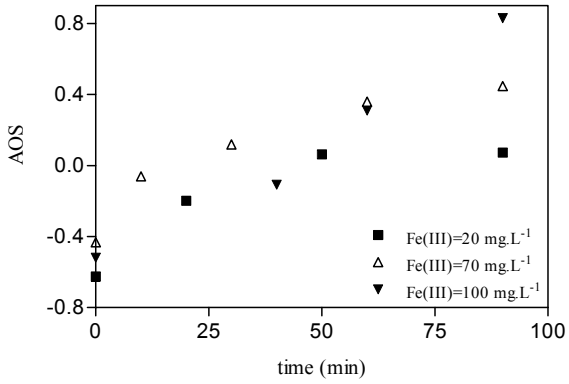

Figure 8.16: Evolution of AOS as function of reaction time in UVA/Fe(III) process, for different initial Fe(III) concentrations in multi lamps reactor.

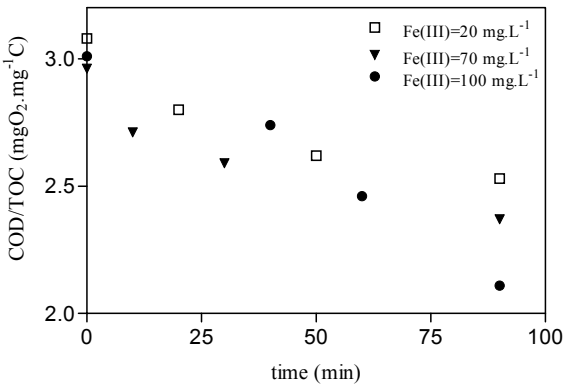

Figure 8.17: Evolution of COD/TOC as function of reaction time in UVA/Fe(III) process, for different initial Fe(III) concentrations in multi lamps reactor.

8.3. Treatment of DCP by Photo-Fenton:

8.3.1 Photo-degradation

DCP degradation by photo-Fenton reaction was studied in both reactors, in this section all photo-Fenton operating conditions that affect hydroxyl radical formation will be discussed in detail as well as biodegradability improvement.

Effect of initial H_2O_2 concentrations

Photo-Fenton reaction were carried out at different initial concentration of H_2O_2 in both reactors. Figures 8.18 and 8.19 present the evolution of DCP and TOC as function of time in single lamp reactor and fixed initial Fe(II) concentration to 10 mg.L^{-1}. It can be seen that, DCP degradation rate is dependent on initial H_2O_2 concentration, due to production of more $OH^{\bullet}$ radicals that can attack the organic matter.

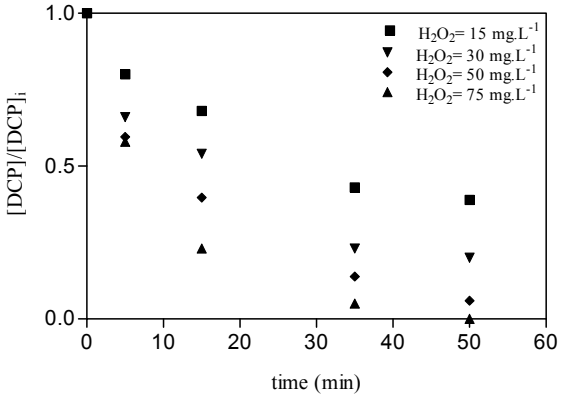

Figure 8.18. Evolution of DCP as function of irradiation time at different H_2O_2 in single lamp photo-reactor $[Fe(II)]_i = 10$ mg. L^{-1}

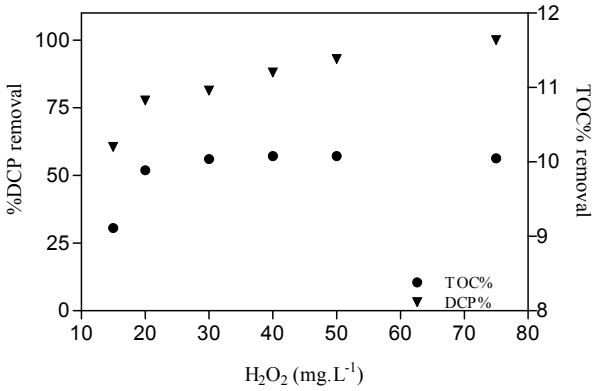

Figure 8.19: DCP removal as function of different initial H_2O_2 concentration in single lamp photo-reactor $[Fe(II)]_i = 10$ mg. L^{-1} or

In photo-Fenton reaction H_2O_2 concentrations decline significantly over the reaction periods, and this leads to significant degradation of DCP. In this reactor 100% DCP elimination was obtained with following conditions: 75 $mg.L^{-1}$ H_2O_2, 10 $mg.L^{-1}$ Fe(II) and 50 min reaction. This elimination was combined with 10% TOC reduction.

The same tendency was detected in multi lam reactor (see figure 8.20 and 8.21). With this reactor 65 $mg.L^{-1}$ H_2O_2, 10 $mg.L^{-1}$ Fe(II) and 35 min irradiation time was sufficient to reach100% DCP elimination. Again TOC reduction of 12% was obtained in this reactor.

In both reactors, it was noticed that, not all the added H_2O_2 degraded, and small non reacted fraction of initial H_2O_2 was noticed to remain in reactor (15% of initial H_2O_2 concentration for single lamp and 8% for multi lamp reactor). An explanation of that may be due to H_2O_2 lower absorption coefficient at the working wavelength (350 and 360 nm), that may limited the photolysis of H_2O_2.

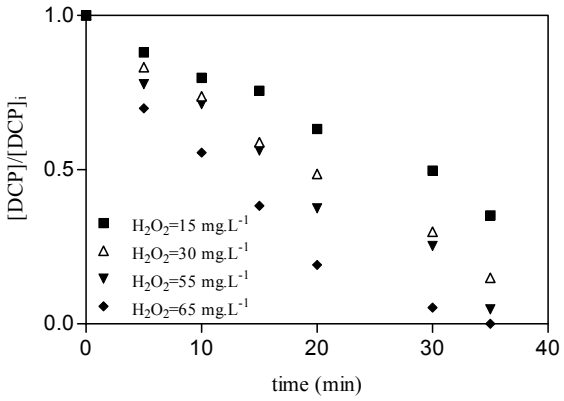

Figure 8.20. Evolution of DCP as function of irradiation time at different H_2O_2 in multi lamps photo-reactor. $[Fe(II)]_i = 10$ mg. L^{-1}

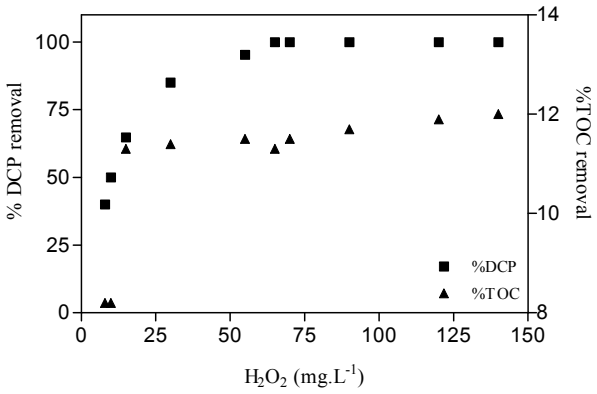

Figure 8.21: DCP and TOC removals as function of irradiation time at different H_2O_2 in multi lamps photo-reactor .$[Fe(II)]_i = 10$ mg. L^{-1}.

As a comparison between UV light reactor and multi lamp UVA reactor in DCP degradation via photo-Fenton process. It was noticed that both reactor are able to eliminate all DCP from the solution, this was achieved in UV reactor by 50 $mg.L^{-1}$ H_2O_2, 10 $mg.L^{-1}$ Fe(II) and 40 min and 65 $mg.L^{-1}$ H_2O_2, 10 $mg.L^{-1}$ Fe(II) and 35 min irradiation in multi lamp reactor. Based on the present results, it can be confirm that using multi lamp UVA (with 24W) is strongly comparable with UV (60W). with respect to TOC reduction it was noticed that multi lamp reactor is 50% less that UV reactor.

First order kinetic constant and half-life were checked, Table 8.3 presents results with respect to both reactors. It can be seen that multi lamp reactor show faster kinetic than single lamp reactor. As a comparison, K_0 values at initial H_2O_2 concentration of 30 $mg.L^{-1}$ was found to be 0.045 for multi lamps reactor and 0.038 for single lamp. Also, table 8.3 shows that multi lamps reactor has smaller half-life time than that of single lamp reactor. Which confirm the previous observation.

As a comparison K_0 and half-life obtained in multi lamp reactor and UV reactor, it was found that multi lamp reactor K_0 and half-life are smaller by an order of magnitude than that that achieved by UV reactor; at 50 $mg.L^{-1}$ H_2O_2, K_0 and half-life time are 0.057 min^{-1} 10 min for multi lamp UVA reactor and 0.11 min^{-1} and 4.5 min for and UV reactor. The difference could be point to favourable H_2O_2 absorption spectra at wavelength 254nm.

Table 8.3: First order kinetics for DCP degradation by photo-Fenton process. At different H_2O_2 initial concentration. $[Fe(II)]_i$= 10 mg. L^{-1}, 50 min irradiation time and free pH evolution.

Single lamp (4W)			*Multi lamps (24W)*		
$[H_2O_2]$ (mg. L^{-1})	*$t_{1/2}$ (min)*	*K_0 (min^{-1})*	*$[H_2O_2]$, (mg. L^{-1})*	*$t_{1/2}$ (min)*	*K_0 (min^{-1})*
15	> 50	0.021	15	30	0.026
30	18	0.038	30	15	0.045
50	12	0.057	55	12	0.046
75	8	0.087	65	5	0.091

Effect of iron ion concentrations

The effect of the initial Fe(II) concentration was tested. In single lamp reactor, different sets of experiments with various amounts of the iron salt and fixed amount of initial

H_2O_2 (15, 30 and 50 $mg.L^{-1}$) were carried out. The evolution of normalized DCP as function of irradiation time at different initial Fe(II) concentration and 15 $mg.L^{-1}H_2O_2$ is shown in figure 8.22. DCP elimination was observed to increase by increasing the initial Fe(II) concentration, as a result of more hydroxyl radicals formation via iron photo-redox reaction. As mentioned before, Fe(II) may act as $OH^{\bullet}$ scavenger, but under theses experimental conditions scavenging effect was not clear. Moreover, it was found that the major degradation occurs during the first 30 min of the reaction, and only a small degradation fraction could be achieved in the remaining 20 min.

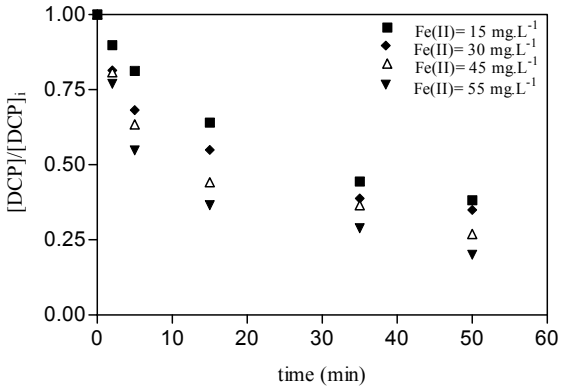

Figure 8.22: Evolution of normalized DCP concentration as function of time at different initial Fe(II) concentration in single lamp reactor. $[H_2O_2]_i$ =15 $mg.L^{-1}$

Figures 8.23 and 8.24 present results obtained by photo-Fenton reaction done with initial H_2O_2 of 30 $mg.L^{-1}$. Under these conditions, it was noticed that;

- at the beginning DCP degradation increases by increasing the iron concentration until it reach to the point where addition more iron has no effect in the degradation, and degradation carve take a plateau form.
- The degradation continue all over the reaction time, this may be as a results of presence high reagents (H_2O_2 and Fe(II)) that produce continuously hydroxyl radicals.
- Fe(II) scavenging effect was observed to take place at Fe(II) concentration of 40 $mg.L^{-1}$. this may be due to the formation of brown turbidity in the solution that cause the recombination of hydroxyl radicals(Ghaly et al., 2001).

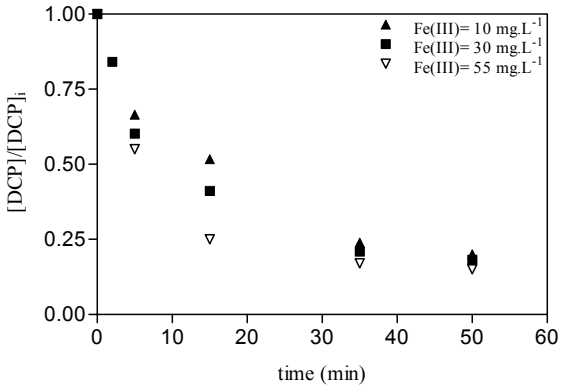

Figure 8.23: Evolution of normalized DCP concentration as function of time at different initial Fe(II) concentration in single lamp reactor. $[H_2O_2]_i$ =30 mg.L^{-1}

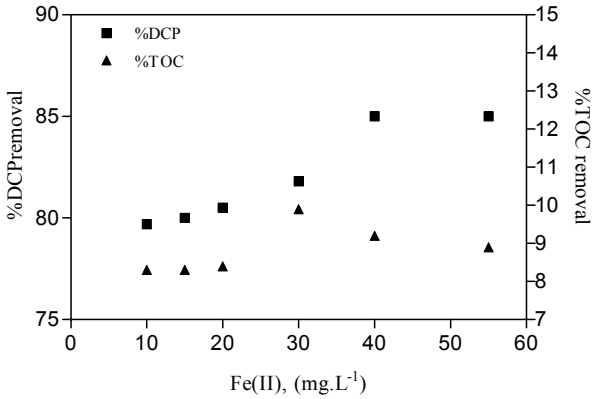

Figure 8.24: DCP and TOC degradation as function of iron catalyst in photo-Fenton process in single lamp reactor. $[H_2O_2]_i$ =30 mg.L^{-1} and 50 min irradiation.

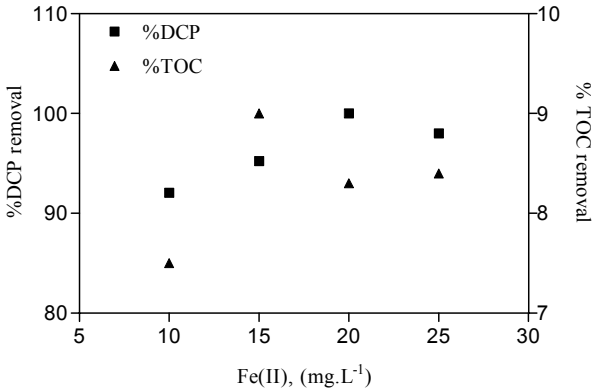

Figure 8.25: DCP and TOC degradation as function of iron initial concentration in single lamp photo-reactor. $[H_2O_2]_i$ =50 mg.L^{-1} and 50 min irradiation.

In all earlier experiments, 100% DCP elimination only could be achieved with experiments carried out with a minimum of 50 $mg.L^{-1}$ initial H_2O_2 concentration (see figure 8.25). The reaction conditions were: 50 min irradiation time , free pH evolution and 20 $mg.L^{-1}$ Fe(II). For these experimental conditions only 9% TOC reduction was achieved.

In case of multi lamps reactor (see figure 8.26), DCP degradation tendency achieved in this reactor is the same for single lamp reactor with two principle differences:

- Total DCP elimination could be acquired under small initial reactant concentration and short irradiation time; 100% DCP removal was gained under the following conditions: 15 $mg.L^{-1}$ H_2O_2 , 60 $mg.L^{-1}$ Fe(II) and 35 min irradiation time.

- At higher Fe (II) initial concentration no scavenging effect of iron ion was noticed, this may be attributed to enough concentrations of iron ion that goes a photo-redox reaction and so produce more hydroxyl radicals.

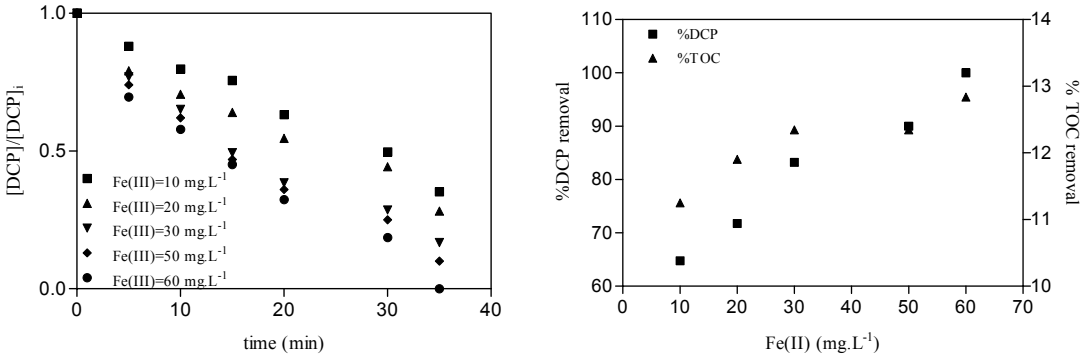

Figure 8.26: DCP degradation as function of iron catalyst in photo-Fenton process in multi lamps reactor. $[H_2O_2]_i$ =15 $mg.L^{-1}$ and 35 min irradiation.

As before, first order kinetic model and half-life time were examined. Results are summarized in table 8.4 for both the upper preceding experimental sets. Multi lamps reactor has high kinetic constant compare with single lamp reactor, also in this section it can be seen that half-life time for multi lamps reactor is smaller than that of single lamp reactor to the same reason explained before. It is interesting to remake that, the validity of first order model is affected by initial iron concentration. For the two reactors at small initial iron concentration (e.g 30 $mg.L^{-1}$) regression analysis shows a good experimental data distributions around straight line (R^2 =0.95 as an average), but as

initial iron concentration increase the validity of first order decrease (for initial H_2O_2 of 50 $mg.L^{-1}$ R^2 is 0.67 for single lamp reactor). Again, multi lamps reactor has better kinetic constant than single lamp reactor, as an indication of continuous hydroxyl radical production, that lead to more degradation efficiency.

Table 8.4: First order kinetics for DCP degradation by photo-Fenton process. At different H_2O_2 and Fe(II) initial concentration for single and multi lamps reactors. 50 min irradiation time and free pH evolution.

	Single lamp reactor (4W)				*Multi lamps reactor (24W)*			
H_2O_2 ($mg.L^{-1}$)	Fe(II) ($mg.L^{-1}$)	K_0 (min^{-1})	R^2	$t_{1/2}$ (min)	Fe(II) ($mg.L^{-1}$)	K_0 (min^{-1})	R^2	$t_{1/2}$ (min)
15	15	0.021	0.95	34	10	0.026	0.94	30
	30	0.024	0.97	25	20	0.032	0.95	20
	45	0.028	0.95	22	50	0.053	0.93	13
	55	0.034	0.85	18	60	0.056	0.99	11
30	10	0.036	0.91	18.5	10	0.045	0.93	16
	30	0.039	0.88	15.4	30	0.057	0.85	13
	55	0.042	0.67	15.53	50	0.067	0.70	10

Effect of temperature :

The effect of temperature on DCP degradation rates was determined for both reactors (see figure 8.27), where the removal percentage of DCP and TOC are plotted vs. reaction temperature. It was noticed that in single lamp reactor, increase the temperature from 25 to 45 ºC, and under the same initial reactant concentrations (H_2O_2 30 $mg.L^{-1}$,Fe(II) =10 $mg.L^{-1}$ and reaction time 50) leads to improve in DCP% removal from 60.5% to 80%. The same tendency was observed in multi lamps reactor, the same change in temperature (25 to 45 ºC) under photo-Fenton conditions of 30 $mg.L^{-1}H_2O_2$, 10 $mg.L^{-1}$Fe(II), and reaction time 35 min improve DCP elimination from 85 to 99%. In fact, it was expected that increase the temperature will lead to the point where optimum temperature could be deduced, because when temperature increase, H_2O_2 decompose to H_2O and O_2, with an expected negative effect on the availability of H_2O_2 and hence hydroxyl radicals. Also radical

reactions have very low activation energies and consequently, are not influenced by temperature. Nevertheless, not all the contributing reactions are radical ones, like the Fenton reaction itself, and some of photo-Fenton reactions, these elementary reactions can be affected by temperature (Utset et al., 2000). In any case for both experimental conditions data are clear, pointing towered better DCP degradation at higher temperature when the temperature increased. However, the effect of this temperature increment was weak in %TOC reduction (9.09 to 9.7 %) in single lamp reactor and (11.4 to 12.4%) for multi one.

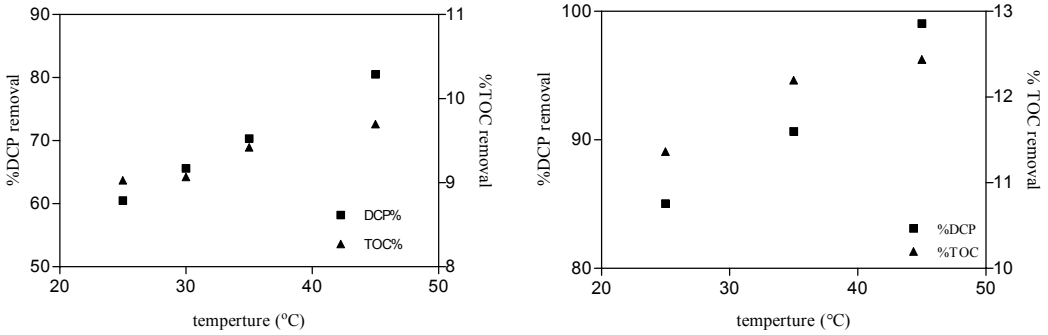

Figure 8.27: DCP% removal and TOC elimination for different initial temperature. A) single lamp reactor, $[H_2O_2]_i$= 30 mg.L^{-1},$[Fe(II)]_i$ =10 mg.L^{-1}, free pH evolution and reaction time 50 B) multi lamps reactor, $[H_2O_2]_i$= 30 mg.L^{-1},$[Fe(II)]_i$ =10 mg.L^{-1}, free pH evolution and reaction time 35 min

Effect of initial DCP concentration

Finally, the change of initial DCP concentration was studied. Fixed concentrations of hydrogen peroxide and iron (II) was chosen to study the degradation rate. All experiments were held at room temperature and the following reaction conditions: H_2O_2 and Fe(II) initial concentrations of 30 and 10 mg.L^{-1} and free pH evolution. Figure 8.28 presents the evolution of DCP and percentage removal of DCP and TOC as function of time for single lamp reactor.

It was observed that, the rate degradation decrease by increasing the initial contaminant concentration (DCP). Even it was started in the same initial reactant concentrations (H_2O_2= 30 mg.L^{-1}, Fe(II)= 10 mg.L^{-1} and 50 min reaction time). 83% of 2.4-DCP was removed when 100 mg.L^{-1} initial concentration was used, while only 57% DCP was removed for 200 mg.L^{-1}. However, it is interesting to note that TOC% removal in all concentration is in the same order of magnitude (10 to 12%).

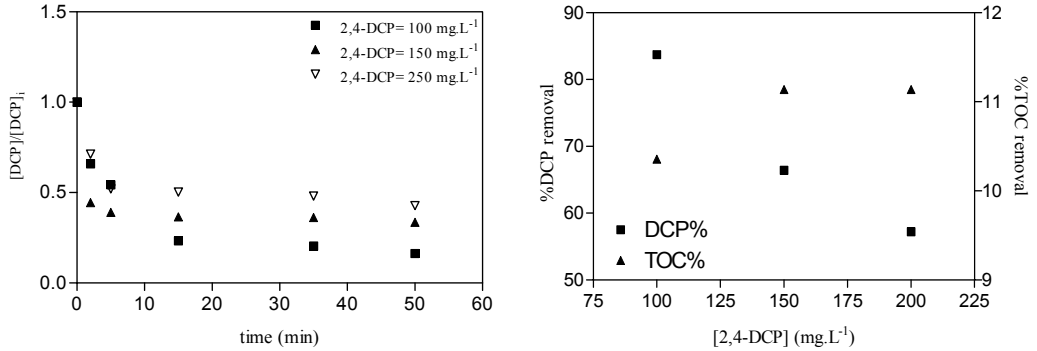

Figure 8.28: Evolution of DCP vs. irradiation time for different initial DCP for single lamp photo-reactor. $[H_2O_2]_i$= 30 mg.L^{-1}, $[Fe(II)]_i$= 10 mg.L^{-1}.

The same tendency was observed in multi lamps reactor (result not shown), at photo-Fenton conditions of 30 mg.L^{-1}H_2O_2, 10 mg.L^{-1}Fe(II), and reaction time 35 min, DCP elimination DCP was 85%. At the same initial conditions and 200 mg.L^{-1} DCP the degradation decreased down to 62%. Again the TOC reduction for all the initial DCP concentration was at the same order (11-13%).

8.3.2 Dechlorination during photo-Fenton

The chlorine liberation through photo-Fenton reactions was also examined in both reactors. Result showed that in single reactor at 83% of DCP elimination (reactant initial concentrations of 30 mg.L^{-1}H_2O_2, 10 mg.L^{-1}Fe(II) and 50 min irradiation time) 32% of the stiochiometric Cl^- was obtained, while it is ~61%for 100% DCP elimination (reactant initial concentrations of 75 mg.L^{-1} H_2O_2, 10 mg.L^{-1}Fe(II) and 50 min irradiation time).

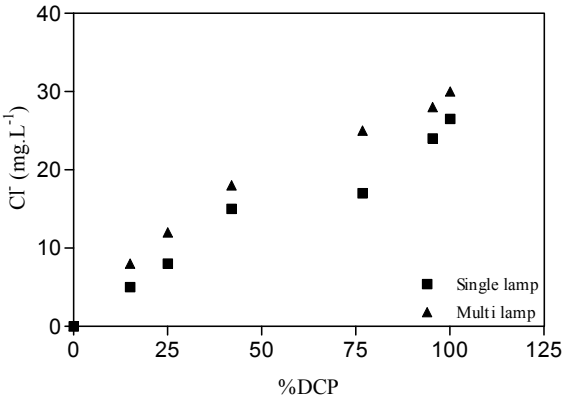

Figure 8.29: Dechlorination as function of DCP removal in single and multi lamps reactors.

In multi lamps reactor and for DCP elimination percentage of 83% and 100 %, Cl^- production was 59 and 69 % of the stiochiometric Cl^- (see figure 8.29). Comparing the

rates of DCP degradation and Cl^- liberation suggests that, during DCP degradation aromatic and aliphatic chlorinated compounds form Abe and Tanaka (1997), identified chloro-benzoquinone as reaction by-products.

8.3.3. Effect of photo-Fenton in biodegradability

The biodegradability improvement all over photo-Fenton reaction in both reactors will be followed by measuring the change in BOD_n. BOD_n/COD and BODn/TOC for treated solution. Accordingly, in this section photo-Fenton operational conditions that affect DCP elimination will be taken in account.

Effect of initial H_2O_2 concentrations

Photo-Fenton treated solutions with different initial hydrogen peroxide and fixed initial Fe(II) were tested for their BOD_n. It was observed no significant difference between BOD_5 and BOD_{21}. So, in this section all BOD measurements will be taken as BOD_5 (BOD_{21} was checked frequently to confirm the small difference). Figures 8.30 and 8.31 present the evolution of BOD_n as function of initial H_2O_2 concentration for single and multi lamps reactors, it was noticed that, BOD_5 and BOD_{21} increase by increasing the initial hydrogen peroxide as a results of DCP oxidation into other intermediates which are more biodegradable, at 75 $mg.L^{-1}$ H_2O_2 (concentration necessary for 100% DCP elimination in single lamp reactor), BOD_5 and BOD_{21} increase from zero for original DCP solution up to 14 and 15 $mgO_2.L^{-1}$ respectively.

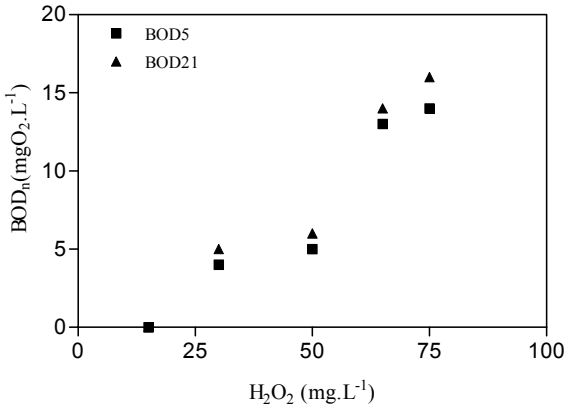

Figure 8.30: Evolution of BOD_n as function of initial H_2O_2 in single lamp photo-reactor.$[Fe(II)]_i$= 10 $mg.L^{-1}$, 50 min irradiation time and free pH evolution.

For multi lamps reactor the hydrogen peroxide concentration needed to eliminate all DCP was 65 $mg.L^{-1}$ (with 10 $mg.L^{-1}$ Fe(II) and 35 min irradiation time) the corresponding BOD_5 and BOD_{21} at this point were 11 and 13 $mgO_2.L^{-1}$ respectively.

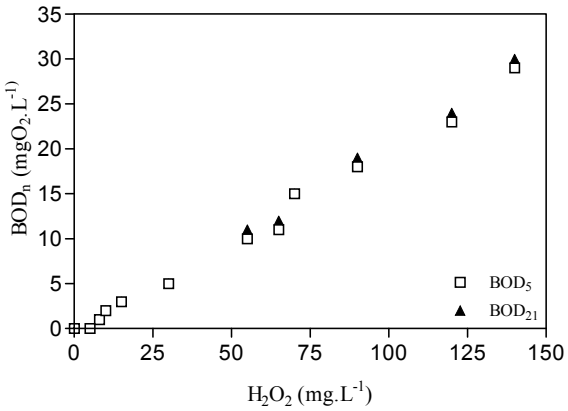

Figure 8.31: Evolution of BOD_n as function of initial H_2O_2 in multi lamps photo-reactor.$[Fe(II)]_i$= 10 $mg.L^{-1}$, 35 min irradiation time and free pH evolution.

To check the proportion of contained organic matter (measured as COD and TOC) able to bio-oxidation, BOD_n/COD and BOD_n/COD is presented in figures 8.32 and 8.33 for both reactor under the same previous conditions. As expected BOD_5/COD and BOD_5/TOC ratios increased by increasing initial hydrogen peroxide used in the reaction.

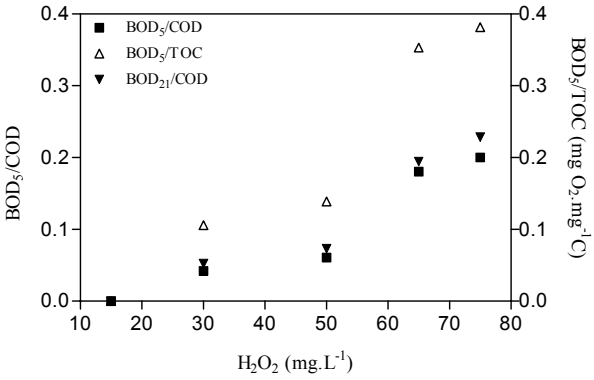

Figure 8.32: Evolution of BOD_n/COD and BOD_n/TOC as function of initial H_2O_2 in single lamp photo-reactor.$[Fe(II)]_i$= 10 $mg.L^{-1}$, 50 min irradiation time and free pH evolution.

The increase in BOD_5/COD and BOD_5/TOC ratios after pre-treatment is an indication of increase in contained organic matter proportion (COD or TOC) able to biodegradation. Both ratios increase by elimination more DCP. At the moment where

100% DCP removed, BOD_5/COD and BOD_5/TOC ratios increased up to 0.19 and 0.36 (0.23 and 0.44 for BOD_{21}/COD and BOD_{21}/TOC) in single lamp reactor, and 0.15 and 0.29 (0.22 and 0.37 for BOD_{21}/COD and BOD_{21}/TOC) in multi lamps reactor.

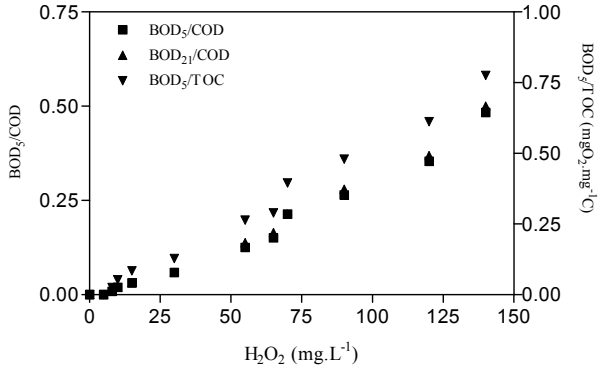

Figure 8.33: Evolution of BOD_n/COD and BOD_n/TOC as function of initial H_2O_2 in multi lamps photo-reactor.$[Fe(II)]_i$= 10 $mg.L^{-1}$, 35 min irradiation time and free pH evolution

As it was seen that the biodegradability improve by elimination more DCP. It was decided to follow biodegradability change as function of DCP removals in both reactors. Figure 8.34 presents the change in BOD_5/COD ratio as function of DCP removed in both reactors. For single lamp reactor, it was observed that, BOD_5/COD and BOD_5/TOC ratios start to increase slightly when DCP removed is more than 20% of the original concentration, elimination more DCP leads to more development in organic matter biodegradability and finally moderate value obtained at 100% DCP elimination.

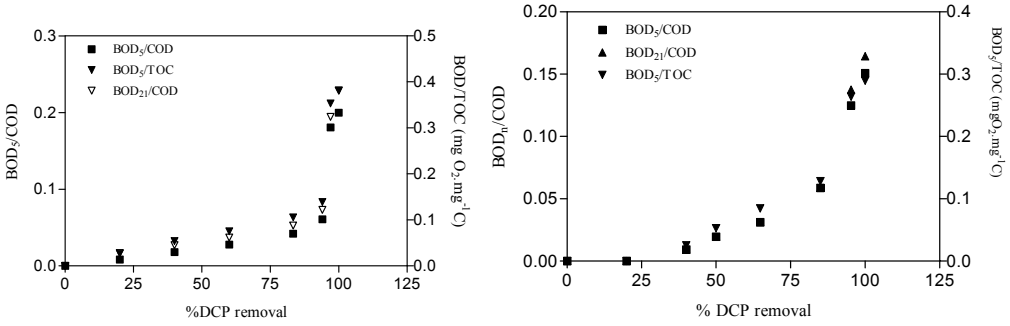

(A) (B)

Figure 8.34: BOD_5/COD and BOD_5/TOC as a function DCP removal percentage A) single lamp reactor with $[H_2O_2]_i$= 75 $mg.L^{-1}$, $[Fe(II)]_i$ =10 $mg.L^{-1}$ 50 min and free pH evolution, B) multi lamps reactor with $[H_2O_2]_i$= 65 $mg.L^{-1}$, $[Fe(II)]_i$ =10 $mg.L^{-1}$ 35 min and free pH evolution.

The same tendency was noticed in multi lamp reactor, the BOD_5/COD growth start at 25% DCP elimination, and significant increment in biodegradability was observed when

all DCP eliminated, 0.0 to 0.20 in single lamp and 0.0 to 0.23 in multi lamps reactor, on BOD_5/COD base.

Effect of initial iron ion concentrations

With respect to initial iron ion concentration, Also solutions treated with photo-Fenton at different initial Fe(II) concentration were tested for their BOD_n. For single lamp reactor, solutions treated with photo-Fenton with 15 $mg.L^{-1}$ H_2O_2, 50 min irradiation time and different Fe(II) initial concentration during lead to no improvement in biodegradability. The reason was referred to high DCP remain in the solution.

Based on above, experiments carried out with higher H_2O_2 initial concentration (30 $mg.L^{-1}$), 50 min irradiation time and different initial Fe(II) concentration were tested. Figure 8.35 presents BOD_n development as function of initial Fe(II) in single lamp reactor.

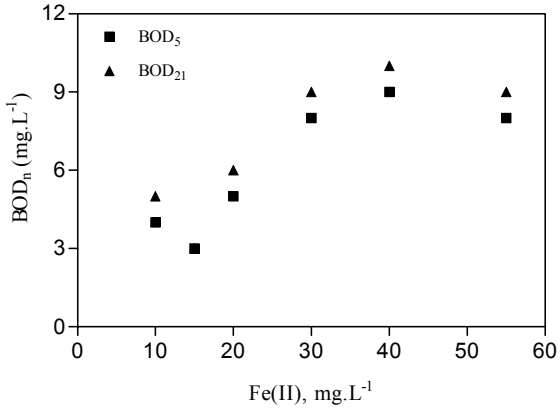

Figure 8.35 : BOD_n as function of initial Fe(II) in single lamp photo-reactor. $[H_2O_2]_i$= 30 $mg.L^{-1}$, 50 min irradiation time and free pH evolution.

As presented in the previous section, during these experiments, significant DCP removal was achieved (up to 85%). Thus, a development in BOD_n was anticipated. It can be seen in figure 8.35 that, at beginning BOD_n start to increase as initial Fe(II) increased, as result of production more hydroxyl radicals and elimination more DCP. BOD_5 and BOD_{21} increased respectively from 0 to 9 and 10 $mgO_2.L^{-1}$ when 30 $mg.L^{-1}$ initial Fe(II) was used. However, at higher Fe(II) concentration (in this case 40 $mg.L^{-1}$), the catalytic effect was noted to diminish and no more BOD_n development take place.

The same tendency was observed in BOD_n evolution in multi lamps reactor at different initial Fe(II) concentration (see figure 8.36). BOD_n increase by increasing initial Fe(II)

concentration However, one difference was noticed in this reactor, all over the reaction increasing the initial Fe(II) concentration guide continuously to BOD_n growth.

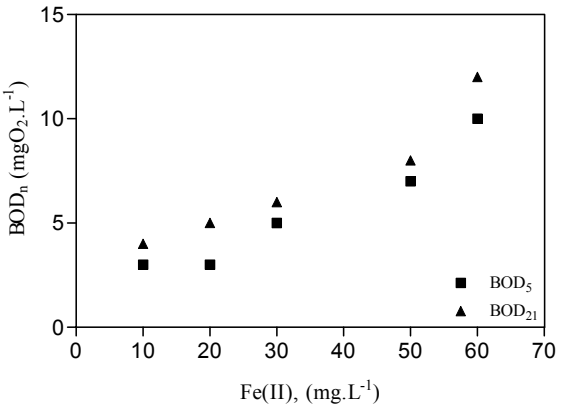

Figure 8.36 : BOD_n as function of initial Fe(II) in multi lamps photo-reactor. $[H_2O_2]_i$= 15 mg.L^{-1}, 35 min irradiation time and free pH evolution.

Figure 8.37 presents the change in organic matter biodegradability (BOD_5/COD and BOD_5/TOC ratios) for photo-Fenton solution carried out with 30 mg.L^{-1} H_2O_2 and different Fe(II) initial concentration in single lamp reactor. At the commencement the enhancement in contained organic matter proportion able to biodegradation increase by increasing the initial iron dosage until it reach a maximum value, after that, when Fe(II) catalytic effect diminished no improvement in BOD_5/COD and BOD_5/TOC was noticed. Accordingly, BOD_5/COD and BOD_5/TOC increased from zero up to 0.11 and 0.22 (corresponding BOD_{21}/COD and BOD_{21}/TOC are 0.13 and 0.25) respectively. As a result of small biodegradability obtained in these experiments, compared with domestic wastewater. It was decided to check the experiments carried out with more initial H_2O_2 (50 mg.L^{-1}) and different Fe(II) initial concentrations. Results point out minor enhancement in biodegradability was obtained by increasing initial Fe(II) concentrations, BOD_5/COD and BOD_5/TOC increase as maximum to 0.22 and 0.43 respectively.

With regard to multi lamps reactor (see figure 8.38), BOD_5/COD and BOD_5/TOC ratios was detected to increase as initial iron concentration increase. At 50 mg.L^{-1} initial iron concentrations and only 15 mg.L^{-1} H_2O_2, BOD_5/COD and BOD_5/TOC increased from 0 up to 0.1 and 0.2 respectively.

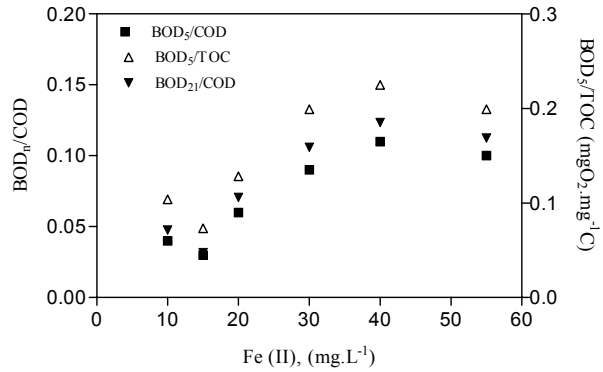

Figure 8.37 : BOD_n/COD and BOD_5/TOC as function of initial Fe(II) in single lamp photo-reactor. $[H_2O_2]_i$= 30 $mg.L^{-1}$, 50 min irradiation time and free pH evolution.

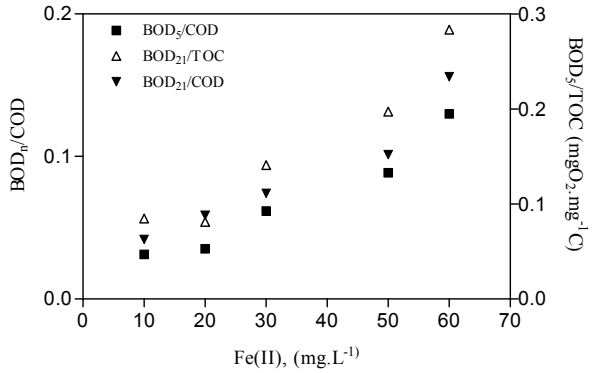

Figure 8.38: BOD_n/COD and BOD_5/TOC as function of initial Fe(II) in multi lamp photo-reactor. $[H_2O_2]_i$= 15 $mg.L^{-1}$, 35 min irradiation time and free pH evolution.

Effect of temperature:

Photo-Fenton pre-treated solution with different operation temperature was tested for biodegradability improvement. Figure 8.39 presents the variation of biodegradability at different photo-Fenton operational temperature in single lamp reactor. It can be seen that, biodegradability of the treated solution enhanced by changing operational temperature, at the same initial reactant initial concentration (30 $mg.L^{-1}H_20_2$, 10 $mg.L^{-1}$Fe(II), 50 min irradiation time) BOD_5/COD increased from 0.03 and 0.08 by increasing the temperature by 10° C, and BOD_5/TOC from 0.08 to 0.20 in single lamp reactor. The same tendency has been attained using multi lamps photo reactor. Nonetheless, problems associated of working at higher at higher temperatures and the biodegradability enhancement recommend working at normal operation temperatures.

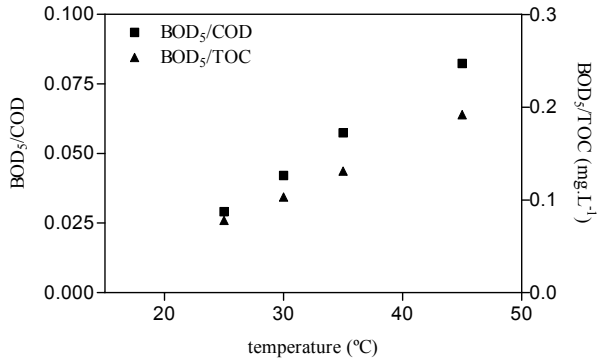

Figure 8.39: Variation of biodegradability as function of operational temperature in single lamp photo-reactor. $[H_20_2]_i$= 30 mg.L^{-1}, $[Fe(II)]_i$= 10 mg.L^{-1}, 50 min irradiation time and free pH evolution.

Effect of initial DCP

Also solutions with different initial DCP treated previously with photo-Fenton reaction was tested for their biodegradability value. As result of high remaining DCP in the treated solutions, only solution with initial DCP 100 mg.L^{-1} showed biodegradability development (BOD_5/COD and BOD_5/TOC 0.04 and 0.11 respectively), while the other showed no increment in biodegradability.

8.3.4. Change on oxidation state

Effect of initial hydrogen peroxide concentration

As it was commented before initial H_2O_2 has significant effect on the oxidation state of organic matter. Concerning this effect on treated solution, figures 8.40 to 8.43 present the change on average oxidation state and COD/TOC ratio as function of initial hydrogen peroxide in both reactors. During photo-Fenton reaction (see figure 8.40), At any initial H_2O_2 both AOS and COD/TOC ratio was perceived to increase throughout the reaction time; with photo-Fenton initial conditions 10 mg.L^{-1}Fe(II), 30 mg.L^{-1} H_2O_2, AOS increased from –0.30 up to 0.8 and COD/TOC ratio decreased from 2,89 to 2.11in single lamp reactor. This may be aim to continuous production of hydroxyl radical and more organic matter degradation. Figure 2.41 presents the variation of final solution oxidation sate as function initial H_2O_2 used and fixed initial Fe(II) concentration (10 mg.L^{-1}) in single lamp reactor, increasing H_2O_2 from 10 to 75 mg.L^{-1} increase the AOS from -0.3 to 1.14 and COD/TOC decreased from 2.89 to 1.6).

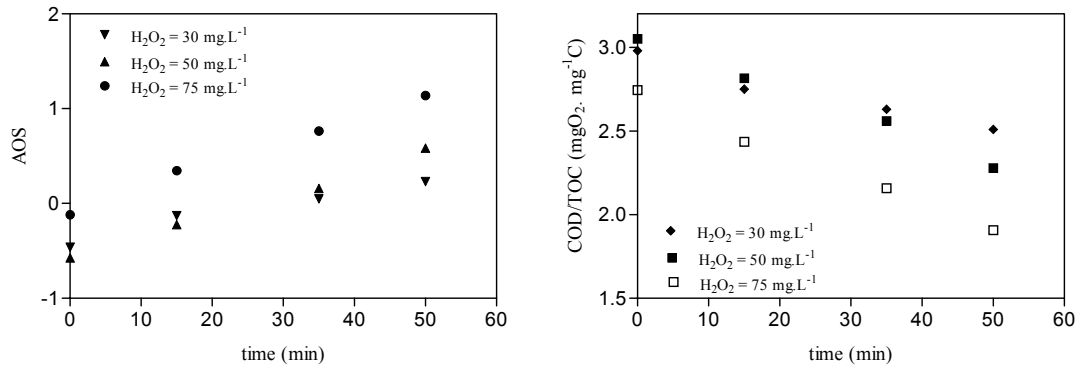

Figure 8.40: AOS and COD/TOC as function of time for different initial H_2O_2 in single lamp photo-reactor.$[Fe(II)]_i$= 10 mg.L^{-1}, 50 min irradiation time and free pH evolution.

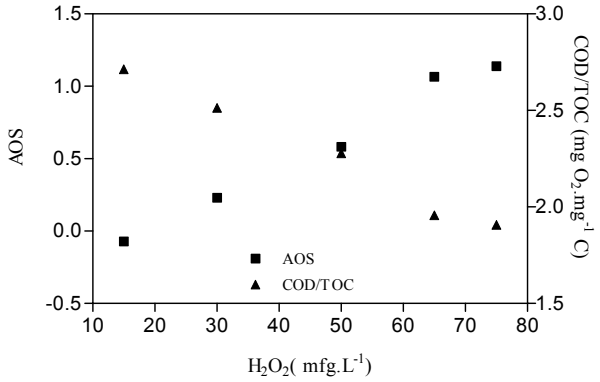

Figure 8.41: AOS and COD/TOC as function of initial H_2O_2 in single lamp photo- reactor. $[Fe(II)]_i$= 10 mg.L^{1}, 50 min irradiation time and free pH evolution.

The same affinity was noticed in multi lamps photo reactor figures 8.42 and 8.43 (AOS increased from -0.18 to 1.65 and COD/TOC from 2.78 to 1.6) by increasing the initial H_2O_2 from 10 up to 65 mg.L^{-1}.

As a comparison between the two reactor, it was found that during 50 min in single lamp and 35 min in multi lamps reactor with the same initial concentrations (30 mg.L^{-1} H_2O_2, 10 mg.L^{-1} Fe(II)), COD/TOC ratio decayed by 31% and 41% in single and multi lamps reactors respectively. This suggest that multi lamps reactor is more able to degrade the organic matter even in short time. The same affinity have been noticed in AOS evolution.

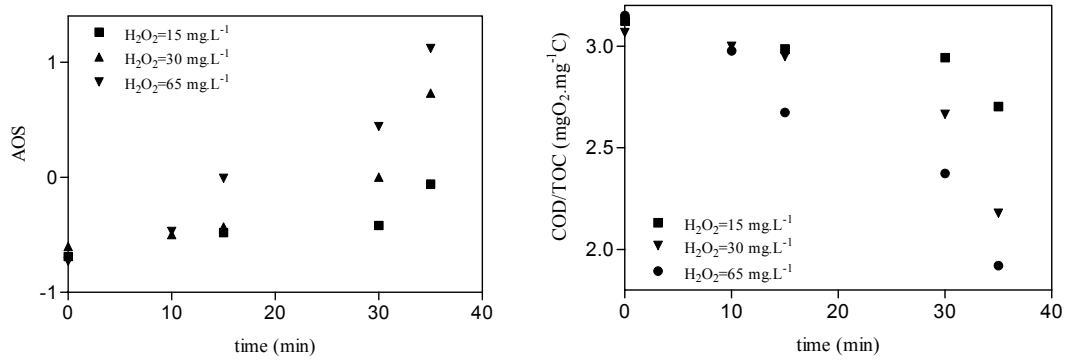

Figure 8.42: AOS and COD/TOC as function of time for different initial H_2O_2 in multi lamps photo-reactor.$[Fe(II)]_i$= 10 mg.L^{-1}, 35 min irradiation time and free pH evolution.

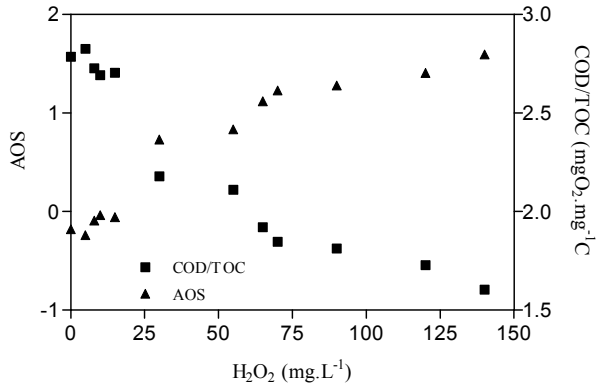

Figure 8.43: AOS and COD/TOC as function of initial H_2O_2 in single lamp photo- reactor. $[Fe(II)]_i$= 10 mg.L^{-1}, 35 min irradiation time and free pH evolution.

Effect of initial iron ion concentrations

The effect of initial Fe(II) concentration in the oxidation state of treated solution is presented in figures 8.44 to 8.47 for both reactors. For single lamp reactor it can be seen that at the beginning, increasing the initial Fe(II) concentrations (from 0 to 30 mg.L^{-1}) direct to increase the oxidation of contained organic matter (AOS increased from -0.02 up to 0.83 and COD/TOC decreased from 2.7 to 2.1) due to hydroxyl radicals production. Nevertheless, at high ferric ion concentration the oxidation of organic matter keep almost constant, at 50 mg.L^{-1} AOS and COD/TOC ratio were 1.0 and 1.99. In contrast of that, oxidation sate in multi lamps reactor increase all over the reaction as initial Fe (II) concentration increase, the case that indicate uninterrupted hydroxyl radical production via iron photo-redox.

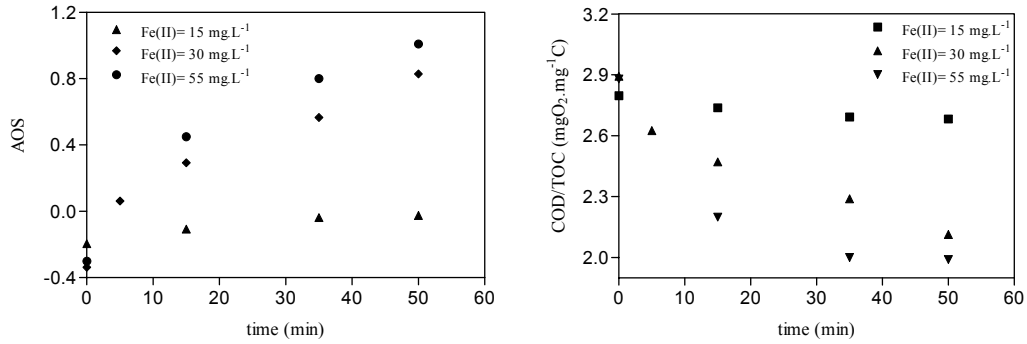

Figure 8.44: AOS and COD/TOC as function of time at different initial Fe(II) in single lamp photo-reactor.$[H_2O_2]_i$= 30 mg.L^{-1}, 50 min irradiation time and free pH evolution.

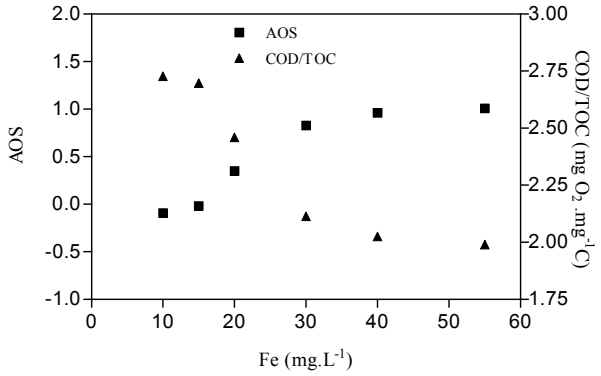

Figure 8.45: AOS and COD/TOC as function of initial Fe(II) in single lamp photo-reactor.$[H_2O_2]_i$= 30 mg.L^{-1} , 50 min irradiation time and free pH evolution.

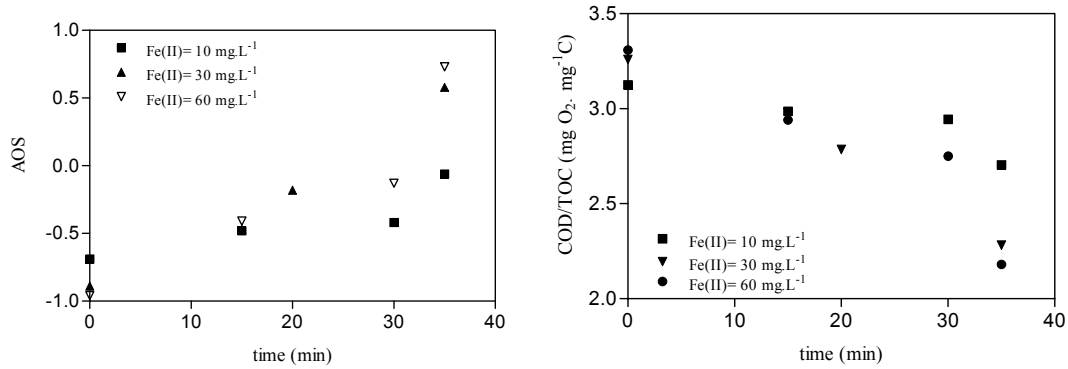

Figure 8.46: AOS and COD/TOC as function of time at different initial Fe(II) in multi lamps photo-reactor.$[H_2O_2]_i$= 15 mg.L^{-1}, 50 min irradiation time and free pH evolution.

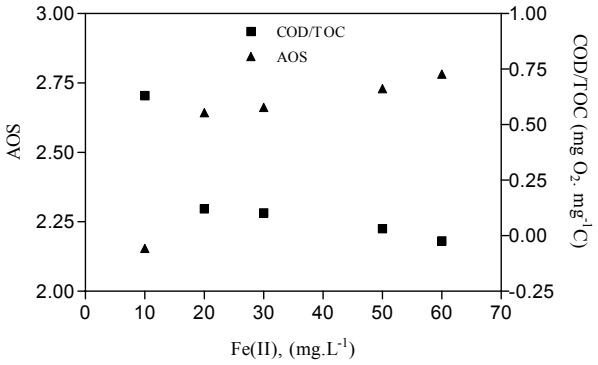

Figure 8.47: AOS and COD/TOC as function of initial Fe(II) in multi lamps photo-reactor. $[H_2O_2]_i$= 15 $mg.L^{-1}$, 50 min irradiation time and free pH evolution.

Effect of temperature

Since the rate of photo degradation change by changing the temperature, it was decided to study the temperature effect in oxidation of organic matter. The degradation tendency as function of temperature in both reactors was the same. Thus, in this section; only the solutions treated with single lamp reactor will be used to examine the change of AOS and COD/TOC ratios. Figure 8.48 presents the evolution of both parameters (AOS, COD/TOC) as function of reaction temperature, results indicated that, at photo-Fenton initial conditions 30 $mg.L^{-1}$ H_2O_2, 10 $mg.L^{-1}$ Fe(II) and 50 min irradiation time, increasing the temperature from 25 to 45ºC guide to insignificant increase in organic matter oxidation state (AOS from 0.88 to 1.28 and COD/TOC from 2.1 to 1.8).

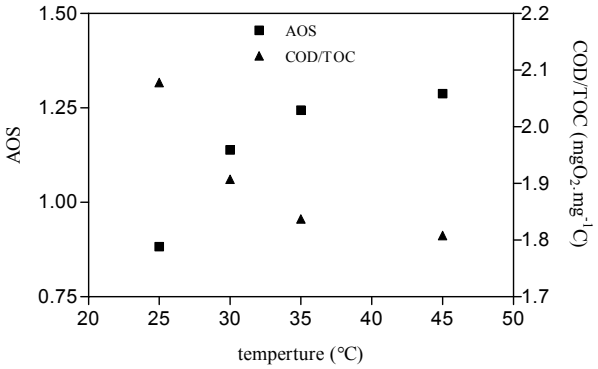

Figure 8.48: AOS and COD/TOC as function of operational temperature in photo-Fenton reaction. $[H_2O_2]_i$= 30 $mg.L^{-1}$, $[Fe(II)]_i$= 10, 50 min irradiation time and free pH evolution.

8.4. Mineralization

As commented before AOP´s can be used efficiently for organic matter total mineralization. In view of that, photo-Fenton reaction carried out in both reactors was tested for mineralization. Based on the previous experiments, the following conditions were used:

- ✓ For single lamp reactor, initial Fe(II) concentration of 40 $mg.L^{-1}$, 60 min irradiation time, free pH evolution and different hydrogen peroxide concentration
- ✓ For multi lamps reactor, initial Fe(II) concentration of 40 $mg.L^{-1}$, 35 min irradiation time, free pH evolution and different hydrogen peroxide concentration.

Figure 8.49 presents the normalized TOC evolution as function of time at different initial H_2O_2 for both reactors. It can be seen that, by increasing the initial hydrogen peroxide normalized TOC decreases, and total organic matter (TOC) mineralization was found to take place when 460 and 410 $mg.L^{-1}$ H_2O_2 were used in single and multi lamps reactor respectively. These concentration corresponding to molar ratio between DCP and H_2O_2 of 8.3 and 7.35 respectively. From total reactant consumption and irradiation time point of view, the results show that, using multi lamps reactor is more competent method for 100 $mg.L^{-1}$ DCP mineralization compared with single lamp reactor.

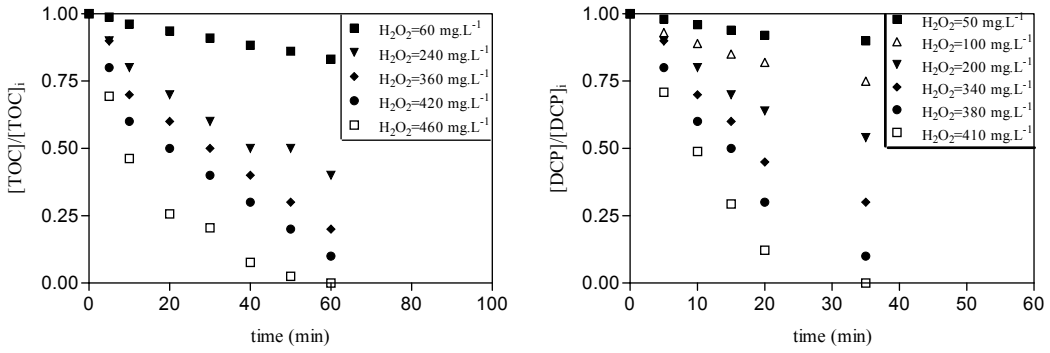

(A) (B)

Figure 8.49: Normalized TOC evolution as function of time at different initial H_2O_2 A) single lamp reactor B) multi lamps reactor. $[Fe(II)]_i$= 10 $mg.L^{-1}$ and Free pH evolution

First order mineralization kinetic was calculated for the two reactions. table 8.5 are shown the first order kinetic constants and half-life time for total organic carbon (TOC) mineralization.

Table 8.5: First order kinetic constant and half-life time for TOC mineralization in single and multi lamps reactor. $[Fe(II)]_i$= 10 $mg.L^{-1}$, 60 min (35 in multi lamps) and Free pH evolution

Single lamp reactor (4W)			*Multi lamps reactor (24 W)*		
H_2O_2 ($mg.L^{-1}$)	$K_{TOC\,(}min^{-1}$)	$t_{1/2}$ (min)	H_2O_2 ($mg.L^{-1}$)	$K_{TOC\,(}min^{-1}$)	$t_{1/2}$ (min)
60	0.0031	> 60	50	0.0035	> 35
120	0.0051	> 60	100	0.0091	> 35
240	0.016	40	200	0.0202	35
420	0.036	21	380	0.0617	12
460	0.067	10	410	0.0924	8

As a comparison between mineralization carried out with UV-light and UVA-light, result show that the use of photon-Fenton based UV-light is more efficient for DCP mineralization than UVA-light. 270 $mg.L^{-1}$ H_2O_2 during 50 min irradiation was sufficient for total DCP mineralization in UV reactor, while as minimum 410 $mg.L^{-1}$ H_2O_2 was needed in multi lamps reactor. From kinetic data point of view, at the same previous concentrations first order mineralization constant (0.069 min^{-1} for UV-light at 254nm and 0.067 for UVA-light at 360 nm)and half life-time (8 min for UV-light at 254nm and 10 for UVA-light at 360 nm) are in the same order of magnitude for the two reactor. The required high initial amount of hydrogen peroxide in multi lamps reactor may credited to the low H_2O_2 absorption coefficient at the working wavelength (360 nm), the case that affect on the production of hydroxyl radicals, and hence the mineralization.

8.5. Intermediates identification:

Solutions treated by AOP´s based on UVA-light were analyzed for intermediates identifications. Different standard found in literatures were used: among these standards chlorobenzoquinone and other acids have been identified as reaction by-product. As the same intermediates were found in both reactors (single and multi lamps), and for simplicity, in this part only chromatograms corresponding to single lamp reactor will be presented.

UVA-light: During DCP degradation by UVA-light process only chlorobenzoquinone was identified. This compound was found to produce after 25 min of irradiation time in single and after 15 min in multi lamps reactor, and keep in reaction solution until the end of the reaction (experiment DCP-UVA). The presence of DCP and

chlorobenzoquinone may account for the no improvement of biodegradability observed at this process.

UVA/H_2O_2: Figures A5.1 and A5.2 present the chromatograms corresponding to samples at 20 and 30 min of UVA irradiation experiment UVA/H_2O_2-2 (appendix A5). During DCP degradation, chlorobenzoquinone (retention time 6.6 min), Glotamic acid (retention time 2.37) and formic acid (retention time 2.93) were identified between reaction intermediates. The low BOD_5 value could be explained as a result of presence inhibitory components like chlorobenzoquinone and remaining DCP.

UVA/Fe(III): Figure A5.3 presents sample at 30 min of experiment UVA/Fe (III)-1. During DCP degradation by this process just one intermediates could be identified retention time was 2.3 min: this component is suspected to be oxalic acid, since oxalic was injected in the HPLC and seems to appear more o less at the same retention time.

Photo-Fenton: With regarded of photo-Fenton intermediates the same procedure used in the previous section was followed to identify some intermediates. Figure A5.4 and A5.5 show the chromatograms corresponding to samples after 20 and 30 min (experiment DCP-PHFA-2). Chlorobenzoquinone was found to form early in the reaction medium. And glutamic acid (retention time 3.37 min) was identified intermediates at the final by-products. By using high initial concentration of H_2O_2 (experiment DCP-PHFA-4) both chlorobenzoquinone and glutamic acid was degraded, and at the end just small molecular weight compound as oxalic and formic acids were found to be in the solution figure A5.6.

8.6. Comparison of the different studied processes for DCP degradation.

In the present section, in each reactor different AOP's based on UVA-light will be used for comparison purpose, the general conditions for each process can be seen in legend of Figure 8.56.

Figure 8.56 presents the normalized DCP concentrations as function of time for the different processes in both reactors. Photo-Fenton process shows the best capacity in DCP degradation results while UVA irradiation alone shows the slowest degradation efficiency.

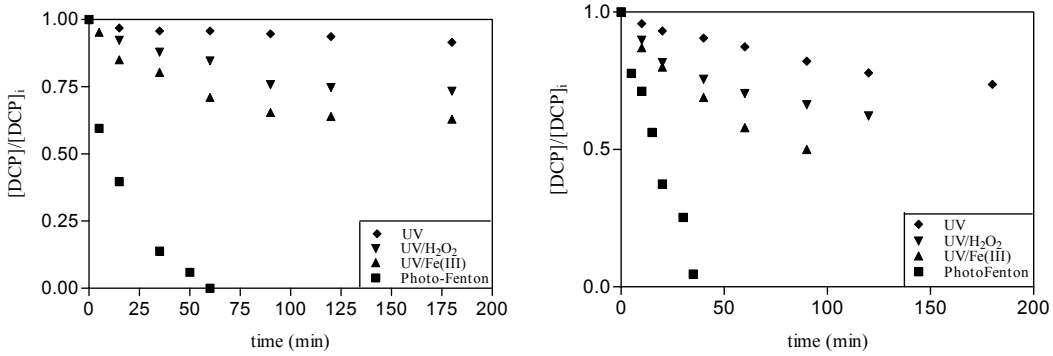

Figure 8.50: DCP evolution as function of time for different AOP´s in single and multi lamps reactor. $[H_2O_2]_i$= 50 mg.L^{-1}, $[Fe(III)]_i$= 70 mg.L^{-1}, $[Fe(II)]_i$= 10 mg.L^{-1} and free ph evolution.

Table 8.6 presents the pseudo-first order kinetic constant and experimental half-life time ($t_{1/2}$) for the same. The results confirm the priority of photo-Fenton in DCP degradation over the other processes. Again the kinetic data confirm the previous observation concern photo-Fenton precedence.

Table 8.6: Values of reaction rate constants of the degradation of DCP by different oxidation processes

	Single lamp reactor (4W)		*Multi lamps reactor (24W)*	
Type of Oxidation process	*$t_{1/2}$ (min)*	*K_0 (min^{-1})*	*$t_{1/2}$ (min)*	*K_0 (min^{-1})*
UVA	>90	0.0005	>180	0.0015
UVA/H_2O_2	>120	0.0026	>120	0.0038
UVA/Fe(III)	>90	0.0062	90	0.0087
Photo-Fenton	14.5	0.028	12	0.053

Figure 8.51 presents the normalized TOC mineralization during different processes in both reactors. between all the processes that use UVA-light as oxidation parameter photo-Fenton shows more TOC mineralization; in single lamp reactor 50 min was sufficient to obtain 10 % TOC mineralization under the following conditions: 50 and 10 mg.L^{-1} of H_2O_2 and Fe(II) respectively. At the same time, UVA/H_2O_2 with initial H_2O_2 of 50 mg.L^{-1} and 120 min irradiation provides only 8%. With respect to UVA-light alone during 180 min only 3% could be mineralized.

With respect to multi lamps reactor, result are consistence with previous observations; Photo-Fenton shows high TOC mineralization rate compared with the other processes, as result of different contribution reactions which produce hydroxyl radicals, so more organic carbon mineralized. In second position comes UVA/Fe(III) reaction and finally direct UVA alone.

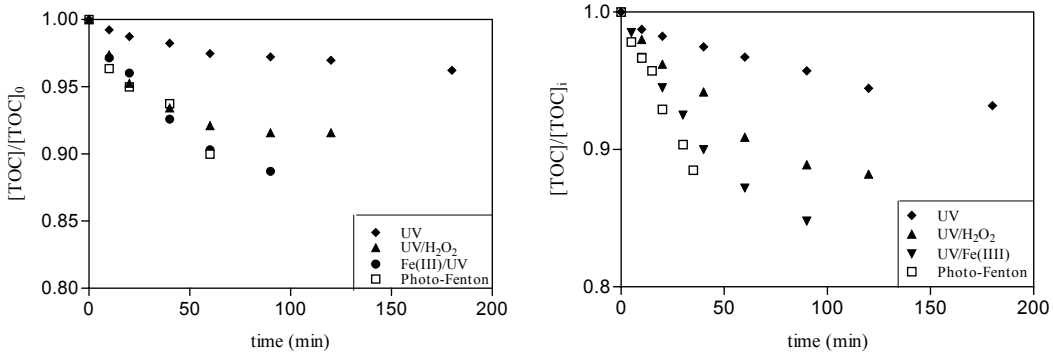

(A) (B)

Figure 8.52: Normalized TOC concentrations as function of time for the different AOP's processes, A) single lamp, B) multi lamps reactor. $[H_2O_2]_i$= 50 mg.L^{-1}, $[Fe(III)]_i$= 70 mg.L^{-1}, $[Fe(II)]_i$= 10 mg.L^{-1} and free pH evolution.

The apparent first order rate constants based in TOC mineralization for the previous process was examined (see table 8.7). Almost all the processes have been found to follow first order kinetics except UVA/H_2O_2 reaction in single lamp reactor, which shows deviation from linearity (R^2=0.70). An explanation could be low photon emission by this lamp, so weak H_2O_2 photolysis could be obtained.

As comparison between two reactors, it is clear that increasing the irradiation power leads to photo-degradation enhancement. However, only in photo-Fenton reaction the increment in mineralization rate is significant.

8.7 the apparent first ordet kinetics based on mineralization

	Single lamp reactor (4W)		Multi lamps reactor (24W)	
Process	K_{TOC} (min^{-1})	R^2	K_{TOC} (min^{-1})	R^2
UVA	0.00037	0.84	0.00044	0.90
UVA/H_2O_2	0.00122	0.70	0.00128	0.90
UVA/Fe (III)	0.0015	0.95	0.0021	0.92
Photo-Fenton	0.0018	0.88	0.0034	0.99

With respect to dechlorination during AOP´s processes, results are compared in figure 8.53 for single lamp reactor (results for multi lamp not shown). It was observed in both reactors that, photo-Fenton process shows better tendency to liberate Cl^- ions than the

other processes. For example, 94 % DCP elimination direct to about 54% and 60% release in Cl^- in single and multi lamp respectively. Other processes showed smaller chlorine ion liberation capacity.

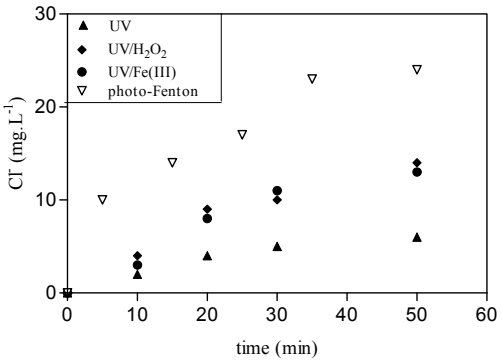

Figure 8.53: Dechlorination during different AOP's different AOP´s. (A) single lamp photo-reactor,$[H_2O_2]_I$= 50 mg.L^{-1}, .$[Fe(III)]_I$= 70 mg.L^{-1}, .$[Fe(II)]_I$= 10 mg.L^{-1},and free pH evolutions.

Oxidation state during different methods are also compared (see figure 8.59). Among the studied oxidation processes, photo-Fenton reaction has more oxidizing capacity: in single lamp reactor, 50 min reaction was sufficient to decrease the COD/TOC ratio by 26%, while maximum reduction in the same parameter was 18 and 4 % for UVA/Fe(III) and UVA/H_2O_2 respectively.

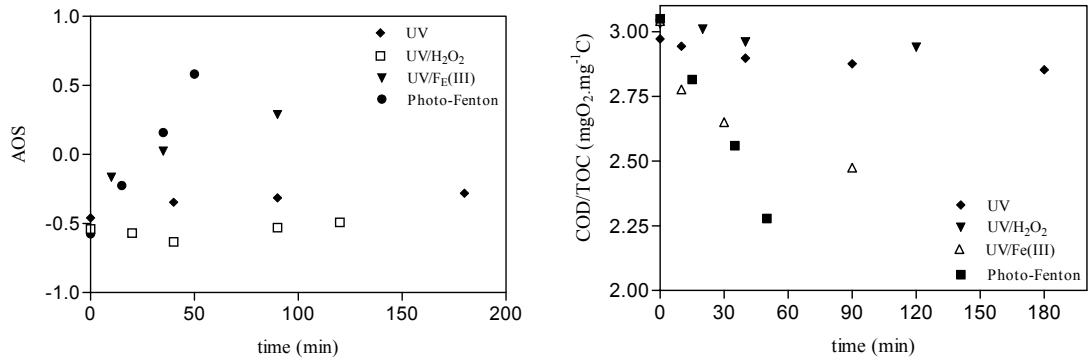

Figure 8.54: Change in oxidation state for the five AOP's, in single lamp photo-reactor. $[H_2O_2]_I$= 50 mg.L^{-1}, $[Fe(III)]_i$= 70 mg.L^{-1}, .$[Fe(II)]_I$= 10 mg.L^{-1},and free pH evolutions.

The same affinity was observed in AOS values; photo-Fenton increased AOS from –0.58 to 0.58 and decreased COD/TOC from –0.56 to 0.29 in UVA/Fe(III). Similar tendency was observed in multi lamps reactor, which also indicate that photo-Fenton

reaction affect more both the change in AOS (–0.69 to 0.83) and COD/TOC ratio (3.129 to 2.11).

With regard to the biodegradability enhancement during the five processes, it was found that, photo-Fenton has more positive effect in biodegradability improvement compare with other AOP's, under moderate initial concentration of reactant, 50 $mg.L^{1}$ $H_2O_2$10 $mg.L^{1}$, Fe(II) and 50 min irradiation time, the BOD_5/COD and BOD_5/TOC ratios increased from 0.0 up to 0.06 and 0.14 respectively. At the same time, other processes could not reach this improvement even under higher initial reactant concentrations.

9. Combined photo-Fenton with biological sequencing batch reactors

In this section a combined processes that include photo-Fenton as pre-treatment step and biological sequencing batch reactor (SBR) for total DCP removal will be performed. The study will concentrate on both aerobic and anaerobic bioreactors. During the experiments, the start up of both reactors (aerobic and anaerobic), the effect of pre-treatment process as well as cycle duration was followed. All photo-Fenton pre-treatment processes were carried out in multi lamp stirred photo-reactor (reactor 3).

9.1. Aerobic sequencing batch reactor

From results presented before in section 8, it was seen that significant biodegradability enhancement occurred when DCP disappeared from the solution. To start up the SBR, it was decided to used photo-Fenton pre-treated solution at this point (100% DCP removal) as substrate for SBR reactor. The initial conditions for photo-Fenton pre-treatment were: 100 mgL^{-1} of DCP: 65 $mg.L^{-1}$ H_2O_2, 10 $mg.L^{-1}$ Fe(III), 35 minutes irradiation time. At these conditions, it was found a positive effect in pre-treated solution biodegradability: BOD_5/COD and BOD_5/TOC were increased up to 0.15 and 0.29 respectively.

9.1.1. Start up

To start up aerobic biological reactor, fresh activated sludge from Gava municipal wastewater treatment plant was acclimated in a sequencing batch reactor (SBR) to photo-Fenton pre-treated solution. The substrate was DCP oxidized intermediates, the solution total organic carbon (TOC) content was around 40 $mgTOC.L^{-1}$ and BOD_5/COD was 0.15. At the beginning, the bioreactor has biomass concentration measured as TVSS of 1.2 $g.L^{-1}$. During the acclimation period, daily measurements of TOC, pH, TSS, and TVSS were performed. Figure 9.1 presents total organic carbon evolution and TVSS as function of acclimation time. It can be seen in figure 9.1 that, the organic matter and TVSS in the effluent decrease irregularly, which is an indication of acclimation process. The duration of acclimation cycle extended to 40 days. All over that, monitoring the SBR showed that about 35 % of initial substrate was degraded, in an organic carbon base (see figure 9.1). At the same time, biomass concentration TVSS decreased to finally stabilized at 0.24 $g.L^{-1}$.

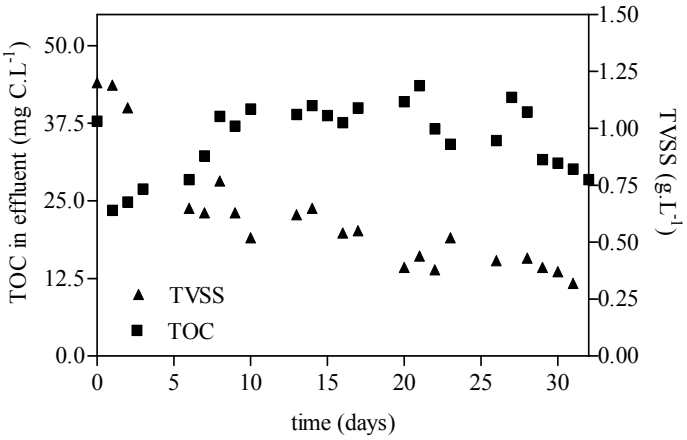

Figure 9.1: Total organic carbon evolution and TVSS as function of time during start up, feed BOD_5/COD= 0.15

9.1.2. Aerobic SBR operation:

After acclimation period, the operation of coupled processes was divided in 12 periods, each running under different operational conditions (varying the cycle time and feed biodegradability). The biological reactor was fed with DCP pre-treated solution, and the exchange volume was 7/8 of total reactor volume. Thus, the concentration in the reactor maintained around 37 $mgTOC.L^{-1}$ as a result of slight dilution with the remaining reactor volume (less than 1/8). Table 9.1 presents the operational conditions at different parts and part of the results obtained during the SBR operations.

Table 9.1: operational conditions and results obtained during operational SBR.

No. Cycles	Cycle duration	H_2O_2 used in Pre-treatment conditions (1) ($mg.L^{-1}$)	Feed BOD_5/COD	Average OLR ($mgC.L^{-1}.day^{-1}$)	%TOC removal in pre-treatment	Average %TOC removal in SBR	% TOC removal in combined processes
2	8 Days	H_2O_2= 70	0.15	4.25	10	40	52
4	8 Days	H_2O_2= 110	0.25	4.25	12	42	54
4	4 Days	H_2O_2= 110	0.25	7.5	12.5	62	74.5
10	3 Days	H_2O_2= 110	0.25	11.33	12.5	68	80.5
3	2 Days	H_2O_2= 110	0.25	16.5	12.5	66	78.5
6	1 Days	H_2O_2= 110	0.25	34	12.5	68	80.5
8	12 h	H_2O_2= 110	0.25	66	12.5	65	67.5
19	8 h	H_2O_2= 110	0.25	104	12.5	68	70.5
7	8 h	H_2O_2= 120	0.35	104	13	70	83
7	8 h	H_2O_2= 140	0.48	104	13.5	77	90.5
4	6 h	H_2O_2= 140	0.48	135	13.5	80	93.5
4	3 h	H_2O_2= 140	0.48	273	13.5	77	90.5

In general, it can be seen in table 9.1 that, all the studied conditions lead to significant organic substrate removal in combined processes at different cycle durations. Under the same pre-treated solution biodegradability (0.25 and 0.48), TOC removals in SBR was increased from 42 up to 80 % diminishing the cycles operation time from 8 days to 8 hours. Moreover, it can be seen that up to 93.5 % total organic matter can be removed in coupled processes, with a major degradation take place in the bio-oxidation process.

From the acclimation period and second operation conditions(first period in table 9.1) formations, the feed solution biodegradability was changed to use the solution pre-treated with photo-Fenton under the following conditions: 100 mgL^{-1} of DCP: 110 $mg.L^{-1}$ H_2O_2, 10 $mg.L^{-1}$ Fe(III) and 35 minutes irradiation time, this solution biodegradability (measured as BOD_5/COD ratio) was 0.25. With this feed SBR reactor was operated for 122 day and 8 day cycle duration and decreasing periodically to reach down to 8 hours. Accordingly the organic load rate increased from 34 up to 104 $mgC.L^{-1}day^{-1}$. Figure 9.2 illustrate the evolution of TOC in effluent as function of operation days. It can be seen in the figure that, the organic matter concentration decrease as function of operational conditions. The use of new pre-treated solution with higher biodegradability showed better biological affinity to DCP organic intermediates, this is in concurrence with biodegradability indicator increment (0.15 up to 0.21 respectively).

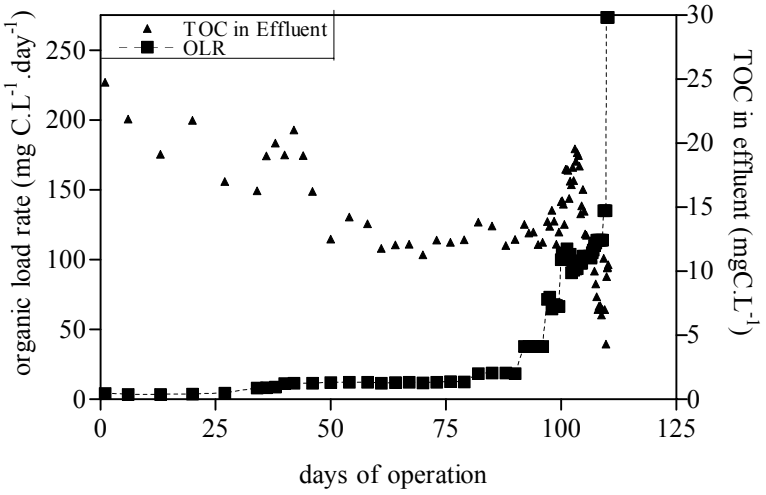

Figure 9.2: TOC in effluent solution as function of operation days for aerobic SBR. Feed BOD_5/COD=0.25.

Figure 9.3 presents TOC evolution and biomass concentration as function of cycle duration when SBR was run at 8 days cycle durations. It can be seen that, organic

matter biodegradation started immediately after reactor feeding and reached a plateau within 50h of bioreaction, after that no more degradation occurred. An average organic matter removal in SBR (TOC%) of 44% was achieved during the 6 cycles, and slight change was noticed in biomass concentration (0.14-0.16 $g.L^{-1}$). Throughout these cycle about 56% organic matter removal in combined processes was acquired.

In literature different models were used to explain the biodegradation tendency of different substrates, two types of substrate were defined only: rapidly biodegradable fraction and refractory fraction (Mamais et al., 1993, Klopp and Koppe. 1990). During the degradation of DCP intermediates by SBR, the two different fractions were identified. The first one (FI in figure 9.3) represents the easily biodegradable substrate. Whereas the second fraction (FII) shows the start of refractory conditions. Taking the maximal slope of the biodegradable fraction the reaction rate was calculated to be 2.33 $mgTOC.L^{-1}.h^{-1}$ and specific rate of 15.6 $mgTOC.gTVSS^{-1}.h^{-1}$.

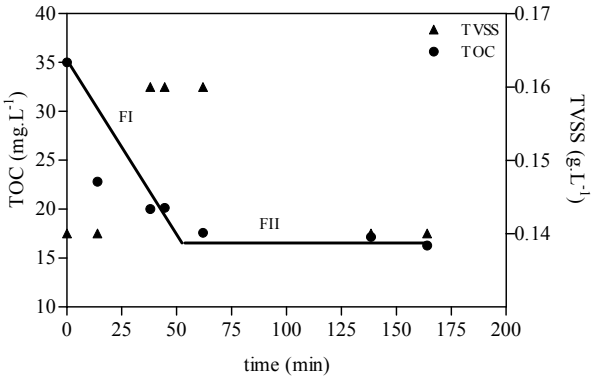

Figure 9.3: Evolution of TOC and TVSS as function of cycle duration, cycle duration 8 days and feed BOD_5/COD= 0.21.

As in the previous part almost all the biodegradation was take place during 50 h, and to make the biological process more feasible, during the next 46 days, SBR cycles were reduced to 4 and then 3 days of duration. Figure 9.4 demonstrates the organic substrate (TOC) evolution and organic mater removal (TOC%) as function of time for both cycle durations. The new conditions enhanced significantly the organic matter biodegradation: with respect to cycle carried out with 4 days duration, it was noticed from the first cycle that biomass is able to degrade more than 62% of the contained organic matter. Moreover, it was noticed that the major degradation took place during the first 24 h and a small proportion was degraded in rest of time. The same influence

was observed in biomass concentrations. TVSS increased from 0.1 $g.L^{-1}$ up to 0.15 $g.L^{-1}$ during the 4 cycles. From reaction rate point of view, reaction rate and specific elimination rate of 0.3345 $mgTOC.(L.h)^{-1}$ and 3.71 $mgTOC.(L.h.\ g\ TVSS)^{-1}$ were obtained respectively.

In case of 3 days cycle duration (see figure 9.4), the same organic matter elimination achieved before was obtained also by this cycle time duration. In average, substrate elimination of 68% and biomass concentration of (0.16 $gTVSS.L^{-1}$) were achieved. Again, it was noticed that the maximum degradation arises during the first 20 h. This may suggest that the SBR cycle time may decrease directly into 20 h. Once more, it can be seen that the degradation tendency in the bioreactor can be represented by biodegradable and non-biodegradable fractions.

60 to 68 % organic matter degradation (74.5 and 80.5% degradation in combined processes) are in agreement with biodegradability value: as it was mentioned before a BOD_5/COD ratio of 0.4 is consider as a cut-off point between biodegradable and difficult biodegradable waste (Metcalf and Eddy, 1985).

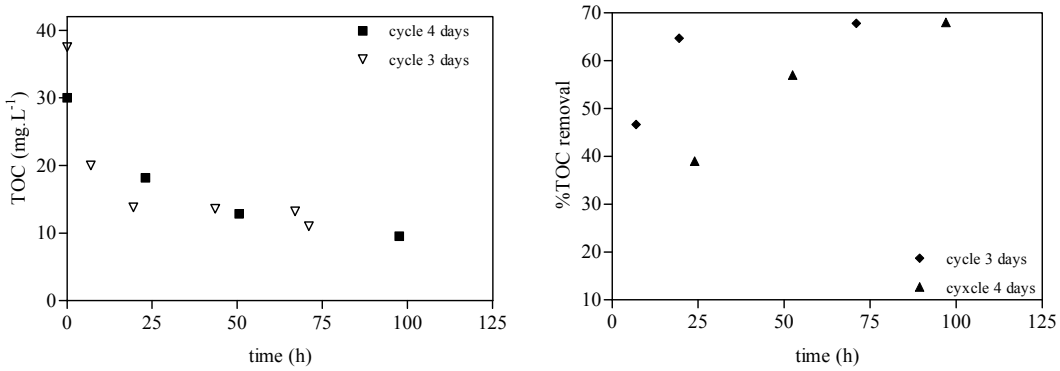

Figure 9.4: TOC evolution and organic matter removals (%TOC) as function of time for SBR operated at 4 and 3 days cycle duration , feed BOD_5/COD= 0.25

Yet, to reach short cycle time duration it was necessary to go through cycle time of 2 and 1 day. The organic matter removal during cycle duration of 2 and 1 days time is presented in figure 9.5. Average TOC removal of 66 and 68 % were achieved for both cycle duration respectively. Moreover the reaction rate, based on maximal slope consideration, and specific elimination rate of both cycle were increased up to 4.2 $mgTOC.(L.h)^{-1}$ and 28 $mgTOC.(L.h.\ g\ TVSS)^{-1}$. What means that an important fraction of the organic content of the pre-treated solution could be aerobically removed form the effluent in a very short retention time (total TOC removal in combined processes was in

order of 80 %). By the other hand, it has also been observed that, for all the working conditions studied, a fraction of the organic matter (less than 20 % of total TOC content) produced as intermediates in photo-Fenton process are still recalcitrant for the biodegradation.

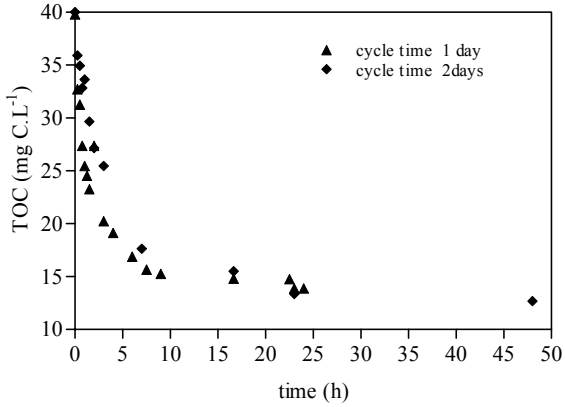

Figure 9.5: TOC evolution as function of time in aerobic SBR, cycle duration 1 and 2 days and feed $BOD_5/COD= 0.25$

Next, shorter cycle duration were studied, the same pre-treated solution was allow to biodegraded for only 12 hr; 6 cycle were carried out at this cycle duration. Figure 9.6 shows the results obtained during one cycle. During all the studied cycle a organic mater removal of 65% (more than 77.5% in combined processes) could be acquired, at this time (after 90 days of operation) biomass can be assume highly acclimated to DCP pre-oxidized solution. Nevertheless, it is interesting to note that the substrate degradation seems to take place all over the 12 h.

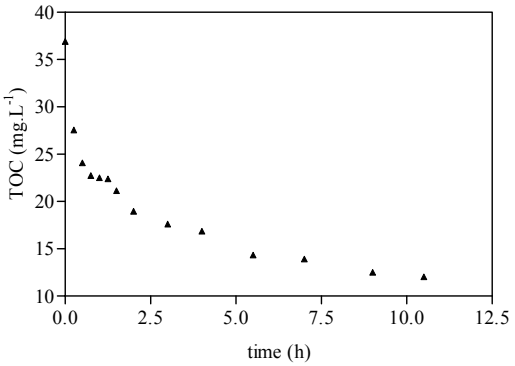

Figure 9.6: TOC evolution in aerobic SBR reactor during cycle of 12 h and feed $BOD_5/COD= 0.25$

.

In spite that TOC removal in cycle of 12h arise during all cycle time, new shorter cycle duration of 8h was tested. Figure 9.7 shows the evolution of initial organic carbon after

feeding the reactor (TOC_i), final organic carbon before next feeding (TOC_f) and organic mater removal (%TOC) for each cycle as function of time. It was observed that, for the first three cycles the biodegradation affinity is in the same order of magnitude of that obtained with 12 h cycle duration (62% TOC removal). Nonetheless, proceeding with bio-oxidation, it was observed that both the degradation efficiency and biomass concentration decrease to 45% and 0.08 $g.L^{-1}$ respectively. As in these cycles it was started in the same pre-treated solution, the new tendency may be due to the change in cycle duration the action that cost the biomass time to get use. Furthermore, after 11 cycles the reactor appear to somewhat recover up and the degradation increase to 58%.

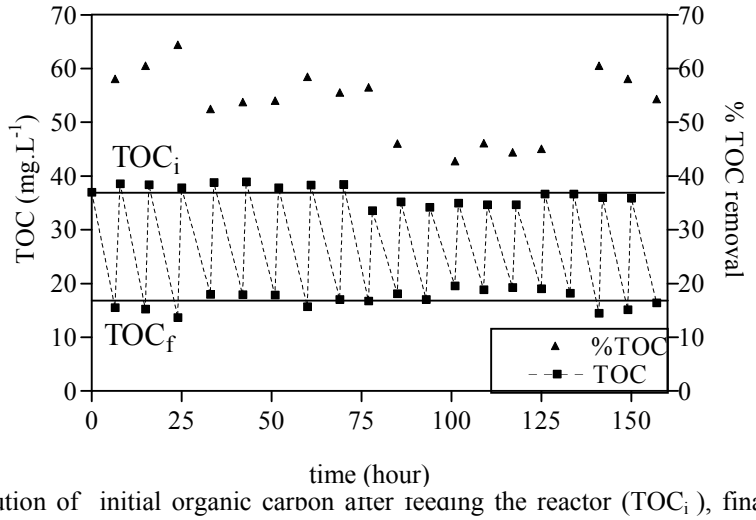

Figure 9.7: Evolution of initial organic carbon after feeding the reactor (TOC_i), final organic carbon before next feeding (TOC_f) and organic mater removal for each cycle (%TOC) as function of time, cycle duration 8 h and feed BOD_5/COD= 0.25.

After it was certain that the degradation efficiency of the SBR with this feed will not pass the 68 % under all condition, due to long feeding time with same pre-treated solution. It was decided to test the bio-oxidation of more biodegradable pre-treated solutions, At this point it was thinking with solution treated with 120 $mg.L^{-1}$ H_2O_2, 10 $mg.L^{-1}$ Fe(II) and 35 irradiation time, this solution has biodegradability (measured as BOD_5/COD) of 0.35 (see table 9.1). The new feed was charged to the reactor and leave to react for 8 hr cycle time, for a period of 7 cycles. Figure 9.8 provides the same previous parameters for the new solution. Organic substrate removal improved from 60% to70 %, in total organic base. In reality it was expected that change in feed biodegradability from 0.25 up to 0.35 will direct to considerable increment in

degradation. Though, it should not be forgot that solution biodegradability is still below the cut–off limit at which organic matter assume easily biodegradable.

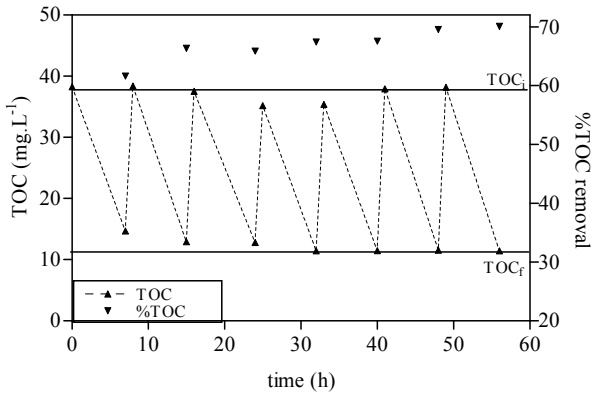

Figure 9.11: Evolution of initial organic carbon after feeding the reactor (TOC_i), final organic carbon before next feeding (TOC_f) and organic mater removal for each cycle (%TOC) as function of time, cycle duration 8 h and feed BOD_5/COD= 0.35.

Thus, it was decided to change the SBR feed solution and to use other pre-treated solution within the cut-off limit. This solution was attained by photo-oxidize DCP solution with 140 $mg.L^{-1}$ H_2O_2, 10 $mg.L^{-1}$ Fe(II) and 35 irradiation time. BOD_5/COD measurements for this pre-treated solution provides a value of 0.48. Figure 9.12 presents the evolution of total organic carbon (TOC) in effluent as function of operation hours for this solution. Actually this solution was allowed to bio-react in SBR for three different cycle durations 8, 6 and 3 hours. During these cycle the OLR increased from 104 up to 273 $mgTOC.L^{-1}.day^{-1}$. The change into feed solution with significant biodegradability value guided to significant progress in the bio-degradation tendency. It can be seen in figure9.12 that during the first 5 cycle the TOC in effluent started to decrease and reached to less than 10 $mg.L^{-1}$ even at short cycle duration (8 to 3 h).

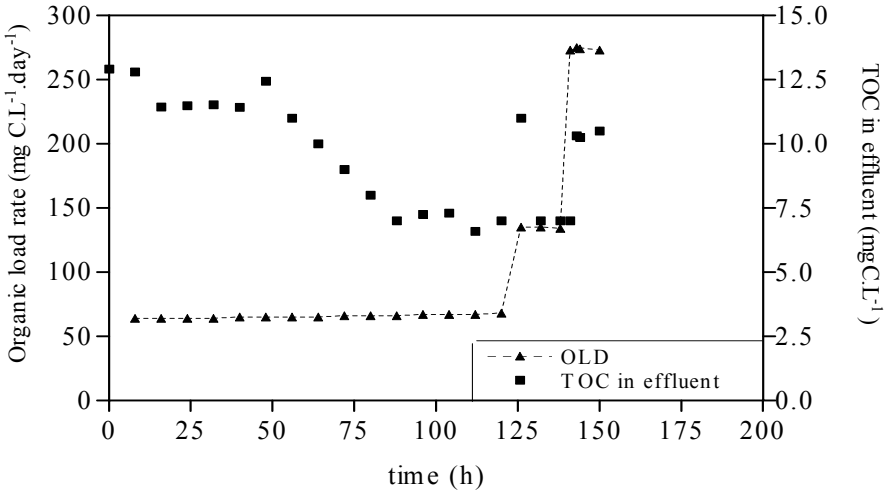

Figure 9.12 Evolution of total organic carbon (TOC) in effluent as function of operation hours.

In periods of 8.6 and 3 hours.

Figure 9.13 presents initial organic carbon (TOC_i), final organic carbon (TOC_f) and organic mater removal (%TOC) as operation function of time, for cycles carried out at 8, 6 and 3 hours using the feed (BOD_5/COD= 0.48). The influence in feed solution biodegradability can be seen from the first three cycles where the degradation increased from 68 up to 73%. what's more important development in elimination tendency was observed during the 10 days, maximum TOC removal of 85% and biomass increment up to 0.2 $g.L^{-1}$was obtained in 8 h cycle duration cycle concentration increased.

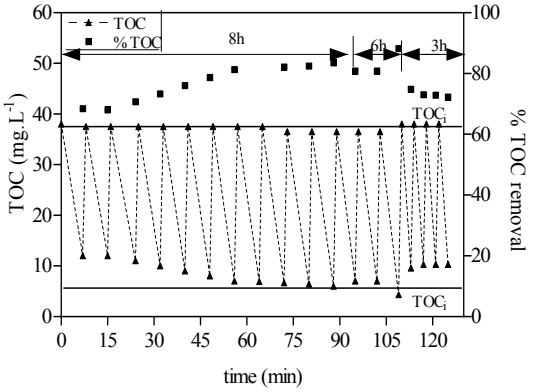

Figure 9.12: Evolution of initial organic carbon after feeding the reactor (TOC_i), final organic carbon before next feeding (TOC_f) and organic mater removal for each cycle (%TOC) as function of time, cycle duration 8 h and feed BOD_5/COD= 0.48.

At this conditions, it was noticed that almost all the degradation took place during the first 3 hours (65%) and only small fraction was eliminated during the remaining 5 h (18%). With regard of reaction rate a value of 7.5 $mgTOC.(L.h)^{-1}$ and specific elimination rate of 75 $mgTOC.(L.h.\ g\ TVSS)^{-1}$ was obtained.

For cycles operated with 6 h duration no effect in biodegradation efficiency was observed and bio-oxidation of 80% (93.5 in combined processes) as an average was achieved. In addition to that, biomass concentration seems to be constant at 0.2 $g.L^{-1}$. for a second time, it was noticed that the major degradation ensue during the first 4 hours. In case of cycles with 3 hour duration, it was noticed that degradation percentage is still acceptable 74 % in SBR and 90.5 in combined processes.

Finally, a full summary for 112 days of operation time is presented; figure 9.14 shows the development of organic substrate removal(TOC%) as function of cycle duration, biodegradability improvement represented as initial H_2O_2 concentration used in photo-Fenton pre-treatment. The change in pre-treated solution conditions affected positively the SBR performance. In fact, important increments in TOC removal were observed

when original DCP solution was more pre-oxidized in photo-Fenton process. By increasing H_2O_2 initial concentration from 65 up to 140 $mg.L^{-1}$, the substrate removal efficiency increased from 42 up to 85 % TOC removal and more than 93.5% total organic carbon can be eliminated even at shorter cycles duration.

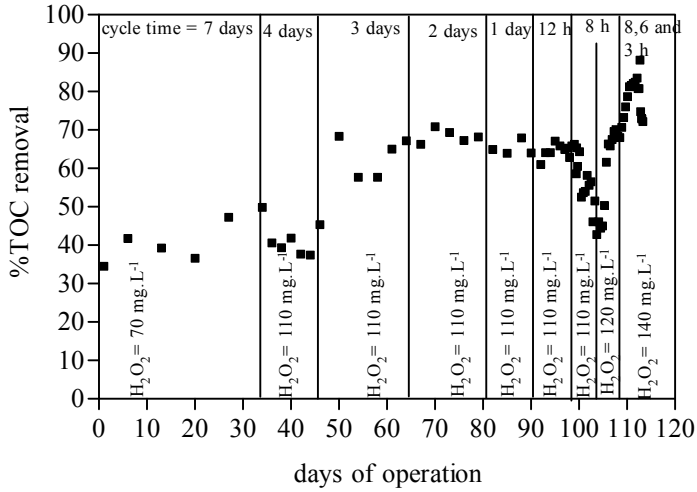

Figure 9.14: TOC removal as function of time at different initial H_2O_2 used in photo-Fenton and cycle duration.

9.2. Anaerobic sequencing batch reactor

the same previous strategy was applied for Anaerobic biological degradation of DCP photo-treated solution. A summary of experimental condition and some results are presented in table 9.2

Table 9.2: operational conditions and results obtained during anaerobic bio-degradation

No. Cycles	Cycle duration Days	H_2O_2 used in Pre-treatment conditions (1) ($mg.L^{-1}$)	Feed BOD_5/COD	Average OLR ($mgC.L^{-1}.day^{-1}$)	%TOC removal in pre-treatment	Average %TOC removal in SBR	% TOC removal in combined processes
4	8	H_2O_2= 65	0.15	8	10	52.3	63.5
2	8	H_2O_2= 70	0.21	4.1	12	42	54
2	8	H_2O_2= 110	0.25	4.1	12.5	55	67.5
6	4	H_2O_2= 110	0.25	8.3	12.5	58	70.5
5	3	H_2O_2= 110	0.25	11	12.5	56	68.5
5	2	H_2O_2= 110	0.25	17	12.5	60	72.5
8	1	H_2O_2= 110	0.25	34	12.5	59	71.5
6	0.5	H_2O_2= 110	0.25	78	12.5	60	72.5
19	0.33	H_2O_2= 110	0.25	102	12.5	45	57.5
8	0.33	H_2O_2= 120	0.35	102	13.0	70	83
4	0.33	H_2O_2= 140	0.48	136	14	82	96
3	0.25	H_2O_2= 140	0.48	170	14	78	92
4	0.125	H_2O_2= 140	0.48	204	14	60	74

9.2.1. Start up:

The start up of biological reactor was performed by feeding the SBR which contain fresh anaerobic loads, with photo-Fenton pre-treated solution according to following conditions: 100 mgL^{-1} of DCP: 65 $mg.L^{-1}$ H_2O_2, 10 $mg.L^{-1}$ Fe(III), 35 minutes irradiation time. At these conditions feed biodegradability (BOD_5/COD) is 0.15. As before, the pre-treated solution contained organic matter concentration around 40 $mgTOC.L^{-1}$. Figure 9.15 presents total organic carbon (TOC) evolution and biomass concentration (TVSS) as function of acclimation time. Anaerobic process present better response for acclimation, 20 days was sufficient to complete the acclimation period. Moreover, dissimilar to aerobic reactor two noticeable difference was observed during acclimation; the organic matter concentration decrease regularly with operational time and moderate organic substrate removal was obtained (52%). In this reactor the initial biomass concentration was 0.6 $g.L^{-1}$, the concentration in acclimation period decrease slightly into 0.53 $g.L^{-1}$.

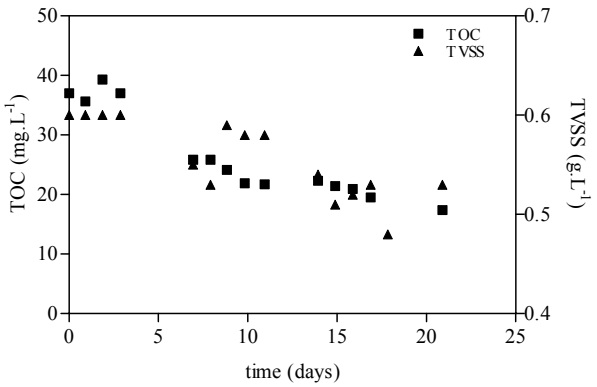

Figure 9.15: Total organic carbon (TOC) evolution and biomass concentration (TVSS) as function of acclimation time, feed BOD_5/COD =0.15.

9.2.2. Anaerobic SBR operation :

Next 4 cycles were carried out with the same pre-treated solution, exchange volume of 7/8 of total reactor volume and 8 days cycle duration. The concentration in the reactor maintained around 33 $mgTOC.L^{-1}$ as a result of slight dilution in reactor. The evolutions of organic matter in effluent and biomass concentration of the first cycle are presented in figure 9.16. Throughout this cycles organic matter (TOC) removal was 52.3% and biomass maintain at average concentration

of 0.36 g.L^{-1}. In next three cycles the degradation decreased to an average value of 42 in SBR and 52 % in combined processes (see table 9.2).

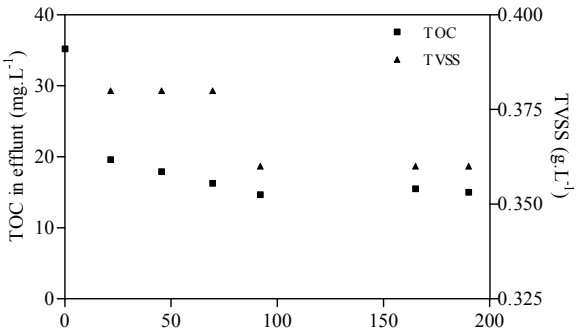

Figure 9.16: Evolution of organic matter and biomass concentration as function of cycle duration, cycle duration 8 days and feed BOD_5/COD =0.15.

To go further in biodegradation and to compare with aerobic treatment process, the pre-treated solution was changed and solution with more biodegradability was used. This feed was obtained in photo-Fenton pre-treated solution with 70 mg.L^{-1} H_2O_2 and the same previous conditions of Fe(II) and irradiation time, biodegradability of this solution was 0.21. Two cycles of 8 days was performed using this pre-treated solution, unexpected response of the bioreactor was noticed. During the two cycles, organic mater removal of 42 % was acquired, and biomass concentration also decreased to 0.14 mg.L^{-1}. In spite all of that, it was noticed that this degradation was occurred during the first 70 hour of reaction time. As the degradation mechanisms in anaerobic reactor is different than aerobic bioreactor, it was thought that 42% degradation is the maximum degradation can be obtained at this biodegradability values.

To check if further improvement in bio-oxidation can be achieved. The same changed done in aerobic reactor was made in this reactor, mainly feed the bioreactor with another pre-treated solution with more biodegradability value, the solution used was treated with photo-Fenton process with 110 mg.L^{-1} H_2O_2 this solution has biodegradability (BOD_5/COD =0.25). To get a good idea about the reaction progress, this feed was allowed to biodegraded anaerobically for 133 days (see table 9.3).

At the beginning two cycles with 8 h cycle duration was tested. Feeding with better biodegradable solution direct to significant improvement in organic substrate removal. More than 55% TOC removal in SBR and 67.5% in combined processes was achieved. Moreover it was observed that almost all the biodegradation took place during the first 70 hours.

Thus after that, it was decided to keep feeding with the same pre-treated solution but with different cycle durations (from 4 down to 1 day). Figure 9.17 presents the evolution of organic matter as function of cycle duration. It was noticed that changing the feed biodegradability did not affect the degradation efficiency and TOC removals almost in the same order of magnitude were obtained for all cycle time (60 % as an average). Moreover, maximum degradation rate was noticed at the beginning of the cycle (rapidly biodegradable fraction) and small fraction degraded in the rest of the time.

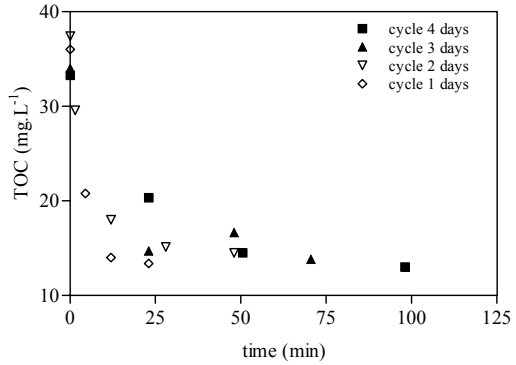

Figure 9.17: Evolution of organic matter as function of cycle duration, cycle duration 4,3, 2 and 1 day and feed BOD_5/COD =0.25.

Based on figure 9.17 details, and taking in account that all the degradation occurs during the first 12 hr, the cycle duration was reduced to this level. Figure 9.18 shows organic matter evolution as function of cycle time, again the degradation efficiency is still around 60 % and the TVSS sustain at 0.10 $g.L^{-1}$. Moreover, based on first time reaction, the reaction rate and the specific elimination were 5.8 mgTOC. $(L.h)^{-1}$and of 29 mgTOC. $(L.h.\ g\ TVSS)^{-1}$ respectively.

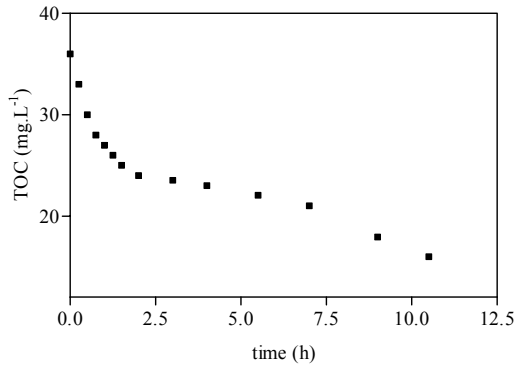

Figure 9.18: Evolution of organic matter as function of cycle duration (12h), and feed BOD_5/COD =0.25.

As in the aerobic biological reactor, shorter cycle was time also tested do see the limit at which the an aerobic reactor can be operated, Figure 9.18 shows the results when the reactor was

operated in cycles with 8 h cycle duration. In the first three cycles it was obtained the same removal TOC as before (60%). Nevertheless, it is clear in the figure the effect of cycle time reduction the proceeding cycles, organic matter elimination decreased to less than 45%. So far, anaerobic process seems to response rapidly to this change and the organic matter removal becomes again to be approximately 60%.

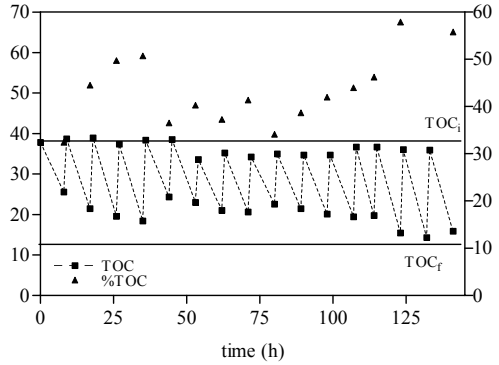

Figure 9.18: Evolution of initial organic carbon after feeding the reactor (TOC_i), final organic carbon before next feeding (TOC_f) and organic mater removal for each cycle (%TOC) as function of time, cycle duration 8h and feed BOD_5/COD= 0.25.

After it was firmed that with this pre-treated solution no more substrate degradation could be obtained, and it was decided to check if an increase in the feed solution biodegradability affects the bioreactor. Feed solution with biodegradability value of 0.35 was tested during 10 cycles. Up to 70% organic matter removal could be achieved. During that, degradation rate of 8.4 $mgTOC.(L.h)^{-1}$ and specific elimination rate of 28 $mgTOC.(L.h.\ g\ TVSS)^{-1}$ were obtained.

Also, solution with biodegradability value of 0.48 was tested. Figure 9.19 presents the evolution of initial organic carbon after feeding the reactor (TOC_i), final organic carbon before next feeding (TOC_f) and organic mater removal for each cycle (%TOC) as function of time for different cycle durations. It can be seen that the change of the feed solution into readily biodegradable solution leads to significant improvement in biodegradation efficiency. The change can be noticed from the first two cycles, throughout the 8 cycles with 8 h. duration more than 82% can be acquired. In addition to that, it was observed that a considerable degradation occurred during the first 2 hours and only small fraction was degraded in the remaining time. Again a degradation kinetic reaction rate of 9 $mgTOC.(L.h)^{-1}$ and specific elimination rate of 30 $mgTOC.(L.h.\ g\ TVSS)^{-1}$ was attained.

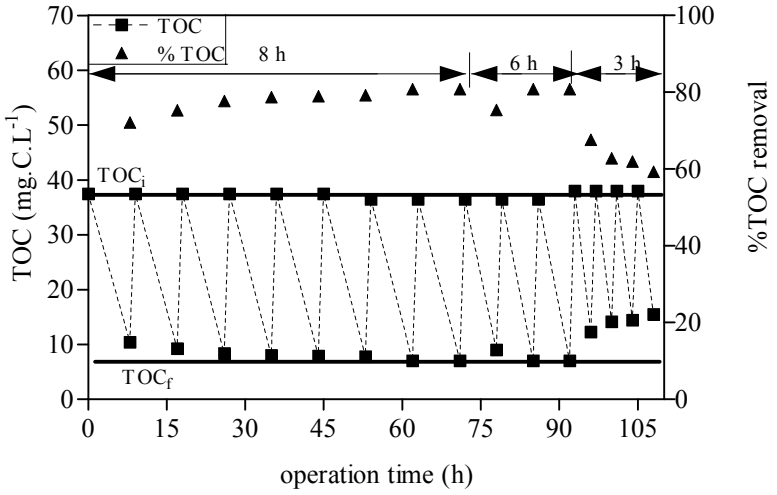

Figure 9.19: Evolution of initial organic carbon after feeding the reactor (TOC_i), final organic carbon before next feeding (TOC_f) and organic mater removal for each cycle (%TOC) as function of time, cycle duration 8. 6 and 3 h and feed BOD_5/COD= 0.48.

It was noticed that, decrease the cycle time did not lead to the same degradation efficiency, it can be seen in figure 9.19 that from the first cycle of 6 h duration organic matter removal start to decrease, but still within the acceptable range (78%). With respect to cycles at 3 h duration the removal efficiency also decreased and no more than 60 % organic matter can be eliminated.

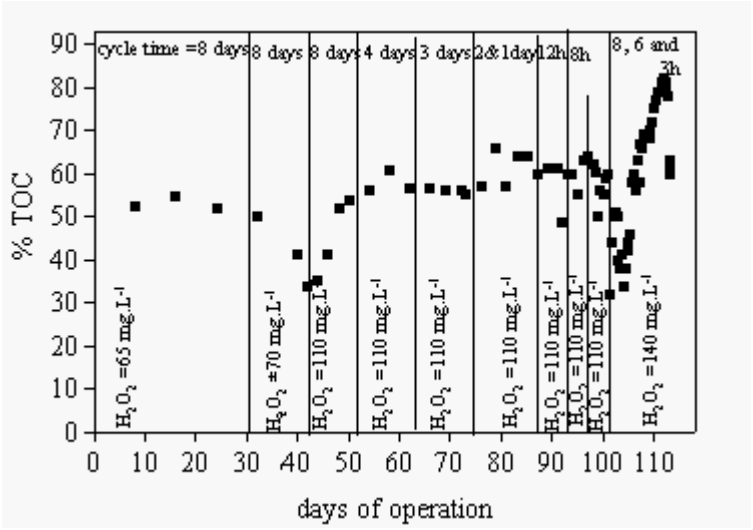

Figure 9.14: TOC removal as function of time at different initial H_2O_2 used in photo-Fenton and cycle duration.

Again summary of 120 days of anaerobic degradation is presented: figure 9.20 shows the development of organic substrate removal (TOC%) as function of cycle duration, pre-treated solution biodegradability improvement. The change in pre-treated solution conditions affected positively the SBR performance.

Significant improvement in organic matter removal was observed by oxidized DCP solution, and hence increase intermediates biodegradability. Considerable biodegradation was achieved at different cycle duration, up to 80% of organic substrate elimination can be achieved at short cycle time (6 h), moreover SBR can be operated with only 3 hr cycle time with noteworthy elimination capacity.

9.3. Kinetic study:

Aerobic and an aerobic biodegradation in SBR kinetics were examined for a simple first order kinetics according to Eq. (7.24). Good distributions of experimental data around straight prove the validity of this model to explain the present bioreactor kinetic. Table 9.1 summarize the first order kinetic constants for aerobic and anaerobic bioreactor at different cycle duration and different biodegradability.

Table 9.3 first order kinetic constants for aerobic and anaerobic bioreactor at different cycle duration and different biodegradability.

Cycle duration (day)	feed BOD_5/COD	Aerobic reactor K_{ob} ($L.gTVSS^{-1}\ h^{-1}$)	Anaerobic reactor K_{ob} ($L.gTVSS\text{-}1\ h^{-1}$)
2	0.25	0.011±0.003	0.008±0.0005
1	0.25	0.034±0.004	0.025±0.002
0.5	0.25	0.060±0.003	0.0255±0.001
0.33 (8h)	0.35	0.324±0.004	0.0414±0.002

First order kinetic constant indicates that aerobic biodegradation rate is faster than anaerobic process, this tendency was observed clearly at different cycle during the operation of both reactors. It is interesting to mention that during kinetic data treatment, it was noticed the presence of two possible kinetics. The first one is so fast and it took place during the first 8 hours of bioreactor and the second is slow and occurred all over the remaining reaction time. The presence of two kinetics in the reactors could be aimed to the presence two kind of biodegradable material that degraded in different time periods.

9.4 Cost Estimation

Costs estimation based on operating costs and required reagents has been compared between TOC mineralization in photo-Fenton process and total organic matter elimination via combined processes (photo-Fenton and SBR). Costs have been calculated for the amount of TOC

mineralized in each process . Results are shown in Table 9.4. With regard to photo-Fenton process cost was calculated for different %TOC removal (100, 90 and 80%). Whereas different operational condition of the combined processes cost were tabulated. It can be seen in the table that, under the same mineralization efficiency, combined processes show lower costs than photo-Fenton processes. Despite that the biological part was operated at large cycle duration of 8 days. For 90% TOC removal the cost in photo-Fenton process is 110 €.kg^{-1} TOC treated. at the same time, only 25 and 34 € was needed in combined processes operating the SBR with 8 and 3 h cycle durations. Thus, it can conclude that using the combined process can save at least 70 up to 110 €.kg^{-1} TOC treated.

Table 9.4 Comparison of costs among photo-Fenton process and coupled processes (photo-Fenton and SBR)

Process		Photo-Fenton		combined with SBR						
Average %TOC removal	100	90	80	54	81	80.5	67.5	90.5	93.5	90.5
Amount of reagents used										
H_2O_2 (mg.L^{-1})	410	380	350	110	110	110	110	140	140	140
Fe(II) (mg.L^{-1})	40	40	40	10	10	10	10	10	10	10
Irradiation time (min)	60	60	60	35	35	35	35	35	35	35
Cycle duration (days)	-	-	-	8	3	1	0.5	0.33	0.25	0.125
Feed biodegradability	-	-	-	0.25	0.25	0.25	0.25	0.48	0.48	0.48
Cost €/kg TOC	120	110	101	95	75	50	50	34	30	25

Moreover. it can be seen the reduce in combined processes costs as function of pre-treated oxidation and biodegradability enhancement. Combined processes fed with pre-treated solution with BOD_5/COD of 0.25 guide to total organic carbon removal from 54 up to 80 throughout different cycle durations (8 days to 12h), and this was cost about 95 to 50 €.kg^{-1} TOC treated respectively. But, solution with biodegradability of 0.48 direct to more than 90% TOC removal and less than 30 €.kg^{-1}TOC at all tested cycle duration.

10. Treatment of textile dyes and textile wastewater

In this part photodegradation and biodegradability improvement have been studied for three different non-biodegradable textile dyes families (Intracron reactive dyes, Optisal dyes and Nylanthrene acid dyes) and a textile wastewater. The influence of pH, VUV-light and UV-light was examined in addition to the effect of all these conditions in pre-treated solutions biodegradability. Furthermore, first order kinetic constant were determined.

10.1 Effect of pH in dye solution:

Physico-chemical characteristics of studied dyes (100 $mg.L^{-1}$) are summarized in Table 10.1. The chosen concentration is the maximal concentration that can be observed in most discharge textile wastewater.

Table 10.1: Physico-chemical characteristics of studied dyes (100 $mg.L^{-1}$)

Family	Dyes	pH	COD ($mgO_2.L^{-1}$)	Conductivity ($\mu S.cm^{-1}$)	BOD_5/COD
Nylanthrene	Yellow	6.3	128	40	0.09
	Red	6.1	110	20	0.03
	Blue	7.9	140	23	0.05
Intracron	Red	5.1	112	23	0.0
	Orange	5.5	133	38	0.02
	Black	5.5	71	26	0.0
	Yellow	5.8	88	105	0.01
Optisal	Yellow	5.4	90	57	0.09
	Red	5.3	122	30	0.02
	Blue	5.5	100	18	0.09
Textile wastewater		6.8	325	1730	0.0

Before starting in the photo degradation, the effect of pH on dyes solution were studied for the three dye families. The pH effect is presented in figure (10.1-10.3). Basic conditions has no effect on Intracron dyes, since the dye spectra show no change by changing the pH from initial dye pH to 3. But, under acidic conditions some changes was noticed in dye colour and hence in UV-visible spectra. Acidic pH leads to bathochromic shift in dye spectra which suggests the effect of basic condition in dye chemical structur. In the case of Nylathrene dyes (figure 3), small effect was noticed under basic pH (specially for Blue dye). However, acidity has more noticeable

effect in dyes, acidic conditions direct the dye spectra to go through hypsochromic and hypochromic shift. The different tendency of the previous two dye families may indicate a big variety in the basic functional group the dyes family may contain.

With respect to the third dye family (Optisal dye), non regular tendency was noticed between dyes. While Optisal yellow dye show no effect neither to acidic nor basic pH, Optisal blue dye show obvious effect of both pH, specially at acidic pH where almost all the colour could be eliminated by just pH change. No valuable effect by pH change was noticed for Optisal red dye.

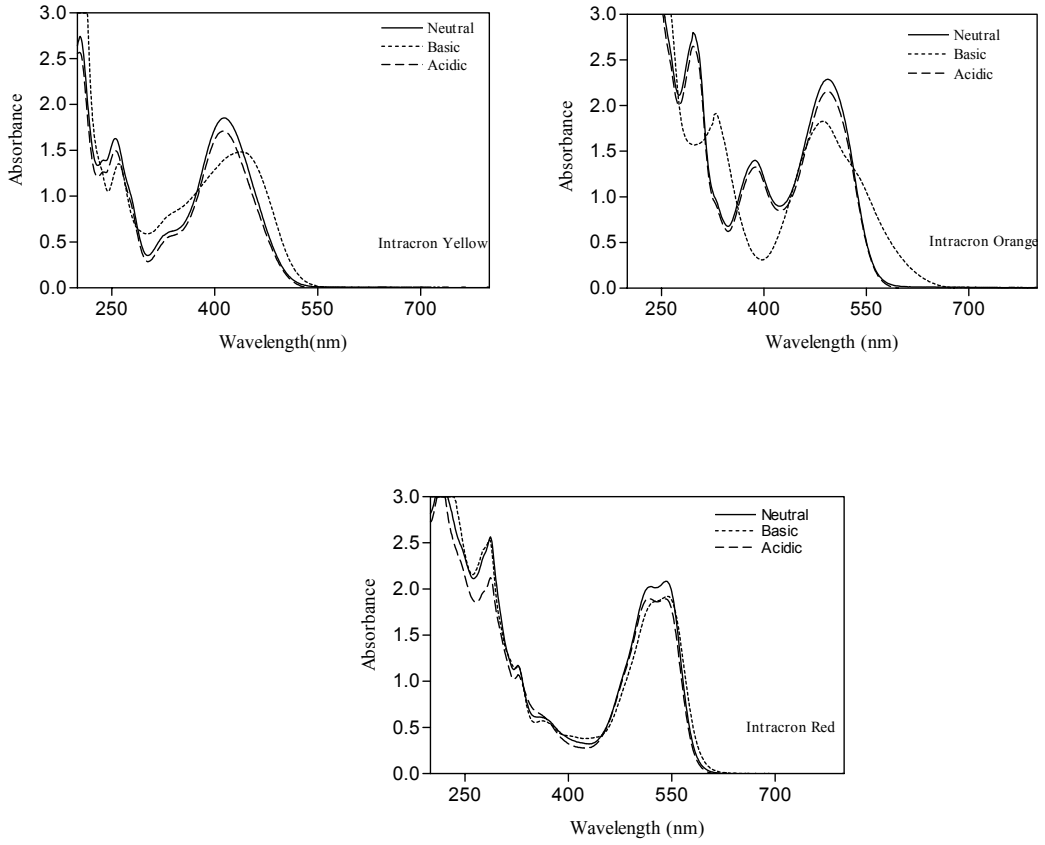

Figure 10.1: pH effect in UV-Vis. Spectra for intracron dyes

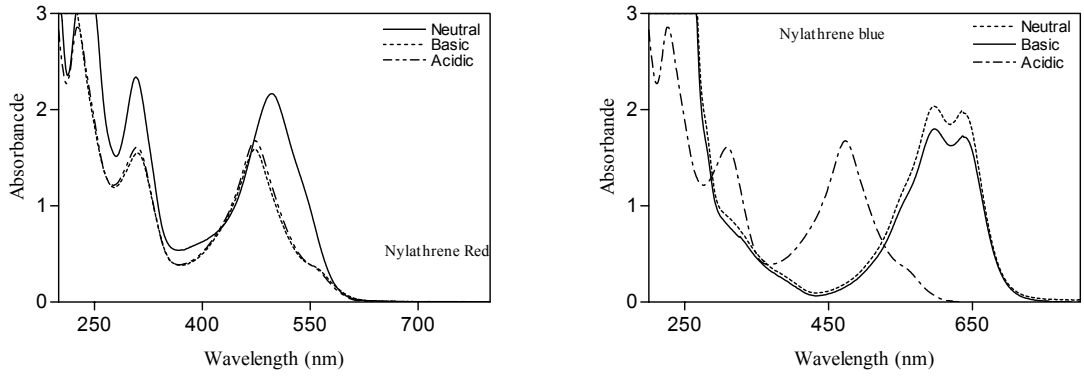

Figure 10.2: pH effect in UV-Vis. spectra for Nylathrene dyes

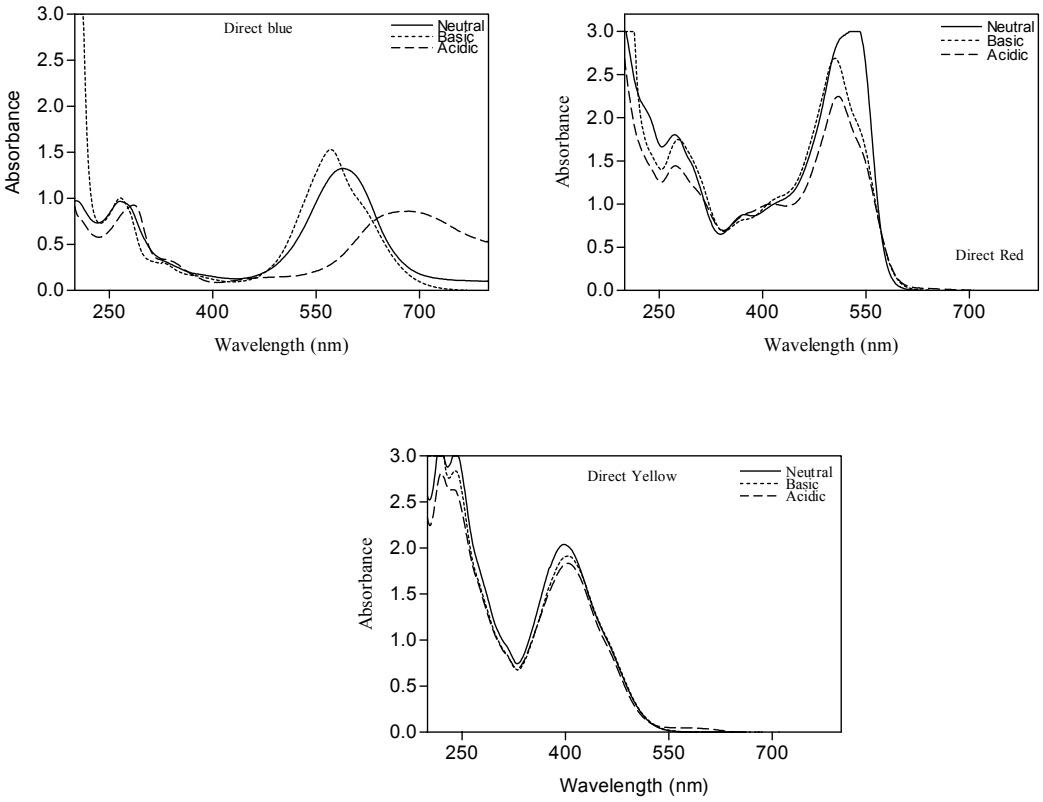

Figure 10.3: pH effect in UV-Vis. spectra for Optisal dirct dyes

10.2. Biodegradability tendency

Before proceeding with any pre-treatment, the ability of the original dye to go through biodegradation was verified, beside biodegradability (measured as BOD_5/COD ratio) inhibition test of oxygen consumption by activated sludge for the studied dyes was tested. Indeed, inhibition test allows a rapid indication of the toxicity of water medium for non-acclimated biomass population. Moreover, it may advantageously take place of BOD_5 measurements, due to its short application time. As it was commented before, domestic wastewater can be considered substantially biodegradable if it has a BOD_5/COD ratio between 0.4 to 0.8 [Metcalf and Eddy 1985]. The biodegradability measurements shows that all the studied dyes are non-biodegradable (Table 10.1). The inhibition effect on activated sludge for one dye of each family is presented in Figure 10.4, the sludge used in this test is taken from the municipal wastewater plant in Ales (France). As it can be seen in figure 10.4, the presence of these dyes in small concentration leads to the inhibition of oxygen consumption by the activated sludge. This fact can be imputed, either to the toxicity of the dyes for the bacterial culture which leads to bacteria death, or to the non-biodegradable character of the organic load. Textile dyes, azoïc or non azoïc, were studied and have been classified as hardly biodegradable pollutants [Hitz et al., 1978, Porter et al., 1973], so the second hypothesis could account for BOD_5 and inhibition test behaviour.

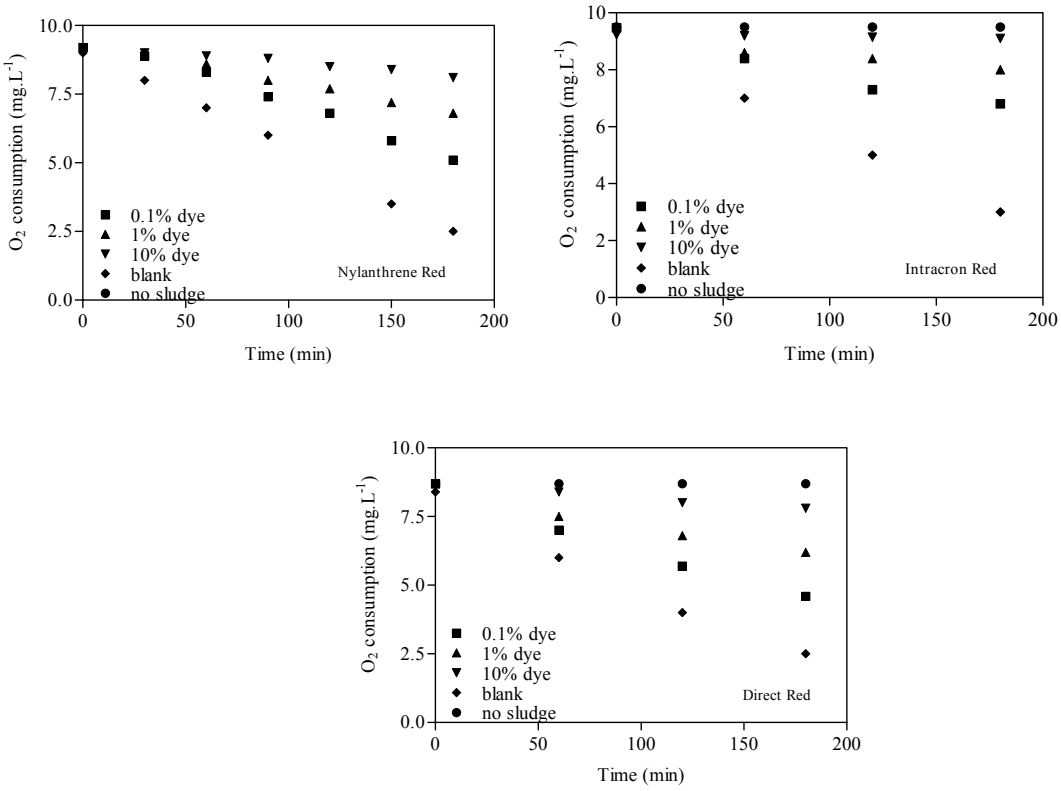

Figure 10.4 : Inhibition of O_2 consumption by activated sludge for three dye solutions ($100mg.L^{-1}$, pH= 7.0± 0.2)

10.3. Vacuum ultraviolet light photolysis (VUV) :

Color removal of the three dyes families was tested first by direct photolysis, for that two type of UV light was used, VUV light and UV light. VUV photolysis use light with two main wavelength (3% at λ= 184.7 nm)and (95% at λ= 253.7 nm). At the same time UV light used light at λ= 253.7nm, in the photo-reactor to get ride of light at λ= 184.7 nm special type of quartz was used (Infrasil quartz). In fact, this quartz prevents VUV irradiation (184.9nm) to reach the reaction zone, hence only UV light can be use in UV photolysis (see reactor 4 installations part).

10.3.1. VUV photolysis

On-line dye discoloration was monitored by UV-Visible spectrophotometry. VUV photolysis appears to be efficient as color abatement process for all studied dyes solutions (100 $mg.L^{-1}$).
Figure 10.5 shows the evolution of UV as function of irradiation time for Nylanthrene dyes. Direct examination of UV-Visible spectra shows that, after few minutes of irradiation, the

intensity of absorption peaks in the visible range decreases as well as the coloration of the sample. In a global way, an absorbance decrease is observed in the whole range of wavelength and the structuration of the spectrum vanishes more or less quickly according to the irradiation time. Moreover, a common phenomenon is noticed for studied dyes: UV-visible spectra go through an isosbestic point during the first minutes of irradiation, this suggest that during this time the dye global structure is preserved. This phenomenon is especially marked for Nylanthrene Blue which shows more resistance to degradation. However, continuing with direct photolysis guide to total discolorations of dyes molecule. During dyes discoloration mineralization of contained organic matter was determined. Total discoloration was combined with 18% chemical oxygen demand removal (COD). Moderate time (4.5 min) was sufficient for 90% discoloration of all Nylanthrene dyes.

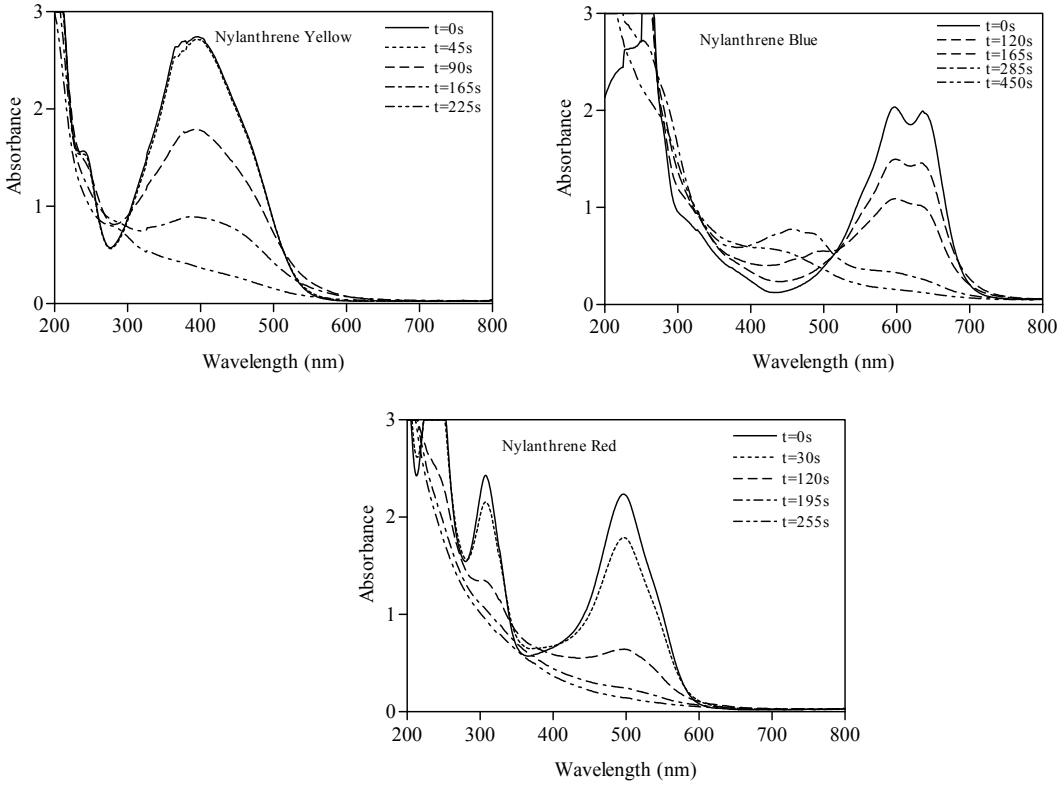

Figure 10.5 : VUV photolysis of Nylanthrene acid dyes (100 mg.L^{-1}).

Optisal dyes can be considered also as an easily photo-degradable dyes. For two reasons: 90% color removal was obtained during the first 5min irradiation time (Figure 10.6). Moreover, these days showed more mineralization ability. At 90% color removal the COD removal was 30% . it is interesting to remark that during Optisal dyes photo-Degradation, the conductivity increase in the solution by a factor of 5.0 this may give an indication that these degraded forming an ionic molecules.

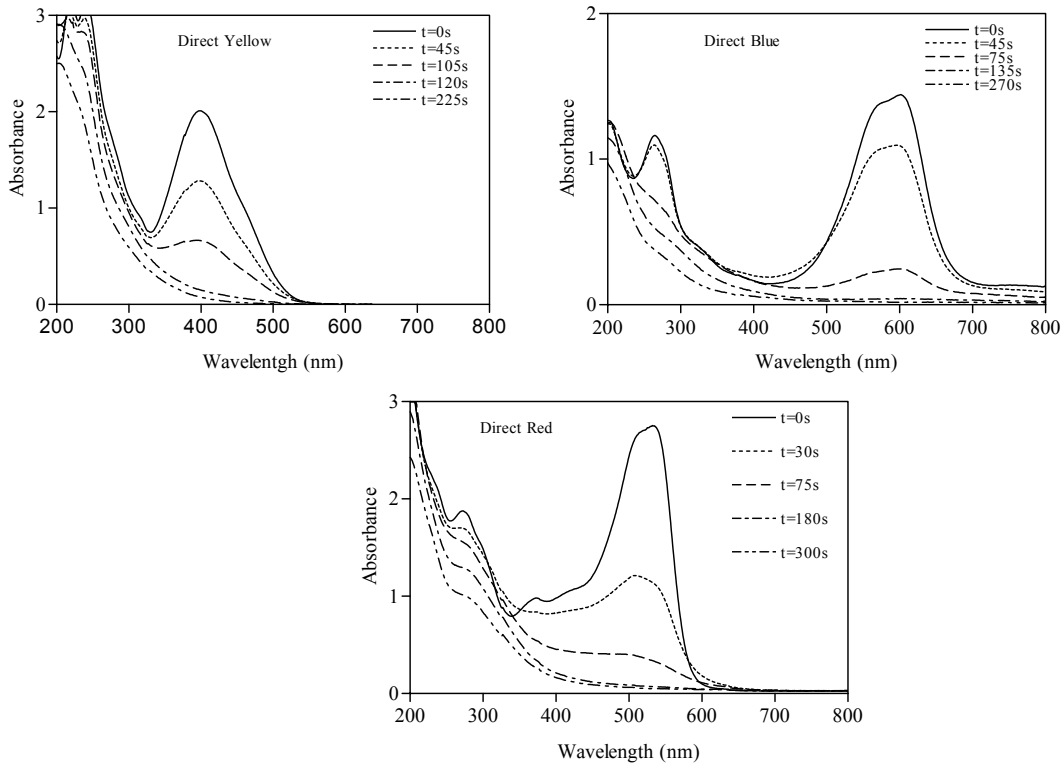

Figure 10.5 : UV photolysis of Optisal dyes (100 mg.L^{-1}).

Intracron family gives a similar behavior during VUV photolysis. Total color removal occurs during the first 4.2 min. As it can be seen on the UV-visible spectra (figure 10.6), more than 80% color abatement is achieved within 1.7 min. this degradation provides only 17% COD removal, and some increment in conductivity was detected in the reaction solution.

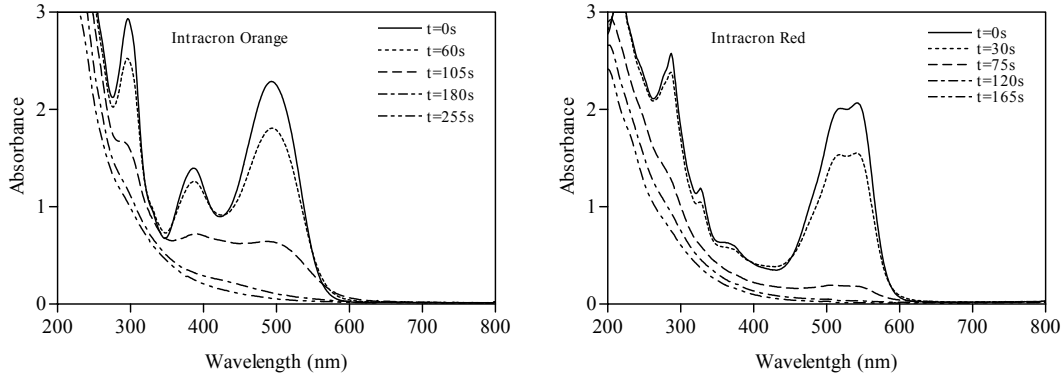

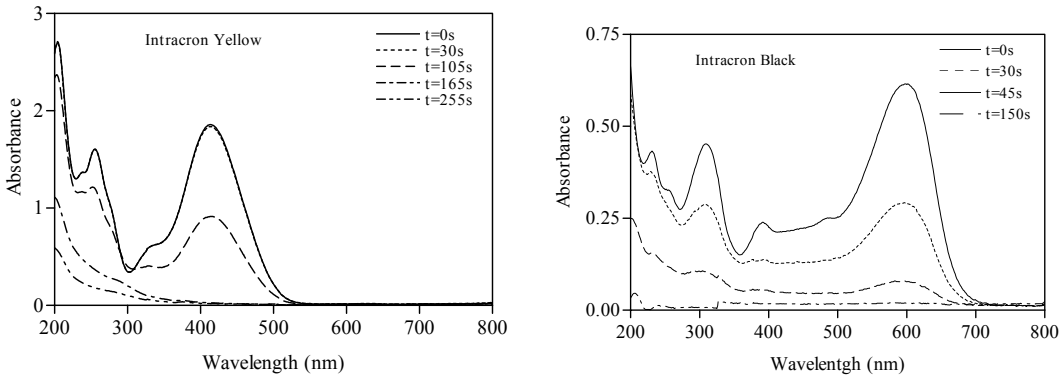

Figure 10.6 : UV Photolysis of Intracron reactive dyes (100 mg.L^{-1}).

10.3.2. Biodegradability improvement:

After photolysis, the treated dye solutions have been tested for their BOD_5, COD, conductivity (Table 10.2) and inhibition of oxygen consumption. As shown in Figure 10.7 for Intracron Red and Nylanthrene Red dyes, BOD_5 of the dye solution is increased through out photolysis, while COD decreased during the reaction. Table 10.2 shows the biodegradability of all studied dyes when colour removal is 90%, and the COD abatement. The increase of BOD_5 may imply that the biodegradability can be enhanced by the photolysis oxidation converting the non-biodegradable organic substrates into more biodegradable compounds.

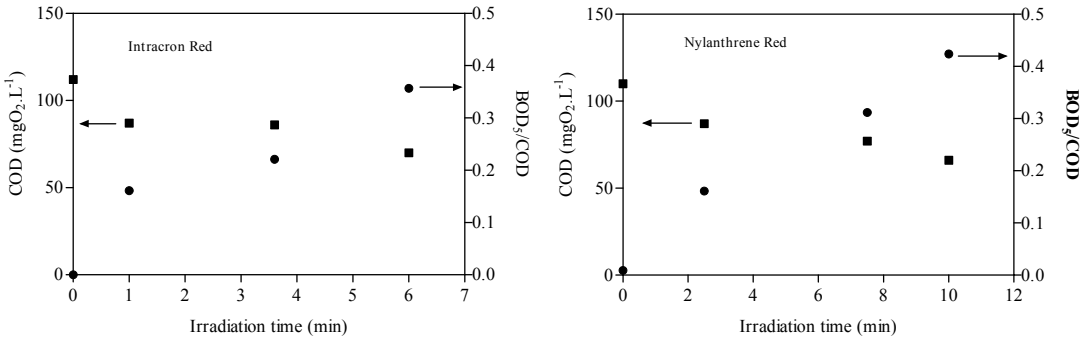

Figure 10.7: Evolution of BOD_5/COD ratio and COD vs irradiation time for Intracron Red and Nylanthrene Red (100 mg.L^{-1}).

Figure 10.8 shows the BOD_5/COD ratio for initial and treated solutions, It can be seen that using the VUV light, as pre-treatment step, leads to noticeable improvement in the biodegradability (BOD_5/COD) for the three dyes families depending on the structure of initial dyes. This improvement in biodegradability is reached with moderate COD conversion and short irradiation time. As mentioned before, a wastewater sample is considered as readily biodegradable when a BOD_5/COD value is in the range 0.40-0.80. This limit was reached easily for Optisal dyes, which

indicates that this family is degraded into intermediates that are readily biodegradable. Modern dyes are known to contain high composition ratio of aromatic rings in dye molecule.

Table 10.2 : BOD_5/COD, COD% removal and irradiation time of studied dyes (100 $mg.L^{-1}$) after VUV photolysis

Family	Dyes	pH_f	COD Removal (%)	Conductivity ($\mu S.cm^{-1}$)	BOD_5/COD	Irradiation time (min)
Nylanthrene	Yellow	2.8	30	66	0.27	7.5
	Red	2.7	30	21	0.31	7.5
	Blue	2.8	37	46	0.21	7.5
Intracron	Red	2.7	23	27	0.22	3.4
	Orange	2.9	33	155	0.23	5.1
	Black	2.8	18	109	0.26	2.5
	Yellow	2.9	39	186	0.27	2.5
Optisal	Yellow	3.0	31	116	0.42	4.5
	Red	3.0	22	78	0.41	5.2
	Blue	2.9	23	63	0.42	4.0

These molecules are degraded into toxic compounds such as aromatic amines [Beydilli et al., 1998]. As an increase of biodegradability is observed after phtoloysis, it can be assume that this process do not generate such compounds. For the other two families (Nylanthrene acid dyes and Intracron reactive dyes), results show that the biodegrdablity is less than the domestic level. So, it was decided for these families to go further more in photolysis, to see if the final BOD_5/COD ratio could be increased. The results shows that BOD_5/COD ratio increased for Intracron Red and Nylanthrene Red until to 0.39 and 0.38 with 2.0 and 2.5 min overtime of irradiation respectivley. This effect was combined with COD removal of 28 % and 40% respectively and a total discoloration. Other studied dyes show the same tendency in increasing the biodegradability as the colour disappeared completely.

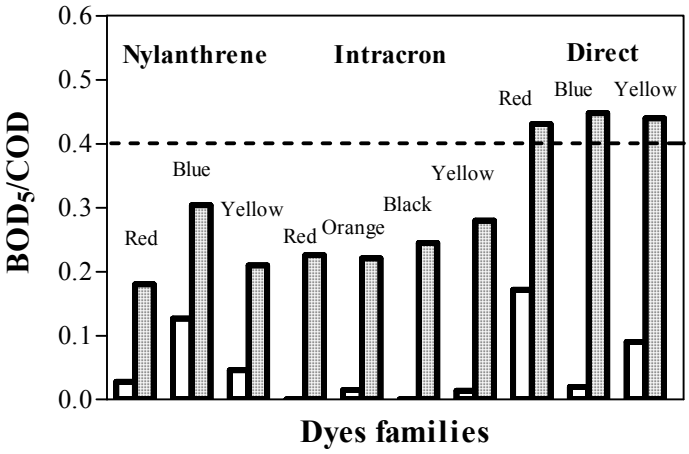

Figure 10.8: BOD_5/COD evolution for initial and photolyzed dyes solutions (100 $mg.L^{-1}$)

The by-products arising from total discoloration were tested for inhibition on activated sludge : no inhibition in oxygen consumption for activated sludge is observed during the 3 hours test and the sludge behavior is the same as for the blank solution (Figure 10.9).

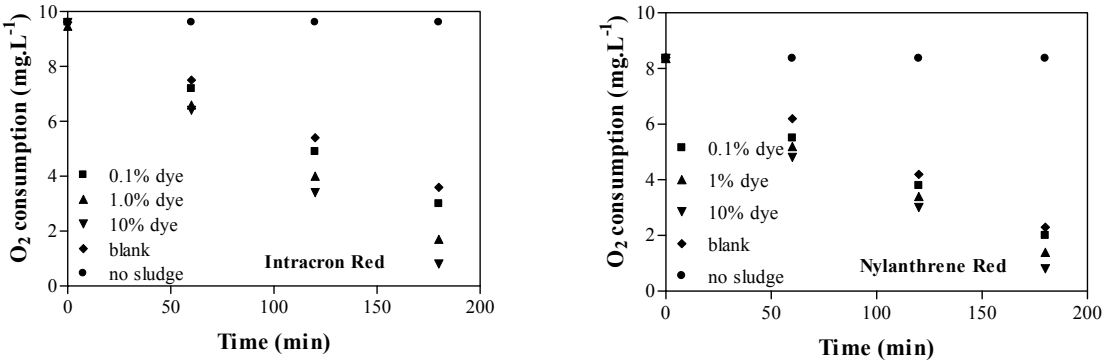

Figure 10.9: Inhibition of O_2 consumption by activated sludge for photolyzed Nylanthrene Red dye and Intracron Red dye (100$mg.L^{-1}$, pH=7.0± 0.2, irradiation time : 7.5 and 3.4 min respectively).

10.4. UV photolysis:

In order to see the effect of absence VUV light (λ =184.9 nm), the same experiments were repeated with UV light only at wavelength 184.9 νμ. Table 10.3 presents a comparison between UV and VUV photolyzed for some of the studied dye solutions at the same irradiation time. Experimental results show that VUV irradiation is more efficient in color removal and biodegradability enhancement than UV light lone.

Table 10.3 : Comparison between UV and VUV photolyzed solutions

Family	Dye	VUV		UV		
		COD removal (%)	BOD_5/COD	COD removal %	BOD_5/COD	Irradiation time (min)
Nylanthrene	Red	30	0.31	24	0.2	7.5
	Blue	37	0.21	24	0.16	7.5
Intracron	Red	23	0.22	15	0.15	3.5
	Orange	33	0.23	28	0.15	5.0
Optisal	Red	22	0.41	26	0.3	5.2
	Blue	23	0.42	20	0.39	4.0

However, the tendency depends on the dye family: for Optisal and Nylanthrene groups, the difference between UV and VUV is not significant (COD% and BOD_5/COD are in the same order of magnitude), while it can be noticed a valuable difference for Intracron family. In this case, the BOD_5/COD value decreases by 40 % by changing the photolysis process from VUV to UV. More efforts should be done to investigate the degradation mechanism and by products identification.

10.5. Kinetic study

A kinetic study has been done, considering that the absorbance of the solution (A_λ) at the maximal wavelength in the visible range is representative of the dye concentration, according to the Beer Lambert law :

$$A_\lambda = \varepsilon_\lambda C.L \qquad (10.1)$$

where : ε, absorptivity at the wavelength λ ($mol.L^{-1}\ cm^{-1}$),

C, concentration of dye ($mol.L^{-1}$),

L, pathlength (cm^{-1}).

The major kinetic pathway of dye degradation could be expressed by the differential rate equation:

$$-\frac{dC}{dt} = KC + k_T \qquad (10.2)$$

with : K, First order kinetic constant (min^{-1}),

k_T, zero order kinetic constant ($mol.L^{-1}.min^{-1}$),

C, concentration of dye ($mol.L^{-1}$).

However the photodegradation of dyes in aqueous solution were found to be controlled, and has small zero order kinetic constant. So the value of k_T in equation (10.2) can be neglected. Substitution of C value from equation (10.1) gives equation (10.3) :

$$-\frac{dA_\lambda}{dt} = K_{ab}A_\lambda \quad (10.3)$$

So, during the first minutes of photolysis, photo-degradation of the dyes is governed by a first order kinetic. Therefore, equation (10.3) is integrated with initial conditions $A=A_o$ for $t=0$ and leads to equation (10.4) :

$$\ln(\frac{A}{A_\circ}) = -K_{ab}t \quad (10.4)$$

According to Eq.(10.4), plot of $\ln(A/A_o)$ versus time must lead to straight lines. A good agreement of the experimental points around straight line confirms the validity of the proposed kinetic model.

Table 10.4 provides the values of the apparent kinetic constant, K, calculated during the first minutes of reaction, for all studied dyes. Direct examination of Table 10.4 shows that reactive dyes (Intracron families) are more rapidly degraded by VUV photolysis than direct (Optisal family)and acid (Nylanthrene) dyes. This observation is interesting as reactive dyes have been identified as problematic compounds in textile wastewater. Indeed, they are soluble and cannot be easily removed by conventional aerobic biological treatment systems (Thongchai et al., 1999).

Table 10.4 : Apparent kinetic constants of studied dyes

Dyes	K_{ab} (min) (1)	R^2
Nylanthrene Blue	0.063 ± 0.003	0.980
Nylanthrene Yellow	0.165 ± 0.006	0.987
Nylanthrene Red	0.139 ± 0.003	0.990
Intracron Red	0.613 ± 0.028	0.989
Intracron Black	1.06 ± 0.041	0.995
Intracron Yellow	0.679 ± 0.036	0.986
Optisal Red	0.321 ± 0.009	0.993
Optisal Blue	0.548 ± 0.032	0.980
Optisal Yellow	0.396 ± 0.026	0.975

(1) Values calculated for 95% confidence level

The discoloration of the studied dye solutions is governed by a first order kinetic. Kinetics rate constant (K_{ab}) depends on many factors, which can be articulated in as a simple equation[Feng et al., 1999]

$$K_{ab}= f\{pH, T, I, C_{dye}, C_{oxidantes}, I, DO, E(I_{irr}, \lambda)\} \qquad (10.5)$$

Where T represent the reaction temperature, I dyes ionic strength, DO represents dissolved oxygen on the solution, C is the concentration and E represents irradiation energy which depends on the intensity and the wavelength of the light.

Since the studied dyes molecular structure is not supplied, the relation between the dye maximal wavelength in the visible range and the discoloration constant rate was used to compare between dyes chemical structure and its photo- stability during photolysis. Indeed, for each dye molecule, the absorption in the visible range can be attribute to the extension of the chromophore conjugation and the nature of auxochromic substitutents connected to the chromophore. Figure 10.10 shows the apparent kinetic constants of dyes versus the absorption wavelength in the visible range.

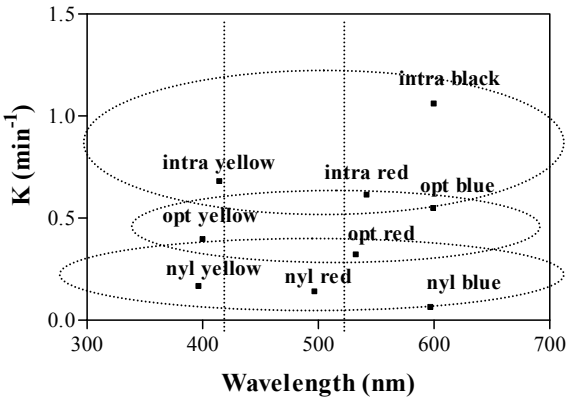

Figure 10.10 : Apparent kinetic constants vs. λ_{max} in the visible range.

As expected, there were a good relationship between color maximal absorbance wavelength and it is photo-degradability. The variability of kinetic constant increases as maximal absorption wavelength in the visible range is shifted towards blue light. In view of the fact that, all the studied dyes are of azo-dye family, for both blue and black ones. It can be assumed that conjugation in the dye molecule is important due to the presence of two or more azo bonds. It is interesting to note also that, the nature of auxochromic group and the ionic strength are an important factor which characterized photo-sensitivity of dye family. The reaction kinetic constant for the same dye family is in same order of magnitude. For example, Nylanthrene dyes

low reactivity could point to high ionic strength between dyes molecules, this can give an explanation to the low COD% and the small change in conductivity in the reaction solution. However, there were a lot of other factors that should not be forgotten. Galindo et al., 1999 reported during the study of azodyes oxidation that, the absence of any labile hydrogen atom in the molecule may also induces a low reactivity. This could be an explanation for Nylanthrene dyes lower reactivity.

In Eq.(10.5) the lamp irradiation energy has also effect on the photo-treatability of dyes. Low pressure mercury lamps used in dyes discolorations emits UV light with wavelength 253.7nm. This light transmitted to absorbed as photolysis photon intensity, work in transfer the dye molecule from fundamental to excited state, which may assume as photochemical initiation step. The transmitted photon intensity could be related to photon absorptivity of dye molecule at 254nm. Photon absorptivity can be estimated by measuring the absorbance value at 254nm weighted to dye mass. Figure 10.11 presents the dye kinetic constants as function of absorptivity at 254nm.

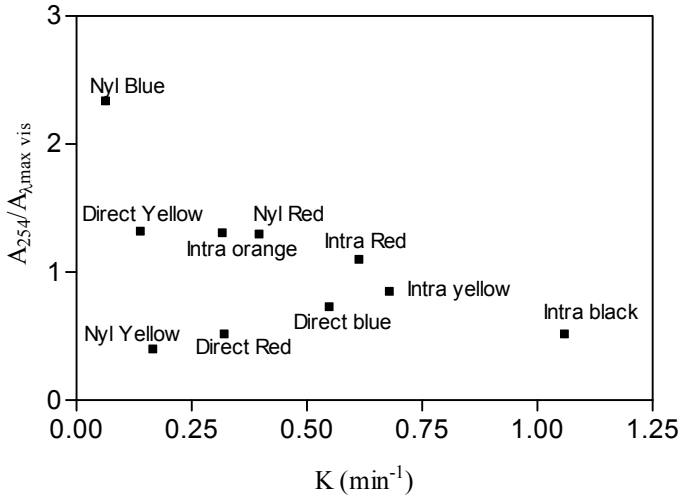

Figure 10.11 : Dye kinetic apparent constants versus specific absorbance at 254nm.

It can be figure out that, for Nylanthrene and Optisal dyes photo-reactivity are quite not affected by the dye absorptivity at 254nm. while, Intracron dyes involve variation in its reactivity as their absorptivity at 254nm change, the more absorptivity is the low is photo-reactivity. This imply that, Intracron reactive dyes show a high sensitivity towards UV light. Thongchai et al., 2000 remarks during the decolorization and treatment of reactive dyes that these days are not affected

by municipal biological treatment processes, based on the present results, UV photolysis can be advantageously utilized as a pretreatment step.

10.6. Industrial textile wastewater:

The same treatment has been applied to an industrial wastewater coming from textile industry that uses the same studied dyes for specific applications. Clearly, this wastewater can not be biodegraded according to its BOD_5/COD value equal to zero (see table 1) and inhibition test observations. Direct VUV photolysis was used efficiently for colour removal. Total discoloration is achieved for about 13 minutes of irradiation. At the same time, the COD conversion of the wastewater was 18 %. Concurrently, the ratio BOD_5/COD increased up to 0.22 (Figure 10.12). It is interesting to note that the BOD_5/COD with irradiation time follows a linear tendency. It can be explained by the fact that more biodegradable by products are generated during organic matter oxidation. The biodegradability has been enhanced up to the previous limit (BOD_5/COD>0.40) by further photo-degradation. The limit was reached after 28 minutes of irradiation and, during this time, 39% COD conversion is obtained. The difference between VUV and UV irradiation is about 25%. Previous study of industrial wastewater gives the same order of magnitude [Hitz et al., 1978]

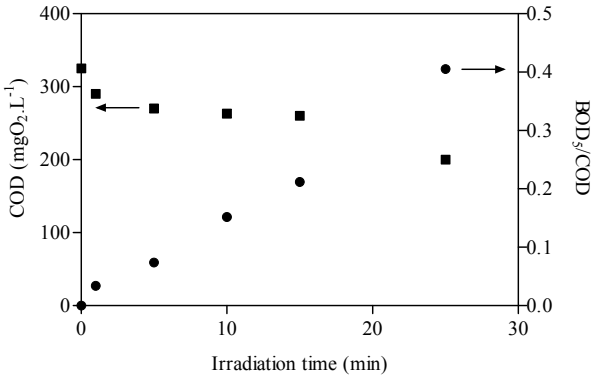

Figure 10.12: Evolution of BOD_5/COD and COD Vs irradiation time for textile industrial water

11. Conclusions.

The results obtained in the study have allowed to formulate the following conclusions**:**

I. The degradation rate and biodegradability improvement of DCP and POH were developed by going from simple photochemical oxidation processes (UV or UVA photolysis) to photo-catalytical oxidation (Photo-Fenton). Throughout that, the degradation rate was influenced by many factors such as: initial hydrogen peroxide concentrations, initial iron concentrations, pH, and temperature in addition to contaminants (DCP and POH) initial concentrations.

II. Involving all the studied photo-oxidation processes, photo-Fenton reaction shows a good precedence in DCP and POH elimination rate. at initial concentrations of 100mg.L^{-1}, total DCP removal was obtained in 40 min experimental time, and initial reactant concentrations of 50 mg.L^{-1} H_2O_2 and 10 mg.L^{-1} Fe(II), with 21 % TOC reduction. At the same time 82 % phenol total elimination was reached at 15 min, 210 mg.L^{-1} H_2O_2 and 10 mg.L^{-1} Fe(II).

III. The concentration evolution of both substances through degradation follows a first-order kinetics with respect to the pollutant concentration. First order kinetic constants were found to be improve by about 18 times higher for photo-Fenton than direct UV photolysis for both (POH and DCP). The corresponding first order kinetic constants at 82%POH 100 and% DCP removals were 0.11min^{-1} and 0.13 min^{-1} respectively.

IV. Higher initial iron concentrations showed negative effect in compound degradation, with clearer effect for DCP than POH and UV-light than UVA. This can be attributed to iron absorption coefficient at the studied wavelength.

V. Photo-Fenton process showed to be an efficient pre-treatment method to enhance the biodegradability of POH and DCP solutions. In the case of 100 mg.L^{-1} POH solutions, BOD_5/COD ratio was increased from 0 to 0.92, during 15 min and with initial conditions: 50 mg.$L^{-1}$$H_2O_2$, 75 mg.$L^{-1}$ Fe(II) and free pH evolution. For 100 mg.L^{-1} DCP aqueous solutions, BOD_5/COD ratio were improved from 0.0 to 0.18 by photo-oxidation based on UV-light, and 0 to 0.19 by UVA. This was achieved with low Fe(II) initial concentration 10 mg.L^{-1} and 50 mg.L^{-1} H_2O_2 in UV case and 75 mg.L^{-1} H_2O_2 in UVA case. Moreover, further by additional oxidation DCP solution biodegradability (BOD_5/COD) can be improved up to 0.48.

VI. Photo-Fenton process increases the biodegradability of 1000 mg.L^{-1} phenol solution. Maximum biodegradability of 0.92 was reached under the studied conditions. Both hydrogen peroxide and Fe (II) have been shown a good effect on the biodegradability enhancement.

VII. Good relation between biodegradability and organic matter oxidation sate was established. Better biodegradability was found to occur when a significant change in the contained organic matter oxidation increased.

VIII. For both compounds (DCP and POH) with initial concentrations of 100 $mg.L^{-1}$, total mineralization can be achieved with following conditions: initial Fe (II) concentration of 40, 60 $mg.L^{-1}$, hydrogen peroxide concentration of 270 and 750 $mg.L^{-1}$ for DCP and POH respectively. The amounts of hydrogen peroxide used is less than the stoichiometric amount by 62% and 40% respectively. The effect can be due to hydroxyl radical production from UV light and iron photo-redox process.

IX. Chlorobenzoquinone and hydroquinone have been identified as preliminary intermediates generated in DCP treated solutions in different process. Moreover, oxalic acid and glotamic acid were detected as final by-products.

X. POH and its pre-treated solutions were biologically oxidized in two batch stirred tank reactors, one containing phenol (100 $mg.L^{-1}$) and activated sludge and the second containing activated sludge with POH pre-treated solution. Better efficiency for organic matter removals were obtained by reactor feed with POH pre-treated solution. A maximum TOC removal of 95 % during cycle duration of 55hour was obtained in coupled process, while it was required 130 hours to obtain 80 % removal in single biological process.

XI. Also DCP pre-treated solutions were biologically oxidized in two semi-continuous stirred tank reactors, one with biomass acclimated previously to phenol and the second containing non-acclimated activated sludge. Slightly better TOC removals were obtained by acclimated reactor. A maximum TOC removal between 81.4 and 89 % was obtained by co-digesting pre-treated solution (70%V/V) with municipal wastewater (20% V/V) and 2 days HRT. Moreover, TOC removal of approximately 57 % was achieved in both reactors when feeding 100% pre-treated solution, and 12 HRT.

XII. Full biological chemical coupled process was established by combine photo-Fenton and sequencing batch biological reactors, DCP photo-treated solutions were bio-oxidized in Aerobic and anaerobic reactors. The effect of pre-treated solution biodegradability as well as cycle duration on bioreactor performance were followed. Manipulating both parameters allow to achieve organic substrate removal up to 82% within short cycle duration (8 to 6 h). at this points, reaction rate of order 9 $mgTOC.(L.h)^{-1}$ and specific elimination rate of 30 $mgTOC.(L.h.\ g\ TVSS)^{-1}$ was obtained.

XIII. Operating costs for the treatment of DCP by means of combined processes (photo-Fenton and SBR) and total mineralization via photo-Fenton were compared. Under the same mineralization efficiency, combined processes show lower costs than photo-Fenton processes. Despite that the biological part was operated at large cycle duration (8 days). using the combined process can save at least 70 €.kg^{-1} TOC treated.

XIV. By using VUV photolysis More than 90% colour removal of most dyes solutions were achieved after a round 7.5 min treatment. During the same time, 30% in average of COD is eliminated. Moreover, it was found that the BOD_5 of the dye solution increases after photolysis. This indicates that the biodegradability of textile dyes can be enhanced after only few minutes of treatment. The BOD_5/COD of dyes was increased up to the value for which organic matter is consider readily biodegradable (BOD_5/COD>0.40) when colour disappeared totally.

XV. Textile dyes -decolouration follows a first order kinetic. Results showed that that each dyes family has it's own behaviour. Reactive dyes are the most sensitive to UV irradiation. Kinetic constants are found to be (0.06–0.17, 0.3–0.55 and 0.61–1.1min^{-1}), for Nylanthrene, Optisal, and Intracron families, respectively.

Recommendations

- As photo-Fenton process has shown to be very effective in degradation of both DCP and POH, it is interesting to carry out this process in a more practical way. This can be achieved by:
    - ⊕ To study the possibility of replacing the artificial light sources with solar irradiation.
    - ⊕ To establish the strategy for iron recirculation which support positively the use of photo-oxidation processes.
    - ⊕ To identify the contaminants intermediates to establish a possible mechanism of reaction and to obtain more biodegradability enhancement.
- Regarding coupled processes (AOPs and biological treatment):
    - ➢ It is interesting to examine the effect of other operating conditions (pH, temperature, hydrogen peroxide, iron concentration and feed characteristics) in reactor performance.
    - ➢ To improve bioreactor configuration.
    - ➢ To operate the coupled processes in continues operation.

Nomenclature

BOD_n	n-days chemical oxygen demand [$mgO_2.L^{-1}$]
CBOD	Carbonaceous biological oxygen demand [mg $O_2.L^{-1}$]
COD%	Chemical oxygen demand removal percentage %
COD_f	Final chemical oxygen demand [mg O_2L^{-1}]
COD_i	Initial chemical oxygen demand [mg $O_2.L^{-1}$]
D_b	BOD_5 measured for the blank
D_s	BOD_5 measured for the sample
K	Monod first order kinetic constant [L g VSS h^{-1}]
K_{ab}	Dyes first order kinetic constant [h^{-1}]
K_d	Biomass death phase kinetic constant [h^{-1}]
K_o	First order kinetic constant [h^{-1}]
K_{ob}	Biological first order kinetic constant [L. $gTVSS^{-1}h^{-1}$]
k_s	Half velocity constant, substrate concentration at one-half the maximum growth rate, [$g.L^{-1}$]
K_S	The Monod saturation constant [mg COD L^{-1}]
K_{TOC}	First order mineralization constant [h^{-1}]
L	The BOD remaining at time zero(the total or ultimate first-stage BOD)
N	Multiplication factor
NBOD	Nitrogenous biological oxygen demand mg $O_2.L^{-1}$
O_3	Ozone
q_λ	Modulus radiation flux density factor
q_{max}	The maximum specific decomposition rate of substrate [mg COD g $VSS^{-1}h^{-1}$]
r_d	Endogenous decay coefficient [h^{-1}]
r_g	Rate of bacterial growth, [$g.(L.h)^{-1}$]
r_{su}	Substrate utilization rate, [$g.(L.h)^{-1}$]
r_g	Rate of bacterial growth, [$g.(L.h)^{-1}$]
μ	Specific biomass growth rate [h^{-1}]
R_R	Intensive reaction rate of oxalic acid
S	The biodegradable substrate concentration [mg COD L^{-1}]
t	Time (h)

TOC%	Total organic carbon removal percentage %
TOC_f	Final total organic carbon [$mgC.L^{-1}$]
TOC_i	Initial total organic carbon [$mgC.L^{-1}$]
V	Volume of the reaction (L)
$W_{abs, \lambda}$	Photon absorbed at wavelength λ
X	Biomass concentration [g VSS. L^{-1}]
Y	Maximum yield coefficient, mg/mg (defined as the ratio of the mass of cell formed to the mass of substrate consumed, measured during any Finite period of logarithmic growth)
$Y_{X/S}$	Cellular yield coefficient [g VSS g COD^{-1}]
φ	Quantum yield
λ	Wavelength (nm)
μ_m	Maximum specific growth rate, h^{-1}

ABE K. and TANAKA K. (1997) "Fe^{3+} and UV-enhanced ozonation of chlorophenolic compounds in aqueous medium", *Chemosphere*, **35,** (12), 2747-2752.

ABE K. and TANAKA K. (1999) "Effect of Fe^{3+} on UV-illuminated ozonation of nitrophenolic compounds", *Chemosphere*, **38,** (12), 2837-2847.

ADAMS C.D., COZZENS R.A. and KIM B.J. (1997) "Effects of ozonation on the biodegradability of substituted phenols", *Wat. Res.,* **31,** (10), 2655-2663.

ADAMS C.D., SCANLAN P. A. and SECRIST N.S. (1994) "Oxidation and biodegradablity enhancement of 1,4-dioxane using hydrogen peroxide and ozone", *Environ.Sci.& Technol.,* **28**, 1812-1818

ADAMS C. E and ECKENFELDER W.W. (1974) " Process Design Techniques for Industrial Waste Treatment", *Enviro*., Nashville

AHLBORG U.B. and THUNBERG T.M. (1980) "Chlorinated phenols: occurrence, toxicity, metabolism and environmental impact", *CRC Crit. Rev. Toxicol*., **7**, 1-35.

ALNAIZY R. and AKGERMAN A. (2000) "Advanced oxidation of phenolic compounds**",** *Advances in Environmental Research,* **4**, (3), 233-244

ANDREOZZI R., CAPRIO V., INSOLA A. and MAROTTA, R. (1999)"Advanced oxidation processes (AOP) for water purification and recovery", *Catalysis Today***, 53**, 51-59.

ARORA M. L., BARTH E. F. and UMPHRES M. B. (1985) " Technology evolution of sequencing batch reactors", *WPCF*, **57**, (8).

ATKISON B., DAVIES J. and YU S (1974)" How : the overall rate of substrate uptake by microbial films part I and II", *Trans. Inst. Chem. Eng.*

ATSDR (1999), www.atsdr.cdc.gov/toxfaq.html.

AYRANCI E. and BRIAN E.C. (2001) "Removal of phenol, phenoxide and chlorophenols from wastewaters by adsorption and electrosorption at high-area carbon felt electrodes", *Journal of Electroanalytical Chemistry*, **513**, (2), 100-110

BALZANI V. C. and CARASSITI V. (1970)" Photochemistry of coordination compounds", *acadimic:New York,* 172-174

BARAZA J. and ESPLUGAS S. (2000)"Oxidación avanzada en el tratamiento de agua residuales", *Tecnología del Agua*, **(197)**, 82-92

BARBINI M., MINERO C. and PELEZZITTI E., 1987, *Chemosphere*, 16, 2225-2237

BAUM G. and OPPENLAENDER T. (1995) "Vacuum-UV-oxidation of chloroorganic compounds in an excimer flow through photoreactor", *Chemosphere*, **30,** (9), 1781-1790.

BEBEFIELD L.D. and RANDALL C.W (1980) " Biological process design for wastewater treatment", *Prentice-Hall, Englewood Cliffs*, NJ

BELTRÁN F.J., GONZALEZ M. and ALVAREZ P. (1997a) "Tratamiento de agua mediante oxidación avanzada (I): Procesos con ozono, radiación ultravioleta y combinación ozono / radiación ultravioleta", *Ingeniería Química*, 331, 161-168.

BELTRÁN F.J., ENCINAR J.M. and ALONSO M. (1998a) "Nitroaromatic hydrocarbon ozonation in water. 1. Single ozonation", *Ind. Eng. Chem. Res.*, **37**, 25-31.

BELTRÁN F.J., ENCINAR J.M. and ALONSO M. (1998b) "Nitroaromatic hydrocarbon ozonation in water. 2. Combined ozonation with hydrogen peroxide or UV radiation", *Ind. Eng. Chem. Res.*, **37**, 32-40.

BELTRÁN F.J., GONZÁLEZ M. and ÁLVAREZ P. (1997a) "Tratamiento de aguas mediante oxidación avanzada (I): Procesos con ozono, radiación ultravioleta y combinación ozono/radiación ultravioleta", *Ingeniería Química*, **331**, 161-168.

BELTRÁN F.J., GONZÁLEZ M. and ÁLVAREZ P. (1997b) "Tratamiento de aguas mediante oxidación avanzada (II): Procesos con peróxido de hidrógeno", *Ingeniería Química*, **332**, 165-169.

BELTRAN J. H., TORREGROSA J., DOMÍNGUEZ J. R. and GRACIA J. (2000)"Treatment of black-olive wastewater by ozonation and aerobic biological degradation", *Wat. Res*., **34,** (14), 3515-3522

BENÍTEZ F.J., BELTRÁN-HEREDIA J., ACERO J.L. and RUBIO F.J. (2000b) "Contribution of free radicals to chlorophenols decomposition by several advanced oxidation processes", *Chemosphere*, **41,** (8), 1271-1277.

BEYDILLI M.I., PAVLOSTAHIS S. G. and TINCHER W.C. (1998), "Decolorization and toxicity screening of selected reactive azo dyes under methanogenic conditions ", *Water Sci. and Technol.*, **38, (** 4-5), 225-232.

BIGDA R.J. (1995) "Consider fenton's Chemistry for Wastewater Treatment", *Chem. Eng. Progr*., **12**, 62-66

BOSSMANN S.H., OLIVEROS E., GOB S., SIEGWART S., DAHLEN E.P., PAYAWAN L., STRAUB M., WOORNER M. and BRAUN A.M. (1998) "New evidence against hydroxyl radicals as reactive intermediates in the thermal and photochemically enhanced Fenton reactions", *.J.Phys.Chem.,* **102**, 5542 –5550.

BRILLAS E., CALPE J.C. and CASADO J. (2000) "Mineralization of 2,4-D by advanced electrochemical oxidation processes", *Wat. Res*., **34,** (8), 2253-2262.

BRILLAS E., MUR E., SAULEDA R., SÁNCHEZ L., PERAL J., DOMÉNECH X. and CASADO J. (1998a) "Aniline mineralization by AOPs: anodic oxidation, photocatalysis, electro-Fenton and photoelectro-Fenton processes", *Appl. Catal. B: Environ*., **16**, 31-42.

CROSB R. M. and BENDER J. H. (1980) "Hydraulic consideration that affect clarifier performance", *EPA Technology Transfer*, **march.**

BRILLAS E., SAULEDA R. and CASADO J. (1998b) "Degradation of 4-chlorophenol by anodic oxidation, electro-Fenton, photoelectro-Fenton and peroxicoagulation processes", *J. Electrochem. Soc.*, **145,** (3), 759-765.

BUITRÓN G., SOTO G., VITE G. and MORENO J. (2001). "Strategies to enhance the biodegradation of toxic compounds using discontinuous processes", *Wat. Sci.& Technol*., **43,** (3), 283-290.

CERVERA S. and ESPLUGAS S. (1983) " Obtención de hidrógeno mediante fotólisis del agua", *Energía*, **9**, 103-107.

CHAMARRO E., MARCO A. and ESPLUGAS S. (2001) "Use of Fenton reagent to improve organic chemical biodegradability", *Wat. Res*., **35,** (4), 1047-1051

CHAMARRO E., MARCO A., PRADO J. and ESPLUGAS S. (1996) "Tratamiento de aguas y aguas residuales mediante utilización de procesos de oxidación avanzada", *Química & Industria*, *½*, *Sociedad Chilena de Química*, **1**, 28-32.

CHEN F., WU S., CHEN J. and RONG S. (2001) "COD removal efficiencies of some aromatic compounds in supercritical water oxidation", *Chinese Journal of Chemical Engineering*, **9,** (2), 137-140.

CHEN R. and PIGNATELLO J.J. (1997) "Role of quinone intermediates as electron shuttles in Fenton and photoassisted Fenton oxidation or aromatic compounds", *Environ. Sci.& Technol.*, **31,** (8), 2399-2406.

DE LAAT J. and GALLARD H. (1999) "Catalytic decomposition of hydrogen peroxide by Fe(III) in homogeneous aqueous solution: mechanism and kinetic modelling", *Environ. Sci .& Technol.,* **33**, 2726 –2732.

DIRECTIVE 2000/60/EC of the Euripean Parliament and of the Council of 23 October 2000 establishing a framework for Community action in the field of water policy (L 327 of 22.12.2000)

DUGUET J.P., DUSSERT B., MALLEVIALLE J. and FIESSINGER F. (1987) "Polymerization effects of ozone: applications to the removal of phenolic compounds from industrial wastewaters", *Water Sci.& Technol.*, **19**, 919-930.

ECKENFELDER W.W. (1963) " Biological phosphorus removal: state of Art review", *pollution engineering* , pp 88

EISENHUAR H. R. (1964) *J. Water Poll Contr. Fed*. **36**,1116-1128, EPA site, www.scorecard.org , visited on April, 2003.

ESPLUGAS S. and VICENTE M. (1983) "Calibrado del fotorreactor anular", *Afinidad*, **40**, 453-457.

ESPLUGAS S., GIMÉNEZ J., CONTRERAS S., PASCUAL E. and RODRÍGUEZ M. (2002) Comparison of different advanced oxidation processes for phenol degradation", *Water Research,* **36***,* (4), 1034-1042

ESPLUGAS S., YUE P.L. and PERVEZ M.I. (1994) "Degradation of 4-chlorophenol by photolytic Oxidation", *Wat. Res*., **28**, 1323-1328.

FAIR G. M., GEYER J.C., and OKUM D. A. (1966): "Water and Wastewater Engineering", vol. 2, Wily, New York

FAUST B.C. and HOIGNE J. (1990) " Photolysis Fe(III)-hydrixy complexes as sources of OH radicals in clouds, fog and rain", *Atoms Environ* , **22**, (5-6),79-89

FENG WU, NASHENG DENG and YUEGANG ZUO (1999),"Discolorarion of dye solutions induced by solar photolysis of ferrioxalate in aqueous solution", *Chemosphere,* **39**, (12), 2079-2085

FENTON H.J.H. (1884), "Oxidation of tartaric acid in presence of iron", *J. Chem. Soc*., **65,** 889-910.

GALINDO C., JACQUES P. and KALT A. (2001) "Photochemical and photocatalytic degradation of an indigoïd dye: a case study of acid blue 74", *J. Photochem. & Photobio.,* **141,** 47-56.

GALINDO C. and KALT A. (1999) "UV/H_2O_2 oxidation of azodyes in aqueous media : evidence of a structure – degradability relationship", *Dyes and Pigments*, **42,** 199-207

GHALY M. Y., HARTEL G., MAYER R. and HASENEDER R., (2001),"Photochemical oxidation of p-chlorophenol by UV/H2O2 and photo-Fenton process. A comparative study", *Wat. Management*, **21**, 41-47

GILBERT E. (1987) "Biodegradability of ozonation products as a function of COD and DOC elimination by example of substituted aromatic substances", *Wat. Res*., **21,** (10), 1273-1278.

GILBERT G. and ZINEDNER H. (1980) "Ozonation of aromatic amines in water", *Wat. Res.*, **25,** (7), 1563-1570.

GIMÉNEZ J., CURCO D. and QUERAL M.A. (1999) "Photocatalytic treatment of phenol and 2,4-dichlorophenol in a solar plant in the way to scaling-up", *Catalysis Today*, **45**, 229-243

GLAZE W.H., KANG. J.W. and CHAPIN D.H. (1987) "The chemistry of water treatment processes involving ozone, hydrogen peroxide and ultraviolet radiation", *Ozone Sci. & Eng.*, **9,** (4), 335-342.

GRADY C.P.L. JR. and LIM H.C. (1980) " Biological wastewater treatment: theory and application", Marcel Dekker, New York.

HA S.R., QISHAN L. and VINITNANTHARAT S. (2000) "COD removal of phenolic wastewater by biological activated carbon-sequencing batch reactor in the presence of 2,4-DCP", *Water Sci. & Technol*., **42,** (5-6), 171-178.

HA S.R., VINITNANTHARAT S. and ISHIBESHI Y. (2001) "A modelling approach to bioregeneration of granular activated carbon loaded with phenol and 2,4-dichlorophenol", *Journal of Environmental Science and Health, Part A: Toxic/Hazardous Substances & Environmental Engineering*, **A36,** (3), 275-292.

HAUTANIEMI M., KALLAS J., MUNTER R. and TRAPIDO M. (1998) "Modelling of chlorophenol treatment in aqueous solutions. 1. Ozonation and ozonation combined with UV radiation under acidic conditions", *Ozone Sci. & Eng.,* **20,** (4), 259-282.

HAYWARD K. (1999), "Drinking water contaminant hit-list for US EPA", *Water,* 21, September-October, 4.

HEIDT L.J. TREGAY G.W. and MIDDLETON F.A. (1979) "Influence of the pH upon the photolysis of the uranyl oxalate actinometer system", *J. Phys. Chem.*, **74**, 1876-1882.

HEINZLE E., STOCKINGER H., STERN M., FAHMY M. and KUT, O.M. (1995) "Combined biological-chemical (ozone) treatment of wastewaters containing chloroguaiacols", *J. Chem. Tech.& Biotechnol*., **62**, 241-252.

HERRERA F., PULGARIN C., NADTOCHENKO V. and J. KIWI (1998) "Accelerated photo-oxidation of concentrated *p*-coumaric acid in homogeneous solution. Mechanistic studies, intermediates and precursors formed in the dark**",** *Applied Catalysis B: Environmental,* **17***,*(1-2), 141-156

HIRVONEN A., TRAPIDO M., HENTUNEN J. and TAKHAREN J. (2000) "Formation of hydroxylated and dimeric intermediates during oxidation of chlorinated phenols in aqueous solution", *Chemosphere*, **41**, (8), 1211-1218.

HITZ H.R., HUBER W. and REED R.H. (1978) " The adsorption of dyes on activated sludge", *J Soc, Dyers Colorists*, **94**, 71-76

HOIGNÉ J. and BADER H. (1979), "Ozonation of water: selectivity and rate of oxidation of solutes", *Ozone Sci. & Eng*., **1** (1), 73-85.

HOIGNÉ J. and BADER H. (1983a) "Rate constants of reaction of ozone with organic and inorganic compounds in water. Part I. Non-Dissociating organic compounds" *Wat. Res.*, **17**, 173-183.

HOIGNÉ J. and BADER H. (1983b) "Rate constants of reaction of ozone with organic and inorganic compounds in water. Part II. Dissociating organic compounds", *Wat. Res.*, **17**, 185-194.

HOWARD P.H. (1989) "Handbook of environmental fate and exposure data for organic chemical. Volume I Large production and priority pollutants", Lewis Publishers, Chelsea, Michigan (USA)

HU CHUN and WANG YIZHONG (1999) " Decolorization and biodegradablity of photocatalytic treated azo dyes and wool textile wastewater", *Chemosphere*, **39**, (12), 2107-2115

HUANG C.P. and CHU C.S. (1992) "Electrochemical oxidation of phenolic compounds from dilute aqueous solutions", *Chem. Oxid. Proc. Int. Symp. 1st*, 239-253.

KANG J-W., HUNG H-M. , LIN A. and HOFFMANN M.R.(1999)"Sonolytic destruction of methyl tert-butyl ether by ultrasonic irradiation: the role of O_3, H_2O_2, frequency and power density", *Environ. Sci .& Technol.*, **33**, 3199 –3205.

KANG S.F., LIAO C. H. and HUNG H.P. (1999) "Peroxideation treatment of dye manufacturing wastewater in the presence of ultraviolet light and ferrous ions", *J. Hazardous mat. B*, **65**, 317-333

KIM S.M., GEISSEN S. and VOGELPOHL, A., (1999)," Landfill leachate treatment by a photoassistid fenton reaction", *Wat. Sci. & Technol.*, **35**, 239-248

KLOPP R. and KOPPE P. (1990) " die quantitative charakterisierung von abwassern hinsichtlich ihrer despresivitat und abbaubarkeit" Vom Wasser. **75**, 307-329.

KU Y. and HSIEH C.B. (1992) "Photocatalytic decomposition of 2,4-dichlorophenol in aqueous TiO_2 suspensions", *Wat. Res*., **26**, (11), 1451-1456.

KU Y., SU W.J. and SHEN Y.S. (1996) "Decomposition of phenols in aqueous solution by a UV/O_3 process", *Ozone Sci. & Eng.*, **18**, (5), 443-460.

KUO W.S. (1999) "Synergistic effects of combination of photolysis and ozonation on destruction of chlorophenols in water", *Chemosphere*, **39,** (11), 1853-1860.

Kyu Cheol Namkung, Paul Sharratt, "Fenton and Photo-Fenton Processes for Treatment of Aqueous Wastes", www1.york.ac.uk/res/gcrn/OXNamkung.ppt. visited at 20/04/2003.

LA GREGA M.D., BUCKINGHAM P.L. and EVANS J.C.(1994) "Hazardous Waste Management", McGraw-Hill, New York, NY.

LEDAKOWICZ S. (1998) "Integrated processes of chemical and biological oxidation of wastewaters", *Environment Protection Engineering*, **24,** (1-2), 35-47.

LEDAKOWICZ S. and GONERA M. (1999) "Optimisation of oxidant dose for combined chemical and biological treatment of textile wastewater", *Wat. Res.*, **33,** (11), 2511-2516.

LEE D.S., GLOYNE E.F. and LI L. (1990) "Efficiency of hydrogen peroxide and oxygen in supercritical water oxidation of 2,4-dichlorophenol and acetic acid", *J. of Supercritical Fluids*, **3**, (4), 249-255.

LEE G., NUNOURA T., MATSUMURA Y. and YAMAMOTO K.(2002) " Comparison of the effects of the addition of NaOH on the decomposition of 2-chlorophenol and phenol in supercritical water and under supercritical water oxidation conditions", *Journal of Supercritical Fluids*, **24**, (3), 239-250

LEGRINI O., OLIVEROS E. and BRAUN A.M. (1983) "Photochemical processes for water treatment", *Chem. Rev.*, **93**, 671-698.

LEVINE A. D., TCHOBANOGLOUS G. and ASANO T. (1985)" Characterization of the size distribution of contaminants in wastewater: treatment and reuse implications" *J. of WPCF*, 57

LI L., CRAIN N., KANTHASAMY A., MATTHEWS C.P., ROLLANS S.W. and GLOYNE E.F. (1994) "Supercritical water oxidation model development for selected EPA priority pollutants", *Proc. Annual Meeting - Air & Waste Management Association 87th*, **13**, 94.

LI L., PEISHI C. and EARNEST F.G. (1991) "Generalized kinetic model for wet oxidation of organic compounds", *AIChE J.*, **37**, (11), 1687-1697.

LIAO C. H. and GUROL M.D. (1995), *Environ. Sci. & Technol.*, **29** (12), 3007

LIN K.S., WANG H.P. and LI M.C. (1998) "Oxidation of 2,4-dichlorophenol in supercritical water", *Chemosphere*, **36**, (9), 2075-2083.

LIPCZYNSKA-KOCHANY E. (1991) "Degradation of aqueous nitrophenols and nitrobenzene by means of the Fenton reaction", *Chemosphere*, **22**, (5-6), 529-536.

Lopez R., Espinoza A. and Litter M. (2002) " Photodegradation of an azo dye of textile industry", *Chemosphere*, **48,** 393-399.

LUNAK S. and SEDLEK P. (1992) "Photoinitiated reactions of hydrogen peroxide in the liquid phase", *J. Photochem. &Photobio. A: Chemistry,* **68***,* (1)*,* 1-33

MALATO S., BLANCO J., FERNÁNDEZ-IBÁÑEZ P. and CÁCERES J. (2001) "Treatment of 2,4-dicholorophenol by solar photocatalysis: comparison of coupled photocatalytic-active carbon vs. active carbon", *Journal of Solar Energy Engineering*, **123**, (2), 138-142.

MAMAIS D., JENKINS D. and PITT P. (193) " A rapid physical-chemical method for the determintion of readily biodegradable soluble COD in municipal wastewater" Wat. Res., **27**, (1), 195-197.

MALETZKY P. and BAUER R. (1998) "The photo-Fenton method – Degradation of nitrogen containing organic compounds", *Chemosphere*, **24**, (9), 1369-1380**.**

MARA D.D (1974) " Bacteriology for sanitary engineers" *Churchill Livingston*, Edinburgh.

MARCO A., ESPLUGAS S. and SAUM G., (1997) "How and why combine chemical and biological processes for wastewater treatment" *Wat. Sci. Technol.,* **35**, (4), 321-327

MARK H.F., OTHMER D.F., OVERBERGER C.G. and SEABURG G.T. (1992) "Kirk-Othmer Encyclopedia of Chemical Technology", 4ª ed., Wiley-Interscience Publication, New York (USA).

MATHEWS W. R., PELIZZETTI E. and SHIAVELLO M. (1991) "In photochemical conversion and storage of Energy, Eds.; Kluwer: Dochecht, the Netherlands, pp427-449.

MATTHEWS R.W. (1990) "Purification of water with near-UV illuminated suspensions of titanium dioxide", *Wat. Res*., **24**, (5), 653-660.

MAZELLIER P., SARAKHA M. and BOLTE M. (1999),"primary mechanism for the iron (III) photoinduced degradation of 4-Chlorophenol in aqueous solution", *New J. Chem.,* **23**, (2), 133-135

MAZELLIER R., MAILHOT G. and BOLTE M. (1997) "Photochemical behaviour of the Iron(III)/2,6-dimethylphenol system", *New J. Chem.*, **21**, (3), 389-397.

METCALF and EDDY, INC (1995) "Wastewater engineering: treatment, disposal and reuse (Spanish version)", 3rd ed., McGraw-Hill, New York, USA.

METCALF and EDDY, INC (1979) "Wastewater Engineering :Treatment, disposal. Reuse", 2nd ed., McGraw-Hill, New York

METCALF and EDDY, INC (1981) "Wastewater Engineering : Collection and Pumping of Wastewater", McGraw-Hill, New York

MOKRINI A., OUSSI D. and ESPLUGAS S. (1997) "Oxidation of aromatic compounds with UV radiation/ozone/hydrogen peroxide", *Wat. Sci.& Technol.*, **35**, 95-102.

MONOD J. (1949) "The growth of bacteria cultures", *Annu. Rev.Mircobial*, **79**, 390,

MOORE E. W., THOMAS H.A. and SNOW W.B (1950) "Simplified method for analysis of BOD data", *Sewage ind. Wastes,* 22, (3), 487-506.

MUNTER R., PREIS S., KALLAS J., TRAPIDO M. and VERESSININA Y. (2001) "Advanced oxidation processes (AOPs): Water treatment technology for the twenty-first century", *Kemia-Kemi*, **28**, (5), 354-362.

MURPHY A.P., BOEGLI W.J., PRICE M.K. and MOODY C.D. (1989) "A Fenton-like reaction to neutralize formaldehyde waste solutions", *Environ. Sci. & Technol.,* **23**, 166 –169.

NESHEIWAT F.K. and SWANSON A.G. (2000) "Clean Contaminated Sites Using Fenton's Reagent", *Chem. Eng. Prog.*, **96, (**4), 61-66.

OGATA M., YAMASAKI Y. and KAWAI T. (1986) "Significance of urinary phenyl sulfate and phenyl glucuronide as indices of exposure to phenol", *International Archives of Occupational and Environmental Health*, 58, (3), 197-202.

OHTSUJI H., and IKEDA M. (1972) "Quantitative relation between atmospheric phenol vapor and vapor in the urine of workers in Bakelite factories", *J Ind. Med.,* 29, 70-73.

OPPENLÄNDER T. and GLIESE S. (2000) "Mineralization of organic micropollutants (homologous alcohols and phenols) in water by vacuum-UV-oxidation (H_2O-VUV) with an incoherent xenon-excimer lamp at 172 nm", *Chemosphere,* **40**, (1), 15-21.

OPPT Chemical Fact Sheets (1995), www.epa.gov/chemfact. Visited march 2003

ORMAD M.P., OVELLEIRO J.L. and KIWI J. (2001)," Photocatalytic degradation of concentrated solution of 2,4-dichlorophenol using low energy light Identification of intermediates", *Applied catalysis B: Environmental*, 32,157-166

OUSSI D., ASMAE M. and ESPLUGAS S., (1997), " Removal of aromatic comounds using UV/H_2O_2", *Recent Res. Devel. In Photochem & Photobiol*, **1**, 77-83

PAILLARD H., BRUNET R. and DORÉ M. (1988) " Conditions optimals d'application du systeme oxydant ozone-peroxide d'hydrogene", *Wat. Res.*, 22, 91-103.

PALAU R. (1999) "Contribución al estudio de la eliminación de contaminantes acuosos mediante reacción electroquímica –degradación del herbicida NCPA" Master in chemistry, Dpt. of Chemical Engineering and Metallurgy, University of Barcelona

PHILIPPE C.V., ROBERTO B. and WILLY V. (1998) "Treatment and reuse of wastewater from the textile wet-processing industry: review of emerging technologies", *J Chem. Technol. Biotechnol*, **72**, 289-302

PIGNATELLO J.J. (1992) "Dark and photoassisted ion (3+)-catalyzed degradation of chlorophenoxy herbicides by hydrogen peroxide", *Environ. Sci.& Technol.*, **26**, (5), 944-951.

PORTER J.J. (1973) "A study of the photodegradation of commercial dyes", *EPA Report-R2*-73-058.Washington.DC.

QIU Y., KUO C-H. and ZAPPI M.E. (2002) "Ozonation kinetics of six dichlorophenol isomers", *Ozone Sci. & Eng.*, **24**, (2), 123-131.

RODGERS J.D., JEDRAL W. and BUNCE N.J. (1999) "Electrochemical oxidation of chlorinated phenols", *Environ. Sci.& Technol.*, **33**, (9), 1453-1457.

RODRÍGUEZ M., BEN ABDERRAZIK N., CONTRERAS S., CHAMARRO E., GIMENEZ J. and ESPLUGAS S. (2002) "Iron(III) photoxidation of organic compounds in aqueous solutions**",** *Applied Catalysis B: Environmental,* **37**, (2), 131-137

RODRÍGUEZ M., KIRCHNER A., CONTRERAS S. CHAMARRO E. and ESPLUGAS S. (2000) "Influence of H_2O_2 and Fe(III) in the photodegradation of nitrobenzene", *J. Photochem. Photobiol. A: Chemistry*, 133, 123-127.

RODRÍGUEZ M., TIMOKHIN V., CONTRERAS S., CHAMARRO E. and ESPLUGAS S. (2002b) "Rate equation for the degradation of nitrobenzene by Fenton-like reagent", *Adv. Environ. Res*. **7**, 583-595.

RUPPERT G., BAUER R. and HEISLER G. (1994) "UV-O_3, UV-H_2O_2, UV-TiO_2 and the photo-Fenton reaction. Comparison of advanced oxidation processes for waste water treatment", *Chemosphere*, **28**, (8), 1447-1454.

RUPPERT G., BAUER R. and HEISLER G. (1993) "The photo-Fenton reaction — an effective photochemical wastewater treatment process", *Journal of Photochem. & Photobio. A: Chemistry,* **73**, (1), 75-78.

SACHER F., KARRENBROCK F., KNEPPER T and LINDNER K. (2001) "Adsorption studies of organic compounds for the assessment of their relevancies for drinking water production", *Vom Wasser*, **96**, 173-191.

SAFARZADEH-AMIRI A. BOLTON J.R. and CATER, S.R. (1996a) "The use of iron in Advanced Oxidation Processes", *J. Adv. Oxid. Technol.*, **1**, (1), 18-26.

SAFARZADEH-AMIRI A., BOLTON J.R. and CATER S.R. (1996b) "Ferrioxalate-mediated solar degradation of organic contaminants in water", *Solar Energy*, **56**, (5), 439-443.

SAKURIA H., SHIOTANI M. and ICHIKAWA T., (1999) "Hydrogen molecule detachment in irradiated 1,2-dimethyl cyclohexane: stereo-selective, reaction*", Radiat. Phys Chem*., **54**, (3), 235-240.

SAULEDA R. and BRILLAS E. (2001) "Mineralization of aniline and 4-chlorophenol in acidic solution by ozonation catalyzed with Fe^{2+} and UVA light", *Applied Catalysis B:Environmental,* **29**, (2), 135-145.

SCOTT D.B.M. and LESHER E.C. (1963) "Effect of ozone on survival and permeability of *Escherichia coli*", *Journal of Bacteriology*, **85**, 567-576.

SCOTT G.P. (1997) "Design, characterization and performance of a bench-scale continuous wet oxidation system", *Chem. Oxidation. Technol. Nineties*, **6**, 156-186.

SCOTT J. and OLLIS D.F. (1997), "Integration of Chemical and Biological Oxidation Processes for Water Treatment: II. Recent Illustrations and Experiences", *J. Adv. Oxidation Technology*, **2**, 374-381.

SCOTT J.P and OLLIS, D.F.(1996)"Engineering model of combined chemical and biological processes", *J. Enviromental Engineering*, **122**,1110-1114

SCOTT J.P. and OLLIS D.F. (1995) "Integration of chemical and biological oxidation processes for water treatment: review and recommendations", *Environ. Prog*., **14**, (2), 88-103

SCRUDATO R.J and CHIARENZELLI J.R. (1996) "Electrochemical Preoxidation of PCBs and VOCs in Suspended Site Water and Sedmints" presented at the pacific Basin Conference in Hazardous Waste, Kuala Lumpar, Sponsored by Pacific Basin Consortium for Hazardous Waste Research and Management.

SIENLIEWICZ A., FERRIERA A.M.D., DANNER B. and SCHOLES C.P., (1999), "Electron-spin-resonance center of dangling bonds in undoped a Si:H", *J. Electrochem. Soc.*, **136**, (2),137-142.

STAEHELIN S. and HOIGNÉ, J. (1982) "Decomposition of ozone in water: Rate of initiation by hydroxide ions and hydrogen peroxide", *Environ. Sci. & Technol.*, **16**, 676-681.

STANDARD METHODS (1985) for the examination of water and wastewater, *American Public Health Association*.

STEFAN M.I., HOY A.R. and BOLTON J.R.(1996) "Kinetics and mechanism of the degradation and mineralization of acetone in dilute aqueous solution sensitized by the UV photolysis of hydrogen peroxide", *Environ.Sci. & Technol.,***30**,2382 –2390.

STUMM W. and MORGAN J.J. (1991) "Aquatic chemistry", 2nd edition, Wiley, New York.

STREETER H. W. and PHELPS E. B. (1925) "A study of the pollution and narural purification of the Ohio river", *public Health Bulletin*, **146,** Us public Health Service, Washington DC.

TACHIEV (1998) "Hydrogen peroxide Oxidation of Phnol Catalyzed by Iron Ions," *Chemical Oxidation Symposium*

TAKAHASHI N., NAKAI T., SATOH Y. and KATOH Y. (1994) "Variation of biodegradability of nitrogenous organic compounds by ozonation", *Wat. Res.*, **28**, (7), 1563-1570.

THONGCHAI P. and WORRAWIT L. (2000) "Decolorization of reactive dyes with different molecular structures under different environmental conditions", *Wat. Res.*, **34**, (17), 4177-4184.

THOMAS R. G. (1982) " Volatilization from water", *Handbook of Chemical Property Estimation Methods*, McGraw-Hill, New York.

TRAPIDO M., HIRVONEN A., VERESSINA Y., HENTUNEN J. and MUNTER R. (1997) "Ozonation, Ozone/UV and UV/H_2O_2 degradation of chlorophenols", *Ozone Sci. & Eng.*, **19**, (1), 75-96.

ULLMANN S. (1991) "Encyclopedia of Industrial Chemistry", 5ª ed., 415-419, VCH Verlagsgesellschaft (Germany).

UTSET B., GRACIA J., CASADO J., DOMÉNECH X. and PERAL J., (2000) "Replacement of H_2O_2 by O_2 in Fenton and Photo-Fenton reactions", *Chemosphere*, **41**, 1187-1192

VAN U.N. (1967)" Transport-limited Growth in the Chemostat an its Competitive Inhibition; A Theoritical Treatment" *Arch.Mikrobial.,* vol 58

WALLING C. (1975) "Fenton's reagent revisited", *Acc. Chem. Res*., **8**, 125-131.

WATTS R.J., UDELL M.D. and MONSEN R.M. (1993) "UV/H2O2 and photo-Fenton process. A comparative study" *Water Environ. Res*., **65**, 839-844

WILCOCK R.J. (1988) " Study of river reaeration at different flow rates " *J. Environ. Eng.,* **114**, (1).

YOO E.S. (2002)"Kinetics of chemical decolorization of the azo dye C.I. Reactive Orange 96 by sulfide" *Chemosphere*, **47**, 925-931

YU Y.H. and HU S.T. (1994) "Preoxidation of chlorophenolic wastewaters for their subsequent biological treatment", *Wat. Sci. & Technol*., **29**, 313-320.

ZEFF J.D. and BARICH J.T. (1990) "Symposium on Advanced Oxidation Processes and Treatment of Contaminated Water and Air: Wastewater Technologies", *Center, Ontario (Canadá).*

Publication derived from this work

- BEN ABDERRAZIK N., AL MOMANI F., SANS C. and ESPLUGAS S. (2001) "Combined advanced oxidation with biological treatment", *AFINIDAD,* **Tomo LIX**, (498), 141-151.

- AL-MOMANI F., TOURAUD E., DEGORCE-DUMAS J.R., ROUSSY J., and THOMAS O. (2002) "Biodegradability Enhancement of Textile Dyes and Textile Wastewater by VUV photolysis", *J. of Photochem. & Photobiology,* **153**,(1-3)*,* 191-197.

- BEN ABDERRAZIK N., AL MOMANI F., RODRIGUEZ M., AZMANI A., SANS C. and ESPLUGAS S. (2002) "Biodegradability Improvement by Photo Fenton Reaction", *Afinidad*, 59, 391-398.

- AL MOMANI F., SANS C., CONTRERAS S. and ESPLUGAS S. (2003) "Sequential Degradation of 2,4-dichlorophenol by Photo-assisted Fenton reaction and biological treatment", *Water Environmental research*, sent for publication.

- CONTRERAS S., RODRÍGUEZ M., AL MOMANI F., SANS C. AND ESPLUGAS S. (2003) "Contribution of the ozonation pre-treatment to the biodegradability of aqueous solution of 2,4-dichlorophenol, , *Wat. Res.,* in press

- AL MOMANI F., GONZALEZ O., SANS C., and ESPLUGAS S. (2003) "Combined Photo-Fenton with Biological Sequencing Batch Reactor for Degradation of 2,4-dichlorophenol", *sent for publication in Journal of water Sci. & Technol.*

- AL MOMANI F., GONZALEZ O., SANS C., and ESPLUGAS S. (2003) "UVA Photo-oxidation of 2,4-dichlorophenol. A comparative study", *Sent for publication in Journal of Hazardous material.*

- AL- MOMANI F., TOURAUD E., AND O. THOMAS (2003) "VUV Photolysis of commercial textile dyes: Kinetic study and UV sensitivity, *Sent for publication in Journal of dyes and pigments.*

Communications

- The 2nd European Workshop on Water, Air and Soil: Treatment by Advanced Oxidation Technologies, Poitiers, France, 28-02-2001 "Biodegradability improvement by Photo-Fenton Reaction".

- The 7th International Conference on Advanced oxidation technology for water and Air remediation, Niagara Falls, Ontario, Canada, 25-06-2001, "Impact of photo-Fenton reaction on biological treatment, effect on TOC removal and biodegradability".

- The 2nd European Meeting: solar-chemistry and photo catalysis: environmental Applications, Saint Avold, France, 2002, "Sequential photo-Fenton and biological oxidation, strategy for biodegradability improvement"

- The 5th IWA chemical industry group conference, France 13-15 November 2002, "UV and VUV photolysis, strategy for biodegradability improvement".

- The 5th IWA chemical industry group conference, France 13-15 November 2002, "Effect of photo-Fenton reaction on the biodegradability of 2,4-dichlorophenol".

- The 9th Mediterranean conference of chemical engineering, "Photochemical degradation of reactive dyes: colour removal and biodegradability improvement".

- The 9th Mediterranean conference of chemical engineering, "Biodegradability enhancement of 2,4-DCP using photo-Fenton"

- The 9th Mediterranean conference of chemical engineering, "Ozonation as a pre-treatment to improve the biodegradability of aqueous 2,4-DCP solution".

- the 9th Mediterranean conference of chemical engineering, "Homogeneous and heterogeneous photo-catalytic processes in the treatment of phenolic compounds"

A1.1 Actinometry

Before the starting in photo-oxidation experiments, it was necessary to determine the real flux of radiation enter the reactor. As it was discussed before, the actinometry system depends on the photochemical decomposition of oxalic acid in the presence of uranly nitrate (Esplugas et al, 1983). The mechanism of the reaction is complicated, many products seems to produce like CO, CO_2, CHOOH, U^{4+} and H_2O. For pH in the range of 3-7, and oxalic acid conversion is less than 20%, the reaction that takes place is:

$$UO_2^{2+} + H_2C_2O_4 \rightarrow UO_2^{2+} + CO_2 + CO + H_2O \quad \text{(A1.1)}$$

Mathematical treatment:

The intensive reaction rate is defined by:

$$r_R = -\sum_{\lambda} \Phi_{\lambda}.\mu_{\lambda}.I_{\lambda} = -\sum_{\lambda} \Phi_{\lambda}\mu_{\lambda}\, q_{\lambda} \quad \text{(A1.2)}$$

Where;

Φ is quantum yield

μ_{λ} is uranly absorption for each wavelength I_{λ}, q_{λ} the modulus of the radiation flux density vector at wavelength λ .

As the uranly is not consumed during the reaction, the absorbance remains constant, and the kinetic is zero order with respect to the concentration of the reactant and first order with respect to the density radiation.

By introducing the mass balance Eq.(A1.2), and integrating

$$n_{ox}^0 - n_{ox} = R_{ox}t = -\int_v \sum_{\lambda} \Phi_{\lambda}.\mu_{\lambda}.q_{\lambda}.t.dv \quad \text{(A1.3)}$$

from geometrical parameters of photo-reactor and imply the emission model for the lamp. The absorbed photon flow at any wavelength λ given by the equation

$$W_{abs,\lambda} = \int_v \mu_{\lambda}.q_{\lambda}.dv \quad \text{(A1.4)}$$

Where v is the volume of the photochemical reactor

by substitution (A1.4) in (A1.2)

$$n_{ox}^0 - n_{ox} = -\sum_{\lambda} \Phi_{\lambda}.W_{abs,\lambda}.t \quad \text{(A1.5)}$$

Since the lamp emit just one wavelength, so Eq. (A1.5) can be simplified as

$$n_{ox}^{0} - n_{ox} = - \Phi_{\lambda} . W_{abs,\lambda} . t \qquad \text{(A1.6)}$$

Experimental method

The test was carried out as follow:

solution of 0.05 M oxalic acid and 0.01M urinal nitrate was prepared

the solution charged to the reactor and switch on the ultraviolet light.

Samples were taken at time intervals of 2-3 min and titrate it with solution $KMnO_4$ 0.1N

- **Reactor 1**

Table (A1.1) Actinometrical results

Time (min)	$KMnO_4$, ml	$[C_2H_20_4]$, mole/L	n.^{0} $C_2H_20_4$ Mole	n^0_{C2H204}-n_{C2H204} (mole)
0	4,80	0,0480	0,120	0,0000
3	4,56	0,0456	0,114	0,0060
6	4,54	0,0454	0,114	0,0065
9	4,52	0,0452	0,113	0,0070
12	4,30	0,0430	0,113	0,0070
15	4,25	0,0425	0,110	0,0100
18	4,20	0,0420	0,108	0,0120
21	4,15	0,0415	0,107	0,0130
24	4,10	0,0410	0,105	0,0150
27	4,00	0,0400	0,103	0,0170
33	4,00	0,0400	0,100	0,0200
36	3,95	0,0395	0,099	0,0210
39	3,85	0,0385	0,096	0,0237
42	3,80	0,0380	0,095	0,0250
45	3,75	0,0375	0,094	0,0252

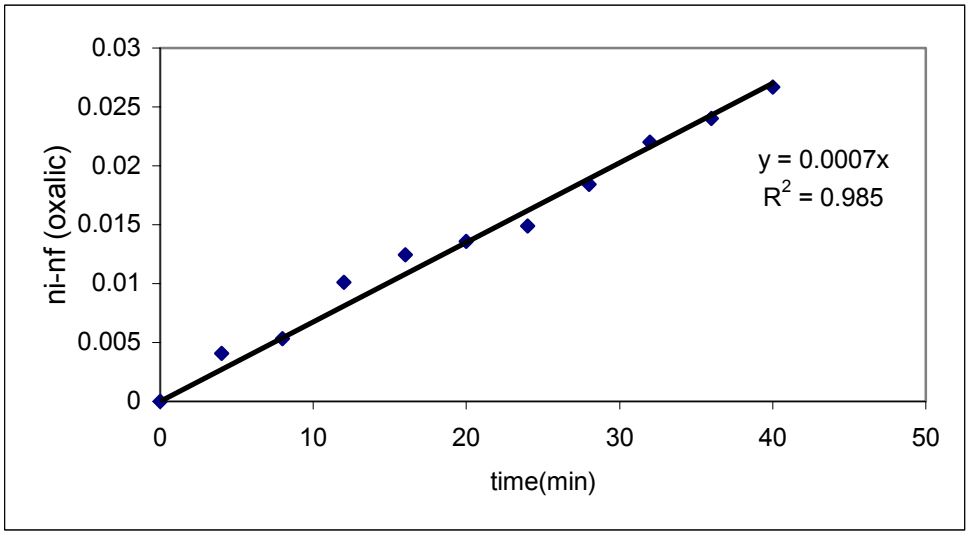

Figure A1.1 actinometrical curve

The value of φ at the lamp wavelength (254 nm) is 0.6

Results

$\text{Slope} = \Phi_{\lambda} W_{abs,\lambda}$

So the value for

$W_{abs,\lambda}$ =13.8888μ eins.s^{-1}

The same procedure was followed for the other lamps, table A1.2 presents summary for the actinometrical results of all the reactors:

Table A1.2: photo-reactor actinometrical results

Reactor	Slope	$W_{abs,\lambda}$ (μ eins.s^{-1})
Reactor 1	7 X10^{-4}	13.9
Reactor 2	8X10^{-4}	2.4
Reactor 3	3X10^{-4}	9.3

DCP

Table DCP-V

Volatilization of DCP

Operational conditions

$[DCP]_i$ ($mg.L^{-1}$)	Temperture (ºC)	pH
106	45	free

Time (min)	Temperature (ºC)	[DCP] ($mgC.L^{-1}$)	TOC ($mgC.L^{-1}$)
0	45	106.0	46.6
20	45	103.2	46.2
40	45	102.0	44.9
60	45	101.3	44.9
80	45	101.0	44.7
100	45	97.9	44.0
120	45	97.5	43.6
% removal	-	8%	6.5%

Table DCP-S

Stripping of DCP

Operations conditions

$[DCP]_i$ ($mg.L.^{-1}$)	Temperture (ºC)	pH
100	25	free

Time (min)	Temperature (ºC)	[DCP] ($mgC.L^{-1}$)	TOC ($mgC.L^{-1}$)º
0	25	100.0	45.5
20	25	97.2	46.2
40	25	94.7	44.2
60	25	93.6	43.6
80	25	92.3	43.2
100	25	92.56	42.2
120	25	90.4	40.0
% removal	-	9.6%	12.1%

Degradation of DCP by direct UV-light

Table DCP-UV

Operational conditions

$[DCP]_i$ ($mg.L^{-1}$)	Temperture (ºC)	pH
100	25	free

Time (min)	DCP ($mg.L^{-1}$)	TOC ($mg\ C.L^{-1}$)	AOS	COD/TOC ($mg\ O_2.\ mg^{-1}\ C$)	BOD_5 ($mgO_2.L^{-1}$)	COD ($mgO_2.L^{-1}$)
0	85	39.2	-0.061	2.71	0.0	106
5	80	38.6				
10	77	37.0				
20	73	36.0				
30	68	35.2				
40	65	35.0				
60	55	34.5				
90	48	34.2				
120	40	34.0	0.51	2.32	0.0	79
% removal	52.9	13.2				

Degradation of DCP by direct U/H_2O_2

Table DCP-UV/H_2O_2 –1

Operation conditions			
$[DCP]_i$ ($mg.L^{-1}$)	H_2O_2 ($mg.L^{-1}$)	Temperature (ºC)	pH
100	200	25	free

time (min)	pH	TOC ($mg\ C.L^{-1}$)	DCP ($mg.L^{-1}$)	BOD5
0	6.37	41.0	98.0	0
1	2.67	40.0	77.0	
5	2.79	39.2	51.0	
10	2.67	38.0	31.0	
20	2.66	37.1	18.0	
30	2.62	36.1	12.0	
50	2.61	34.5	8.0	
60	2.39	34.0	6.0	
90	2.60	32.0	0.0	2

Table DCP-UV/H_2O_2 -2

Operation conditions			
$[DCP]_i$ ($mg.L^{-1}$)	H_2O_2 ($mg.L^{-1}$)	Temperature (ºC)	pH
100	100	25	free

time (min)	TOC ($mg\ C.L^{-1}$)	DCP ($mg.L^{-1}$)	COD ($mg\ O_2.L^{-1}$)	BOD_5 ($mg\ O_2.L^{-1}$)
0	40.1	95.0	122	0
5	39.1	80.0		
10	39.0	62.0		
20	39.0	38.0		
30	38.7	24.0		
40	37.0	18.0		
50	36.0	12.0		
60	35.4	10.0		
70	33.0	5.5		
90	31.5	3.0	72	1
% Removal	21.4	96.8		

Table DCP-UV/H_2O_2 –3

Operation conditions			
$[DCP]_i$ ($mg.L^{-1}$)	H_2O_2 ($mg.L^{-1}$)	Temperature (ºC)	pH
100	50	25	free

time (min)	TOC ($mg\ C.L^{-1}$)	DCP ($mg.L^{-1}$)	COD ($mg\ O_2.L^{-1}$)	BOD_5 ($mg\ O_2.L^{-1}$)
0	41.1	108	135	0
5	37.5	85	106	
20	35.8	60	98	
30	35.1	45		
60	34.1	20		
90	32.6	10	82	1
% removal	20.7	90.7		

Table DCP-UV/H_2O_2-4 Operation conditions

$[[DCP]_i$ ($mg.L^{-1}$)	H_2O_2 ($mg.L^{-1}$)	Temperature (ºC)	pH
100	30	25	free

time (min)	TOC (mg $C.L^{-1}$)	DCP ($mg.L^{-1}$)	COD (mg $O_2.L^{-1}$)	BOD_5 (mg $O_2.L^{-1}$)
0	40.3	91.5	116	0
20	38	75		
40	36.4	55		
60	35.2	36		
80	34.0	22		
90	32.0	18		
100	33.7	15		
120	32.0	11	82	0
% removal	20.6	80.3		

Table DCP-UV/H_2O_2-5 Operation conditions

$[DCP]_i$ ($mg.L^{-1}$)	H_2O_2 ($mg.L^{-1}$)	Temperature (ºC)	pH
100	10	25	free

time (min)	DCP ($mg.L^{-1}$)	TOC (mg $C.L^{-1}$)	COD (mg $O_2.L^{-1}$)	BOD_5 (mg $O_2.L^{-1}$)
0	98	42.0	122	0
10	88	39.5		
15	80	39.0		
20	78	38.7		
40	67	36.2		
60	56	34.4		
90	55	33.8	86	0
% removal	43.9	19.5		

Table DCP-UV/H_2O_2-6 summary

Operation conditions		
$[DCP]_i$ ($mg.L^{-1}$)	Temperature (ºC)	pH
100	25	free

H_2O_2 ($mg.L^{-1}$)	T0C%	DCP%	BOD_5/COD	AOS	COD/TOC (mg O_2. mg^{-1} C)
200	21.9	100.0	0.0303	0.91	2.06
100	21.4	96.8	0.0139	0.57	2.29
50	20.7	90.7	0.0122	0.23	2.51
30	20.6	80.3	0	0.27	2.48
25	21.0	68.8	0	0.24	2.53
10	19.5	43.8	0	0.20	2.82

Degradation of DCP by UV/Fe(III)

Table DCP-UV/Fe(III) –1 Operational conditions

$[DCP]_i$ ($mg.L^{-1}$)	Fe(III) ($mg.L^{-1}$)	Temperature (ºC)	pH
100	10	25	free

time (min)	TOC ($mg\ C.L^{-1}$)	DCP ($mg.L^{-1}$)	COD ($mg\ O_2.L^{-1}$)	BOD_5 ($mg\ O_2.L^{-1}$)
0	43.7	107	133	0
5	43.0	102		
10	42.1	98		
20	39.4	96		
30	38.5	90		
40	37.5	86		
60	37.0	77		
90	35.0	59	98	0
% removal	20.0	44.9		

Table DCP-UV/Fe(III) –2 Operational conditions

$[DCP]_i$ ($mg.L^{-1}$)	Fe(III) ($mg.L^{-1}$)	Temperature (ºC)	pH
100	20	25	free

time (min)	TOC ($mg\ C.L^{-1}$)	DCP ($mg.L^{-1}$)	COD ($mg\ O_2.L^{-1}$)	BOD_5 ($mg\ O_2.L^{-1}$)
0	40.8	94	121	0
10	39.4	84		
20	38.6	77		
40	36.2	66		
80	33.9	49		
90	33.0	46	96	0
% removal	19.3	51.1		

Table DCP-UV/Fe(III) –3 Operational conditions

$[DCP]_i$ ($mg.L^{-1}$)	Fe(III) ($mg.L^{-1}$)	Temperature (ºC)	pH
100	70	25	free

time (min)	TOC ($mg\ C.L^{-1}$)	DCP ($mg.L^{-1}$)	COD ($mg\ O_2.L^{-1}$)	BOD_5 ($mg\ O_2.L^{-1}$)
0	41.5	97	122	0
5	38.0	92		
20	36.2	73		
40	35.8	59		
60	34.5	51		
90	31.5	38	88	0
% removal	24.1	60.8		

Table DCP-UV/Fe(III) – 4 summary

Operation conditions			
$[DCP]_i$ ($mg.L^{-1}$)	Fe(III) ($mg.L^{-1}$)	Temperature (ºC)	pH
100	70	25	free

Fe(III) ($mg.L^{-1}$)	BOD/COD	COD%	AOS	COD/TOC (mg O_2. mg^{-1} C)
10	0	26.3	-0.45	2.97
20	0	20.7	-0.36	2.91
25	0	19.7	-0.45	2.97
45	0	24.0	-0.31	2.88
60	0	26.2	-0.35	2.90
70	0	27.9	-0.19	2.79

Degradation of DCP by Fenton process

A) Effect of H_2O_2

Table DCP-H_2O_2/Fe(II)-1 Operation conditions

$[DCP]_i$ ($mg.L^{-1}$)	H_2O_2. ($mg.L^{-1}$)	Fe(II) ($mg.L^{-1}$)	Temperature (ºC)	pH
100	85	10	25	free

time (min)	TOC (mg $C.L^{-1}$)	DCP ($mg.L^{-1}$)	COD (mg $O_2.L^{-1}$)	BOD_5 (mg $O_2.L^{-1}$)
0	42.6	98	120	0
20	38.5	62		
40	37.5	25		
50	37.0	15		
60	36.2	5	71	5
% removal	15.0	94.90		

Table DCP-H_2O_2/Fe(II)-2 Operational conditions

$[DCP]_i$ ($mg.L^{-1}$)	H_2O_2. ($mg.L^{-1}$)	Fe(II) ($mg.L^{-1}$)	Temperature (ºC)	pH
100	50	10	25	free

Time (min)	TOC (mg $C.L^{-1}$)	DCP ($mg.L^{-1}$)	BOD_5 (mg $O_2.L^{-1}$)	COD (mg $O_2.L^{-1}$)
0	40.6	98	0	120
5	39.0	85		
10	38.0	72		
20	37.5	66		
30	35.2	50		
40	34.8	38		
60	34.7	22	0	83
% removal	14.5	77.6		

Table DCP-H_2O_2/Fe(II)-3 Operation conditions

$[DCP]_i$ ($mg.L^{-1}$)	H_2O_2. ($mg.L^{-1}$)	Fe(II) ($mg.L^{-1}$)	Temperature (ºC)	pH
100	20	10	25	free

Time (min)	TOC ($mg\ C.L^{-1}$)	DCP ($mg.L^{-1}$)	BOD_5 ($mg\ O_2.L^{-1}$)	COD ($mg\ O_2.L^{-1}$)
0	40.6	98	0	120
10	38.5	76		
20	37.5	69		
40	36.0	55		
60	35.0	49		0
	13.8	50.0		

B)Effect of Fe(II)

Table DCP-H_2O_2/Fe(II)-4 Operation conditions

$[DCP]_i$ ($mg.L^{-1}$)	H_2O_2. ($mg.L^{-1}$)	Fe(II) ($mg.L^{-1}$)	Temperature (ºC)	pH
100	20	30	25	free

time (min)	TOC ($mg\ C.L^{-1}$)	DCP ($mg.L^{-1}$)	BOD_5 ($mg\ O_2.L^{-1}$)	COD ($mg\ O_2.L^{-1}$)
0	41.0	98	0	121
5	40.0	86		
20	37.5	68		
30	36.5	64		
40	36.2	57		
60	35.8	49	0	92
% removal	12.7	50		

Table DCP-H_2O_2/Fe(II)-5 Operational conditions

$[DCP]_i$ ($mg.L^{-1}$)	H_2O_2. ($mg.L^{-1}$)	Fe(II) ($mg.L^{-1}$)	Temperature (ºC)	pH
100	20	50	25	free

time (min)	TOC ($mg\ C.L^{-1}$)	DCP ($mg.L^{-1}$)	BOD_5 ($mg\ O_2.L^{-1}$)	COD ($mg\ O_2.L^{-1}$)
0	41.0	98	0	121
5	40.0	88		
10	38.5	80		
20	37.5	72		
30	36.5	68		
40	36.2	61		
60	35.8	54	0	97
	12.7	44.9		

Table DCP-H_2O_2/Fe(II)-6

Operation conditions

$[DCP]_i$ ($mg.L^{-1}$)	H_2O_2. ($mg.L^{-1}$)	Fe(II) ($mg.L^{-1}$)	Temperature (ºC)	pH
100	20	100	25	free

time (min)	TOC ($mg\ C.L^{-1}$)	DCP ($mg.L^{-1}$)	BOD_5 ($mg\ O_2.L^{-1}$)	COD ($mg\ O_2.L^{-1}$)
0	42.6	100	0	120
10	39.0	77		
20	38.0	58		
30	37.5	38		
40	37.0	22		
50	36.5	10		
60	36.0	0	8	65
	15.49	100.00		

Table DCP-H_2O_2/Fe(II)- 7 **summary-1**

Operation conditions

$[DCP]_i$ ($mg.L^{-1}$)	Fe(II) ($mg.L^{-1}$)	Temperature (ºC)	pH
100	10	25	free

H_2O_2 ($mg.L^{-1}$)	BOD_5 ($mg\ O_2.L^{-1}$)	BOD_{10} ($mg\ O_2.L^{-1}$)	BOD_{21} ($mg\ O_2.L^{-1}$)	COD%	AOS	BOD_5/COD	BOD21/COD
20	0	0	0	23.3	0.057	0.0000	0.0000
40	0	1	2	26.7	0.174	0.0000	0.0227
50	1	3	3	30.8	0.412	0.0120	0.0361
85	5	8	11	40.8	1.058	0.0704	0.1549
100	8	15	23	45.8	1.299	0.1231	0.3538
120	9	17	25	48.3	1.409	0.1452	0.4032
140	10	19	26	52.9	1.592	0.1754	0.4561

Table DCP-H_2O_2/Fe(II)-8 **summary-2**

Operational conditions

$[DCP]_i$ ($mg.L^{-1}$)	Fe(II) ($mg.L^{-1}$)	Temperature (ºC)	pH
100	10	25	free

H_2O_2 ($mg.L^{-1}$)	BOD10/COD	BOD_5/TOC	BOD_{10}/TOC	BOD_{21}/TOC	COD/TOC
20	0.00000	0.0000	0.0000	0.0000	2.63
40	0.01136	0.0000	0.0290	0.0580	2.55
50	0.03614	0.0288	0.0865	0.0865	2.39
85	0.11268	0.1381	0.2210	0.3039	1.96
100	0.23077	0.2216	0.4155	0.6371	1.80
120	0.27419	0.2507	0.4735	0.6964	1.73
140	0.33333	0.2817	0.5352	0.7324	1.61

Table DCP-H_2O_2/Fe(II)- 9 summary-3

Operation conditions

$[DCP]_i$ ($mg.L^{-1}$)	H_2O_2 ($mg.L^{-1}$)	Temperature (ºC)	pH
100	20	25	free

Fe ($mg.L^{-1}$)	COD%	COD/TOC (mg O_2. mg^{-1} O_2)	AOS
30	24.0	2.63	0.057
50	19.8	2.71	-0.064
10	19.8	2.76	-0.134
60	18.2	2.73	-0.102

Degradation of DCP by modified Fenton process

Table DCP-H_2O_2/Fe(III)-1 Operational conditions

$[DCP]_i$ ($mg.L^{-1}$)	H_2O_2 ($mg.L^{-1}$)	Fe(III) ($mg.L^{-1}$)	Temperature (ºC)	pH
100	85	10	25	free

time (min)	TOC (mg $C.L^{-1}$)	DCP ($mg.L^{-1}$)	BOD_5 (mg $O_2.L^{-1}$)	COD (mg $O_2.L^{-1}$)
0	42.0	97.8	120	0
10	40.6	88.0		
20	39.8	70.0		
30	39.0	52.0		
40	38.5	42.0		
50	37.5	32.0		
60	36.5	12.0	1	721
	13.1	87.7		

Table DCP-H_2O_2/Fe(III)-2 Operation conditions

$[DCP]_i$ ($mg.L^{-1}$)	H_2O_2 ($mg.L^{-1}$)	Fe(III) ($mg.L^{-1}$)	Temperature (ºC)	pH
100	50	10	25	free

time (min)	TOC (mg $C.L^{-1}$)	DCP ($mg.L^{-1}$)	BOD_5 (mg $O_2.L^{-1}$)	COD (mg $O_2.L^{-1}$)
0	40.7	98	0	120
5	39.9	91		
10	37	79		
20	36.5	68		
30	36	59		
40	35.8	45		
60	35.2	27	0	96
	13.5	72.4		

Table DCP-H_2O_2/Fe(III)-3 Operation conditions

$[DCP]_i$ ($mg.L^{-1}$)	H_2O_2 ($mg.L^{-1}$)	Fe(III) ($mg.L^{-1}$)	Temperature (ºC)	pH
100	20	10	25	free

time (min)	TOC ($mg\ C.L^{-1}$)	DCP ($mg.L^{-1}$)	BOD_5 ($mg\ O_2.L^{-1}$)	COD ($mg\ O_2.L^{-1}$)
0	41.0	98	0	120
5	40.0	92		
10	38.5	82		
20	37.5	73		
30	36.5	69		
40	36.2	61		
60	35.8	55	0	95
	12.7	43.9		

Table DCP-H_2O_2/Fe(III)- 4 Summary

Operation conditions

$[DCP]_i$ ($mg.L^{-1}$)	Fe(III) ($mg.L^{-1}$)	Temperature (ºC)	pH
100	10	25	free

H_2O_2 ($mg.L^{-1}$)	BOD_5 ($mg\ O_2.L^{-1}$)	BOD_{10} ($mg\ O_2.L^{-1}$)	BOD_{21} ($mg\ O_2.L^{-1}$)	COD_i ($mg\ O_2.L^{-1}$)	COD_f ($mg\ O_2.L^{-1}$)	COD%	BOD_5/COD	BOD_{10}/COD
85	2	6	9	120	72	40	0.0278	0.0833
50	1	2	3	120	96	20	0.0104	0.0208
20	0	0	0	120	95		0.0000	0.0000
40	0	0	0	120	100	16.7	0.0000	0.0000
100	3	8	11	120	69	42.5	0.0435	0.1159
115	7	14	20	120	64	46.7	0.1094	0.2187
125	8	16	22	120	61	49.2	0.1312	0.2623

Table DCP-H_2O_2/Fe(III)- 5 Summary

Operation conditions

$[DCP]_i$ ($mg.L^{-1}$)	Fe(III) ($mg.L^{-1}$)	Temperature (ºC)	pH
100	10	25	free

H_2O_2 ($mg.L^{-1}$)	BOD_{21}/COD	BOD_5/TOC ($mg\ O_2$. mg C)	BOD_{10}/TOC ($mg\ O_2$. mg C)	BOD_{21}/TOC ($mg\ O_2$. mg C)	AOS	COD/TOC ($mg\ O_2$. mg C)
85	0.1250	0.0548	0.1644	0.2466	1.04	1.97
50	0.0313	0.0279	0.0559	0.0838	-0.02	2.68
20	0.0000	0.0000	0.0000	0.0000	-0.003	2.67
40	0.0000	0.0000	0.0000	0.0000	-0.26	2.84
100	0.1594	0.0855	0.2279	0.3134	1.05	1.97
115	0.3125	0.2000	0.4000	0.5714	1.26	1.83

125	0.36066	0.2292	0.4585	0.6304	1.378	1.75

Degradation of DCP by photo-Fenton process

A) Effect of initial H_2O_2

Table DCP-PHF-1 Operation conditions

[DCP]i ($mg.L^{-1}$)	H_2O_2 ($mg.L^{-1}$)	Fe(II) ($mg.L^{-1}$)	Temperature (ºC)	pH
100	0	10	25	free

Time (min)	BOD_5/COD	COD ($mg\ O_2.L^{-1}$)	DCP ($mg\ .L^{-1}$)	BOD5 ($mg\ O_2.L^{-1}$)	TOC ($mg\ C.L^{-1}$)	AOS	BOD/TOC ($mg\ O_2.\ (mg^{-1}C)$)
0	0	106	85	0	39	-0.08	0
5	0	98	80	0	38.2	0.15	0
10	0	96	75	0	37.4	0.15	0
20	0	95	71	0	37	0.15	0
25	0	94	69	0	36.7	0.16	0
40	0	93	65	0	36	0.13	0

Table DCP-PHF-2 **Operation conditions**

[DCP]i ($mg.L^{-1}$)	H_2O_2 ($mg.L^{-1}$)	Fe(II) ($mg.L^{-1}$)	Temperature (ºC)	pH
100	10	10	25	free

Time (min)	BOD_5/COD	COD ($mg\ O_2.L^{-1}$)	DCP ($mg\ .L^{-1}$)	BOD5 ($mg\ O_2.L^{-1}$)	TOC ($mg\ C.L^{-1}$)	cl^- ($mg.L^{-1}$)	AOS	BOD/TOC ($mg\ O_2.\ (mg^{-1}C)$)
0	0	106	85	0	39.0	0.00	-0.08	0
5	0	98	70	0	38.0	4.00	0.13	0
10		96	65		37.0	10.00	0.11	
20	0	95	48	0	36.4	13.00	0.09	0
25	0	94	43.3	0	36.0	18.00	0.08	0
40	0	91	40	0	35.0	20.00	0.10	0
% removal			52.9		10.3			

Table DCP-PHF-3 Operation conditions

[DCP]i ($mg.L^{-1}$)	H_2O_2 ($mg.L^{-1}$)	Fe(II) ($mg.L^{-1}$)	Temperature (ºC)	pH
100	40	10	25	free

Time (min)	BOD_5/COD	COD ($mg\ O_2.L^{-1}$)	DCP ($mg\ .L^{-1}$)	BOD5 ($mg\ O_2.L^{-1}$)	TOC ($mg\ C.L^{-1}$)	cl^- ($mg.L^{-1}$)	AOS	BOD/TOC ($mg\ O_2.\ (mg^{-1}C)$)
0	0.0000	125	100	0	42.1	0.00	-0.46	0.0000
5	0.0182	110	56	2	41.5	7	0.02	0.0482
10		98	32		40.0	13.00	0.33	
20	0.0444	91	15	4	38.0	18.00	0.45	0.1053
25	0.0568	88	10	5	36.0	20.00	0.67	0.1389
40	0.0843	83	6	7	34.0	23.00	0.82	0.2059
% removal			94		19.1			

Table DCP-PHF-4 Operation conditions

[DCP]i ($mg.L^{-1}$)	H_2O_2 ($mg.L^{-1}$)	Fe(II) ($mg.L^{-1}$)	Temperature (ºC)	pH
100	50	10	25	free

Time (min)	BOD_5/COD	COD ($mg\ O_2.L^{-1}$)	DCP ($mg\ .L^{-1}$)	BOD5 ($mg\ O_2.L^{-1}$)	TOC ($mg\ C.L^{-1}$)	cl^- ($mg.L^{-1)}$	AOS	BOD/TOC ($mg\ O_2.\ (mg^{-1}C)$
0	0.0000	120	98	0	42.01	0.00	-0.28	0
5	0.0300	100	48.5	3	40.5	9.00	0.30	0.0741
10	0.0610	10	20	5	39	17.00	0.85	0.1282
20	0.0741	89	4	6	38	24.00	0.80	0.1579
25	0.1143	80	2	8	36	28	1.08	0.2222
40	0.1857	74	0.01	13	35.4	32.00	1.03	0.3672

Table DCP-PHF-5 Operation conditions

[DCP]i ($mg.L^{-1}$)	H_2O_2 ($mg.L^{-1}$)	Fe(II) ($mg.L^{-1}$)	Temperature (ºC)	pH
100	60	10	25	free

Time (min)	BOD_5/COD	COD ($mg\ O_2.L^{-1}$)	DCP ($mg\ .L^{-1}$)	BOD5 ($mg\ O_2.L^{-1}$)	TOC ($mg\ C.L^{-1}$)	cl^- ($mg.L^{-1)}$	AOS	BOD_5/TOC ($mg\ O_2.\ mg^{-1}C$)
0	0.0000	110	88	0	40.51	0.00	-0.073	0.0000
5			45			11		
10			20			19.00		
20	0.0750	80	8	6	34.11	27.00	0.482	0.1759
25			0			30		
30	0.2333	62	0	14	33	32.00	1.273	0.4242
% removal			100		18.5			

Summary

Table DCP-PHF-6 Operation conditions

[DCP]I ($mg.L^{-1}$)	Fe(II) ($mg.L^{-1}$)	Temperature (ºC)	pH
100	10	25	free

H_2O_2 ($mg.L^{-1}$)	%DCP	`%TOC	%COD	BOD21	BOD_{21}/COD	COD/TOC ($mg\ O_2.\ mg^{-1}C$)
0	23.53	7.692	11%	0	0.00	2.58
10	52.94	10.26	14%		0.00	2.60
20	65.98	14.63	30%		0.00	2.46
30	83.16	17.56	36%	5	0.060	2.28
40	94	19.14	40%	10	0.125	2.12
50	99.99	15.73	42%	17.5	0.24	1.98
60	100	18.54	45%		0.00	1.82
65	100	23.57	57%	22	0.34	1.58
70	100	23.92	55%		0.00	1.67

75	100	25	63%	23	0.575	1.33

B) Effect of Fe(II)

Table DCP-PHF-7 Operation conditions

[DCP]i ($mg.L^{-1}$)	H_2O_2 ($mg.L^{-1}$)	Fe(II) ($mg.L^{-1}$)	Temperature (ºC)	pH
100	10	0	25	free

Time (min)	BOD_5/COD	COD ($mg\ O_2.L^{-1}$)	DCP ($mg\ .L^{-1}$)	BOD5 ($mg\ O_2.L^{-1}$)	TOC ($mg\ C.L^{-1}$)	AOS	BOD/TOC ($mg\ O_2.mg^{-1}C$)
0	0.0000	128	106	0	42.5	-0.51	0.0000
5		115	96	0	38.5	-0.48	0.0000
10		109	88		36.7	-0.46	
20	0.0000	108	78	0	36.4	-0.45	0.0000
25		106	71	0	36.2	-0.39	0.0000
40	0.0000	102	67	0	36.2	-0.23	0.0000
%removal			36.8		14.9		

Table DCP-PHF-8 Operation conditions

[DCP]i ($mg.L^{-1}$)	H_2O_2 ($mg.L^{-1}$)	Fe(II) ($mg.L^{-1}$)	Temperature (ºC)	pH
100	10	10	25	free

Time (min)	BOD_5/COD	COD ($mg\ O_2.L^{-1}$)	DCP ($mg\ .L^{-1}$)	BOD5 ($mg\ O_2.L^{-1}$)	TOC ($mg\ C.L^{-1}$)	AOS	BOD/TOC ($mg\ O_2.mg^{-1}C$)
0	0.0000	106	85	0	39.0	-0.08	0
5	0.0000	98	70	0	38.0	0.13	0
10		96	65		37.0	0.11	
20	0.0000	95	48	0	36.4	0.09	0
25	0.0000	94	43.3	0	36.0	0.08	0
40	0.0000	89	40	0	33.3	-0.02	0
% removal			52.9		14.7		

Table DCP-PHF-9

Operation conditions

[DCP]I ($mg.L^{-1}$)	H_2O_2 ($mg.L^{-1}$)	Fe(II) ($mg.L^{-1}$)	Temperature (ºC)	PH
100	10	30	25	Free

Time (min)	BOD_5/COD	COD ($mg\ O_2.L^{-1}$)	DCP ($mg\ .L^{-1}$)	BOD5 ($mg\ O_2.L^{-1}$)	TOC ($mg\ C.L^{-1}$)	AOS	BOD/TOC ($mg\ O_2.mg^{-1}C$)
0	0.0000	118	102	0	41.6	-0.25	0.0000
5		108	80	0	40.0	-0.05	0.0000
10		95	68		39.0	0.35	
20	0.0000	93	56	0	38.0	0.33	0.0000
25		88.5	47.5	0	36.0	0.31	0.0000
40	0.0000	87	46.0	0.0	35.4	0.31	0.0000
% removal			54.9		14.9		

Table DCP-PHF-10 Operation conditions

[DCP]i ($mg.L^{-1}$)	H_2O_2 ($mg.L^{-1}$)	Fe(II) ($mg.L^{-1}$)	Temperature (ºC)	pH
100	10	50	25	free

Time (min)	BOD_5/COD	COD ($mg\ O_2.L^{-1}$)	DCP ($mg\ .L^{-1}$)	BOD5 ($mg\ O_2.L^{-1}$)	TOC ($mg\ C.L^{-1}$)	AOS	BOD/TOC ($mg\ O_2.mg^{-1}C$)
0	0.0000	118	95	0	39.0	-0.54	0.0000
5		113	62	0	38.6	-0.39	0.0000
10		97	44		37.0	0.07	
20	0.0000	92.5	30	0	35.6	0.10	0.0000
25		87	22	1	33.5	0.10	0.0299
40	0.01299	77	12	1	32.8	0.48	0.0305
			87.4		15.9		

Table DCP-PHF-11 Operation conditions

[DCP]i ($mg.L^{-1}$)	H_2O_2 ($mg.L^{-1}$)	Fe(II) ($mg.L^{-1}$)	Temperature (ºC)	pH
100	10	60	25	free

Time (min)	BOD_5/COD	COD ($mg\ O_2.L^{-1}$)	DCP ($mg\ .L^{-1}$)	BOD5 ($mg\ O_2.L^{-1}$)	TOC ($mg\ C.L^{-1}$)	AOS	BOD5/TOC ($mg\ O_2.mg^{-1}C$)
0	0.0000	115	95	0	40.0	-0.31	0.0000
5		110	84	0	38.6	-0.27	0.0000
10		98	70		35.6	-0.13	
20	0.0000	92	60	0	34.0	-0.06	0.0000
25		90	54.5	0	33.7	-0.01	0.0000
40	0.0000	80	49	0	33.5	0.42	0.0000
			48.4		16.3		

Summary

Table DCP-PHF-12 Operation conditions

[DCP]i ($mg.L^{-1}$)	H_2O_2 ($mg.L^{-1}$)	Temperature (ºC)	pH
100	10	25	free

Fe(II) ($mg.L^{-1}$)	%DCP	%TOC	%COD	COD/TOC ($mg\ O_2.\ mg^{-1}C$)
0	36.8	14.9	16%	2.82
10	52.9	14.74	16%	2.95
20	53.7	14.6	16%	2.39
30	54.9	14.9	26%	2.23
40	64.7	15.4	25%	2.33
50	87.4	15.9	19%	2.66
60	48.4	16.3	19%	2.39

Table DCP-PHF-13 Operation conditions

[DCP]i ($mg.L^{-1}$)	H_2O_2 ($mg.L^{-1}$)	Fe(II) ($mg.L^{-1}$)	Temperature (ºC)	pH
100	30	0	25	free

Time (min)	BOD_5/COD	COD ($mg\ O_2.L^{-1}$)	DCP ($mg\ .L^{-1}$)	BOD5 ($mg\ O_2.L^{-1}$)	TOC ($mg\ C.L^{-1}$)	AOS	BOD/TOC ($mg\ O_2.mg^{-1}C$)
0	0.0000	133	106	0	42.5	-0.69	0.0000
5		118	90	0	38.2	-0.63	0.0000
10		110	81		36.4	-0.53	
20	0.0000	104	72	0	36.2	-0.31	0.0000
25		98	66	0	36.0	-0.08	0.0000
30	0.0000	92	50	0	35.6	0.12	0.0000
			52.8		16.3		

Table DCP-PHF-13 Operation conditions

[DCP]i ($mg.L^{-1}$)	H_2O_2 ($mg.L^{-1}$)	Fe(II) ($mg.L^{-1}$)	Temperature (ºC)	pH
100	30	10	25	free

Time (min)	BOD_5/COD	COD ($mg\ O_2.L^{-1}$)	DCP ($mg\ .L^{-1}$)	BOD5 ($mg\ O_2.L^{-1}$)	TOC ($mg\ C.L^{-1}$)	AOS	BOD/TOC ($mg\ O_2.mg^{-1}C$)
0	0.0000	120	95	0	41.0	-0.39	0
5	0.0174	115	35	2	40.0	-0.31	0.05
10		110	25		39.7	-0.16	
20	0.0200	100	20	2	38.0	0.05	0.052632
25	0.0345	87	19	3	37.5	0.52	0.08
30	0.0390	77	16	3	33.8	0.58	0.088757
			83.2		17.6		

Table DCP-PHF-14 Operation conditions

[DCP]i ($mg.L^{-1}$)	H_2O_2 ($mg.L^{-1}$)	Fe(II) ($mg.L^{-1}$)	Temperature (ºC)	pH
100	30	30	25	free

Time (min)	BOD_5/COD	COD ($mg\ O_2.L^{-1}$)	DCP ($mg\ .L^{-1}$)	BOD5 ($mg\ O_2.L^{-1}$)	TOC ($mg\ C.L^{-1}$)	AOS	BOD/TOC ($mg\ O_2.mg^{-1}C$)
0	0.0000	129	102	0	41.6	-0.65	0.0000
5		109	77	0	40.0	-0.09	0.0000
10		95	55		39.0	0.35	
20	0.0323	93	51	3	38.0	0.33	0.0789
25		88	39	4	36.0	0.33	0.1111
30	0.0811	74	6	6	35.4	0.86	0.1695
			94.1		14.9		

Table DCP-PHF-14 Operation conditions

[DCP]i ($mg.L^{-1}$)	H_2O_2 ($mg.L^{-1}$)	Fe(II) ($mg.L^{-1}$)	Temperature (ºC)	pH
100	30	50	25	free

Time (min)	BOD_5/COD	COD ($mg\ O_2.L^{-1}$)	DCP ($mg\ .L^{-1}$)	BOD5 ($mg\ O_2.L^{-1}$)	TOC ($mg\ C.L^{-1}$)	AOS	BOD/TOC ($mg\ O_2.mg^{-1}C$)
0	0.0000	117	95	0	39.0	-0.5	0.0000
5		100	62	0.5	38.6	0.11399	0.0130
10		93	44	1	37.0	0.22973	
20	0.0345	87	30	3	35.6	0.33427	0.0843
25		82	22	6	33.5	0.328358	0.1791
30	0.1692	65	0	11	32.8	1.027439	0.3354
			100.0		15.90		

Summary

Table DCP-PHF-15 Operation conditions

[DCP]I ($mg.L^{-1}$)	H_2O_2 ($mg.L^{-1}$)	Temperature (ºC)	pH
100	30	25	free

Fe(II) ($mg.L^{-1}$)	%COD	BOD_{21} ($mg\ O_2.L^{-1}$)	BOD_{10}/COD	BOD_{21}/COD	BOD_{10}/TOC	BOD_{21}/TOC	COD/TOC ($mg\ O_2.mg^{-1}C$)
0	28%	0	0	0	0	0	2.58
10	29%	6	0.051948	0.07792	0.118343	0.177515	2.28
20	40%	7	0.060811	0.09459	0.127841	0.198864	2.10
30	37%	8.5	0.090278	0.11806	0.183616	0.240113	2.03
40	31%	12	0.130769	0.18462	0.264798	0.373832	2.02
50	38%	14	0.169231	0.21538	0.341615	0.434783	2.02
60	33%	11	0.111111	0.15278	0.242424	0.333333	2.18
70	26%	10	0.0875	0.125	0.213415	0.304878	2.44

C) Effect of pH

Table DCP-PHF-16 Operation conditions

[DCP]i ($mg.L^{-1}$)	H_2O_2 ($mg.L^{-1}$)	Fe(II) ($mg.L^{-1}$)	Temperature (ºC)	pH
100	10	10	25	4.86

Time (min)	COD ($mg.O_2.L^{-1}$)	DCP ($mg.L^{-1}$)	BOD_5 ($mg.O_2.L^{-1}$)	TOC ($mg.C.L^{-1}$)	AOS	BOD/TOC ($mg.O_2.mg^{-1}C$)
0	106	85	0	39.0	-0.08	0
5	98	70	0	38.0	0.13	0
10	96	65		37.0	0.11	
20	95	48	0	36.4	0.09	0
25	94	43.3	0	36.0	0.08	0
30	93	40	0	35.0	0.01	0
% removal		52.9		10.3		

Table DCP-PHF-17 Operation conditions

[DCP]i ($mg.L^{-1}$)	H_2O_2 ($mg.L^{-1}$)	Fe(II) ($mg.L^{-1}$)	Temperature (ºC)	pH
100	10	10	25	3.0

Time (min)	COD ($mg.O_2.L^{-1}$)	DCP ($mg.L^{-1}$)	BOD_5 ($mg.O_2.L^{-1}$)	TOC ($mg.C.L^{-1}$)	AOS	BOD/TOC ($mg.O_2.mg^{-1}C$)
0	106	85	0	39.0	-0.08	0
5	98	70	0	38.0	0.13	0
10	96	65		37.0	0.11	
20	95	43	0	36.4	0.09	0
25	93	39	0	35.5	0.07	0
30	90	37	0	34.9	0.13	0
% removal		56.5		10.5		

Table DCP-PHF-18 Operation conditions

[DCP]i ($mg.L^{-1}$)	H_2O_2 ($mg.L^{-1}$)	Fe(II) ($mg.L^{-1}$)	Temperature (ºC)	pH
100	10	10	25	7.5

Time (min)	COD ($mg.O_2.L^{-1}$)	DCP ($mg.L^{-1}$)	BOD_5 ($mg.O_2.L^{-1}$)	TOC ($mg.C.L^{-1}$)	AOS	BOD/TOC ($mg.O_2.mg^{-1}C$)
0	106	85	0	39.0	-0.08	0
5	98	70	0	38.0	0.13	0
10	96	65		37.0	0.11	
20	95	55	0	36.8	0.13	0
25	93	50	0	36.2	0.15	0
30	90	48	0	35.4	0.19	0
% removal		43.5		9.2		

Table DCP-PHF-19

Operation conditions

[DCP]i ($mg.L^{-1}$)	H_2O_2 ($mg.L^{-1}$)	Fe(II) ($mg.L^{-1}$)	Temperature (ºC)	pH
100	40	10	25	4.86

Time (min)	COD ($mg.O_2.L^{-1}$)	DCP ($mg.L^{-1}$)	BOD_5 ($mg.O_2.L^{-1}$)	TOC ($mg.C.L^{-1}$)	AOS	BOD/TOC ($mg.O_2.mg^{-1}C$)
0	125	100	0	42.0	-0.46	0.0000
5	110	56	2	41.0	-0.02	0.0488
10	98	32		40.0	0.33	
20	90	15	4	38.0	0.45	0.1053
25	80	10	5	36.0	0.67	0.1389
30	72	6	7	34.0	0.82	0.2059
% removal		94.0		19.0		

Table DCP-PHF-20

Operation conditions

[DCP]i ($mg.L^{-1}$)	H_2O_2 ($mg.L^{-1}$)	Fe(II) ($mg.L^{-1}$)	Temperature (ºC)	pH
100	40	10	25	3.0

Time (min)	COD ($mg.O_2.L^{-1}$)	DCP ($mg.L^{-1}$)	BOD_5 ($mg.O_2.L^{-1}$)	TOC ($mg.C.L^{-1}$)	AOS	BOD/TOC ($mg.O_2.mg^{-1}C$)
0	122	98	0	41.8	-0.3780	0.0000
5	108	49	2	40.5	0.0000	0.0494
10	95	24		39.5	0.3924	
20	80	10	5	37.2	0.7742	0.1344
25	72	5	5	36.1	1.0083	0.1385
30	70	2	8	34.1	0.920821114	0.2346
% removal		98.0		18.4		

Table DCP-PHF-21 Operation conditions

[DCP]i ($mg.L^{-1}$)	H_2O_2 ($mg.L^{-1}$)	Fe(II) ($mg.L^{-1}$)	Temperature (ºC)	pH
100	40	10	25	7.5

Time (min)	COD ($mg.O_2.L^{-1}$)	DCP ($mg.L^{-1}$)	BOD_5 ($mg.O_2.L^{-1}$)	TOC ($mg.C.L^{-1}$)	AOS	BOD/TOC ($mg.O_2.mg^{-1}C$)
0	123	99	0	42.0	-0.39	0.0000
5	115	60	2	41.0	-0.21	0.0488
10	105	38		40.5	0.11	
20	95	25	4	38.5	0.30	0.1039
25	93	18	4	36.7	0.20	0.1090
30	72	10	7	34.6	0.88	0.2023
% removal		89.9		17.6		

D) effect of initial DCP concentration

Table DCP-PHF-22 Operation conditions

[DCP]i ($mg.L^{-1}$)	H_2O_2 ($mg.L^{-1}$)	Fe(II) ($mg.L^{-1}$)	Temperature (ºC)	pH
100	50	10	25	free

	$[DCP]_i$=100 $mg.L^{-1}$		$[DCP]_i$=150 $mg.L^{-1}$		$[DCP]_i$=200 $mg.L^{-1}$	
Time (min)	DCP ($mg.L^{-1}$)	TOC ($mgC.L^{-1}$)	DCP ($mg.L^{-1}$)	TOC ($mgC.L^{-1}$)	DCP ($mg.L^{-1}$)	TOC ($mgC.L^{-1}$)
0	96	42.9	150	57.8	194.9	84.8
5	48.5	40.5	100	54.0	140	76.6
10	20	38.0	80	53.4	110	72.0
20	4	36.0	60	47.8	88	68.8
30	1	33.5	55	44.0	80	63.0
60	0.01	22.0	52	57.8	78	84.8

E) Effect of UV-irradiation time

Table DCP-PHF-23 Operation conditions

[DCP]i ($mg.L^{-1}$)	H_2O_2 ($mg.L^{-1}$)	Temperature (ºC)	pH
100	50	25	free

Time (min)	PH	DCP ($mg.L^{-1}$)	TOC ($mgC.L^{-1}$)
0	5.76	95	39.5
3	5.89	84	39.5
6	5.72	82	37
9	5.66	72.2	36.13
10	5.9	72.1	36.1
14	4.2	68	35
18	3.86	52.1	34.95
20	3.41	42.1	34.8
25	3.67	38	34.5
30	3.64	30.67	34.2
% removal		67.7	13.4

Table DCP-PHF-24 Operation conditions

[DCP]i ($mg.L^{-1}$)	H_2O_2 ($mg.L^{-1}$)	Fe(II) ($mg.L^{-1}$)	Temperature (ºC)	pH
100	30	10	25	free

Time (min)	PH	DCP (ppm)	TOC(ppm)
0	5.35	96.0	39.0
1	4.50	80.0	38.0
5	3.47	66.0	35.9
8	3.41	57.0	35.9
10	3.38	30.0	35.5
15	3.34	18.0	34.1
20	3.32	18.0	34.0
30	3.34	17.0	34.0
% removal		82.6	12.8

Mineralization of DCP by photo-Fenton process

Table DCP-PHF-25 Operation conditions

[DCP]i ($mg.L^{-1}$)	H_2O_2 ($mg.L^{-1}$)	Fe(II) ($mg.L^{-1}$)	Temperature (ºC)	pH
100	50	10	25	free

time (min)	[H2O2]=60 ($mg.L^{-1}$)	[H2O2]=100 ($mg.L^{-1}$)	[H2O2]=150 ($mg.L^{-1}$)	[H2O2]=200 ($mg.L^{-1}$)	[H2O2]=250 ($mg.L^{-1}$)	[H2O2]=270 ($mg.L^{-1}$)
0	38.5	39.3	39.5	38.4	37.4	38.6
5	33.8	33.3	28.4	22.7	23.2	28.6
10	33.5	31.3	25.4	11.3	11.9	17.1
20	33.2	31.0	23.7	9.6	10.9	8.6
30	32.8	28.7	21.9	8.4	6.8	6.1
40	32.4	26.8	19.4	7.1	5.9	3.2
50	32.2	26.3	17.6	6.6	4.3	1.2

POH

Degradation of POH by direct UV-light

Table POH-UV

Operational conditions		
[DCP]i ($mg.L^{-1}$)	Temperture (ºC)	pH
100	25	free

time (min)	POH ($mg.L^{-1}$)	TOC ($mgC.L^{-1}$)	COD ($mgO_2.L^{-1}$)	BOD_5 ($mgO_2.L^{-1}$)	BOD_5/COD	BOD_5/TOC ($mgO_2.mg^{-1}C$)	COD/TOC ($mgO_2.mg^{-1}C$)	AOS
0	106	78	220	27	0.1227	0.3462	2.82	-0.23
5	100							
10	94	76						
20	86	73	200				2.74	-0.11
30	80							
40	74	70						
50	66							
80	57	68						
120	46	65	160	30	0.1875	0.462	2.46153846	0.31
% removal	56.6	16.6	27.2					

Degradation of POH by direct UV/H_2O_2

Table POH- UV/H_2O_2-1

Operational conditions			
[DCP]i ($mg.L^{-1}$)	H_2O_2 ($mg.L^{-1}$)	Temperture (ºC)	pH
100	150	25	free

time (min)	POH ($mg.L^{-1}$)	TOC ($mgC.L^{-1}$)	COD ($mgO_2.L^{-1}$)	BOD_5 ($mgO_2.L^{-1}$)	BOD_5/COD	BOD_5/TOC ($mgO_2.mg^{-1}C$)	COD/TOC ($mgO_2.mg^{-1}C$)	AOS
0	103	78	218	27	0.1238	0.3461	2.79	-0.19
5	92	76						
30	73							
40	67	67						
80	44	63						
120	30	60	145	30	0.2070	0.500	2.42	0.375
% removal	70.9	23.1	33.5					

Table POH- UV/H_2O_2-2

Operational conditions			
[DCP]i ($mg.L^{-1}$)	H_2O_2 ($mg.L^{-1}$)	Temperture (ºC)	PH
100	200	25	Free

time (min)	POH ($mg.L^{-1}$)	TOC ($mgC.L^{-1}$)	COD ($mgO_2.L^{-1}$)	BOD_5 ($mgO_2.L^{-1}$)	BOD_5/COD	BOD_5/TOC ($mgO_2.mg^{-1}C$)	COD/TOC ($mgO_2.mg^{-1}C$)	AOS
0	103	78	218	27	0.1238	0.346	2.80	-0.19
5	85	71						
10	70	67						
40	34	63						
50	20							
80	10	61						
120	4	59	138	31	0.2246	0.525	2.338	0.49
% removal	96.1	24.4	36.7					

Table POH- UV/H_2O_2-3

Operational conditions			
[DCP]i ($mg.L^{-1}$)	H_2O_2 ($mg.L^{-1}$)	Temperture (ºC)	pH
100	400	25	free

time (min)	POH ($mg.L^{-1}$)	TOC ($mgC.L^{-1}$)	COD ($mgO_2.L^{-1}$)	BOD_5 ($mgO_2.L^{-1}$)	BOD_5/COD	BOD_5/TOC ($mgO_2.mg^{-1}C$)	COD/TOC ($mgO_2.mg^{-1}C$)	AOS
0	103	78	218	27	0.12385321	0.3461	2.79	-0.19230769
5	82	68						
30	40							
40	28	60						
50	19							
80	5	58						
120	0.1	55	126	33	0.26190476	0.600	2.29	0.56
	99.9	29.4	42.2				0.18	

Degradation of POH by UV/Fe(III)

Table POH- UV/Fe(III)-1

Operational conditions			
[DCP]i ($mg.L^{-1}$)	Fe(III) ($mg.L^{-1}$)	Temperture (ºC)	pH
100	20	25	free

time (min)	TOC ($mgC.L^{-1}$)	POH ($mg.L^{-1}$)	COD ($mgO_2.L^{-1}$)	BOD_5 ($mgO_2.L^{-1}$)	BOD_5/COD	BOD_5/TOC ($mgO_2.mg^{-1}C$)	COD/TOC ($mgO_2.mg^{-1}C$)	AOS
0	76	106	218	27	0.1238	0.355	2.86	-0.30
5		102						
10	74	96	210	28	0.1333	0.378	2.83	-0.25
30	71	83	205	30	0.1463	0.422	2.88	-0.33
60	67	57	200	32	0.1600	0.477	2.98	-0.47
90	64	38	164	34	0.2073	0.531	2.56	0.15
% removal	15.8	64.1	24.7					

Table POH- UV/Fe(III)-2

Operational conditions			
[DCP]i ($mg.L^{-1}$)	Fe(III) ($mg.L^{-1}$)	Temperature (ºC)	pH
100	10	25	free

time (min)	TOC ($mgC.L^{-1}$)	POH ($mg.L^{-1}$)	COD ($mgO_2.L^{-1}$)	BOD_5 ($mgO_2.L^{-1}$)	BOD_5/COD	BOD_5/TOC ($mgO_2.mg^{-1}C$)	COD/TOC ($mgO_2.mg^{-1}C$)	AOS
0	78	108	223	27	0.121	0.346	2.859	-0.29
10	75	100	215	29	0.135	0.386	2.866	-0.30
30	73	92	210	31	0.147	0.424	2.876	-0.315
60	69	65	207	33	0.159	0.478	3	-0.5
90	66	44	170	33	0.194	0.5	2.575	0.13
% removal	15.4	59.3	23.8					

Table POH- UV/Fe(III)-3

Operational conditions			
[DCP]i ($mg.L^{-1}$)	Fe(III) ($mg.L^{-1}$)	Temperature (ºC)	pH
100	50	25	free

time (min)	TOC ($mgC.L^{-1}$)	POH ($mg.L^{-1}$)	COD ($mgO_2.L^{-1}$)	BOD_5 ($mgO_2.L^{-1}$)	BOD_5/COD	BOD_5/TOC ($mgO_2.mg^{-1}C$)	COD/TOC ($mgO_2.mg^{-1}C$)	AOS
0	78	106	224	27	0.120	0.3461	2.87	-0.31
5		97						
10	73	90	212	29	0.138	0.397	2.90	-0.36
20		84						
30	70	73	207	31	0.149	0.442	2.95	-0.43
60	67	53	204	33	0.162	0.492	3.04	-0.56
90	64	33	162	35	0.216	0.546	2.53	0.20
% removal	17.9	68.8	27.6					

Table POH- UV/Fe(III)-4

Operational conditions			
[DCP]i ($mg.L^{-1}$)	Fe(III) ($mg.L^{-1}$)	Temperature (ºC)	pH
100	70	25	free

time (min)	TOC ($mgC.L^{-1}$)	POH ($mg.L^{-1}$)	COD ($mgO_2.L^{-1}$)	BOD_5 ($mgO_2.L^{-1}$)	BOD_5/COD	BOD_5/TOC ($mgO_2.mg^{-1}C$)	COD/TOC ($mgO_2.mg^{-1}C$)	AOS
0	78	106	223	27	0.121	0.346	2.858	-0.28
10	72	84	214	30	0.1401	0.416	2.972	-0.45
30	69	65	209	32	0.153	0.463	3.028	-0.54
60	65	41	203	34	0.167	0.523	3.123	-0.68
80		32.5					#¡DIV/0!	
90	63	28	157	36	0.229	0.571	2.492	0.26
% removal	19.2	73.5	29.5					

Degradation by Fenton reaction

A) Effect of H_2O_2

Table POH- H_2O_2/Fe(II)-1

Operational conditions				
[DCP]i ($mg.L^{-1}$)	H_2O_2 ($mg.L^{-1}$)	Fe(II) ($mg.L^{-1}$)	Temperature (ºC)	pH
100	60	10	25	free

Time (min)	POH ($mg.L^{-1}$)	TOC ($mgC.L^{-1}$)	COD ($mgO_2.L^{-1}$)	BOD_5 ($mgO_2.L^{-1}$)	BOD_5/COD	BOD_5/TOC ($mgO_2.mg^{-1}C$)	COD/TOC ($mgO_2.mg^{-1}C$)	AOS
0	102	78	222	27	0.121	0.346	2.84	-0.26
5	90	72						
20	57	69						
30	47	67	194	31	0.159	0.462	2.89	-0.34
40	41	66						
60	39	65	177	34	0.192	0.523	2.72	-0.08
% removal	61.7	16.6	20.2					

Table POH- H_2O_2/Fe(II)-2 Operational conditions

[DCP]i ($mg.L^{-1}$)	H_2O_2 ($mg.L^{-1}$)	Fe(II) ($mg.L^{-1}$)	Temperature (ºC)	pH
100	250	10	25	free

Time (min)	POH ($mg.L^{-1}$)	TOC ($mgC.L^{-1}$)	COD ($mgO_2.L^{-1}$)	BOD_5 ($mgO_2.L^{-1}$)	BOD_5/COD	BOD_5/TOC ($mgO_2.mg^{-1}C$)	COD/TOC ($mgO_2.mg^{-1}C$)	AOS
0	102	78	222	27	0.121	0.346	2.8	-0.26
5	77	74						
10	43.5	72	204	29	0.142		2.83	-0.25
20	27	70						
30	18	68	192	32	0.166	0.470	2.82	-0.23
40	15	65						
60	10	63	159	35	0.220	0.555	2.52	0.21
% removal	90.1	19.2	28.3					

B) effect of Fe(II

Table POH- H_2O_2/Fe(II)-3 Operational conditions

[DCP]i ($mg.L^{-1}$)	H_2O_2 ($mg.L^{-1}$)	Fe(II) ($mg.L^{-1}$)	Temperature (ºC)	pH
100	30	10	25	free

time (min)	POH ($mg.L^{-1}$)	TOC ($mgC.L^{-1}$)	COD ($mgO_2.L^{-1}$)	BOD_5 ($mgO_2.L^{-1}$)	BOD_5/COD	BOD_5/TOC ($mgO_2.mg^{-1}C$)	COD/TOC ($mgO_2.mg^{-1}C$)	AOS
0	102	78	222	27	0.121	0.346	2.84	-0.27
5	40	73						
10	16	70	190	32	0.168		2.71	-0.071
20	11	67						
30	5	64	180	35	0.194	0.546	2.81	-0.22
40	1	62						
60	0	61	135	38	0.281	0.622	2.21	0.68
% removal	100	21.7	39.18					

)

Table POH- H_2O_2/Fe(4II)-4
Operational conditions

[DCP]i ($mg.L^{-1}$)	H_2O_2 ($mg.L^{-1}$)	Fe(II) ($mg.L^{-1}$)	Temperature (ºC)	pH
100	30	45	25	free

time (min)	POH ($mg.L^{-1}$)	TOC ($mgC.L^{-1}$)	COD ($mgO_2.L^{-1}$)	BOD_5 ($mgO_2.L^{-1}$)	BOD_5/COD	BOD_5/TOC ($mgO_2.mg^{-1}C$)	COD/TOC ($mgO_2.mg^{-1}C$)	AOS
0	102	78	222	27	0.121	0.346	2.8461	-0.26
5	86	73						
10	71	70	205	30	0.146		2.928	-0.39
20	52	68						
30	44	66	191	32	0.167	0.484	2.893	-0.34
40	37	64						
60	31	63	172	35	0.203	0.555	2.730	-0.095
% removal	69.6	19.2	22.5					

Table POH- H_2O_2/Fe(II)-5 Operational conditions

[DCP]i ($mg.L^{-1}$)	H_2O_2 ($mg.L^{-1}$)	Fe(II) ($mg.L^{-1}$)	Temperature (ºC)	pH
100	30	60	25	free

time (min)	POH ($mg.L^{-1}$)	TOC ($mgC.L^{-1}$)	COD ($mgO_2.L^{-1}$)	BOD_5 ($mgO_2.L^{-1}$)	BOD_5/COD	BOD_5/TOC ($mgO_2.mg^{-1}C$)	COD/TOC ($mgO_2.mg^{-1}C$)	AOS
0	102	78	222	27	0.121	0.346	2.84	-0.26923077
5	82	71						
10	66	67	201	30	0.149			-0.5
20	46	65						
30	40	63	189	32	0.169	0.507		-0.5
40	34	62						
60	26	61	169	36	0.213	0.590	2.77	-0.15
% removal	74.5	21.8	23.9					

Table POH- H_2O_2/Fe(III)-6 Operational conditions

[DCP]i ($mg.L^{-1}$)	H_2O_2 ($mg.L^{-1}$)	Fe(II) ($mg.L^{-1}$)	Temperature (ºC)	pH
100	30	90	25	free

time (min)	POH ($mg.L^{-1}$)	TOC ($mgC.L^{-1}$)	COD ($mgO_2.L^{-1}$)	BOD_5 ($mgO_2.L^{-1}$)	BOD_5/COD	BOD_5/TOC ($mgO_2.mg^{-1}C$)	COD/TOC ($mgO_2.mg^{-1}C$)	AOS
0	102	78	222	27	0.121	0.346	2.84	-0.26
5	84	73						
10	72	71	206	31	0.150		2.90	-0.35
20	50	68						
30	43	66	193	33	0.170	0.500	2.92	-0.38
40	38	64						
60	34	63	168	37	0.220	0.587	2.66	
% removal	66.6	19.2	24.3					

Degradation of POH by modified Fenton

Table POH- H_2O_2/Fe(III)-1 Operational conditions

[DCP]i ($mg.L^{-1}$)	H_2O_2 ($mg.L^{-1}$)	Fe(III) ($mg.L^{-1}$)	Temperature (ºC)	pH
100	60	10	25	free

time (min)	POH ($mg.L^{-1}$)	TOC ($mgC.L^{-1}$)	COD ($mgO_2.L^{-1}$)	BOD_5 ($mgO_2.L^{-1}$)	BOD_5/COD	BOD_5/TOC ($mgO_2.mg^{-1}C$)	COD/TOC ($mgO_2.mg^{-1}C$)	AOS
0	102	78	222	27	0.121	0.346	2.84	-0.26
5	82	75						
10	68	72	221	28	0.12		30.72	
20	56	70						
30	48	68	198	30	0.151	0.441	2.91	-0.36
40	44	67						
60	42	65.5	168	32	0.190	0.488	2.56	0.15
% removal	58.8	16.0	24.3					

Table POH- H_2O_2/Fe(III)-2 Operational conditions

[DCP]i ($mg.L^{-1}$)	H_2O_2 ($mg.L^{-1}$)	Fe(III) ($mg.L^{-1}$)	Temperature (ºC)	pH
100	250	10	25	free

time (min)	POH ($mg.L^{-1}$)	TOC ($mgC.L^{-1}$)	COD ($mgO_2.L^{-1}$)	BOD_5 ($mgO_2.L^{-1}$)	BOD_5/COD	BOD_5/TOC ($mgO_2.mg^{-1}C$)	COD/TOC ($mgO_2.mg^{-1}C$)	AOS
0	102	78	222	27	0.121	0.346	2.84	-0.26
5	73	74						
10	48	71	200	30	0.15		2.81	-0.22
20	29	69						
30	20	67	188	33	0.175	0.492	2.80	-0.21
40	16	65						
60	13	63	154	37	0.240	0.587	2.44	0.33
% removal	87.2	19.2	30.6					

Table POH- H_2O_2/Fe(III)-3
Operational conditions

[DCP]i ($mg.L^{-1}$)	H_2O_2 ($mg.L^{-1}$)	Fe(III) ($mg.L^{-1}$)	Temperature (ºC)	pH
100	350	10	25	free

time (min)	POH ($mg.L^{-1}$)	TOC ($mgC.L^{-1}$)	COD ($mgO_2.L^{-1}$)	BOD_5 ($mgO_2.L^{-1}$)	BOD_5/COD	BOD_5/TOC ($mgO_2.mg^{-1}C$)	COD/TOC ($mgO_2.mg^{-1}C$)	AOS
0	102	78	222	27	0.121	0.346	2.84	-0.26
5	55	74						
10	40	71	192	31	0.161		2.70	-0.056
20	30	68						
30	20	65	184	34	0.184	0.523	2.83	-0.25
40	13	63						
60	3	61	149	37	0.248	0.606	2.44	0.34
% removal	98.0	21.7	32.8					

Degradation of POH by photo-Fenton
A) Effect of H_2O_2
Table POH- H_2O_2/PHF-1 Operational conditions

[DCP]i ($mg.L^{-1}$)	H_2O_2 ($mg.L^{-1}$)	Fe(III) ($mg.L^{-1}$)	Temperature (ºC)	pH
100	30	10	25	free

time (min)	POH ($mg.L^{-1}$)	TOC ($mgC.L^{-1}$)	COD ($mgO_2.L^{-1}$)	BOD_5 ($mgO_2.L^{-1}$)	BOD_5/COD	BOD_5/TOC ($mgO_2.mg^{-1}C$)	COD/TOC ($mgO_2.mg^{-1}C$)	AOS
0	102	78	222	27	0.122	0.346	2.84	-0.26
2	85	74						
5	70	69	205	29	0.141		2.97	-0.45
10	40	64	190	31	0.163	0.484	2.96	-0.45
15	22	62.5	170	35				
					0.205	0.560	2.72	-0.08
	78.4	19.8	23.4					

Table POH- H_2O_2/PHF-2 Operational conditions

[DCP]i ($mg.L^{-1}$)	H_2O_2 ($mg.L^{-1}$)	Fe(III) ($mg.L^{-1}$)	Temperature (ºC)	pH
100	120	10	25	free

time (min)	POH ($mg.L^{-1}$)	TOC ($mgC.L^{-1}$)	COD ($mgO_2.L^{-1}$)	BOD_5 ($mgO_2.L^{-1}$)	BOD_5/COD	BOD_5/TOC ($mgO_2.mg^{-1}C$)	COD/TOC ($mgO_2.mg^{-1}C$)	AOS
0	102	78	222	27	0.121	0.346	2.84	-0.26
2	77	71						
5	43.5	67	204	29	0.142		3.04	-0.56
8	27	65						
10	22	63	192	32	0.166	0.508	3.04	-0.57
15	18	62	159	38	0.239	0.612	2.56	0.15
% removal	82.3	20.5	28.3					

Table POH- H_2O_2/PHF-3 Operational conditions

[DCP]i ($mg.L^{-1}$)	H_2O_2 ($mg.L^{-1}$)	Fe(III) ($mg.L^{-1}$)	Temperature (ºC)	pH
100	220	10	25	free

time (min)	POH ($mg.L^{-1}$)	TOC ($mgC.L^{-1}$)	COD ($mgO_2.L^{-1}$)	BOD_5 ($mgO_2.L^{-1}$)	BOD_5/COD	BOD_5/TOC ($mgO_2.mg^{-1}C$)	COD/TOC ($mgO_2.mg^{-1}C$)	AOS
0	102	78	222	27	0.122	0.346	2.84	-0.26
2	70	70						
5	36	68	190	32	0.168		2.79	-0.19
8	24	65						
10	19	63	180	35	0.194	0.555	2.85	-0.28
15	14	61	135	44	0.325	0.721	2.21	0.68
% removal	86.2	21.7	39.1					

Table POH- H_2O_2/PHF-4 Operational conditions

[DCP]i ($mg.L^{-1}$)	H_2O_2 ($mg.L^{-1}$)	Fe(III) ($mg.L^{-1}$)	Temperature (ºC)	pH
100	200	60	25	Free

time (min)	POH ($mg.L^{-1}$)	TOC ($mgC.L^{-1}$)
0	100	80
2	77	77
4	55	75.55
6	32	70
8	22	67
10	9	63.4
% removal	91	20.75

Table POH- H_2O_2/PHF-5 Operational conditions

[DCP]i ($mg.L^{-1}$)	H_2O_2 ($mg.L^{-1}$)	Fe(III) ($mg.L^{-1}$)	Temperature (ºC)	pH
100	100	60	25	Free

time (min)	POH ($mg.L^{-1}$)	TOC ($mgC.L^{-1}$)
0	100	77
2	85	74
4	65	72
6	40	71
8	32	69
10	10	60.3
% removal	90	21.6

Table POH- H_2O_2/PHF-6 Operational conditions

[DCP]i ($mg.L^{-1}$)	H_2O_2 ($mg.L^{-1}$)	Fe(III) ($mg.L^{-1}$)	Temperature (ºC)	pH
100	300	60	25	Free

time (min)	POH ($mg.L^{-1}$)	TOC ($mgC.L^{-1}$)
0	95	60
2	72	58
4	50	55
6	38	50
8	15	45
10	0	42.8
% removal	100	28.6

Table POH- H_2O_2/PHF-7 Operational conditions

[DCP]i ($mg.L^{-1}$)	H_2O_2 ($mg.L^{-1}$)	Fe(III) ($mg.L^{-1}$)	Temperature (ºC)	pH
100	50	60	25	Free

time (min)	POH ($mg.L^{-1}$)	TOC ($mgC.L^{-1}$)
0	100	76
2	75	74
4	54	72
6	42	71
8	20	65
10	12	60.4
% removal	88	20.5

B) Effect of Fe(II)

Table POH- H_2O_2/PHF-9 Operational conditions

[DCP]i ($mg.L^{-1}$)	H_2O_2 ($mg.L^{-1}$)	Fe(III) ($mg.L^{-1}$)	Temperature (ºC)	pH
100	50	30	25	Free

i

time (min)	POH ($mg.L^{-1}$)	TOC ($mgC.L^{-1}$)
0	100	83.47
2	75	80
4	54	77
6	42	76.5
10	33	75
15	28	74.9
% removal	72	10.2

Table POH- H_2O_2/PHF-10 Operational conditions

[DCP]i ($mg.L^{-1}$)	H_2O_2 ($mg.L^{-1}$)	Fe(III) ($mg.L^{-1}$)	Temperature (ºC)	pH
100	50	75	25	Free

Time (min)	POH ($mg.L^{-1}$)	TOC ($mgC.L^{-1}$)
0	100	77
2	75	74
4	54	73
6	42	72
8	20	70
10	10	62.4
% removal	90	18.9

Table POH- H_2O_2/PHF-11 Operational conditions

[DCP]i ($mg.L^{-1}$)	H_2O_2 ($mg.L^{-1}$)	Fe(III) ($mg.L^{-1}$)	Temperature (ºC)	pH
100	50	90	25	Free

time (min)	POH ($mg.L^{-1}$)	TOC ($mgC.L^{-1}$)
0	100	81
2	75	74
4	54	73
6	42	72
8	20	70
10	14	65.5
% removal	86	19.1358025

POH- H_2O_2/PHF-12
Operational conditions

H_2O_2 ($mg.L^{-1}$)	Fe(III) ($mg.L^{-1}$)	Temperature (ºC)	pH
50	60	25	Free

	$[poh]_I$= 100 ($mg.L^{-1}$)		$[poh]_I$= 150 ($mg.L^{-1}$)		$[poh]_I$= 200 ($mg.L^{-1}$)	
time (min)	POH	TOC(ppm)	POH ($mg.L^{-1}$)	TOC ($mgC.L^{-1}$)	POH ($mg.L^{-1}$)	TOC ($mgC.L^{-1}$)
0	100	81	150	114	200	153
2	75	74	125	110	175	148
6	42	71	85	105	135	140
10	20	70	65	103	120	137
15	12	69	50	100	110	135
% removal	88	14.8	66.6	12.2	45	11.7

High concentrated POH solutions
POH- H_2O_2/PHF-13

Run	H_2O_2 ($mg.L^{-1}$)	Fe(II) ($mg.L^{-1}$)	BOD_5 ($mg\ O_2.L^{-1}$)	TOC ($mg.L^{-1}$)	COD ($mg\ O_2.L^{-1}$)	BOD_5/COD	COD/TOC ($mg\ O_2$/mg C)
Phenol (1000$mg.L^{-1}$)	-	-	35	766	2020	0.0173	2.63
1	100	60	20	760	1760	0.011	2.31
2	200	60	55	600	1350	0.041	2.25
4	400	60	70	593	1292	0.054	2.18
6	600	60	240	740	1580	0.152	2.13
7	1000	60	300	703	1500	0.200	2.13
8	2000	60	120	570	520	0.231	0.91
9	3000	60	130	639	330	0.394	0.52
10	500	1000	40	686	2000	0.020	3.29
11	1000	1000	400	508	1407	0.284	2.76
12	2000	1000	200	260	563	0.355	2.16
13	3000	1000	180	213	264	0.681	1.24
14	3500	1000	210	427	290	0.724	0.72
15	1000	240	420	608	1341	0.313	2.21
16	1000	500	340	585	1223	0.278	2.09
17	1000	1500	430	480	1431	0.300	2.98
19	2000	240	220	700	1060	0.207	1.51
20	2000	500	220	332	544	0.404	1.64
21	2000	1000	200	260	563	0.355	2.16
22	2000	1500	260	327	753	0.345	2.30
23	3000	60	130	639	330	0.394	0.52
24	3000	240	275	435	613	0.448	1.41
25	3000	500	260	366	499	0.521	1.36
26	3000	1000	180	213	264	0.682	1.24
27	3000	1500	285	200	309	0.922	1.54

Kinetic results of DCP treated solution biodegradation

Acclimated reactor

Table DCP-BIO-1

TVSS ($mg.L^{-1}$)	HRT (day)	Fe(II) ($mg.L^{-1}$)	Temperature (ºC)	pH
350	2	10	22	7.2

Time (min)	TOC ($mg.L^{-1}$)	S ($mgTOC.L^{-1}$)	S/S_0
0	37.5	37.50	1.000
15	37.3	37.30	0.994
30	34.8	34.80	0.928
45	33.2	33.20	0.885
60	32	32.00	0.853
90	28.8	28.80	0.768
105	27.4	27.40	0.731
120	24	24.00	0.640
150	22.8	23	0.608
180	22.5	23	0.600
210	22.1	22	0.589
240	21.8	22	0.581
360	20.4	20	0.544
420	20	20	0.533
480	18.7	19	0.499
540	18.34	18	0.489
720	17.78	18	0.474
1470	15.1	15	0.403

Table DCP-BIO-2

TVSS ($mg.L^{-1}$)	HRT (day)	Fe(II) ($mg.L^{-1}$)	Temperature (ºC)	pH
130	12	10	22	7.2

Time (min)	TOC ($mg.L^{-1}$)	S ($mgTOC.L^{-1}$)	S/S_0
0	34.79	34.79	1.000
15	34	34.00	0.977
30	32	32.00	0.920
60	28	28.00	0.805
90	26.4	26.40	0.759
120	25	25.00	0.719
150	23	23.00	0.661
180	21.5	21.50	0.618
240	19	19.00	0.546
300	16	16.00	0.460
420	15.8	15.80	0.454
540	15.3	15.30	0.440
660	15	15.00	0.431

Non-acclimated reactor

Table DCP-BIO-3

TVSS ($mg.L^{-1}$)	HRT (day)	Fe(II) ($mg.L^{-1}$)	Temperature (ºC)	pH
350	2	10	22	7.2

Time (min)	TOC ($mg.L^{-1}$)	S ($mgTOC.L^{-1}$)	S/S_0
0	24.7	24.7	1.000
15	23.8	24.1	0.976
30	23.7	23.6	0.955
45	23	23.1	0.935
60	22.6	22	0.891
90	21.2	21	0.850
120	19.4	19.4	0.785
150	18.39	18.39	0.745
180	16	16	0.648
240	14	14	0.567
300	12.4	12	0.486
420	10.73	10.73	0.434
540	10.6	10.6	0.429
660	10.3	10	0.4048583

Table DCP-BIO-

TVSS ($mg.L^{-1}$)	HRT (day)	Fe(II) ($mg.L^{-1}$)	Temperature (ºC)	pH
130	1	10	22	7.2

Time (min)	TOC ($mg.L^{-1}$)	S ($mgTOC.L^{-1}$)	S/S_0
0	27.8	27.8	1.000
30	26	26.0	0.935
60	24.68	24.7	0.888
90	24.5	24.5	0.881
120	21.8	21.8	0.784
150	20.8	20.8	0.748
180	18.5	18.5	0.665
240	16.8	16.8	0.604
360	13.5	13.0	0.468
480	11.8	11.0	0.396
540	10.8	10.0	0.360
660	9.9	9.7	0.349
1680	9.8	9.6	0.345

Multi lamps reactor
Degradation of 2.4-DCP by direct UVA-light

Table DCP-UVA

Operational conditions

[DCP]i ($mg.L^{-1}$)	Temperture (ºC)	pH
100	25	free

Time (min)	TOC ($mgC.L^{-1}$)	DCP ($mg.L^{-1}$)	COD ($mgO_2.L^{-1}$)	BOD_5 ($mgO_2.L^{-1}$)	AOS	COD/TOC ($mgO_2.mg^{-1}C$)
0	39.7	95.0	120	0	-0.5340	3.02
10	39.2	91.0	115		-0.4005	2.93
20	39.0	88.5			4.0000	0.00
40	38.7	86.0	111	0	-0.3023	2.87
60	38.4	83.0			4.0000	0.00
90	38.0	78.0	109		-0.3026	2.87
120	37.5	74.0			4.0000	0.00
180	37.0	70.0	100	.0	-0.0541	2.70
%removal	6.8	26.3				

Degradation of 2.4-DCP by direct UVA/H_2O_2

Table DCP-UVA/H_2O_2 –1 Operational conditions

[DCP]i ($mg.L^{-1}$)	H_2O_2 ($mg.L^{-1}$)	Temperature (ºC)	pH
100	15	25	free

Time (min)	TOC ($mgC.L^{-1}$)	DCP ($mg.L^{-1}$)	COD ($mgO_2.L^{-1}$)	BOD_5 ($mgO_2.L^{-1}$)	AOS	COD/TOC ($mgO_2.mg^{-1}C$)
0	40.8	100.0	122		-0.4853	2.99
10	40.2	95.0				
20	39.8	91.0	114		-0.2965	2.86
40	39.0	87.0	107	0	-0.1154	2.74
60	38.2	82.0	104		-0.0838	2.72
90	37.3	77.0				
120	36.8	72.0	99	0	-0.0353	2.69
%removal	9.8	28.0	18.9			

Table DCP-UVA/H_2O_2 –2 Operational conditions

[DCP]i ($mg.L^{-1}$)	H_2O_2 ($mg.L^{-1}$)	Temperature (ºC)	pH
100	50	25	free

Time (min)	TOC ($mgC.L^{-1}$)	DCP ($mg.L^{-1}$)	COD ($mgO_2.L^{-1}$)	BOD_5 ($mgO_2.L^{-1}$)	AOS	COD/TOC ($mgO_2.mg^{-1}C$)
0	40.0	98.0	123		-0.6125	3.08
20	38.5	80.0	109		-0.2468	2.83
40	37.6	74.0	102	0	-0.0691	2.71
60	36.2	69.0				
90	35.6	65.0				
120	35.5	61.0	92	0	0.1127	2.59
%removal	11.3	37.8				

Table DCP-UVA/H_2O_2 –2 Operational conditions

[DCP]i ($mg.L^{-1}$)	H_2O_2 ($mg.L^{-1}$)	Temperature (ºC)	pH
100	100	25	free

Time (min)	TOC ($mgC.L^{-1}$)	DCP ($mg.L^{-1}$)	COD ($mgO_2.L^{-1}$)	BOD_5 ($mgO_2.L^{-1}$)	AOS	COD/TOC ($mgO_2.mg^{-1}C$)
0	39.5	98.0	122		-0.6329	3.09
10	39.2	86.0				
20	38.4	78.0	111		-0.3359	2.89
40	37.6	70.0		0		
60	36.2	65.0	96		0.0221	2.65
90	35.4	60.0				0.00
120	34.0	55.0	92		-0.0588	2.71
%removal	13.9	43.9				

Table DCP-UVA/H_2O_2 –2 Operational conditions

[DCP]i ($mg.L^{-1}$)	H_2O_2 ($mg.L^{-1}$)	Temperature (ºC)	pH
100	200	25	free

Time (min)	TOC ($mgC.L^{-1}$)	DCP ($mg.L^{-1}$)	COD ($mgO_2.L^{-1}$)	BOD_5 ($mgO_2.L^{-1}$)	AOS	COD/TOC ($mgO_2.mg^{-1}C$)
0	40.0	98.0	122		-0.5750	3.05
10	39.5	85.0				
20	38.7	74.0				
40	36.7	67.0	95	0	0.1172	2.59
60	36.2	62.0				
90	35.4	58.0				
120	34.3	50.0	85	6	0.2828	2.48
%removal	14.3	49.0				

Table DCP-UVA/H_2O_2 –5 Summary
Operational conditions

[DCP]i ($mg.L^{-1}$)	Temperature (ºC)	pH
100	25	free

H_2O_2 ($mg.L^{-1}$)	DCP%	TOC%	COD ($mgO_2.L^{-1}$)	BOD ($mgO_2.L^{-1}$)	BOD_5/COD	BOD/TOC ($mgO_2.mg^{-1}C$)
15	28.0	9.8	107	0	0.0000	0
30	31.0	12.2	97	0	0.0000	0
50	37.8	11.3	92	0	0.0000	0
70	39.0	13.8	92	1	0.0109	0.0256
100	43.9	13.9	92	3	0.0326	0.068
200	49.0	14.25	85	5	0.0588	0.102

Degradation of 2.4-DCP by UVA/Fe(III)

Table DCP-UVA/Fe(III) –1 Operational conditions

[DCP]i ($mg.L^{-1}$)	Fe(III) ($mg.L^{-1}$)	Temperature (ºC)	pH
100	20	25	free

Time (min)	TOC ($mgC.L^{-1}$)	DCP ($mg.L^{-1}$)	COD ($mgO_2.L^{-1}$)	BOD_5 ($mgO_2.L^{-1}$)	AOS	COD/TOC ($mgO_2.mg^{-1}C$)
0	40.9	100.0	126	0	-0.6244	3.08
5	40.1	97.0				
10	39.7	92.0				
20	39.3	88.0	110		-0.1985	2.80
30	39.0	83.0				
40	38.5	78.0				
50	38.1	76.0	100		0.0630	2.62
60	37.3	72.0				
80	37.0	67.0				
90	36.8	62.0	93	0	0.2092	2.53
%removal	10.0	38.0				

Table DCP-UVA/Fe(III) –2 Operational conditions

[DCP]i ($mg.L^{-1}$)	Fe(III) ($mg.L^{-1}$)	Temperature (ºC)	pH
100	70	25	free

Time (min)	TOC ($mgC.L^{-1}$)	DCP ($mg.L^{-1}$)	COD ($mgO_2.L^{-1}$)	BOD_5 ($mgO_2.L^{-1}$)	AOS	COD/TOC ($mgO_2.mg^{-1}C$)
0	42.3	100.0	125	0	-0.4326	2.96
5	41.5	93.0				
10	40.8	87.0	111		-0.0809	2.72
20	39.8	80.0				
30	39.2	75.0	103		0.0587	2.63
40	38.2	69.0				
60	37.2	58.0				
90	36.2	50.0	90		0.2707	2.49

Table DCP-UVA/Fe(III) –3 Operational conditions

[DCP]i ($mg.L^{-1}$)	Fe(III) ($mg.L^{-1}$)	Temperature (ºC)	pH
100	100	25	free

Time (min)	TOC ($mgC.L^{-1}$)	DCP ($mg.L^{-1}$)	COD ($mgO_2.L^{-1}$)	BOD_5 ($mgO_2.L^{-1}$)	AOS	COD/TOC ($mgO_2.mg^{-1}C$)
0	41.5	101.0	125	0	-0.5181	3.01
5	41.0	90.0				
15	40.2	80.0	115		-0.2910	2.86
20	39.7	72.0				
40	38.7	56.0	106		-0.1085	2.74
60	37.8	41.0	93		0.3095	2.46
70	37.2	38.0				
90	36.9	30.0	78	0	0.8293	2.11
%removal	11.1	70.3				

Degradation of 2.4-DCP by photo-Fenton process

A) Effect of initial H_2O_2

Table DCP-PHFA-1 Operational conditions

[DCP]I ($mg.L^{-1}$)	H_2O_2 ($mg.L^{-1}$)	Fe(II) ($mg.L^{-1}$)	Temperature (ºC)	pH
100	15	10	25	free

Time (min)	TOC ($mgC.L^{-1}$)	DCP ($mg.L^{-1}$)	COD ($mgO_2.L^{-1}$)	BOD_5 ($mgO_2.L^{-1}$)	AOS	COD/TOC ($mgO_2.mg^{-1}C$)
0	40	96.5	125	0	-0.69	3.125
10	38	77				
15	38.5	73	115		-0.48	2.987
30	36	48	106		-0.42	2.944
35	35.5	34	96	3	-0.06	2.704
%removal	11.25	64.7				

Table DCP-PHFA-2 Operational conditions

[DCP]i ($mg.L^{-1}$)	H_2O_2 ($mg.L^{-1}$)	Fe(II) ($mg.L^{-1}$)	Temperature (ºC)	pH
100	30	10	25	free

Time (min)	TOC ($mgC.L^{-1}$)	DCP ($mg.L^{-1}$)	COD ($mgO_2.L^{-1}$)	BOD_5 ($mgO_2.L^{-1}$)	AOS	COD/TOC ($mgO_2.mg^{-1}C$)	cl-
0	44	107	135		-0.60	3.068	0
15	40	63	118		-0.43	2.950	15
30	39.4	32	105		0.00	2.665	21
35	39	16	85	4	0.73	2.179	26
%removal	11.3	85.0					

Table DCP-PHFA-3 Operational conditions

[DCP]i ($mg.L^{-1}$)	H_2O_2 ($mg.L^{-1}$)	Fe(II) ($mg.L^{-1}$)	Temperature (ºC)	pH
100	55	10	25	free

Time (min)	TOC ($mgC.L^{-1}$)	DCP ($mg.L^{-1}$)	COD ($mgO_2.L^{-1}$)	BOD_5 ($mgO_2.L^{-1}$)	AOS	COD/TOC ($mgO_2.mg^{-1}C$)
0	42.83	106.77	134	0	-0.69	3.129
5	41.9	83		0		
10	41.4	76	123	0	-0.46	2.971
15	41	60	112	0	-0.10	2.732
20	39.8	40		1		
30	38.7	27	99	4	0.16	2.558
35	37.9	5	80	6	0.83	2.111
%removal	11.5	95.3				

Table DCP-PHFA-4 Operational conditions

[DCP]i ($mg.L^{-1}$)	H_2O_2 ($mg.L^{-1}$)	Fe(II) ($mg.L^{-1}$)	Temperature (ºC)	pH
100	65	10	25	free

Time (min)	TOC ($mgC.L^{-1}$)	DCP ($mg.L^{-1}$)	COD ($mgO_2.L^{-1}$)	BOD_5 ($mgO_2.L^{-1}$)	AOS	COD/TOC ($mgO_2.mg^{-1}C$)	cl^- ($mg.L^{-1}$)
0	42.8	104.5	135		3.152	-0.73	0
5	41.0	73					
10	40.3	58	120		2.978	-0.47	12
15	40	40	107		2.675	-0.01	18
20	38.9	20					
30	39.6	5.5	94		2.374	0.44	28
35	38.0	0	73	7	1.921	1.12	30
%removal	11.2	100					

Table DCP-PHFB-5

Operational conditions summary

[DCP]i ($mg.L^{-1}$)	Fe(II) ($mg.L^{-1}$)	Temperature (ºC)	PH
100	10	25	free

H_2O_2 ($mgO_2.L^{-1}$)	%DCP	%TOC	BOD_5/COD	BOD_{21} ($mgO_2.L^{-1}$)	BOD_{21}/COD	BOD_5/TOC ($mgO_2.mg^{-1}C$)	BOD_{21}/TOC ($mgO_2.mg^{-1}C$)
0	0.0	7.9	0.0000	0	0.0000	0.0000	0
5	20.0	8.1	0.0000	0	0.0000	0.0000	0
8	40.0	8.2	0.0093	1	0.0093	0.0253	0.0252
10	50.0	8.2	0.0196	2	0.0196	0.0528	0.053
15	64.8	11.3	0.0313	3	0.0313	0.0845	0.084
30	85.0	11.4	0.0588	5	0.0588	0.1282	0.128
55	95.3	11.5	0.1250	11	0.1375	0.2639	0.290
65	100.0	11.3	0.1507	12	0.1644	0.2895	0.315
70	100.0	11.5	0.2143	15	0.2143	0.3958	0.395
120	100.0	11.9	0.3538	24	0.3692	0.6117	0.638

140	100.0	12	0.4833	30	0.5000	0.7754	0.802

Table DCP-PHFA-6 Operational conditions

[DCP]i ($mg.L^{-1}$)	H_2O_2 ($mg.L^{-1}$)	Fe(II) ($mg.L^{-1}$)	Temperature (ºC)	pH
100	15	30	25	free

Time (min)	TOC ($mgC.L^{-1}$)	DCP ($mg.L^{-1}$)	COD ($mgO_2.L^{-1}$)	BOD_5 ($mgO_2.L^{-1}$)	AOS	COD/TOC ($mgO_2.mg^{-1}C$)
0	40.5	101.3	132		-0.89	3.259
5	40	78				
10	39.9	66				
15	38.6	50	115		-0.47	2.979
20	37.7	39	105		-0.18	2.785
30	36.3	29				
35	35.5	17	81	5	0.58	2.282
%removal	12.3	83.21				

Table DCP-PHFA-7 Operational conditions

[DCP]i ($mg.L^{-1}$)	H_2O_2 ($mg.L^{-1}$)	Fe(II) ($mg.L^{-1}$)	Temperature (ºC)	pH
100	30	30	25	free

Time (min)	TOC ($mgC.L^{-1}$)	DCP ($mg.L^{-1}$)	COD ($mgO_2.L^{-1}$)	BOD_5 ($mgO_2.L^{-1}$)	AOS	COD/TOC ($mgO_2.mg^{-1}C$)
0	41	102	133	0	3.244	-0.87
5	40	72				
10	39	61				
15	38.5	47	110		2.857	-0.29
20	38	33				
30	37	23	97		2.622	0.07
35	36	8	77	6	2.139	0.79
%removal	12.19	92.15				

Table DCP-PHFA-8 Operational conditions

[DCP]i ($mg.L^{-1}$)	H_2O_2 ($mg.L^{-1}$)	Fe(II) ($mg.L^{-1}$)	Temperature (ºC)	pH
100	60	30	25	free

Time (min)	TOC ($mgC.L^{-1}$)	DCP ($mg.L^{-1}$)	COD ($mgO_2.L^{-1}$)	BOD_5 ($mgO_2.L^{-1}$)	AOS	COD/TOC ($mgO_2.mg^{-1}C$)
0	42	106	133		-0.75	3.167
5	39.5	50				
10	38	33				
15	37.5	11	102		-0.08	2.720
20	37	4				
30	36.9	0	89		0.38	2.412
35	36.5	0	74	9	0.96	2.027
%removal	13.1	100				

B) Effect of initial Fe(II)

Table DCP-PHFA-9 Operational conditions

[DCP]I ($mg.L^{-1}$)	H_2O_2 ($mg.L^{-1}$)	Fe(II) ($mg.L^{-1}$)	Temperature (ºC)	pH
100	15	15	25	free

Time (min)	TOC ($mgC.L^{-1}$)	DCP ($mg.L^{-1}$)	COD ($mgO_2.L^{-1}$)	BOD_5 ($mgO_2.L^{-1}$)	AOS	COD/TOC ($mgO_2.mg^{-1}C$)
0	40	96.5	125	0	-0.69	3.125
5	39.12	85				
10	38	77				
15	38.5	73	115		-0.48	2.987
20	37	61				
30	36	48	106		-0.42	2.944
35	35.5	34	96	3	-0.06	2.704
%removal	11.25	64.7				

Table DCP-PHFA-10 Operational conditions

[DCP]i ($mg.L^{-1}$)	H_2O_2 ($mg.L^{-1}$)	Fe(II) ($mg.L^{-1}$)	Temperature (ºC)	pH
100	15	30	25	free

Time (min)	TOC ($mgC.L^{-1}$)	DCP ($mg.L^{-1}$)	COD ($mgO_2.L^{-1}$)	BOD_5 ($mgO_2.L^{-1}$)	AOS	COD/TOC ($mgO_2.mg^{-1}C$)
0	40.5	101.3	132		3.259	-0.89
5	40	78				
10	39.9	66				
15	38.6	50	115		2.979	-0.47
20	37.7	39	105		2.785	-0.18
30	36.3	29				
35	35.5	17	81	5	2.282	0.58
%removal	12.3	83.2				4.00

Table DCP-PHFA-11 Operational conditions

[DCP]i ($mg.L^{-1}$)	H_2O_2 ($mg.L^{-1}$)	Fe(II) ($mg.L^{-1}$)	Temperature (ºC)	pH
100	15	60	25	free

Time (min)	TOC ($mgC.L^{-1}$)	DCP ($mg.L^{-1}$)	COD ($mgO_2.L^{-1}$)	BOD_5 ($mgO_2.L^{-1}$)	AOS	COD/TOC ($mgO_2.mg^{-1}C$)
0	40.5	102	134		3.309	-0.96
5	40	71				
10	39	59				
15	38.1	46	112		2.940	-0.41
20	37.2	33				
30	36	19	99		2.750	-0.13
35	35.3	0	77	10	2.181	0.73
%removal	12.8	100				

Table DCP-PHFA-12

Operational conditions Summary

[DCP]i ($mg.L^{-1}$)	H_2O_2 ($mg.L^{-1}$)	Temperature (ºC)	pH
100	15	25	free

Fe(II) ($mg.L^{-1}$)	BOD_5 ($mgO_2.L^{-1}$)	BOD_5/COD	BOD_5/TOC ($mgO_2.mg^{-1}C$)	COD/TOC ($mgO_2.mg^{-1}C$)	AOS	BOD_{21} ($mgO_2.L^{-1}$)	BOD_{21}/COD
10	3	0.031	0.08	2.70	-0.05	4	0.041
20	3	0.035	0.08	2.29	0.55	5	0.058
30	5	0.061	0.14	2.28	0.58	6	0.074
50	7	0.088	0.19	2.22	0.66	8	0.110
60	10	0.12	0.28	2.18	0.73	12	0.156

Mineralization

Table DCP-PHFB-13 Operational conditions

[DCP]i ($mg.L^{-1}$)	Fe(II) ($mg.L^{-1}$)	Temperature (ºC)	pH
200	40	25	free

t (min)	[H2O2]=50 ($mg.L^{-1}$)	[H2O2]=100 ($mg.L^{-1}$)	[H2O2]=200 ($mg.L^{-1}$)	[H2O2]=340 ($mg.L^{-1}$)	[H2O2]=380 ($mg.L^{-1}$)	[H2O2]=410 ($mg.L^{-1}$)
0	41.500	41.3	41.5	40.4	41.0	40.9
5	40.800	38.5	37.0	36.2	32.8	29.0
10	40.000	36.7	32.0	29.0	24.5	20.0
15	39.000	35.0	28.0	24.0	20.5	12.0
20	38.000	34.0	26.0	18.0	12.5	5.0
35	37.200	31.0	22.5	12.0	4.0	0.0

Single lamp reactor
Degradation of 2.4-DCP by direct UV-light

Table DCP-UVA Operational conditions

[DCP]i ($mg.L^{-1}$)	Temperture (ºC)	pH
100	25	free

Time (min)	TOC ($mgC.L^{-1}$)	DCP ($mg.L^{-1}$)	COD ($mgO_2.L^{-1}$)	BOD_5 ($mgO_2.L^{-1}$)	AOS	COD/TOC ($mgO_2.mg^{-1}C$)
0	39.7	95.0	118	0.0	-0.4584	2.97
20	39.2	92.0				
40	39.0	91.0	113		-0.3462	2.90
60	38.7	91.0				
90	38.6	90.0	111		-0.3135	2.88
180	38.2	88.0	109	0.0	-0.2801	2.85

Degradation of 2.4-DCP by direct UVA/H_2O_2

Table DCP-UVA/H_2O_2 –1 Operational conditions

[DCP]i ($mg.L^{-1}$)	H_2O_2 ($mg.L^{-1}$)	Temperature (ºC)	pH
100	15	25	free

Time (min)	TOC ($mgC.L^{-1}$)	DCP ($mg.L^{-1}$)	COD ($mgO_2.L^{-1}$)	BOD_5 ($mgO_2.L^{-1}$)	AOS	COD/TOC ($mgO_2.mg^{-1}C$)
0	40.8	100.0	124		-0.5588	3.04
10	40.3	98.0				
20	39.9	95.0	116		-0.3609	2.91
40	39.0	94.9	110	0	-0.2308	2.82
60	38.4	92.0	106		-0.1406	2.76
90	37.5	91.0				
120	37.0	90.0	103	0	-0.1757	2.78
%removal	9.3	9.0				

Table DCP-UVA/H_2O_2 –2 Operational conditions

[DCP]i ($mg.L^{-1}$)	H_2O_2 ($mg.L^{-1}$)	Temperature (ºC)	pH
100	50	25	free

Time (min)	TOC ($mgC.L^{-1}$)	DCP ($mg.L^{-1}$)	COD ($mgO_2.L^{-1}$)	BOD_5 ($mgO_2.L^{-1}$)	AOS	COD/TOC ($mgO_2.mg^{-1}C$)
0	38.0	91.0	115		-0.5395	3.03
10	35.5	88.0				
20	34.5	84.0	109		-0.7391	3.16
40	34.0	80.0	105	0	-0.6324	3.09
60	33.8	77.0				
90	33.8	69.0				
120	33.4	68.0	100		-0.4910	2.99
	12.1	25.3				

Table DCP-UVA/H_2O_2 –3 Operational conditions

[DCP]i ($mg.L^{-1}$)	H_2O_2 ($mg.L^{-1}$)	Temperature (ºC)	pH
100	30	25	free

Time (min)	TOC ($mgC.L^{-1}$)	DCP ($mg.L^{-1}$)	COD ($mgO_2.L^{-1}$)	BOD_5 ($mgO_2.L^{-1}$)	AOS	COD/TOC ($mgO_2.mg^{-1}C$)
0	39.0	95.0	120		-0.61538	3.08
10	38.0	94.0				
20	37.0	93.0	115		-0.66216	3.11
40	36.5	89.0	110		-0.52055	3.01
60	36.0	84.0				
120	35.0	77.0	104	0	-0.45714	2.97
%removal	10.3	18.9				

Table DCP-UVA/H_2O_2 –4 Operational conditions

[DCP]i ($mg.L^{-1}$)	H_2O_2 ($mg.L^{-1}$)	Temperature (ºC)	pH
100	30	25	free

Time (min)	TOC ($mgC.L^{-1}$)	DCP ($mg.L^{-1}$)	COD ($mgO_2.L^{-1}$)	BOD_5 ($mgO_2.L^{-1}$)	AOS	COD/TOC ($mgO_2.mg^{-1}C$)
0	39.5	98.0	122		-0.6329	3.09
10	39.2	93.0				
20	38.4	89.5	111		-0.3359	2.89
40	37.6	83.0				
60	36.2	78.0	96		0.0221	2.65
90	35.4	72.0				
120	34.7	66.0	92		0.0231	2.65
%removal	12.2	32.7				

Table DCP-UVA/H_2O_2 –5

Operational conditions

[DCP]i ($mg.L^{-1}$)	H_2O_2 ($mg.L^{-1}$)	Temperature (ºC)	pH
100	250	25	free

Time (min)	TOC ($mgC.L^{-1}$)	DCP ($mg.L^{-1}$)	COD ($mgO_2.L^{-1}$)	BOD_5 ($mgO_2.L^{-1}$)	AOS	COD/TOC ($mgO_2.mg^{-1}C$)
0	40.0	98.0	122		-0.5750	3.05
10	39.5	90.5			4.0000	0.00
20	38.7	87.0			4.0000	0.00
40	36.7	80.0	95		0.1172	2.59
60	36.2	72.0			4.0000	0.00
90	35.4	66.0			4.0000	0.00
120	34.8	62.0	90	0	0.1207	2.59
%removal	13.0	36.7			4.0000	15.21

Table DCP-UVA/H_2O_2 –6 Summary
Operational conditions

[DCP]i ($mg.L^{-1}$)	Temperature (ºC)	pH
100	25	free

H_2O_2 ($mg.L^{-1}$)	DCP%	TOC%	COD ($mgO_2.L^{-1}$)	BOD_5 ($mgO_2.L^{-1}$)	BOD_5/COD
15	9.0	9.3	110	0	0.0000
30	18.9	10.3	104	0	0.0000
50	25.3	12.1	100	0	0.0000
70	28.6	12.3	98	0	0.0000
100	32.7	12.2	92	1	0.0109
250	36.7	13	90	1	0.0111

Degradation of 2.4-DCP by UVA/Fe(III)

Table DCP-UVA/Fe(III) –1 Operational conditions

[DCP]i ($mg.L^{-1}$)	Fe(III) ($mg.L^{-1}$)	Temperature (ºC)	pH
100	20	25	free

Time (min)	TOC ($mgC.L^{-1}$)	DCP ($mg.L^{-1}$)	COD ($mgO_2.L^{-1}$)	BOD_5 ($mgO_2.L^{-1}$)	AOS	COD/TOC ($mgO_2.mg^{-1}C$)
0	40.9	100.0	127	0	-0.6611	3.11
20	39.5	90.0	114		-0.3291	2.89
30	39.0	86.0				
50	38.1	79.0	103		-0.0551	2.70
60	37.8	75.0				
80	37.4	72.0				
90	37.1	70.0	96	0	0.1186	2.59
%removal	9.2	30.0				

Table DCP-UVA/Fe(III) –2 Operational conditions

[DCP]i ($mg.L^{-1}$)	Fe(III) ($mg.L^{-1}$)	Temperature (ºC)	pH
100	70	25	free

Time (min)	TOC ($mgC.L^{-1}$)	DCP ($mg.L^{-1}$)	COD ($mgO_2.L^{-1}$)	BOD_5 ($mgO_2.L^{-1}$)	AOS	COD/TOC ($mgO_2.mg^{-1}C$)
0	43.7	107.0	133	0	-0.5610	3.04
10	42.5	95.0	118		-0.1647	2.78
20	42.0	91.0				
30	41.5	86.0	110		0.0241	2.65
40	40.5	81.0				
60	39.5	76.0				
90	38.8	70.0	96		0.2887	2.47
%removal	11.3	34.6				

Table DCP-UVA/Fe(III) -3

Operational conditions

[DCP]i ($mg.L^{-1}$)	Fe(III) ($mg.L^{-1}$)	Temperature (ºC)	pH
100	120	25	free

Time (min)	TOC ($mgC.L^{-1}$)	DCP ($mg.L^{-1}$)	COD ($mgO_2.L^{-1}$)	BOD_5 ($mgO_2.L^{-1}$)	COD/TOC ($mgO_2.mg^{-1}C$)	AOS
0	41.5	97.0	122	0	2.94	-0.4096
15	40.2	72.0	117		2.91	-0.3657
40	38.7	58.0	108		2.79	-0.1860
50	38.1	47.0			0.00	
60	37.8	50.0	96		2.54	0.1905
90	36.5	37.0	82	0	2.25	0.6301
%removal	12.0	61.9				

summary

Table DCP-UV/Fe(III) – 4 Operational conditions

[DCP]i ($mg.L^{-1}$)	Temperature (ºC)	pH
100	25	free

Fe(III) ($mg.L^{-1}$)	BOD_5/COD	COD%	AOS	COD/TOC ($mgO_2.\ mg^{-1}C$)	BOD/TOC ($mgO_2.\ mgC$)
20	0	24.41	0.1186	2.59	0.0000
70	0	27.82	0.2887	2.47	0.0000
120	0	32.79	0.6301	2.25	0.0007
150	0	28.93	0.3662	2.42	0.0003
180	0	27.87	0.2606	2.49	0.0000

Degradation of DCP by photo-Fenton process

A) Effect of initial H_2O_2

Table DCP-PHFA-1 Operational conditions

[DCP]i ($mg.L^{-1}$)	H_2O_2 ($mg.L^{-1}$)	Fe(II) ($mg.L^{-1}$)	Temperature (ºC)	pH
100	15	10	25	free

Time (min)	TOC ($mgC.L^{-1}$)	DCP ($mg.L^{-1}$)	Cl^- ($mg.L^{-1}$)	COD/TOC ($mgO_2.\ mg^{-1}C$)	COD ($mgO_2.L^{-1}$)	AOS
0	42.8	114.0	0	3.15	135	-0.7324
5	40.4	91.0	3	0.00		
15	40.0	77.0	5	2.88	115.00	-0.3125
35	39.8	48.8	10	2.76	110.00	-0.1457
50	39.8	45.0	14	2.71	108.00	-0.0704
% removal	9.1	60.5	0.32			

Table DCP-PHFA-2 Operational conditions

[DCP]i ($mg.L^{-1}$)	H_2O_2 ($mg.L^{-1}$)	Fe(II) ($mg.L^{-1}$)	Temperature (ºC)	pH
100	30	10	25	free

Time (min)	TOC ($mgC.L^{-1}$)	DCP ($mg.L^{-1}$)	Cl^- ($mg.L^{-1}$)	COD/TOC (mgO_2. $mg^{-1}C$)	COD ($mgO_2.L^{-1}$)	AOS
0	44.1	129	0	3.0	135	-0.58
2	42.8	85	6			
5	41.1	70	9			
15	40.2	30	12	2.9	120	-0.47
35	40.0	26.4	13	2.7	110	-0.12
50	39.7	21	14	2.3	95	0.41
%removal	10.0	83.7	0.32		29.6	

Table DCP-PHFA-3 Operational conditions

[DCP]i ($mg.L^{-1}$)	H_2O_2 ($mg.L^{-1}$)	Fe(II) ($mg.L^{-1}$)	Temperature (ºC)	pH
100	50	10	25	free

Time (min)	TOC ($mgC.L^{-1}$)	DCP ($mg.L^{-1}$)	Cl^- ($mg.L^{-1}$)	COD/TOC (mgO_2. $mg^{-1}C$)	COD ($mgO_2.L^{-1}$)	AOS
0	40.0	100.8	0	3.05	122	-0.5750
5	38.5	60.0	10	0.00		
15	38.0	40.0	14	2.82	107	-0.2237
35	37.5	14.0	23	2.56	96	0.1600
50	36.0	6.0	24	2.28	82	0.5833
%removal	10.0	94.0			32.8	

Table DCP-PHFA-4 Operational conditions

[DCP]i ($mg.L^{-1}$)	H_2O_2 ($mg.L^{-1}$)	Fe(II) ($mg.L^{-1}$)	Temperature (ºC)	pH
100	75	10	25	free

Time (min)	TOC ($mgC.L^{-1}$)	DCP ($mg.L^{-1}$)	Cl^- ($mg.L^{-1}$)	COD/TOC (mgO_2. $mg^{-1}C$)	COD ($mgO_2.L^{-1}$)	AOS
0	40.8	86.2	0	2.65	108.0	0.0294
5	40.0	50.0	15	0.00		
15	39.0	20.0	17	2.38	93.0	0.4231
35	38.0	4.0	24	2.29	87.0	0.5658
50	36.7	0.0	26.5	1.91	70.0	1.1390
%removal	10.0	100.0	0.61		35.2	

Table DCP-PHFB-5

Operational conditions summary

[DCP]i ($mg.L^{-1}$)	Fe(II) ($mg.L^{-1}$)	Temperature (ºC)	pH
100	10	25	free

H_2O_2 ($mg.L^{-1}$)	BOD_5 ($mgO_2.L^{-1}$)	BOD_{21} ($mgO_2.L^{-1}$)	BOD_5/COD	BOD/TOC ($mgO_2.mg^{-1}C$)	BOD_{21}/COD	BOD_{21}/TOC
15	0.0	0.0	0.0000	0.0000	0.0000	0.0000
50	5.0	6.0	0.0610	0.1389	0.0732	0.1667
30	4.0	5.0	0.0412	0.1058	0.0515	0.1323
65	13.0	14.0	0.1566	0.3533	0.1687	0.3804
75	14.0	16.0	0.2000	0.3815	0.2286	0.4360

B) Effect of initial Fe(II)

Table DCP-PHFA-6 Operational conditions

[DCP]I ($mg.L^{-1}$)	H_2O_2 ($mg.L^{-1}$)	Fe(II) ($mg.L^{-1}$)	Temperature (ºC)	pH
100	15	15	25	free

Time (min)	TOC ($mgC.L^{-1}$)	[DCP]i ($mg.L^{-1}$)	Cl^- ($mg.L^{-1}$)	BOD_5 ($mgO_2.L^{-1}$)
0	44.6	104.6	0	0
2	44.5	94.0	1	
5	44.2	85.0	3	
15	43.7	67.0	5	
35	41.5	46.5	10	
50	40.8	40.0	13	0
%removal	8.5	61.8		

Table DCP-PHFA-7 Operational conditions

[DCP]i ($mg.L^{-1}$)	H_2O_2 ($mg.L^{-1}$)	Fe(II) ($mg.L^{-1}$)	Temperature (ºC)	pH
100	15	30	25	free

Time (min)	TOC ($mgC.L^{-1}$)	[DCP]i ($mg.L^{-1}$)	Cl^- ($mg.L^{-1}$)	BOD_5 ($mgO_2.L^{-1}$)
0	45.9	105.6	0	0
2	43.2	84.0	2	
5	43.0	72.0	4	
15	43.0	58.0	7	
35	43.0	41.0	12	
50	41.8	37.0	14	0
%removal	8.9	65.0		

Table DCP-PHFA-8 Operational conditions

[DCP]i ($mg.L^{-1}$)	H_2O_2 ($mg.L^{-1}$)	Fe(II) ($mg.L^{-1}$)	Temperature (ºC)	pH
100	15	45	25	free

Time (min)	TOC ($mgC.L^{-1}$)	[DCP]i ($mg.L^{-1}$)	Cl^- ($mg.L^{-1}$)	BOD_5 ($mgO_2.L^{-1}$)
0	44.6	104.0	0	0
2	44.5	84.0	3	
5	44.2	66.0	6	
10	43.7	46.0	13	
20	41.5	38.0	15	
40	40.8	28.0	17	0
%removal	8.5	73.1		

Table DCP-PHFA-9 Operational conditions

[DCP]i ($mg.L^{-1}$)	H_2O_2 ($mg.L^{-1}$)	Fe(II) ($mg.L^{-1}$)	Temperature (ºC)	pH
100	15	55	25	free

Time (min)	TOC ($mgC.L^{-1}$)	[DCP]i ($mg.L^{-1}$)	Cl^- ($mg.L^{-1}$)	BOD_5 ($mgO_2.L^{-1}$)
0	44.6	104	0	0
2	44.5	80	5	
5	44.18	57	9	
10	43.7	38	13	
20	41.5	30	17	
40	40.8	21	19	0
%removal	8.5	79.8		

Table DCP-PHFA-10 Operational conditions

[DCP]i ($mg.L^{-1}$)	H_2O_2 ($mg.L^{-1}$)	Fe(II) ($mg.L^{-1}$)	Temperature (ºC)	pH
100	30	10	25	free

Time (min)	TOC ($mgC.L^{-1}$)	[DCP]i ($mg.L^{-1}$)	Cl^- ($mg.L^{-1}$)	BOD_5 ($mgO_2.L^{-1}$)	COD ($mgO_2.L^{-1}$)	COD/TOC (mgO_2. ($mg^{-1}C$)	AOS
0	42.0	108.3	0	0	132	3.14	-0.7143
5	41.5	72.0	4				
15	40.5	56.0	8				
35	39.5	25.0	9				
50	38.5	22.0	12	4	105	2.73	-0.0909
%removal	8.3	79.7					

Table DCP-PHFA-11 Operational conditions

[DCP]i ($mg.L^{-1}$)	H_2O_2 ($mg.L^{-1}$)	Fe(II) ($mg.L^{-1}$)	Temperature (ºC)	pH
100	30	15	25	free

Time (min)	TOC ($mgC.L^{-1}$)	[DCP]i ($mg.L^{-1}$)	Cl^- ($mg.L^{-1}$)	BOD_5 ($mgO_2.L^{-1}$)	COD ($mgO_2.L^{-1}$)	COD/TOC (mgO_2. ($mg^{-1}C$)	AOS
0	44.7	100.0	0	0	125	2.80	-0.1956
2	42.8	53.0	5				
5	42.4	40.0	10				
15	42.0	35.0	11		115	2.74	-0.1071
35	41.6	24.0	13		112	2.69	-0.0385
50	41.0	20.0	15	3	110	2.68	-0.0244
	8.3	80.0					

Table DCP-PHFA-12 Operational conditions

[DCP]i ($mg.L^{-1}$)	H_2O_2 ($mg.L^{-1}$)	Fe(II) ($mg.L^{-1}$)	Temperature (ºC)	pH
100	30	30	25	free

Time (min)	TOC ($mgC.L^{-1}$)	[DCP]i ($mg.L^{-1}$)	Cl^- ($mg.L^{-1}$)	BOD_5 ($mgO_2.L^{-1}$)	COD ($mgO_2.L^{-1}$)	COD/TOC (mgO_2. ($mg^{-1}C$)	AOS
0	44.6	104.6	0	0	129	2.89	-0.3386
2	44.5	88.0	6				
5	44.2	63.0	8.1		116	2.63	0.0616
15	43.7	42.5	12		108	2.47	0.2929
35	41.5	22.0	14		95	2.29	0.5663
40	40.2	19.0	17	8	85	2.11	0.8284
%removal	9.9	81.8				0	

Table DCP-PHFA-13

Operational conditions Summary

[DCP]i ($mg.L^{-1}$)	H_2O_2 ($mg.L^{-1}$)	Temperature (ºC)	pH
100	30	25	free

Fe(II) ($mg.L^{-1}$)	BOD_{21} ($mgO_2.L^{-1}$)	BOD_5/COD	BOD_5/TOC (mgO_2. ($mg^{-1}C$)	BOD_{21}/COD	BOD21/TOC (mgO_2. ($mg^{-1}C$)	COD/TOC (mgO_2. ($mg^{-1}C$)
15	3	0.03	0.0732	0.0273	0.0732	2.68
20	6	0.06	0.1538	0.0632	0.1538	2.43
30	9	0.09	0.1990	0.1059	0.2239	2.11
10	5	0.04	0.1039	0.0476	0.1299	2.72
40	10	0.11	0.2250	0.1235	0.2500	2.0
55	9	0.10	0.1990	0.1125	0.2239	1.99

Table DCP-PHFA-14 Operational conditions

[DCP]i ($mg.L^{-1}$)	H_2O_2 ($mg.L^{-1}$)	Fe(II) ($mg.L^{-1}$)	Temperature (ºC)	pH
100	50	10	25	free

Time (min)	TOC ($mgC.L^{-1}$)	[DCP]i ($mg.L^{-1}$)	COD ($mgO_2.L^{-1}$)	BOD_5 ($mgO_2.L^{-1}$)	COD/TOC (mgO_2. ($mg^{-1}C$	AOS
0	40.0	100.8	127	0	3.18	-0.7625
5	38.5	18.0				
10	38.0	12.0				
20	37.5	9.0				
40	37.0	8.0	85	8	2.30	0.5541
%removal	7.5	92.1				4.0000

Table DCP-PHFA-15 Operational conditions

[DCP]i ($mg.L^{-1}$)	H_2O_2 ($mg.L^{-1}$)	Fe(II) ($mg.L^{-1}$)	Temperature (ºC)	pH
100	50	40	25	free

Time (min)	TOC ($mgC.L^{-1}$)	[DCP]i ($mg.L^{-1}$)	BOD_5 ($mgO_2.L^{-1}$)	COD ($mgO_2.L^{-1}$)	COD/TOC (mgO_2. ($mg^{-1}C$
0	39.8	100.0	125	0	3.14
5	38.5	1.0			
10	38.0	0.0			
20	36.0	0.0			
40	36.5	0.0	73	9	2.00
%removal	8.3	100.0			

D) Effect of initial temperature

Table DCP-PHFA-16

Operational conditions summary

[DCP]i ($mg.L^{-1}$)	H_2O_2 ($mg.L^{-1}$)	Fe(II) ($mg.L^{-1}$)	pH
100	30	10	free

Temperature (°C)	COD ($mgO_2.L^{-1}$)	BOD_5 ($mgO_2.L^{-1}$)	BOD_5/COD	BOD_5/TOC (mgO_2. $mg^{-1}C$)	AOS	COD/TOC . (mgO_2. $mg^{-1}C$)
25	103	3	0.02913	0.07792	0.8831	2.08
30	95	4	0.04211	0.10309	1.1392	1.91
35	87	5	0.05747	0.13123	1.2441	1.84
45	85	7	0.08235	0.19178	1.2877	1.81

Table DCP-PHFB-17

Operational conditions

[DCP]i ($mg.L^{-1}$)	H_2O_2 ($mg.L^{-1}$)	Fe(II) ($mg.L^{-1}$)	pH
100	15	10	free

Temperature (°C)	DCP%	TOC%	COD ($mgO_2.L^{-1}$)	BOD ($mgO_2.L^{-1}$)	BOD/COD
25	60.5	8.6	115	0.0000	0.0000
30	64.6	9.1	110	0.0000	0.0000
35	70.4	9.4	108	0.0000	0.0000
45	80.5	9.7	103	2.0000	0.0194

Mineralazation

Table DCP-PHFB-18

Operational conditions

[DCP]i ($mg.L^{-1}$)	Fe(II) ($mg.L^{-1}$)	Temperature (ºC)	pH
200	40	25	free

Time (min)	[H2O2]=60 ($mg.L^{-1}$)	[H2O2]=120 ($mg.L^{-1}$)	[H2O2]=240 ($mg.L^{-1}$)	[H2O2]=360 ($mg.L^{-1}$)	[H2O2]=420 ($mg.L^{-1}$)	[H2O2]=460 ($mg.L^{-1}$)
0	38.450	39.3	39.5	38.4	39.0	38.9
5	38.000	38.6	35.0	33.0	30.0	27.0
10	37.000	38.0	30.0	27.0	24.0	18.0
20	36.000	37.3	26.0	22.0	18.0	10.0
30	35.000	35.0	23.0	19.0	15.0	8.0
40	34.000	32.0	20.0	15.0	10.0	3.0
50	33.100	30.0	18.0	11.0	7.0	1.0
60	32.000	28.0	17.0	8.0	4.0	0.0
	10.8	19.0	37.5		58.3	64.8

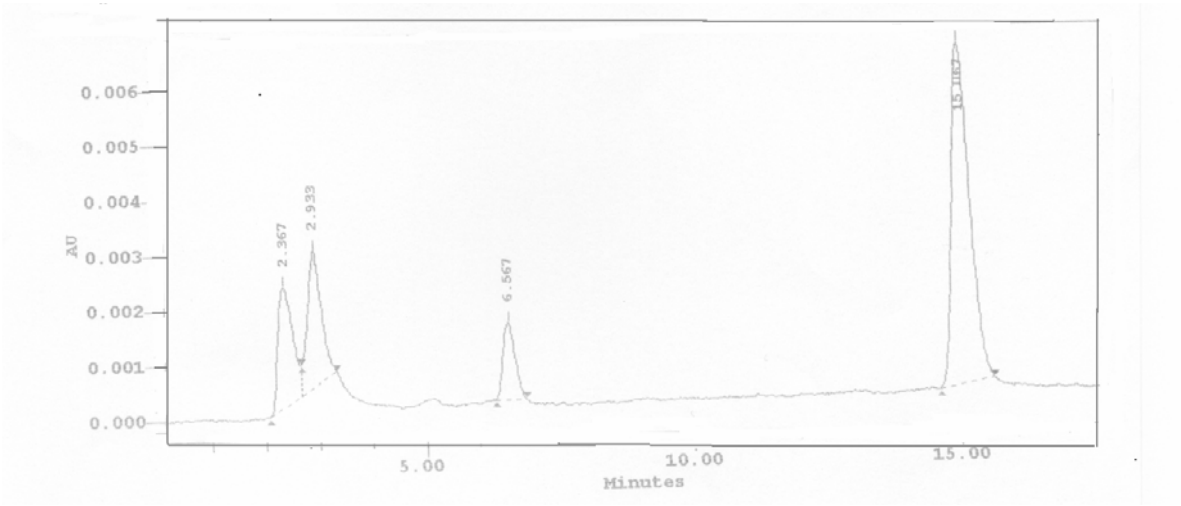

Figure A5.1: Chromatogram corresponding to sample at 20 min in UVA/H_2O_2 process

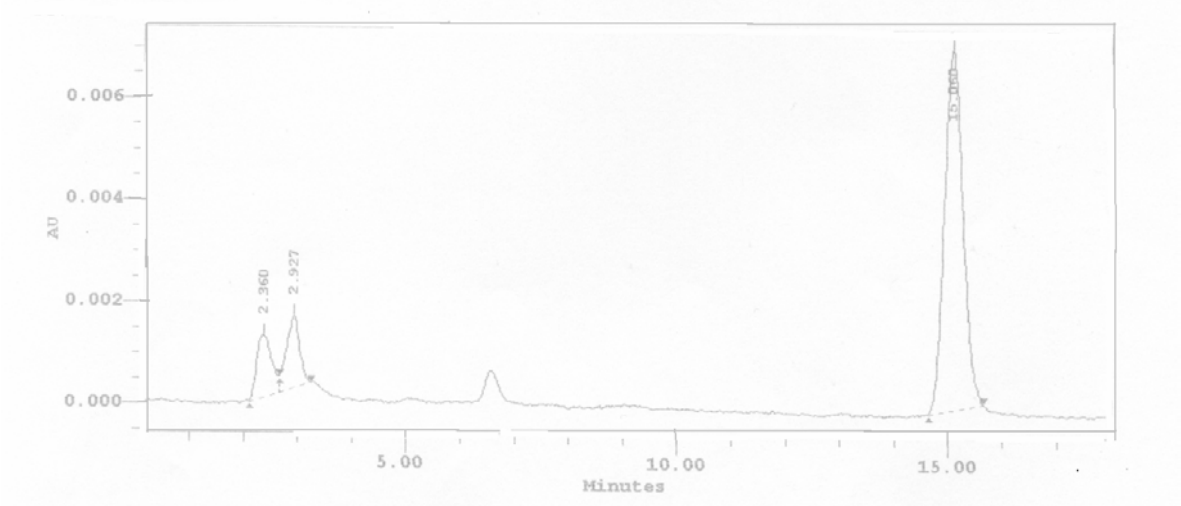

Figure A5.2: Chromatogram corresponding to sample at 30 min in UVA/H_2O_2 process

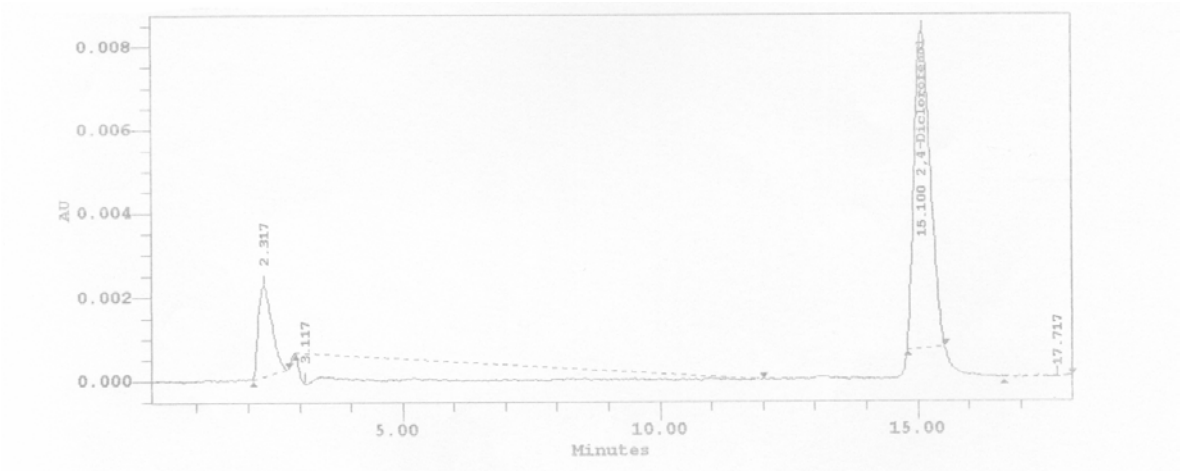

Figure A5.3: Chromatogram corresponding to sample at 30 min in UVA/Fe(III) process

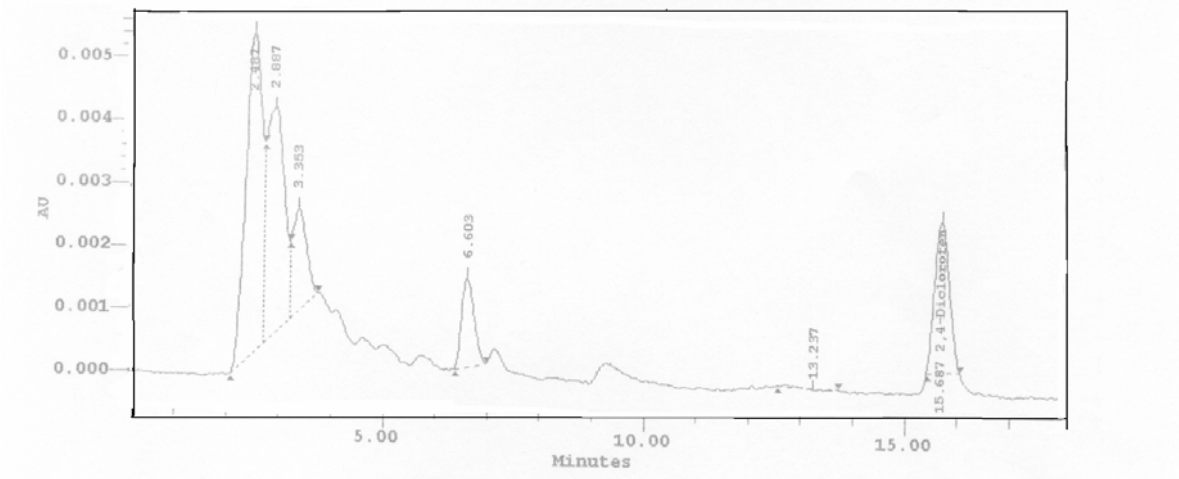

Figure A5.4: Chromatogram corresponding to sample at 2 min in photo-Fenton process

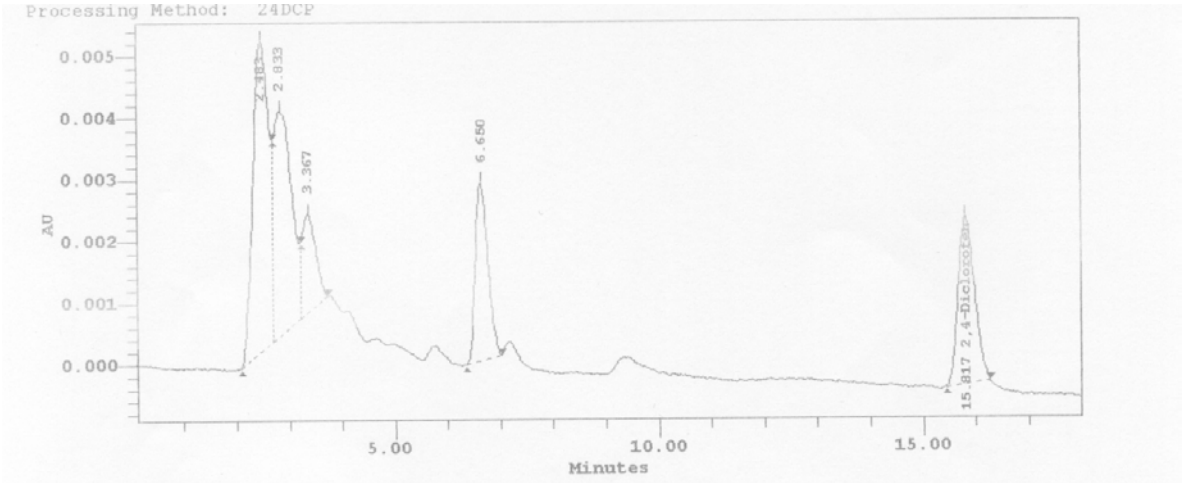

Figure A5.5: Chromatogram corresponding to sample at 20 min in photo-Fenton process

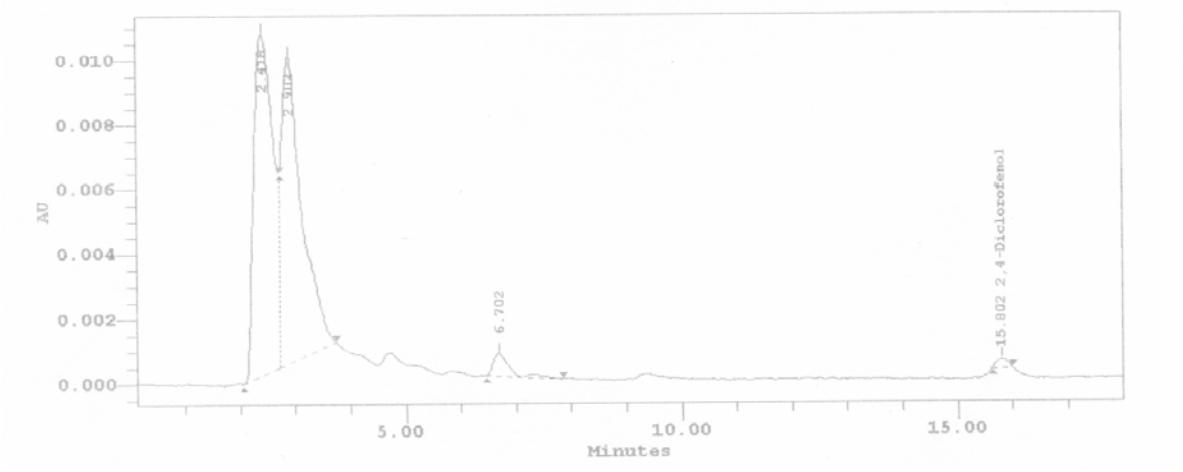

Figure A5.6: Chromatogram corresponding to sample at 30 min in photo-Fenton process

1. Introducción

El agua es indudablemente el recurso natural más precioso que existe en nuestro planeta. Sin el agua, la vida en la tierra sería no existente: es esencial en todo en nuestro planeta para crecer y prosperar. Aunque nosotros como seres humanos reconocemos este hecho constantemente, lo desatendemos contaminando los ríos, lagos y océanos. Como consecuencia de esto, muchos recursos de agua se han visto afectados, además este hecho ha introducido en el medio ambiente muchas enfermedades. Para combatir la contaminación del agua, debemos entender los problemas y ser una parte de la solución. En los últimos años se generó el interés de buscar unos métodos eficaces y económicos para tratar deferentes tipos de agua residual. Esto ha motivado que muchos laboratorios en todo el mundo a llevar a cabo investigaciones en busca a diferentes alternativas para el tratamiento de aguas.

El tratamiento biológico de aguas residuales se considera un alternativa atractiva y barata para eliminar varios tipos de contaminantes cuando se compara con otras opciones de tratamiento. La eficacia del proceso biológico depende de muchos factores tales como la concentración de los contaminantes, la estructura química de los compuestos, el pH y la presencia de otros compuestos inhibitorios. Aunque algunos contaminantes orgánicos se pueden degradar vía el tratamiento biológico, muchos otros compuestos sintéticos y naturales no son biodegradables.

Por el otro lado, Varias procesos químicos como los procesos de oxidación avanzada pueden ser utilizados para mineralizar muchos químicos orgánicos. El inconveniente que presentan estos procesos es el uso de reactivos de elevado coste. Una solución potencial sería la combinación de estos procesos con tratamientos biológicos. En estos procesos combinados, el proceso químico se utilizaría como pre-tratamiento para aumentar la biodegradabilidad de los efluentes o eliminar la toxicidad del mismo, mientras que la mineralización total se completaría en el proceso biológico. Para ello, es interesante seguir los cambios en la biodegradabilidad de los efluentes a tratar a lo largo del tratamiento químico, para determinar el tiempo óptimo que convendría aplicar dicho tratamiento. En la literatura se han propuesto varios indicadores de biodegradabilidad, de los cuales los ratios DBO_5/DQO y DBO_5/COT son los más utilizados (DBO: Demanda Biológica de Oxígeno; DQO: Demanda Química de

Oxígeno; COT: Carbono Orgánico Total). En general, se toman como valores de referencia los correspondientes a un agua residual doméstica. Así, se considera que un efluente es biodegradable cuando la relación DBO5/DQO es mayor de 0.4 o DBO5/COT mayor de 1 (Metcalf & Eddy, 1985).

Los POAs se definen como aquellos procesos que implican la generación de radicales altamente reactivos (especialmente radicales hidroxilo) en cantidades suficientes para el tratamiento de una corriente. Estos radicales son muy poco selectivos, lo que les hace atractivos para el tratamiento de aguas, aunque algunos compuestos orgánicos sencillos como los ácidos acético, maleico y oxálico, la acetona o el cloroformo no son atacados por estos radicales (Bigda, 1995). La versatilidad de los POAs se ve aumentada por el hecho de que estos radicales se pueden formar por medio de distintos procesos.
Como la base de los procesos utilizados en el presente estudio es el POAs, en el primer capítulo de este trabajo se presentan las reacciones en que generan estos radicales. (introducción, sección 3.3) y una serie de métodos para el tratamiento de compuestos refractarios, entre los que se encuentra la adsorción en carbón activo, la oxidación húmeda, la oxidación supercrítica, procesos electroquímicos, procesos fotoquímicos, tratamientos químicos clásicos y procesos de oxidación avanzada o POAs. De todos ellos se ha hecho una pequeña búsqueda bibliográfica en cuanto a su aplicación en la eliminación de fenol (POH) y 2,4-dichlorofenol (DCP). Además representó una explicación básica de las características del tratamiento biológico y sus tipos de operación. Al final de este capitulo (introducción), se ha insertado un grafico (Figure 3.4) que muestra una posible estrategia para seleccionar el tipo de tratamiento satisfactorio para los deferentes tipos de agua dependiendo de la carga orgánica y la biodegradabilidad.

El fenol (POH), 2,4-dichlorofenol (DCP) y efluentes de tintes de textil han sido escogidos en este estudio como compuestos modelos; debido a su presencia en diferentes clases de agua industrial. Los compuestos fenólicos son utilizados en la síntesis de pesticidas, pinturas y disolventes, mientras los clorofenoles derivan del uso incontrolado de pesticidas, funguicidas, herbicidas, así como en subproductos del blanqueo de pulpa de papel con cloro y en la desinfección con cloro para potabilización de agua. Los tintes del textil también causan una problema al medio ambiente por el hecho que la mayoría de ellos y sus subproductos son difíciles de eliminarse usando

métodos biológicos normales. Varios compuestos de estas familias se encuentran incluidos entre los contaminantes prioritarios seleccionados por la Unión Europea (ver *Tabla 2*.3) y han sido listados entre los 130 contaminantes prioritarios dados por la US EPA, por ej. fenol y 2,4-diclorofenol, los cuales han sido también incluidos. Las características principales de estos compuestos, así como la presencia de estas sustancias en algunas aguas se presenta en la sección 4 (studied compounds). Un análisis del comportamiento de estas sustancias en cuanto a una posible degradación microbiana aeróbica ha mostrado que son de baja biodegradabilidad e inhibidores de otras fuentes de carbono, lo que hace necesario buscar alternativas a los procesos biológicos convencionales.

Basado en todos eso, los objetivos generales del presente trabajo son:

1. Estudiar la posibilidad de uso de los procesos de oxidación avanzado (POA), basados en la luz ultravioleta, en el tratamiento de compuestos de baja biodegradabilidad y/o tóxicos, en concreto POH, DCP.

2. Examinar la biodegradación de estos compuesto después de ser tratados

3. Investigar el efecto del proceso de fofolisis (VUV y UV) para la eliminación del color de tintes de textil y agua de textil. Además estudiar el efecto de dichos procesos en la mejora de la biodegradabilidad de estas soluciones.

Para ello, se han establecido los siguientes estrategias:

- Estudio del efecto en la eliminación y mineralización de estos compuestos mediante los procesos. UV, H_2O_2/UV, Fe(III)/H_2O_2, Fenton y foto-Fenton. Esta parte se realizó en dos apartados:

    1. Foto-oxidación basada en el uso de luz UV.
    2. Foto-oxidación basada en el uso la luz UVA. Parte se llevó a cabo vía con dos tipos reactores: foto-reactor con una la lámpara y foto-reactor con 3 lámparas.

- Estudio del efecto de dichos POA en la biodegradabilidad de las soluciones del POH y del DCP, utilizando las relaciones DBO/DQO y DBO/COT como indicadores.
- Identificación de los principales intermedios de las reacciones, intentando relacionarlos con los cambios producidos en la biodegradabilidad.

- Seguir el cambio del estado de oxidación por los procesos antes mencionados anteriores y relacionar este cambio con los de la biodegradabilidad

En la realización de estos objetivos sé han puesto en práctica las siguientes técnicas analíticas: HPLC, para determinar la concentración de los contaminantes; DQO; DBO; COT y el consumo de oxigeno por lodos activos (Ver capítulo 6, *"analytical methods*").

Las instalación experimental utilizadas son:

a) Reactores Químicos:

Reactor1: Reactor tubular de cuarzo consiste básicamente en un depósito de 5 L de carga, 4 lámparas de luz UV de 15W cada una emiten luz con longitud de onda de 253.7 nm, y bomba de circulación.

Reactor 2& 3: Estos dos reactores son de tipo tanque agitado
Reactor 2 consiste en un tanque agitado de 1.5 litro, 1 lámpara de luz negra de 4 W que emite luz con longitud de onda de 350 nm. El reactor esta equipado con agitadores y controladores de temperatura.
Reactor 3 consiste de tanque agitado de 2 L, 3 lámparas de luz negra con 8 W cada una y emiten luz con longitud de onda 360 nm. También este reactor esta equipado con agitadores y controladores de temperatura.

Reactor 4: Es un Reactor tubular: En este reactor se llevó a cabo las reacciones de tintes de textil. El reactor contiene una zona de reacción con capacidad de 420 mL y una lámpara de 120 W que emite luz con longitud de onda de 253.7 y 184.9 nm. En realidad este reactor puede funcionar en dos maneras: con VUV y UV esto se logra

cambiando el cuarzo que está alrededor de la lámpara (Suprasil para VUV y Infrasil cuarzo para UV). El reactor también está equipado con mediadores de absorbancia y pH mediante una bomba centrífuga que logra el circulación del liquido. Para mas detalles sobre estos reactores se puede revisar la sección 6.1.

b) Reactores Biológicos:

Reactor 1: Tanques semicontinuos agitados de 1.5 L, alimentados por aire mediante un difusor y agitador magnético.

Reactor 2: (sequencing batch reactors) SBR. Estos reactores son de 1.5 L, alimentados por aire mediante un difusor y agitador magnético. Además estos reactores están equipados con bombas de alimentación y purgas automáticas

Como inóculo en todos los reactores se ha utilizado lodos de la depuradora de Gavá (Barcelona). Cuando fue necesaria un aclimatación previa para algunas biomasas, esta aclimatación fue realizada en el laboratorio.

2. Resultados y discusión

En primer lugar se realizaron dos experimentos preliminares para comprobar el efecto del stripping por oxígeno, comprobándose que el grado de volatilización debido al paso de oxígeno a través de las soluciones de POH y DCP era insignificante.

2.1. Tratamiento del DCP y POH con POAs basando en el uso de luz UV

En ésta capitulo se ha estudiado deferente procesos:

2.1.1 Tratamiento del DCP y POH con luz UV

En esta parte se ha estudiado efecto de la luz UV sobre la degradación del DCPy POD. La mijora en el biodegradabilidad y el cabio en el estado de oxidación.

Foto-degradación:

Se ha estudiado el efecto de irradiación de la luz UV en la degradación del POH y DCP. Como se puede observar en el *figura 7.1* ambos compuestos se degradan a ciertos limites por la irradiación UV. Durante 2 horas de irradiación, se logro degradar 53% del POH y 56% del DCP. Esto fue combinado con 13% y 16% mineralización en la materia orgánica en los dos compuestos respectivamente.

Para ambos compuestos la cinética de la degradación fue ajustada con un modelo cinético del primer orden. Así, puede verse que bajo las mismas condiciones el POH muestra una mejor reactividad del DCP.

La influencia del UV en la biodegradabilidad

Antes de empezar cualquier test de biodegradabilidad necesario medir la compatibilidad de las soluciones del POH y del DCP antes de ser tratados. Se utilizaron dos parámetros: la demanda biológica de oxigeno y el consumo de oxigeno de lodos activos. Los experimentos han mostrado que el DCP con concentración 100mg.L^{-1} es un compuesto no-biodegradable (DBO_5=0.0). por el contrario el POH ha mostrado biodegradabilidad (DBO_5 =27 mg.L^{-1}).

Posteriormente de esto se han probado la biodegradabilidad de las soluciones de POH y DCP tratadas con UV; Se ha observado que el uso de este proceso con los dos compuestos no ha generado ningún cambio en el valor de la biodegradabilidad, por lo tanto con este proceso no se puede lograr ninguna mejora en la biodegradabilidad del POH y DCP.

El cambio del grado de oxidación:

Una manera simple para efectuar el seguimiento de la oxidación de compuestos orgánicos es realizar medidas y contrastes del grados de oxidación. Dos parámetros fueron seguidos en este seguimientos "Average Oxidation state" (AOS) y el cambio de ratio (DQO/COT). El valor del AOS puede calcularse mediante la ecuación 7.2.

Los soluciones tratadas con luz UV fueron examinadas para el cambio del grado de oxidación. Los resultados muestran poco cambio del grado de oxidación en ambos

compuestos debido a la ineficacia del proceso UV en degradación de la materia orgánica.

2.1.2 Tratamiento del DCP y POH en el proceso UV/H_2O_2

Foto-degradación:

Como el proceso UV de ambos componentes (POH y DCP) era ineficaz, se decidió estudiar el efecto del proceso UV/H_2O_2 en la degradación de DCP y de POH, y la mejora en la biodegradabilidad. En este proceso la degradación está reforzada por la presencia de peróxido de hidrógeno que aumenta la formación radicales hidroxilos.
La combinación de UV con H_2O_2 refuerza fuertemente la eficacia de la degradación (figura 7.4 y 7.5). Basado en los resultados experimentales, se necesita una concentración de 200 $mg.L^{-1}$ H_2O_2 durante 90 minutos de irradiación para eliminar 100% de DCP, asimismo 400 $mg.L^{-1}$ H_2O_2 fueron suficientes para degradar todo el POH con el mismo tiempo de irradiación. Sin embargo, durante la reacción no toda la cantidad agregada de H_2O_2 se consumió. Por otro lado, usando 100 $mg.L^{-1}$ de H_2O_2 para DCP y 300 $mg.L^{-1}$ POH durante el mismo tiempo de irradiación se elimina el 96% del ambos compuestos (DCP y POH) y menor cantidades de H_2O_2 queda sin reaccionar. En esta parte se estudia la cinética de reacción en función del H_2O_2 agregad y el tiempo medio de vida. (Tabla 7.1).

La influencia del UV/ H_2O_2 *en la biodegradabilidad*

Los resultados experimentales muestran que, a pesar que proceso UV/ H_2O_2 tiene la capacidad de eliminar todo el DCP en las soluciones con concentraciones iniciales de H_2O_2 alta, al aplicarse la prueba de biodegradabilidad a las soluciones tratados con este proceso no pudo constatarse ninguna mejora en la biodegradabilidad.

Con respecto al POH, durante el proceso UV/H_2O_2, se notó una mejora en la biodegradabilidad de los soluciones tratadas, como resultado de degradación del POH a otros intermedios más biodegradables (figure 7.6). Con 400 $mg.L^{-1}$ H_2O_2, DBO_5, DBO_5/DQO y DBO_5/COT aumentaron a 33 $mgO_2.L^{-1}$, 0.26 y 0.60 $mgO_2.mg^{-1}C$ para los soluciones tratadas respectivamente.

El cambio del grado de oxidación:

Respecto el grado de oxidación, se observa que el grado de oxidación de la materia orgánica aumenta a incrementarse la concentración inicial del peróxido de hidrógeno. Por otro lado, puede verse que para el DCP y el POH, el cambio en el grado de oxidación de los intermedios es mínimo, por ejemplo con concentración inicial $H_2 O_2$ 200 $mg.L^{-1}$, la ratio DQO/COT se ha deteriorado 26% y 18% para el DCP y el POH respectivamente. Eso significa que la materia orgánica en la solución enfrentó a una oxidación débil.

2.1.3 Tratamiento del DCP y POH en el proceso UV/Fe(III)

También fue estudiada la degradación y el aumento de la biodegradabilidad mediante este proceso. Se experimento el cambio de degradación en el DCP y el POH en función de concentraciones iniciales Fe(III).

Se ha encontrado que aumentando la concentración inicial resulta una mayor biodegradabilidad. El 60% y 90 % de eliminación en el DCP y el POH fueron obtenidos con concentraciones iniciales de Fe(III) 70 $mg.L^{-1}$ (Figura 7.8)

Al respecto de la biodegradabilidad y el cambio del grado de oxidación, mediante esta proceso no hubo un cambio significativo,

2.1.4 Tratamiento del DCP y POH en el proceso Fenton

La degradación del DCP y del POH en el proceso Fenton se ha estudiado en diferentes partes :

Efecto de la concentración inicial del H_2O_2.

Como se puede observar en la figura *7.12*, el aumento de la concentración inicial del $H_2 O_2$ conlleva también un aumento en la degradación del DCP y del POH. A lo largo de este proceso, se logro un eliminación total para los dos compuestos con un tiempo de reacción de 60 minutos y concentraciones iniciales de reactivos significante. La eliminación del 100% del DCP fue completada con 100 H_2O_2 y 10 $mg.L^{-1}$ Fe(II), respecto de POH se llegó al mismo porcentaje de con 350 H_2O_2 and 10 $mg.L^{-1}$.

El mismo efecto se notó con respecto a la biodegradabilidad y el cambio en el grado de oxidación. A mayor la concentración inicial del H_2O_2 aumenta la degradación en las materias orgánicas y mejora el biodegradabilidad, con las mismas concentraciones de H_2O_2 y Fe(II) interiores, el biodegradabilidad del DCP, representada como ratio DBO_5/DQO, aumento desde 0 hasta 0.12 y la del POH hasta el 0.28.
La misma tendencia se ha observado respecto del cambio en el grado de oxidación

Efecto de la concentración inicial del Fe(II)

Un tendencia diferente en la degradación de DCP y POH se observó respecto del cambio en la concentración inicial de Fe(II). Inicialmente al aumentar la concentración inicial de Fe(II) apareció un incremento en la degradación de la materia orgánica. Sin embargo, a concentraciones altas se ha observado poco efecto del Fe(II) en la degradación. Como máximo 50% y 70% de eliminación en el DCP y el POH se ha obtenido variando la concentración de Fe(II).

La misma tendencia se observó en la cambio de la biodegradabilidad y el grado de oxidación, con concentraciones iniciales de Fe(II); la biodegradabilidad de la materia orgánica aumenta hasta el limite que agregar mas Fe(II) ya no afecta a la biodegradabilidad.

2.1.5 Tratamiento del DCP y POH en el proceso foto-Fenton

Con respecto la influencia de la concentraciones iniciales del H_2O_2 y Fe(II), se observó que la degradación del DCP y del POH mejoró en estos procesos, debido a la formación de radicales hidroxilos que atacan la materia orgánica. Además, se encontró que la degradación en esta reacción es muy rápida; y solo se necesitan unos minutos para eliminar todo el DCP y el POH (40 y 15 minutos respectivamente). La mejora en la eficacia de la degradación y el aumento en el biodegradabilidad fue mas proporcional en las concentraciones iniciales del H_2O_2 que las concentraciones iniciales del Fe(II).

A lo largo del proceso, 100% de eliminación del DCP y POH se logró bajo las siguientes condiciones: 50 $mg.L^{-1}$ H_2O_2, 10 $mg.L^{-1}$ Fe(II) y 40 minutos para DCP y 300 $mg.L^{-1}$ H_2O_2, 60 $mg.L^{-1}$ Fe(II) y 15 minutos para POH.

Por otro lado, se ha logrado una mejora significativa en el biodegradabilidad durante estas reacciones. En las mismas condiciones interiores, la biodegradabilidad (DBO_5/DQO) de solución de DCP aumentó hasta 0.20 y la del POH hasta 0.92.

El efecto de esta reacción en el grado de oxidación también fue notable. Es interesante mencionar la relación clara entre el cambio en el grado de oxidación y la mejora en el biodegradabilidad.

2.1.6 condiciones óptimas

Las condiciones óptimas de las reacciones se seleccionaron basándose en la eliminación DCP y POH y la mejora de la biodegradabilidad. Así, las condiciones óptimas para DCP son: H_2O_2 50 $mg.L^{-1}$, 10 mg.L-1 Fe(II) y 40 minutos de tiempo de reacción.

Con respecto al POH, los condiciones óptimas son: H_2O_2 50 $mg.L^{-1}$, 75 $mg.L^{-1}$ Fe(II) y 15 minutos de tiempo de reacción.

2.2 Oxidación aerobia del DCP y POH:

Después de aumentar la biodegradabilidad de los soluciones DCP y POH, se estudió un tratamiento de oxidación biológica de las soluciones pre-tratadas vía foto-Fenton.

Para cada compuesto dos reactores fueron estudiados los reactores;

el caso de fenol se estudió:

- Reactor simple alimentado con fenol
- Reactor combinado alimentado con fenol pre-tratado con foto-Fenton el primer reactor.

En esta parte se observó que el proceso combinado mejora el porcentaje de eliminación del COT y se reduce el tiempo necesario para la eliminación en el proceso biológico (tabla 7.12 y 7.13).

Con el proceso simple, un 80% de la eliminación de COT se logró en 150 horas mientras que solo 24 horas se ha necesitado para obtener al 90%.utilizando el proceso combinado.

En el caso del DCP, el tratamiento directo de este compuesto no fue posible, por lo que se tuvo que hacer uso de dos reactores :

- Reactor no-aclimatado
- Reactor aclimatado a fenol.

En ambos reactores se observó una eliminación del COT (Carbon Organico Total) significativa. Un máximo de eliminación entre el 8.4 y el 89% fue obtenido tras la digestión las soluciones pre-tratadas. Mezclando el 70% de V/V de estas soluciones con 20 % V/V de agua residual y con un tiempo de retención hidráulico (TRH) de 2 días.

Se ha estudiado la cinética de en reactores aplicando condiciones diferentes. Los resultados obtenidos se resumen en las tablas 7.11 y 7.14.

2.3 Mineralización

Como se comentó en la de introducción los procesos POAs pueden ser utilizados eficazmente para mineralizar toda la materia orgánica en soluciones acuosas. Por ello, ambos soluciones del DCP y del POH (100 $mg.L^{-1}$) se probaron para un mineralization total.

Los resultados muestran que, 100 $mg.L^{-1}$ DCP y POH puede mineralizarse mediante el l proceso foto-Fenton bajo los condiciones siguientes:

1. DCP; H_2O_2= 270 $mg.L^{-1}$, Fe(II)= 40 $mg.L^{-1}$ y tiempo de irradiación 60 minutos.
2. POH; H_2O_2= 750 $mg.L^{-1}$, Fe(II)= 60 $mg.L^{-1}$ y tiempo de irradiación 60 minutos.

La cinética de mineralización y el tiempo de vida media para el DCP y el POH se han probado, la degradación de ambos compuesto se ajustó a una cinética de primer orden. La tabla 7.15 presenta los valores para DCP y POH.

2.4. Identificación de los intermedios:

Los dos componentes estudiados se examinaron para la identificación de los intermedios de degradación. De la experimentales cob POH solo se pudo identificar el hydroquinine y resorcinol.

Con el respecto al DCP, se han podido identificar entre los intermedios de reacción la chlorobenzoquinona y el resocinol.

2.5. Comparación de los distintos procesos estudiados para la degradación de DCP y POH

Velocidades de desaparición y mineralización

En este apartado se han comparado los distintos procesos estudiados en cuanto a la velocidad de desaparición del DCP y del POH (ver *figura 7.74*) y de mineralización ver (*figura 7.75*). Se han ajustado las velocidades de desaparición a una cinética de primer orden (*tabla 7.16).* En cuanto al grado de mineralización, los procesos que han mostrado una mayor eficacia han sido: el proceso Fenton y foto-Fenton (ver *figura 7.75 y tabla 7.17*). Se ha realizado también una comparación respecto de la dechlorinacion. Se observa que el foto-fenton es el proceso que resulta con mas liberación del iono Cl^{-1}.

Aumento de la biodegradabilidad

Se han comparado los ratios DBO_5/DQO y DBO_5/COT para los distintos procesos estudiados. Así, se ha encontrado que los mayores valores se han obtenido después de 120 a 60 minutos de tratamiento. Los procesos que han mostrados mejores resultados en cuanto a aumento de la biodegradabilidad han sido el Fenton y foto-Fenton. Con un ratio DBO5/DQO de 0.20 y 0.15 tras 40 y 90 minutos de tratamiento respectivamente para soluciones DCP. La misma tendencia se ha encontrado para los soluciones de POH.

Estimación de costes

Se ha realizado una estimación de los costes de operación, en base al coste de los reactivos utilizados y consumo eléctrico (ver *Table 7.18 y 7.19*). Como base se ha utilizado la cantidad de DCP y POH eliminado (€/kg) y de COT eliminado (€/kg C). Los resultados se presentan en la *Tabla 7.19*. En cuanto a la mineralización de soluciones acuosas de DCP y POH, el proceso que presenta mejores costes es el foto-Fenton.

2.6 Tratamiento del DCP con POAs basando en el uso de luz UVA

2.6.1 Foto-degradación y aumento de biodegradabilidad

En este apartado, la degradación de de DCP se estudió con los mismo procesos indicados interiormente. Los únicos cambios en esta sección son el tipo de irradiación UV. Mientras en el primer apartado la luz UV que se usó es de longitud de onda de 253.7 nm, en esta sección los reactores usados están con energía de irradiación UV con longitud de onda diferente.

Así, se usaron dos tipos de reactores (reactor 2 y 3); un reactor con solo una lámpara (4W) y otro reactor con tres lámparas de 8 W cada una (24 W en total). En tabla 1 se han comparado los distintos procesos estudiados en cuanto las concentraciones iniciales de reactivos usados, el tiempo de reacción (tiempo de irradiación), desaparición del DCP y mineralización en COT. Se observa en la tabla que la mayor desaparición del DCP se obtuvo con el uso del proceso foto-Fenton. De hecho, un 100% del eliminación del DCP ocurrió con concentraciones iniciales de 75 $mg.L^{-1}$ H_2O_2 10 $mg.L^{-1}$ Fe(II) y con un tiempo de reacción de 40 minutos en el reactor simple. La misma degradación se ha encontrado con 65 $mg.L^{-1}$ H_2O_2 y 10 $mg.L^{-1}$ Fe(II) tiempo de reacción de 35 minutes en el reactor con 3 lámparas.

Tabal 1: Resultados obtenidos mediante la degradación del DCP con POA basados al UVA

	Reactor con una lámpara				Reactor con 3 lámpara			
Proceso	UVA	UVA/ H_2O_2	UVA/Fe(II)	Foto-Fenton	UVA	UVA/ H_2O_2	UVA/Fe(II)	Foto-Fenton
H_2O_2 ($mg.L^{-1}$)	-	250	-	75	-	200	-	65
Fe(II) ($mg.L^{-1}$)	-	-	-	10	-	-	-	10
F(III) ($mg.L^{-1}$)	-	-	120	40	-	-	120	35
UV (min)	120	120	90	40	120	120	90	35
DBO_5/DQO	0	0.011	0.024	0.19	0	0.06	0.0385	0.20
ºDBO_5/COT (mgO_2. $mg^{-1}C$)	0	0.05	0.0007	0.36	0	0.1	0.001	0.34
%DCP eliminado	9	37	60	100	22	50	70	100
%COT eliminado	4 12	13 12	12 15	11.5 12.5	4 12	13 12	15	12.5

En la tabla 1 se han reasumido los resultados de la mejora la biodegradabilidad con los procesos de POAs. Con los procesos UVA y UVA/H_2O_2 en los dos reactores, no se ha encontrado ninguna mejora significativa, por el otro lado mejoras importantes fueron obtenidas con los procesos UV/Fe(III) y foto-fenton en los dos reactores.
Otra vez, se han ajustado las velocidades de desaparición del DCP a una cinética de primer orden y se calculó la vida media de eliminación. Los resultados se presentan en tablas 8.1 a 8.3.

2.6.2 Identificación de los intermedios:
También se trato en estos experimentos identificar los intermedios de degradación. Como, en los dos reactores los intermedios identificados son iguales, se decido presentar sólo los del reactor simples. Se han podido identificar entre los intermedios de reacción el chlorobenzoquinona y el resocinol Se identificaron también: el ácido glutámico, el ácido oxálico y el ácido formico dentro los intermedios. En este apartado se ha hecho una comparación dentro todos lo procesos estudiados.

2.7. Combinación el proceso foto-Fenton con reactores biológicos SBR
En esta sección se ha establecido un proceso combinado completo, el proceso combinado incluye la reacción foto-Fenton como un pre-tratamiento que mejora la biodegradabilidad de las soluciones acuosas del DCP las cuales alimentan después a un reactor biológico de tipo SBR para terminar de eliminar toda la materia orgánica que se considera más biodegradable. Esta proceso se hizo en dos tipos de reactores:

1. Reactor SBR aeróbico
2. Reactor SBR anaeróbico.

Esta parte se ha centrado en estudiar el efecto del tratamiento, el rendimiento de los reactores SBR y la duración del ciclo.
Todas las soluciones pre-tratadas utilizadas se han hecho con el reactor 3 (tres lámparas de luz negra). De los resultados obtenidos con este reactor, se ha observado que la biodegradabilidad aumenta el tiempo que el DCP desapareció totalmente de la soluciones. De hecho se decidió utilizar esta solución tratado para poner en marcha el reactor biológico.

En ambos reactores (aeróbico y anaeróbico) se ha empezado con un lodo activo aerobico o anaerobio no aclimatado de la depuradora municipal de Gavá. Los lodos fueron aclimatados a las soluciones pre-tratados en periodo de mas de 30 días. Durante el periodo de aclimatación se midieron diariamente la evolución del COT, pH, sólidos totales suspendidos y volatiles (TSS y TVSS). Se eliminó mas de 30 y 45% de COT en el proceso aeróbico y anaeróbico respectivamente. La concentración de biomasa presentad mediante el valor TVSS se estableció en 0.24 y 0.46.

Después de comprobar que los reactores están aclimatados se empezó alimentar ambos rectores con soluciones pre tratadas mediante el Foto-Fenton, cambiando la duración del ciclo o la biodegradabilidad del alimento. En la tabla 9.1 y 9.2 se puede ver los 12 periodos estudiados en cada reactor.

Al respecto del reactor aeróbico los resultados experimentales han mostrado que empezando con una solución de biodegradabilidad moderada, se puede obtener una eliminación de COT de mas del 60% .
A largo del proceso se observó que, cambiando el tipo de alimento con una solución de biodegradabilidad por encima del limite del agua municipal, resulta una mejora en la eliminación del COT de mas del 80%, incluso con un tiempo de reacción muy corto (3 horas). Este resultado nos orienta hacia una posterior eliminación del COT en el proceso combinado (biológico-químico) de más de 93%.
Por otra parte durante los procesos estudiados se notó que durante el desarrollo del proceso un aumentó de la carga orgánica de 34 a 273 $mgC.L^{-1}.día^{-1}$ y se eliminó el COT en un 80%. El cual resulta en un proceso muy económico (ver figura 9.14).
La misma tendencia fue obtenida en el reactor anaerobico, con la diferencia que el proceso aeróbico muestra mejor porcentaje de degradación y una cinética mas rápida. Durante este proceso también se obtuvo mas del 93% de eliminación del COT, en un tiempo de reacción corto de 8 horas. Al final de estos experimentales re ha realizado un estudio cinético de los reactores basándose en una reacción de primer orden, en la tabla 9.3 se han presentado los valores logrados.

Se estableció una comparación de coste dentro del proceso combinado y el de mineralización total de la materia orgánica con foto-Fenton. Los resultados de esta comparación pueden verse en la tabla 9.4. Al respecto del proceso foto-Fenton, se ha

calculado el coste del proceso bajo tres porcentajes de eliminación del COT (100%, 90% y 80%).

Se utilizaron al mismo tiempo diferentes condiciones de operación de los procesos combinados Se ha observado que, bajo el mismo porcentaje de mineralización, los procesos combinados muestran costos más bajos que proceso de foto-Fenton, a pesar de que la parte biológica se operó a un ciclo de duración amplia de 8 días. Para un 90% de eliminación del COT el coste en foto-Fenton es de 110 €.kg^{-1} de COT tratado. Al mismo tiempo, sólo 25 y 34 €.kg^{-1} de COT tratado fue necesario en los procesos combinados, que se operaron con s de 8 y 3 horas. Así, se concluye que usando el proceso combinado se puede ahorrar por lo menos entre 70 y 85 €.kg^{-1} de COT tratado.

2.8 Tratamiento de tintes de textiles y agua de textil industrial

En este parte, se ha estudiado la foto-degradación y la mejora de la biodegradabilidad para tres familias(Intracron, Optisal y Nylanthrene) de tintes de textiles no-biodegradable y un agua residual. Al inicio se examinó la influencia de pH en el cambio de color de dichos tintes además de examinar la tendencia de biodegradabilidad de la soluciones coloradas, esto se realizó mediando el ratio DBO_5/DQO y la inhibición del consumo de oxigeno de lodos activos. Los resultados experimentales han mostrado que estos tipos de colorantes no son biodegradables (DBO_5/DQO ≈0.0) y además se observó un inhibición total del consume de oxigeno cuando la concentración es de orden 10%V/V. Después se ha estudiado el efecto de ambos procesos de foto-oxidación vía el proceso VUV y el proceso UV-luz para eliminar los colores y mejorar el biodegradabilidad.

Los resultados experimentales han mostrado que la fotolisis mediante los procesos VUV y UV parece ser una técnica eficaz para degradar las soluciones de tintes de textil. Con el proceso VUV, mas de 90% de eliminación de color de la mayoría de las soluciones se puede lograr en un tiempo de tratamiento de 7.5 minutos. Durante el mismo tiempo, se elimina el 30%del DQO.

Además, se ha encontrado que el valor del DBO_5 de las soluciones tratadas aumentan. Esto indica que, mediante esté proceso puede reforzar el valor del biodegradabilidad en sólo pocos minutos de tratamiento. El ratio DBO_5/DQO de todos las soluciones aumentaron a un valor en que la materia orgánica fácilmente biodegradable (DBO5/DQO>0.40) con una desaparecieron total del color.

La reacción foto-química estudiada se ha ajustado con una cinética de primer orden. Se observó que las constantes de reacción de cada familia tiene su propia tendencia. Dentro de ellas se han mostrado que los tintes reactivo (reactive dyes) son los más sensibles a irradiación con UV. Las constantes cinéticas de todos los colorantes estudiados están tabulados en tabla 10.4.

2.9 Conclusiones

Del presente estudio se han extraído principalmente las siguiente conclusiones:

I. La degradación y mejora de la biodegradabilidad para soluciones de DCP y POH fueron desarrolladas mediante el proceso de oxidación avanzada basando en la foto-degradación con luz UV y UVA. A lo largo de este estudio, la influencia de varios parámetros como las concentraciones iniciales de peróxido de hidrógeno, Fe(II), pH, y temperatura fueron investigados.

II. Incluyendo todos los procesos de foto-oxidación estudiados, la reacción foto-Fenton ha mostrado una eficiencia significativa en la eliminación del DCP y del POH. Un 100% de eliminación del DCP se obtuvo durante 40 minutos a concentraciones iniciales de 50mg.L^{-1} H_2O_2 y 10mg.L^{-1} Fe(II). Eso fue combinado con un 21% de la reducción en COT. Al mismo tiempo el 82% de eliminación de fenol se logró 15 minutos a concentraciones iniciales de 210 mg.L^{-1} H_2O_2 y 10 mg.L^{-1} Fe(II).

III. La evolución de la concentración de ambas substancias a través de la degradación se ha ajustado a una cinética del primer-orden con respecto a la concentración del contaminante. Al comprarse las reacciones de los procesos de foto-Fenton y UV directa se ha encontrado que las constantes cinéticas para ambos POH y DCP han aumentado aproximadamente 18 veces. La correspondiente contante cinética en él punto de eliminación de 82%POH y 100%DCP eran respectivamente de 0.11 y 0.13 minutos.

IV. El proceso Foto-Fenton han demostrado de ser un método de pre-tratamiento eficaz para mejorar la biodegradabilidad de soluciones de POH y DCP. En el caso de soluciones de POH, la ratio DBO_5/DQO aumentó de 0 a 0.92 durante 15

minutos, con las siguientes condiciones iniciales: 50 $mg.L^{-1}$ H_2O_2 y 75 $mg.L^{-1}$ Fe(II). Al respecto de las soluciones de DCP en el punto donde todo el DCP desapareció de la solución, la ratio DBO_5/DQO mejoró de 0.0 a 0.18 con foto-oxidación basada en luz UV. Mejoró también de 0 a 0.19 con otra reacción basada en el uso de luz UVA. Esto se logró con una concentración inicial de Fe(II) muy baja (10 $mg.L^{-1}$) 50 $mg.L^{-1}$ de H_2O_2 en el caso de UV y 75 $mg.L^{-1}$ en el caso de UVA. El valor de DBO_5 significativo al punto que los compuestos (DCP y POH) fueron eliminados, se atribuye al carácter inhibitorio de ambas substancias o que los primeros intermedios no son fácilmente biodegradable, requiriendo así mas oxidación para mejorar su biodegradabilidad.

V. Se estableció una buena relación entre la mejora de la biodegradabilidad y el cambio en el grado de oxidación de la materia orgánica. Un cambio significativo en la oxidación de la materia orgánica contenida se deriva del desarrollo de biodegradabilidad.

VI. Para ambos compuestos (DCP y POH), la mineralización total se logro con las condiciones siguientes: tiempo de irradiación de 60 minutos, con 40 y 60 $mg.L^{-1}$ de Fe(II) para DCP y POH respectivamente y unas concentración iniciales de peróxido de hidrógeno de 270 y 750 $mg.L^{-1}$. Así las cantidades de peróxido de hidrógeno usados son menores de 62% y 40% de la cantidades stoichiometricas

VII. Se han identificado clorobenzoquinona y hidroquinona como intermedios preliminares generados en el degradación del DCP en proceso diferentes. Además, se han identificado ácido oxálico y ácido glutámico como intermedios finales.

VIII. El POH y sus soluciones pre-tratadas fueron degradados biológicamente. La eficiencia de eliminación de la materia orgánica fue mejor para el reactor alimentado con POH pre-tratado, Un eliminación del COT de 95% durante ciclos de duración de 55 horas se obtuvo en procesos combinados, mientras se exigió 130 horas para obtener un 80% en el proceso biológico.

IX. Soluciones de DCP tratadas se han oxidado biológicamente en dos reactores; uno con biomasa aclimatada previamente al phenol y el segundo con lodos activados no-aclimatados. Los valores de eliminación del COT obtenidos fueron mejores en el reactor aclimatado. Un máximo del COT eliminado entre 81.4 y 89% fue obtenido a traves de la co-digestión de las soluciones pre-tratadas con aguas residuales y TRH de 2 días. Además, un porcentaje de COT de 57% se logró en ambos reactores al alimentar con 100% de soluciones pre-tratadas en12 horas TRH.

X. Las soluciones de DCP foto-tratado se han oxidado biológicamente en un reactor biológico de tipo SBR que contiene lodos no-aclimatado para estudiar la bio-oxidación aeróbico y anaeróbica. Se estudió el efecto de biodegradabilidad de la solución pre-tratada así como la duración del ciclo en la eficiencia del bio-reactor. Los parámetros manipulandos permiten lograr una eliminación de substratos orgánicos al 82% durante un ciclo de 6 a 8 horas En este punto la proporción de la reacción es en orden de 9mg COT. $(L.h)^{-1}$ y la proporción específica de eliminación es de 30mg COT. $(L.h.\ g\ TVSS)^{-1}$

XI. Se han estimado los costes de operación para el tratamiento del DCP por medio de los procesos combinados (foto-Fenton y SBR) y la mineralización total vía foto-Fenton. Bajo la misma eficacia del mineralization, los procesos combinados muestran costos más bajos que el foto-Fenton usando el proceso combinado, y pueden ahorrar como mínimo 70 $€.kg^{-1}$ del COT tratado.

XII. Las soluciones de tintes de textil fueron tratadas por el proceso VUV para eliminar el color y mejorar el biodegradabilidad. Más del 90% de la eliminación de color de la mayoría de las soluciones se logró durante un tiempo de tratamiento de 7.5 minutos. Durante este mismo tiempo, 30% del DQO fue eliminado. Se ha encontrado que los valores del DBO_5 de las soluciónes aumenta el ratio DBO_5/DQO al valor en que la materia orgánica se considera biodegradable (DBO5/DQO>0.40).

XIII. Las decoloraciones en las soluciones de tintes de textil fueron ajustadas a una cinética de primer orden. Los resultados mostraron que cada familia de tintes tiene su propia tendencia. Los tintes reactivos han mostrado ser los más sensibles a la irradiación de UV. Se observo que la sensibilidad del tinte es inversamente proporcional a la absorbencia, en la longitud de la onda que emite la lámpara (253.7nm).